Novel virulence determinants in *Mycoplasma pneumoniae*: Contribution of transport systems and H$_2$S production to viability and hemolysis

---

Dissertation

For the award of the degree
"Doctor rerum naturalium"
Division of Mathematics and Natural Sciences
of the Georg-August-University Göttingen

In the PhD program
Microbiology and Biochemistry
of the Georg-August-University School of Science (GAUSS)

Submitted by
Stephanie Großhennig
from Wernigerode

Göttingen 2014

Thesis Committee

Prof. Dr. Jörg Stülke
(Institute of Microbiology and Genetics; Department of General Microbiology)

PD Dr. Michael Hoppert
(Institute of Microbiology and Genetics; Department of General Microbiology)

Prof. Dr. Carsten Lüder
(University Medical Center Göttingen; Department of Medical Microbiology)

Members of the Examination Board

First reviewer: Prof. Dr. Jörg Stülke
(Institute of Microbiology and Genetics; Department of General Microbiology)

Second reviewer: PD. Dr. Michael Hoppert
(Institute of Microbiology and Genetics; Department of General Microbiology)

Further Members of the Examination Board

Prof. Dr. Carsten Lüder
(University Medical Center Göttingen; Department of Medical Microbiology)

Prof. Dr. Ivo Feussner
(Albrecht von Haller Institute; Department. of Plant Biochemistry)

Prof. Dr. Stefanie Pöggeler
(Institute of Microbiology and Genetics; Department of Genetics of Eukaryotic Microorganisms)

Prof. Dr. Stefan Pöhlmann
(German Primate Center; Infection Biology Unit)

Date of Oral Examination: 20.01.2014

I hereby declare that the doctoral thesis entitled, "Novel virulence determinants in *Mycoplasma pneumoniae* - Contribution of transport systems and H_2S production to viability and hemolysis" has been written independently and with no other sources and aids than quoted.

Stephanie Großhennig

DANKSAGUNG

Es gibt viele Menschen, die mich auf meinem Weg durch die Höhen und Untiefen dieser Arbeit begleitet haben und denen ich daher unbedingt danken möchte.

Natürlich richte ich traditionell den ersten Dank an Jörg, weil er mich schon im Bachelor für die Mikrobiologie begeistern konnte (damals trug er Chucks mit offenen Schnürsenkeln und Ampelmännchen-T-Shirts in der Vorlesung) und dafür gesorgt hat, dass diese Begeisterung bis heute anhält. Danke, dass Du mir die ehrenvolle Aufgabe anvertraut hast, auch nach der Ära Schmidl die Mycoplasmologie in der Abteilung einigermaßen erfolgreich weiter zu führen. Ich hoffe, dass sich das Vertrauen spätestens mit der grandiosen Entdeckung des Schwefelwasserstoffs in *Mycoplasma* bezahlt gemacht hat!

Außerdem danke ich den weiteren Mitgliedern meines Thesis Committees, Michael Hoppert und Carsten Lüder, für das zuverlässige Erscheinen zu meinen Vorträgen, sowie für ihre Unterstützung und den Zuspruch. Ich hatte nach den Meetings immer ein gutes Gefühl. Ich bin desweiteren Till Ischebeck aus der AG Feussner sehr, sehr dankbar dafür, dass er für mich die wichtigen GC-MS Messungen gemacht und mir immer alle Fragen beantwortet hat.

So, nun zu meinen geliebten (Teilzeit-)Mycoplasmologen Julia, Katrin und Hannes: Ohne Scheiß, ihr habt gefühlt ca. die Hälfte meiner Arbeit auf dem (guten) Gewissen! Und das sag ich jetzt nicht nur, weil man das halt am Ende einer Arbeit netterweise so macht. Vielen Dank, dass ihr mir so viel geholfen habt und dass ihr dabei auch noch gekonnt so getan habt, als würde es euch Spaß machen! ;-) Julia, du bist ganz großartig und ich war froh, dass ich dich die ganzen 50% deiner Zeit zu 100% an meiner Seite hatte! Katrin, ich hab selten so viel Begeisterung, so viel (schwarzen) Humor und so viel Intelligenz neben mir sitzen gehabt! Danke, dass du die Hämolyse mit mir erobert hast und mir nicht zuletzt in schwierigen Zeiten das Gefühl gibst, dass ich stolz auf meine Arbeit sein kann! Hannes, für mich bist du eine bemerkenswerte Kombination aus mega schlau, mega ehrgeizig, mega zuverlässig, mega entspannt und dann auch noch mega angenehm. Ohne dich hätt ich die ganze MPN487-Geschichte in der Kürze der Zeit nie so gut geschafft. Vielen Dank, dass ihr mich alle so gut betreut habt. Ihr macht mich (Achtung, Nerd-Witz!) HapE! :-)

Wo wir gerade bei Betreuung sind: Vielen Dank auch an meine beiden anderen ehemaligen Studenten Julian und Martin, die ich aus den unterschiedlichsten Gründen nie vergessen werde! Martin, du bist sowohl fachlich als auch menschlich eine absolute Bereicherung!

Apropos Bereicherung: Katrin G., Lorena, Dodo, Chris, Arne, Daniel, Jan - mit euch hab ich viele Stunden verbracht, die mich auf verschiedenste Weise bereichert haben. Katrin, ich bin fasziniert, dass du dir jahrelang geduldig meine schlechten Witze und mein Gejammer über *Bacillus*, Haarausfall und allgemeine Verunsicherung angehört hast und wir uns trotzdem immernoch regelmäßig treffen! Du bist ein sehr, sehr wertvoller Mensch und bin froh, dass ich dich kennen darf. Lorena... mir fehlen die Worte, so gern hab ich dich! Und du heiratest bald, wie cool ist das denn!? :-) Dodo und Chris, mit Dresden verbinde ich jetzt immer Duschen hinter Milchglas und nächtliche WhatsApp-Beschwerden über das Verschieben der Grenze. Das war ein großartiges Erlebnis! Und ich danke euch für die herzliche, vorübergehende Beherbergung in eurem Lab! Da war das Arbeiten jeden Tag noch ein bisschen schöner. ;-) Arne und Daniel, eure Bereicherung fand wahrscheinlich maßgeblich über die Sättigung der Büro-Luft mit Alkoholausdünstungen statt, hihi. Bei Arne denk ich auch voller Freude an „Herzilein" und „Fields of Gold" in der Little Britain Variante. Naja und an Bon Jovi, aber das ist eher negativ. ;-) Jan, schön, dass wir die Hürden der vergangenen Jahre seit Beginn der Bachelorarbeit zusammen gemeistert haben und es auch zusammen bis (hoffentlich) auf's Liesel schaffen. Leute, ich hab euch echt gern und ich hab sehr gern mit euch gearbeitet und „gearbeitet"!

Auch meinen übrigen gegenwärtigen oder ehemaligen Kollegen Miriam, Sabine, Raphael, Nora, Bingyao, Christina, Bärbel, Andrea, Jan[2], Joni, Felix, Fredo, Martin, Tini, Frothe, und natürlich nachträglich Sebastian „R" Schmidl danke ich für die Unterstützung und die schöne gemeinsame Zeit!

Zuletzt kommt natürlich der größte, wichtigste und liebevollste Dank von allen Danken auf der ganzen Welt an meine Familie und meine Freunde. Mama, Papa, Juli und Peter, ihr seid die wichtigsten Menschen in meinem Leben und ich bin euch dankbar für alles, was ihr mir in der letzten Zeit und eigentlich schon immer gegeben habt: Zuversicht, Wertschätzung, Ablenkung, Kuchen, Taschentücher zum Tränen trocknen, schöne Urlaube, Aufmunterung und ganz, ganz, ganz viel Liebe! Ohne euch hätte ich es nie so weit geschafft. Mama und Papa, diese Arbeit ist für euch.

CONTENT

ABBREVIATIONS

% (v/v)	% (volume/volume) (volume percent)
% (w/v)	% (weight/volume) (mass percent)
ABC	ATP-binding cassette
amp	Ampicillin
AP	Alkaline phosphatase
ATP	Adenosine triphosphate
BACTH	Bacterial adenylate cyclase two hybrid
BLAST	Basic Local Alignment Search Tool
bsu / BSU	*Bacillus subtilis*
c-di-AMP	Cyclic di-adenosine monophosphate
cAMP	Cyclic adenosine monophosphate
CARDS	Community-acquired respiratory distress syndrome
CDP*	Disodium 2-chloro-5-(4-methoxyspiro {1,2-dioxetane-3,2- (5-chloro) tricyclo[3.3.1.13,7]decan}-4-yl) phenyl phosphate
CE	Crude extract
cm	Chloramphenicol
dH$_2$O	Deionised water
DHAP	Dihydroxyacetone phosphate
DIG	Digoxygenin
DMEM	Dulbecco's Modified Eagle Medium
dNTP	Desoxyribonucleosidtriphosphate
DNA	Desoxyribonucleic acid
dpi	Days past infection
DTE	Dithioerythritol
DUF	Domain of unknown function
ECF	Energy coupling factor
EI	Enzyme I
EII	Enzyme II
EDTA	Ethylene diaminetetraacetate
et al.	Et altera
FBS	Fetal bovine serum
Fig.	Figure
FT	Flow through

fwd.	Forward
GC-MS	Gas chromatography coupled to mass spectrometry
gDNA	Genomic DNA
Glc	Glucose
Gly	Glycerol
GPC	Glycerophosphocholine
G3P	Glycerol-3-phosphate
HeLa cells	Henrietta Lacks (human cervix carcinoma) cells
HMW	High molecular weight
HEPES	4-(2-Hydroxyethyl)-piperazin-1-ethan-sulfonic acid
HPr	Heatstable protein
i.e.	id est
IPTG	Isopropyl-1-thio-β-D-galactoside
kan	Kanamycin
kb	Kilo base pairs
LB	Luria Bertani (Medium)
LFH	Long flanking homology
Mbp	Megabasepairs
MCS	Multiple cloning site
metHB	Methemoglobin
MFS	Major facilitator superfamily
MMR	Multiple mutation reaction
Mox	Methoxylamine
mpn / MPN	*Mycoplasma pneumoniae*
mRNA	Messenger RNA
MSTFA	N-methyl-trimethylsilyltrifluoroacetamid
NAD^+	Nicotinamide-adeninedinucleotide
$NADH_2$	Nicotinamide-adeninedinucleotide (reduced form)
OD_x	Optical density, measured at wavelenght $\lambda = x$ nm
ORF	Open reading frame
PAGE	Polyacrylamide gel electrophoresis
PBS	Phosphate buffered saline
PCR	Polymerase chain reaction
PEP	Phosphoenolpyruvate
pH	Power of hydrogen

PLP	Pyridoxal-5'-phosphate
PMP	Pyridoxamine phosphate
PPLO	Pleuropneumoniae like organisms
qRT-PCR	Reverse transcription quantitative real-time PCR
rev.	Reverse
RNA	Ribonucleic acid
RNase	Ribonuclease
rpm	Rounds per minute
PBS	Phosphate-buffered saline
PTS	Phosphoenolpyruvate:Sugar Phosphotransferasesystem
RBCs	Red blood cells
RT	Room temperature
SDS	Sodium dodecyl sulfate
SSC	Standard saline citrate
SulfHb	Sulfhemoglobin
Tab.	Table
TAE	Tris-acetic acid-EDTA
TCA	Tricarbolic acid
Tn	Transposon
Tris	Tris-(hydroxymethyl)-aminomethan
tRNA	Transfer RNA
U	Units
w/o	Without
wt	Wild type
X-Gal	5-bromo-4-chloro-indolyl-galactopyranoside

Units

°C	Degree Celsius
A	Ampere
bar	Bar
Da	Dalton
F	Farad
g	Gram
h	Hour
l	Liter
m	Meter
min	Minute
mol	Mol
M	Molar
sec	Second
V	Volt

Prefixes

k	Kilo
m	Milli
µ	Micro
n	Nano
p	Pico

Nucleosides

A	Adenine
C	Cytosine
G	Guasine
T	Thymine
U	Uracil

Amino acid nomenclature (IUPAC-IUB-covention 1969)

A	Ala	Alanine	M	Met	Methionine
C	Cys	Cysteine	N	Asn	Asparagine
D	Asp	Aspartate	P	Pro	Proline
E	Glu	Glutamate	Q	Gln	Glutamine
F	Phe	Phenyl alanine	R	Arg	Arginine
G	Gly	Glycine	S	Ser	Serine
H	His	Histidine	T	Thr	Threonine
I	Ile	Isoleucin	T	Tyr	Tyrosine
K	Lys	Lysine	V	Val	Valine
L	Leu	Leucin	W	Trp	Tryptophane

1. INTRODUCTION

1.1 Virulence mechanisms in pathogenic bacteria

Pathogenic bacteria possess a multitude of mechanisms which ensure their survival and spread and which potentially cause disease in their human host. Since infectious diseases represent a major cause of death worldwide, identifying and understanding these pathogenicity mechanisms is a key step to a successful combat. Though many of the microbial pathogens are highly different from each other, plenty of their infection strategies have turned out to be remarkably similar. Microbial pathogenesis usually starts with exposure and adhesion of pathogenic bacteria to the host (cells). For this, bacteria often produce adhesins or capsules which help to withstand the mechanical forces the host employs to get rid of intruders. In many cases, adhesion is an indispensable prerequisite for interaction and pathogenesis. Adhesins can be made of proteins or polysaccharides or a mixture of both. In addition to adherence proteins, some bacteria produce slime layers or capsules. Since most pathogens exhibit host and tissue specificity, they do not adhere to all host cells but selectively e.g. to mucosal surfaces and epithelial cells. For this purpose, microbes may use a variety of host-receptors for recognition, like glycolipids, glycoproteins, membrane-spanning or extracellular matrix proteins like fibronectin (Finlay and Falkow, 1997). Successful adhesion then paves the way for deeper colonization of host tissues in forms of extracellular or intracellular invasion. Invasion is a process which describes the penetration of the epithelium, thereby allowing the pathogen to get access to protected and nutrient-rich niches. Entering the blood or lymphatic circular system, the pathogen might force its way to tissues which are quite distant from the original entry site, potentially leading to a systemic infection. Two general types of invasion can be distinguished: During extracellular invasion, bacteria degrade tissue components and cells using secreted proteins like hyaluronidases or lipases without entering the host cells. In contrast, intracellular invasion is a process in which the pathogen really enters the host cells to survive, proliferate and finally spread. Some pathogens are facultatively intracellular; others like *Chlamydia spp.* have an obligate intracellular lifestyle (Walker, 1998). The host cell types in which (obligate) intracellular pathogens can reside comprise professional phagocytes, like macrophages and neutrophils, and non-phagocytic cells such as epithelial and endothelial cells (Finlay and Falkow, 1997). The clear advantage of intracellular life is an overall elevated protection from host antibodies

15

and possibly applied antibiotics. In fact, both, the establishment of antibiotic resistances and the successful evasion of the host immune system are significant aspects of bacterial virulence. Effective evasion of the immune response mainly relies on the attempts not to be recognized by the host immune cells and antibodies, and consequently not to be eliminated by phagocytosis. In this respect, capsule formation is used widely by pathogenic bacteria to protect themselves from the host immune system or antibiotic substances after entering the infection site. Capsules are sugar coats consisting of exopolysaccharides which are specific for different bacterial species. For example, *Streptococcus pneumoniae* dedicates 24 biosynthetic genes for capsule formation which underlines that the capsular polysaccharide is one of its main virulence factors (Garcia *et al.*, 1999). Moreover, the bare bacterial cell walls can also act as virulence factors which may even lead to a septic shock in the human body. The cell walls might contain toxic molecules like the lipopolysaccharides (LPS) in gram-negative or the peptidoglycan and teichoic acids in gram-positive pathogens. These compounds induce the enhanced release and activation of cytokines, complement components and the coagulation cascade, which together can result in a septic shock (Horn *et al.*, 2000). Typical examples for bacteria being involved in sepsis are *E. coli, Pseudomonas aeruginosa* or *Staphylococcus aureus* (Walker, 1998).

Beside the toxic cell wall components, bacterial pathogens are able to actively produce a spectrum of exotoxins to damage host cells. With regard to their structure and function, there are different groups of exotoxins: (i) The AB toxins are amongst others found in *E. coli, Vibrio cholerae*, and *Bordetella pertussis* (Nakao and Takeda, 2000; Klose, 2001; Stein *et al.*, 1994). These toxins consist of two components: A has enzymatic activity like proteolysis or ADP-ribosylation, whereas B delivers the toxin into the host cell. (ii) Proteolytic toxins decompose host proteins. In case of the botulinum and tetanus toxins from *Clostridium botulinum* and *C. tetani*, synaptobrevin is cleaved. This leads to an inhibition of neurotransmitter release and violent muscular spasm (Schiavo *et al.*, 1992). (iii) Membrane-disrupting and pore-forming toxins insert into the host cell membrane to form holes and finally cause cell lysis (Finlay and Falkow, 1997).

Finally, it is assumed that horizontal gene transfer of pathogenicity islands facilitates the emergence of novel pathogenic bacteria strains carrying new resistance and infection properties. Therefore, the gene transfer might also be considered a part of the virulence machinery (Ochman and Moran, 2001).

1.2 The pathogenic lifestyle of *Mycoplasma pneumoniae*

1.2.1 The minimal organism *M. pneumoniae*

Mycoplasma pneumoniae is a human pathogenic bacterium, which belongs to the group of *Firmicutes -* gram-positive bacteria with low GC-content. Within the *Firmicutes,* the *Mycoplasma* species, like *Ureaplasmas*, *Alcholeplasmas* and *Spiroplasmas*, are members of the *Mollicutes* (Ciccarelli *et al.*, 2006). The term "*Mollicutes*" can be translated as "soft skin", describing the absence of a cell wall in these bacteria, due to the lack of genes for peptidoglycan synthesis (Carstensen *et al.*, 1971). Therefore, mycoplasmas are not surrounded by rigid boundaries which give them defined forms like cocci or rods, but they exhibit pleomorphic cell shapes. A typical cell of *M. pneumoniae* is filamentous or flask-shaped, with a knobby tip and is about 1-2 μm long and 0.1-0.2 μm wide (**Fig. 1.1**). The tip has important functions as attachment organelle, in gliding and in cell division (Baseman, 1993; Miyata, 2008).
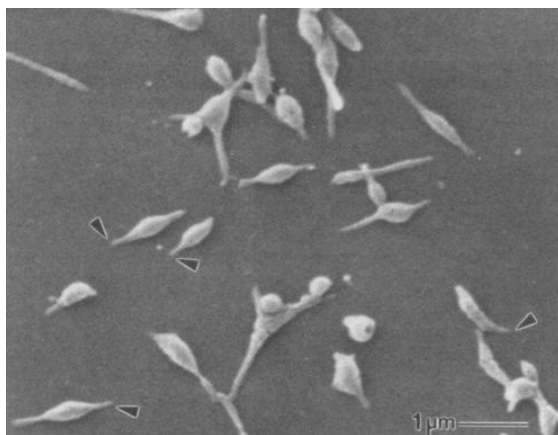
Fig. 1.1. Scanning electron microscopic picture of surface-attached *Mycoplasma pneumoniae* cells. Arrowheads indicate the tip structure which is crucial for adhesion and gliding. (from Krause and Taylor-Robinson, 1992)

The *Mollicutes* are the smallest bacteria that are capable of independent life. They are characterized by extremely reduced genomes as result of a long time degenerative evolution, probably due to their parasitic life style with constantly high nutrient availability and stable conditions in their habitat. Among the *Mycoplasma* spp., the genome size varies between 0.58 Mb in *M. genitalium* and 1.36 Mb in *M. penetrans.* The complete genome sequence of *M. pneumoniae* has been available since 1996. It has a size of 0.86 Mb and contains 688 open reading frames (Himmelreich *et al.*, 1996; Dandekar *et al.*, 2000). Strikingly, in *M. pneumoniae*, as in some other *Mollicutes*, the codon UGA codes for tryptophan

instead of a stop codon as usual (Renaudin *et al.*, 1987; Schaper *et al.*, 1987). Because of their reduced genomes and, yet, their ability to be cultivated in medium without helper cells, these minimal organisms are naturally ideal objects to study the necessity of certain genetic elements for life.

The minimal gene set is not only reflected in the lack of peptidoglycan synthesis. Also, *M. pneumoniae* lacks the genes for most anabolic pathways. Genes coding for amino acid- and vitamin biosynthesis are completely absent and the organism is not able to perform respiration. Concerning the catabolism, glycolysis is the only central catabolic pathway which is complete. The tricarboxylic acid (TCA) cycle is entirely missing and the pentose phosphate shunt is incomplete. Since it lacks its oxidative part, the predominant role of the pentose phosphate shunt is supplying the cell with phosphoribosyl pyrophosphate (PRPP) for nucleotide biosynthesis (Himmelreich *et al.*, 1996; Miles, 1992). Glucose is the carbon-source that is taken up most efficiently and allows the best growth. *M. pneumoniae* can additionally use glycerophosphocholine (GPC), fructose, mannose, glycerol and probably also glycerol-3-phosphate as carbon sources, with all of them entering the glycolysis (Halbedel *et al.*, 2004; Halbedel *et al.*, 2007)). In *M. pneumoniae*, substrate-level phosphorylation in the glycolysis and the pyruvate metabolism is the only way to produce ATP. The degradation of one molecule glucose via the glycolysis yields two molecules pyruvate and two molecules ATP. Pyruvate is converted to either lactate or, after several steps, acetate and ATP. Both lactate and acetate are secreted from the cell and lead to an acidification of the surrounding medium.

Due to its constant conditions in the host tissue, the bacterium has no need to adapt to drastic changes which would require an elaborate regulatory network. Therefore, comparably few genes for regulatory proteins are found (Himmelreich, 1996). Whereas in other bacteria, like *Pseudomonas aeruginosa* or *Streptomyces coelicolor,* transcription factors account for about 10% of the genome, *M. pneumoniae* possesses only an hand full of potential regulators, which make up less than 0.5% of the genome (Stülke *et al.*, 2009). However, this does not mean that *M. pneumoniae* constantly expresses its genes and does not react to extracellular clues. Transcriptome analyses show that *M. pneumoniae* gene expression is indeed altered, e.g. in the presence of different carbon sources, during oxidative stress, heat stress, iron-depletion or temperature imbalance. Also, the regulatory roles of small RNAs and antisense-RNAs were described and the impact of signaling molecules like c-di-AMP is under intense investigation (Güell *et al.*, 2009; Schmeisky, 2013; Treffon, 2014). In addition, there have been several evidences for regulation on a post-translational level, like phosphorylation and acetylation (Halbedel *et al.*, 2004; Schmidl *et al.*, 2010). In fact, the amount of acetylated targets in *Mycoplasma pneumoniae* is three times as high as in *E. coli* (van Noort *et al.*, 2012).

1.2.2 The pathogenicity mechanisms

Disease and epidemiology

M. pneumoniae is one of the most prevalent causes for respiratory tract infections worldwide (Waites and Talkington, 2004). As a human pathogen, it was described for the first time in 1944, after it had been isolated from the sputum of a patient with atypical pneumonia (Meiklejohn, 1944). Transmission usually occurs through aerosols from person to person. Once inside the human host, the bacteria colonize the mucosa of the lower respiratory tract leading to atypical pneumonia (Jacobs, 1997). Although the respiratory tract is the typical habitat, *M. pneumoniae* has also been isolated from several extrapulmonary infection sites like the synovial, the cerebrospinal and the pericardial fluid. Importantly, extrapulmonary manifestations are present in up to 25% of all infected persons (Waites and Talkington, 2004). While, in general, *M. pneumoniae* infections are rather mild, they can cause worse disease patterns in children and immunocompromised patients leading to complications like meningitis, myocarditis (inflammation of the heart muscle) or rheumatoid arthritis (inflammation of the joints) (Taylor *et al.*, 1967; Mackay *et al.*, 1975; Ramirez *et al.*, 2005; Wilson *et al.*, 2007). Due to their natural lack of a cell wall, *Mycoplasma* infections cannot be with treated with common β-lactam antibiotics like penicillin which target the cell wall synthesis machinery. Instead, tetracycline and macrolide-antibiotics are used (Blanchard and Bébéar, 2011).

Adhesion

A prerequisite for colonization and pathogenesis is the ability of *M. pneumoniae* to attach to and grow on smooth surfaces like the human host tissue. This is mediated by an attachment organelle which the bacterium carries at its cell poles (Krause, 1996; Krause und Balish, 2001). This so called tip structure is built up of a network of adhesins e.g. P1, P24, P30, P40 and the P41 and various additional proteins, like the high molecular weight proteins HMW1-3, which allow them to attach to and stay at the host cells (Somerson *et al.*, 1967; Dallo *et al.*, 1990; Inamine *et al.*, 1988). Interestingly, the stability of these cytadherence proteins requires phosphorylation by the protein kinase PrkC. Deletion of this kinase and therefore destabilization of the adhesins clearly demonstrates the importance of cytadherence, since *prkC* mutants turned out to be highly impaired in virulence in a HeLa cell experiment (Schmidl *et al.*, 2010).

Evasion of the host immune system

Surface proteins, like the P1 protein or lipoproteins, are important for the interaction of mycoplasmas with their surroundings. This role, however, makes them also predestined targets for the humoral and cellular immune response. During an *M. pneumoniae* infection, the normal host immune system rapidly produces specific antibodies against protein and glycolipid antigens in the pathogen membrane to eventually get rid of the intruder. To establish a persistent infection, bacterial pathogens need to evade or suppress the host defense response. Mycoplasmas have come up with several mechanisms to protect themselves or hide from immune system: (i) They perform molecular mimicry using the extensive similarity and homology of their own surface proteins and glycolipids with those of the host tissue. This similarity can even cause autoimmune responses in the host through formation of antibodies against its very own substances e.g. myosin, keratin, fibrinogen or lung tissues (Barile, 1979). Also, cross-reactivity can lead to an effect called cold agglutination, in which red blood cells are agglutinated by antibody (IgM) formation following *M. pneumoniae* infection. Therefore, the detection of cold agglutinins in a patient enables diagnosis of *M. pneumoniae* infection. (ii) It has been reported that mycoplasmas exhibit immunomodulatory activities to ensure their survival and that an intracellular lifestyle in the host cells is to be considered (Talkington *et al.*, 2001; Dallo and Baseman, 2000). The latter, for sure, would have indisputable advantages for the bacterium like escaping both the immune system and antibiotic treatment. (iii) *Mycoplasma* species are capable of antigenic phase variation, a process in which the surface antigens of the bacterium are constantly modulated in order to avoid recognition by host antibodies (Citti *et al.*, 2010). In *M. pneumoniae*, DNA rearrangements and recombinatory events in P1 adhesin copies are one example (Kenri *et al.*, 1999). Lipoprotein variation is also widely spread in mycoplasmas and ureaplasmas. This can occur in high frequency via size variation, variation in the number of tandem repeats in one protein or in forms of phase variation (on / off switching of lipoprotein synthesis). Even though *M. pneumoniae* lacks the genes coding for the "classical" lipoprotein families conferring phase variation in other mycoplasma strains, it possesses a large number of lipoprotein encoding genes, some of which are very similar to each other (Markham *et al.*, 1994; Lysnyansky *et al.*, 1999; Rosengarten and Wise, 1991; Bhugra *et al.*, 1991; Hallamaa *et al.*, 2006). Together with the fact that the genes involved in lipoprotein synthesis are essential, this hints at an important role of these proteins for the cell - and possibly also in antigenic variation (Großhennig, 2011).

Toxins and toxic compounds

M. pneumoniae does not possess typical endo- or exotoxins. A fundamental virulence factor is the release of H_2O_2 which has been known as the "hemolysin" of *M. pneumoniae* for a long time (Somerson, 1965). It is assumed that hydrogen peroxide acts together with host endogenous reactive oxygen species to cause oxidative stress in the lung tissue (Tryon and Baseman, 1992). Interaction of H_2O_2 with erythrocytes might lead to oxidation and denaturation of hemoglobin, lipid peroxidation and hemolysis. H_2O_2 is released by *M. pneumoniae* as a side product in glycerol metabolism, more precisely in the conversion of glycerol-3-phosphate (G3P) to dihydroxy acetone phosphate (DHAP), by the glycerol-3-phosphate dehydrogenase GlpD. However, this enzyme actually exhibits oxidase function and transfers electrons to oxygen instead of NAD^+ thus leading to the formation of hydrogen peroxide. Indeed, the *glpD* mutant is not able to produce any hydrogen peroxide and shows a strongly reduced cytotoxicity towards HeLa cells which emphasizes the important role of GlpD in pathogenicity (Hames *et al.*, 2009). Interestingly, *M. pneumoniae* lacks the corresponding enzymes for detoxification: superoxide dismutase and catalase. It is not known how hydrogen peroxide exits the cell and how exactly the minimal organism avoids internal oxidative damage by H_2O_2. In addition to GlpD, *M. pneumoniae* encodes a so called CARDS-Toxin (Community-acquired respiratory distress syndrom), which is similar to a subunit of the pertussis-toxin and has ADP-ribosylating and vacuolating activity (Kannan and Baseman, 2006). While the CARDs toxin appears to be rather irrelevant *in vitro* and in tissue culture, it has been shown to evoke inflammatory responses in a mouse model. Finally, with MPN133, *M. pneumoniae* expresses a lipoprotein which additionally exhibits cytotoxic nuclease function (Somarajan *et al.*, 2010).

Together, these toxic features provide mechanisms to destroy and exploit host cells in order to gain nutrients and compounds which cannot be synthesized by the minimal organism itself but still are absolutely needed for life.

1.3 Transport systems and their impact in virulence

The magnitude of bacterial pathogenicity is significantly determined by their ability to successfully colonize tissues and to spread and persist inside the host. In order to survive, they need to import essential nutrients from their surroundings which makes effective transport systems indispensable. Generally, the function of transport systems is the translocation of solutes over a membrane barrier.

This is not only prerequisite for the uptake of nutrients, but also for the export of metabolic waste or toxic products. The export of drugs is an important aspect in antibiotic resistance therefore having clear clinical relevance. However, it is also a way for bacteria to evolve their ecological niches and prevail over opponents. The secretion of proteins, carbohydrates or lipids can support protection, communication and pathogenesis. Another fundamental aspect of transporters is their relevance in mediating the maintenance of the intracellular osmotic balance by ion in- and efflux. Finally, they can even be involved in the establishment of genetic variety by transferring nucleic acids as part of horizontal gene transfer (Saier, 2000).

1.3.1 Types of transport systems

Transport systems are specifically characterized by their mode of transport, energy coupling mechanism, molecular phylogeny and substrate specificity. According to the transporter classification (TC) system, they can be divided in four major groups regarding their mode of action: channels, secondary transporters, primary active transporters and group translocators (Saier, 2000). These groups are described in more detail in the following.

Channels catalyze an energy-independent, facilitated diffusion process down a concentration gradient which is energy-independent. There are α-type channels, which consist of α-helical spanners and are ubiquitously found in the membranes of all organisms, and β-barrel pores whose transmembrane parts are exclusively made up of β-strands. Even pore-forming toxins, which are produced as cytolysins by one organism to be inserted into the membrane of a target cell, belong to this group. Primary active transporters make use of a primary source of energy, like a chemical reaction, light absorption or electron flow, to transport substrates against a concentration gradient. Their most famous member and actually one of the largest transporter classes are the ATP binding cassette (ABC) transporters, which couple transport to ATP hydrolysis. ABC transporters are usually heteromultimeric complexes consisting of two substrate-translocating and two ATP-hydrolyzing proteins. In addition, ABC transport systems often rely on the collaboration with additional extracytoplasmic substrate binding proteins, which, in gram-positive bacteria, are most often lipoproteins. They bind their substrates with an affinity of 0.01 – 1 μM which makes the binding proteins extremely efficient even at low substrate concentration. In the past years, a new group of ABC transporters has been discovered and aroused interest: the energy-coupling factor (ECF) transporters. These systems do also contain of a small membrane-spanning substrate binding S-component and an energy-coupling module. They catalyze

the uptake of a range of micronutrients, especially water-soluble vitamins (e.g. riboflavin and thiamin) and their precursors. ECF transporters are present in about 50% of all prokaryotes, but are particularly abundant in the Firmicutes (Saier, 2000; Rodionov *et al.*, 2009).

Secondary active transporters are electro-chemically driven transporters. They include uniporters, symporters and antiporters. Uniporters mediate specific transport of a single species, mainly by facilitated diffusion down a concentration gradient. Antiporters transport two or more species in opposite directions, whereas symporters are able to carry two or more species together in the same direction. In both cases, these reactions are coupled only to chemiosmotic energy. The largest known superfamily of secondary transporters is the Major Facilitator Superfamily (MFS), which is ubiquitously distributed in the organisms of all phyla (Saier, 2000: Reddy *et al.*, 2012).

Finally, group translocators include the phosphoenolpyruvate:sugar phosphotransferase systems (PTS). These systems modify their incoming substrate, e.g. glucose, after a series of phosphorylation events starting with phosphoenolpyruvate (PEP) as phosphoryl donor and ending at the sugar as acceptor. Interestingly, PTS systems are only found in prokaryotes (Deutscher *et al.*, 2006; Reizer *et al.*, 1993).

1.3.2   Transport systems in prokaryotes

The particular importance of transport systems for the organism is reflected in their relatively high abundance in prokaryotes. Large-scale genomic analyses of 201 bacterial and archaeal species revealed that in prokaryotes 3 - 16% of all ORFs code for membrane transport proteins (Ren and Paulsen, 2007). However, it has to be noted that, in this study, only proteins possessing actual transmembrane domains are included. Since transport systems do in many cases rely on components with substrate binding or energy coupling functions which do not have transmembrane domains, it appears obvious that the overall number of transport-dedicated proteins is even higher. Interestingly, the percentage of transport systems within one group of bacteria can be quite diverse. This might be due to the differential knowledge about particular transport systems among the bacteria or archaea. Moreover, the amount and also the composition of transporters in a species strongly depend on its lifestyle. While obligate intracellular pathogens tend to encode rather few types of transport systems due to their stable environment, plant- and soil-associated organisms are in need of a variety of transporters to be able to adapt to changing conditions. For example, the soil-bacterium *Bacillus subtilis* possesses 423 total

transport proteins which account for 10.3% of its genome. In contrast, *Leptospira interrogans*, a parasitic pathogenic spirochaete devotes with 147 transmembrane proteins only 3.1% of its genome to transport. *Mycoplasma* species have about 10% of their genome coding for transport proteins (Ren and Paulsen, 2007). Although they have undergone reductive evolution, and the overall number of transporters appears to be comparatively low, these organisms strongly depend on efficient transport systems for the import of the multitude of metabolites that cannot be synthesized by the cells themselves. Therefore, the high percentage of transporters in minimal pathogenic organisms like *M. pneumoniae*, originates from their lack of biosynthetic pathways which makes them constantly reliable on extensive, external nutrient supply. In contrast, the high percentage of transporters in *B. subtilis* arises from the diversity of transported metabolites that might be necessary under specific conditions.

1.3.3   Transport systems in *M. pneumoniae*

Most of the transport systems in *M. pneumoniae* have been annotated only by sequence similarity (Himmelreich *et al.*, 1996). Due to their transmembrane domains, transporters are experimentally challenging. The most intensely studied and therefore best described transporters are import systems for carbon sources. As mentioned above, *M. pneumoniae* can utilize glucose, fructose, mannose, GPC and glycerol (Halbedel *et al.*, 2007). Like in other bacteria, glucose is actively taken up via the phosphoenolpyruvate:glucose phosphotransferase system (PTS). This is also true for fructose and mannose which are both assumed to be transported by the substrate specific protein FruA which represents the EIIABC component of the PTS. Glycerol is taken up by facilitated diffusion using an aquaglyceroporin, GlpF. Since the glycerol metabolism is the basis for hydrogen peroxide production, it seems astonishing that the uptake of its direct precursor is mediated by such comparably inefficient way of import. Indeed, a highly pathogenic form of *M. mycoides*, which produces high rates of H_2O_2 with glycerol, encodes a highly efficient ABC-transport system for glycerol in addition to GlpF (Vilei and Frey, 2001). Recently, it could be shown that GPC is imported by means of a permease, GlpU, which belongs to the major facilitator superfamily. GlpU is accompanied by two accessory proteins, MPN076 and MPN077, which have parallel functions, but with MPN076 being the more prominent one (Großhennig *et al.*, 2013). The phospholipid product GPC is an abundant carbon source in the lung tissue. After its uptake into the Mycoplasma cell, it is converted to G3P by the glycerophosphodiester-phosphodiesterase GlpQ. Since G3P is the substrate for GlpD which produces

the pathogenicity factor H_2O_2, the GPC metabolism is also linked to virulence (Schmidl *et al.*, 2011). Indeed, *M. pneumoniae* strains lacking the genes for GlpQ or the corresponding transporter GlpU show strongly decreased virulence. This example illustrates that, depending on the nature of their substrates, transporters can definitely be crucial for establishment of virulence.

1.3.4 Transport systems in virulence

In addition to the above mentioned indispensability of transporters in nutrient uptake and therefore in assuring the bacterial survival and multiplication, there are other aspects of pathogenicity which involve the function of certain transporters.

Export systems are typically involved in virulence when it comes to the transfer of toxins, hemolysins and antimicrobial or antibiotic substances from the cell into the environment. In gram-negative bacteria, this is mediated by the Type I – Type VI Secretion Systems. To translocate effector molecules and toxins, pathogenic bacteria like *Legionella pneumophila*, *Helicobacter pylori, Brucella* spp. or *Bordetella pertussis* predominantly use the Type IV Secretion System (T4SS) (Vogel *et al.*, 1998; Censini *et al.*, 1997; Boschiroli *et al.*, 2002; Burns, 2003). In gram-positive bacteria, protein secretion is usually mediated by the Sec (secretory) pathway. For that, the desired proteins are tagged with an N-terminal signal peptide which is recognized by the Sec machinery. It has been shown that the exotoxins of *Staphylococcus aureus*, the *Listeria monocytogenes* pore-forming cytolysin listerilolysin O or cytotoxins of *Bacillus cereus* are secreted via the Sec pathway (Fagerlund *et al.*, 2010; Woolridge, 2009). Moreover, antimicrobial peptides can be exported by specific ABC transporters (Wooldridge, 2009).

Another striking and very intensely studied implication of transporters in virulence is the uptake of iron. Since iron is an essential element for growth in nearly all bacterial species, but difficult to access inside the host, pathogenic bacteria evolved efficient iron-acquisition systems. For this, pathogenic bacteria may secrete toxins under iron-limiting conditions that damage the host cells in order to make the intracellular iron sources accessible. Characteristic toxins whose expression is regulated in response to the availability of iron are the diphtheria toxin in *Corynebacterium diphtheriae*, and the Shiga toxins of *Shigella* or *E.coli* strains (Schmitt and Holmes, 1991; Calderwood and Mekalanos, 1987).

1.4   Hemolytic and hemoxidative activities in bacteria

1.4.1   Hemolysis and hemoxidation

The bacterial struggle for iron is often accompanied by hemolysis. Hemolysis describes a process in which red blood cells (RBCs) are destroyed due to the action of lytic compounds. This is a convenient effect, since the bacteria gain access to a lot of nutrients which are released from the lysed erythrocyte. Most importantly, they gain access to iron which is bound inside the hemoglobin molecules of the red blood cell (**Fig. 1.2 A**).

A

Heme   Hemoglobin   Red blood cells

B

Fig. 1.2. Illustration of heme as part of hemoglobin which then again is part of a red blood cell (A) and Types of bacterial hemolysis (B). A. Hemoglobin (1GZX) is made up of four subunits, each of which contains a polypeptide chain called globin and a heme group. Red blood cells (erythrocytes) consist of about 270 million hemoglobin molecules which makes circa 97% (w/w) dry weight (Weed *et al.*, 1963). (modified from www.chem.ucla.edu, www.rcsb.org and Toumey, 2011) **B.** Blood agar plate with alpha-hemolytic (α), beta-hemolytic (β) and non-hemolytic (γ) streptococci recorded with transmission light (www.microbelibrary.org.)

Bacterial hemolysis can be divided into three major types, which are illustrated in **Fig. 1.2 B.**: alpha-, beta-, and gamma hemolysis. Bacteria which exhibit gamma hemolysis do not have hemolytic activity. In contrast, beta-hemolysis describes the process of complete lysis of blood cells leading to a clear yellow halo around the colonies in which no intact red blood cells containing hemoglobin are present anymore. Finally, alpha hemolysis is a process in which the red blood cells are not destroyed, but the hemoglobin is modified. One possibility is, that the Fe^{2+} bound in the middle of the tetrapyrrole ring in

the heme molecule is oxidized to Fe^{3+} resulting in a different form of hemoglobin: methemoglobin (metHb). This process of hemoxidation leads to a brownish discoloration of the blood around the bacterial colonies on the plate. *In vivo*, oxidized hemoglobin has a reduced binding affinity towards oxygen and also the release of oxygen is hindered. However, this process is reversible. Similar to oxididation, hemoglobin can also be sulfenylated resulting in so called sulfhemoglobin (sulfHb), which appears as a greenish-brownish discoloration of blood (Chatfield and La Mar, 1992). As a result, hemoglobin loses its ability to bind oxygen in a non-reversible manner. Both, the formation of sulfHb and metHb are forms of alpha hemolysis. For simplification, the term "hemoxidation" will in this work be referred to as any kind of alpha-hemolysis, whereas the term "hemolysis" is only used for beta-hemolysis.

1.4.2 Hemolysins and hemolytic toxins

Beta-hemolysis is usually induced by the action of proteins which destroy the phospholipid bilayer of the RBC's membrane. This can be mediated by (i) enzymes like phospholipases which hydrolyze the membrane phospholipids, (ii) toxins which exhibit a detergent-like (surfactant) activity that results in membrane solubilization and (or) partial insertion into the hydrophobic regions of target membranes, or (iii) pore-forming toxins which, after their secretion, build oligomers inserting into eukaryotic cell membranes, thereby causing their leakage (Titball, 1993; Braun and Focareta, 1991). The hemolytic actions of phospholipases A and C have been described for several pathogenic bacteria like *Borrelia*, *Staphyloccocci*, *Clostridia* or *Listeria* (Williams and Austin, 1992; Smith and Price, 1938; van Heyningen, 1941; Geofflroy *et al*., 1991). Examples for phospholipases C in gram-positive bacteria are phosphatidylinositol phospholipases C, e.g. PLC-A from *L. monocytogenes*, sphingomyelinases as the beta-hemolysin from *Staphylococcus aureus* or Zinc-metalloenzymes like the alpha-toxin of *Clostridium perfringens*. These enzymes have different preferences concerning their targeted phospholipid: Zinc-dependent phosphilopases C preferentially degrade phosphatidylcholine, whereas sphingomyelinases prefer sphingomyelin (Nakamura *et al*., 1988; Maheswaran and Lindorfer, 1967; Titball, 1993).

The most intensely investigated and best described hemolysins are the numerous pore-forming toxins. Important examples from gram-negative bacteria are the α-hemolysin of *E. coli*, which is encoded by the gene *hlyA,* and the similar hemolysin CyaA of *Bordetella pertussis* (Cavalieri *et al*., 1984; Hackett *et*

al., 1994). HlyA from *E. coli* is a 107 kDa protein that induces hemolysis by creating about 2-nm-wide pores in the erythrocyte membrane. Those pores are thought to increase the permeability thereby producing cell swelling, which ends up in RBC rupture (Bhakdi *et al.*, 1986).

The α-toxin of *S. aureus* is probably the most famous hemolysin from gram-positive bacteria. It is a small β-barrel pore-forming toxin which is secreted as a monomer, but oligomerizes into a heptameric structure when binding the host-cell membrane. This binding leads to formation of a 1-3 nm membrane-perforating barrel pore that allows the efflux of Ca^{2+}, K^+, ATP and low-molecular weight molecules with a maximum size of 4 kDa (Bhakdi and Tranum-Jensen, 1991). Another group of pore-forming toxins which is present in several genera of gram-positive bacteria are the thiol-activated hemolysins. These include the listeriolysin O (*L. monocytogenes*), the pneumolysin (*Streptococcus pneumoniae*), the perfringolysin (*C. perfringens*) and the streptolysin O from *Streptococcus pyogenes*. All these toxins are rapidly inactivated in the presence of oxygen but can be activated again after addition of sulfhydryl compunds. Streptolysin O has been shown to insert into cholesterol-containing membranes, where up to 100 monomers aggregate and assemble as a superstructure forming a transmembrane channel with up to 7.5 nm width (Bhakdi *et al.*, 1985).

In contrast to the hemolytic toxins evoking beta-hemolysis, alpha-hemolysis is not induced by proteins. Secretion of hydrogen peroxide or hydrogen sulfide is the main cause for bacterial oxidation or sulfenylation of hemoglobin. Alpha-hemolysis following production of hydrogen peroxide is used for typing of bacterial species and typically seen in Streptococci like *S. pneumoniae* and *S. mutans* (Duane *et al.*, 1993; Hamada and Slade, 1981).

1.4.3 Hydrogen sulfide

In the recent years, hemoglobin alteration and hemolysis as result of hydrogen sulfide production has been studied in several oral pathogens. Among them, the "cystalysin" of *Treponema denticola* and its hemoxidative and hemolytic activity have been elaborately studied. Cystalysin is a 46 kDa, pyridoxal-5-phosphate (PLP) dependent L-cysteine desulfhydrase, which is homologous to aminotransferases and is able to produce ammonia, pyruvate and H_2S from L-cysteine (Chu *et al.*, 1995; Chu *et al.*, 1997). Heterologous expression of cystalysin in *E. coli* lead to high hemoxidation and hemolysis rates which became apparent in clear halos around the respective *E. coli* colonies (Chu *et al.*, 1995). Detailed investigation of human erythrocytes incubated with the purified enzyme revealed strong

methemoglobin and sulfhemoglobin formation which was attributed to the production of hydrogen sulfide (Kurzban *et al.*, 1999). The production of hydrogen sulfide is a prevalent feature of oral pathogenic bacteria and responsible for periodontal diseases and oral malodor (Tonzetich, 1971). The genera *Fusobacterium, Prevotella* and *Porphyromonas* are amongst the predominant H_2S producers (Persson *et al.*, 1990). For H_2S formation, these bacteria possess PLP dependent βC-S lyases which catalyze the α,β-elimination of L-cysteine. Hemolytic activity correlating with H_2S production has not only been demonstrated for *T. denticola*, but also for *Fusobacterium nucleatum*, *Streptococcus anginosus*, *Streptococcus intermedius* and *Prevotella intermedia* (Fukamachi *et al.*, 2002; Yoshida *et al.*, 2002; Ito *et al.*, 2008; Yano *et al.*, 2009).

1.5   This work

In this work, two potential virulence determinants should be examined and evaluated for their possible roles in virulence and hemolytic activity of *M. pneumoniae.*

Transport systems are necessary for survival of bacteria, especially for genome-reduced pathogens with strict host-specificity. Since not much is known about transport systems in *M. pneumoniae* - except for some sugar uptake transporters -, the identity and function of as many transport systems as possible should be elucidated. For that, (i) mutants for non-essential transporters should be isolated and characterized, and (ii) transport systems of *M. pneumonie* should be expressed heterologously in *B. subtilis* to assess their function in a bacterium that is more convenient for laboratory work. In order to estimate the transporters' importance for host colonization and cell lysis, the respective bacterial strains should be tested in growth assays and in infection studies using HeLa cells and blood culture.

Hemolysis is an important aspect of bacterial pathogenicity which can have severe effects in the human host. Therefore, the hemolytic and hemoxidative activity of *M. pneumoniae* was planned to be studied in detail as well. For a long time, the major pathogenicity factor of *M. pneumoniae*, H_2O_2, has been assumed to be the hemolysin of the organism. However, since also H_2S has been proven to play a role in hemolysis of other bacterial pathogens, *M. pneumoniae* also was to be tested for production of additional hemolytic compounds, like hydrogen sulfide. Also, their importance in the overall virulence of the human pathogen should be evaluated.

2. MATERIAL AND METHODS

2.1 Material

Chemicals, utilities, equipment, commercially available systems as well as antibodies, enzymes and oligonucleotides are listed with their manufacturers in the Appendix.

2.1.1 Bacterial strains and plasmids

The bacterial strains and plasmids used in this work are listed in the Appendix.

2.1.2 Media

Buffers, solutions and media were prepared with deionized water and autoclaved for 20 min at 121°C and 2 bar. Thermally labile substances were solved and filtered sterile. All data refer to water, other solvents are mentioned. For preparation of plates, 18 g/l agar were added to LB-medium and 8 g/l agar were added to MP-Medium while phenol red was left out (Großhennig, 2011).

Media for bacteria and facultative supplements

MP-Medium (400ml)		7.35 g	PPLO Broth
Modified Hayflick medium		11.92 g	HEPES
(Chanock *et al.*, 1962)		2 ml	Phenol red (0.5%)
		14 ml	NaOH (2 N)
		ad 400 ml	deionized H_2O
			pH 7,6-7,8
	autoclave, then addition of:		
		100 ml	Horse serum (heat inactivated)
		5 ml	Penicillin (100,000 U/ml)
		10 ml	Carbon sources (50%)
	+/-	260 µl	Gentamycin (160 mg/ml)

31

LB- Medium (1 l)	10 g	Trypton
	5 g	Yeast extract
	10 g	NaCl
	ad 1 l	deionized H_2O
5 x C-salts (1l)	20 g	KH_2PO_4
	80 g	K_2HPO_4 x 3 H_2O
	16.5 g	$(NH_4)_2SO_4$
	ad 1 l	deionized H_2O
III'-salts	0.232 g	$MnSO_4$ x 4 H_2O
	12.3 g	$MgSO_4$ x 7 H_2O
CSE-glucose medium (100 ml)	20 ml	5 x C-salts
	1 ml	Tryptophan (5 mg/ml)
	1 ml	CAF (2.2 mg/ml)
	1 ml	III'-salts
	2 ml	Potassium glutamate (40%)
	2 ml	Sodium succinate (30%)
	1 ml	Glucose (50%)
	ad 100 ml	deionized H_2O
C-minimal medium (100 ml)	20 ml	5 x C-salts
	1 ml	Tryptophan (5 mg/ml)
	1 ml	CAF (2.2 mg/ml)
	1 ml	III'-salts
+/-	1 ml	Glycerol (50%)
	ad 100 ml	deionized H_2O
SP-medium (1 l)	8 g	Nutrient Broth
	0.25 g	$MgSO_4$ x 7 H_2O
	1 g	KCl
	ad 1 l	deionized H_2O

autoclave, then addition of:

	1 ml	CaCl$_2$ (0.5 M)
	1 ml	MnCl$_2$ (10 mM)
	2 ml	CAF (2.2 mg/ml)

10 x MN-medium (1 l)	136 g	K$_2$HPO$_4$ x 3 H$_2$O
	60 g	KH$_2$PO$_4$
	10 g	Sodium citrate x 2 H$_2$O
	ad 1 l	deionized H$_2$O

MNGE (10 ml)	1 ml	10 x MN-medium
	400 µl	Glucose (50%)
	50 µl	Potassium glutamate (40%)
	50 µl	Ammonium iron citrate (2.2 mg/ml)
	100 µl	Tryptophan (5 mg/ml)
	30 µl	MgSO$_4$ (1 M)
+ / -	100 µl	Casamino acids (10%)

X-Gal	Stock solution: 40 mg/ml X-Gal in DMF
	Working concentration in media: 40 µg/ml

IPTG	Stock solution: 1 M in H$_2$O
	Working concentration in media: 1 mM

Antibiotics

All used antibiotics were prepared as 1,000 fold concentrated stock solutions. Ampicillin, gentamycin, kanamycin, lincomycin and tetracycline were dissolved in water; chloramphenicol and erythromycin were dissolved in 70% ethanol, filtered sterile and stored at -20°C. Penicillin was dissolved in water, filtered sterile and stored at 4°C. After the media had cooled to about 50°C, antibiotics were added in respective concentrations.

Selection concentration for *E. coli*:	Ampicillin	100 µg/ml
	Kanamycin	50 µg/ml

Selection concentration for *M. pneumoniae*:   Gentamycin   80 µg/ml

                                                Penicillin   1000 U/ml

                                                Tetracycline   2 µg/ml

Selection concentration for *B. subtilis:*   Chloramphenicol   100 µg/ml

                                                Erythromycin   2 µg/ml

                                                Kanamycin   10 µg/ml

                                                Lincomycin   25 µg/ml

2.2   Methods

2.2.1 Standard methods

General methods that were described previously and used in this work are listed in **Tab. 2.3**.

Tab. 2.3 Standard methods

Method	Reference
Measurement of optical density	Sambrook *et al.,* 1989
Precipitation of nucleic acids	Sambrook *et al.,* 1989
DNA gel electrophoresis	Sambrook *et al.,* 1989
Ethidium bromide staining of DNA	Sambrook *et al.,* 1989
Ligation of DNA fragments	Sambrook *et al.,* 1989
Plasmid isolation from *E. coli*	Sambrook *et al.,* 1989
Chain terminator sequencing	Sanger *et al.*, 1977
Gel electrophoresis of proteins	Laemmli, 1970
Determination of protein amounts	Bradford, 1976

2.2.2 Cultivation techniques

Cultivation of *E. coli* and *B. subtilis*

Unless stated otherwise, *E. coli* was grown in LB-Medium at 37°C and 200-220 rpm in test tubes. *B. subtilis* was grown in LB medium, CSE-glucose medium, C-glycerol medium or MNGE medium at 30°C or 37°C and 200 rpm in test tubes or flasks. Inoculation was done with single colonies from fresh plates.

Cultivation of *M. pneumoniae*

1 ml of *M. pneumoniae* culture was added to 100 ml MP-Medium. The cultures were grown in 150 cm^2 tissue culture flasks for 4 days at 37°C. When more cell material was needed, 200 ml MP-medium were inoculated with 2 ml of the preculture and incubated in a 300 cm^2 tissue culture flask at 37°C.

Cultivation of human cervix carcinoma cell lines (HeLa) and determination of cell count

HeLa cells were grown in Dulbecco's Modified Eagle Medium (DMEM) supplemented with 10% FCS at 37°C and 5% CO_2 for 3-4 days in 25 cm^2 or 75 cm^2 culture flasks. The supernatant of a confluent grown culture was removed with a sterile serological single-use pipet. Depending on the size of the flask and the cell density, 1-5 ml fresh DMEM were added and the adherent cells were scraped off with a cell scraper.

For passaging of HeLa cells, the scraped cells were separated by gently pipetting up and down and 100 µl – 1 ml were used for inoculation of new flasks containing 5 – 15 ml DMEM. Again, the cells were grown for 3-4 days at 37°C and 5% CO_2.

For subsequent determination of cell count, the previously harvested cells were transferred to a 50 ml Falcon tube und pelleted by centrifugation at 1,400 rpm and 5 min. Afterwards, the supernatant was discarded and, depending on the size of the pellet, the HeLa cells were resuspended in 2-4 ml DMEM. For cell counting, a Neubauer chamber (0.1 mm depth, 0.0025 mm^2 surface) was used. 10 µl of the cell suspension were mixed with 10 µl trypan blue and 10 µl of the mixture were pipetted between chamber and cover slip. Living cells were counted in 4 big squares (each with 16 small squares). The number of cells per ml was calculated by multiplying the average number of cells per big square by the dilution factor 2 and the volume factor 1×10^4 (Großhennig, 2011).

Storage of bacteria

E. coli strains were kept on LB medium agar plates for several weeks at 4°C. For long-term storage at -70°C, glycerol cultures were prepared by adding 300 µl of 50% glycerol to 100 µl of a fresh overnight culture in a screw-cap tube.

B. subtilis was stored on SP agar plates at room temperature or as cryo-cultures in DMSO at -70°C. For that, 900 µl of an overnight culture was mixed with 100 µl DMSO and subsequently frozen.

For long-term storage of *Mycoplasma pneumoniae* strains, the cells of a freshly grown 100 ml culture were harvested by scraping in 10 ml fresh MP medium. The cells were transferred into a falcon tube and stored without any further supplement at -70°C.

Growth experiments with *B. subtilis*

Liquid medium

The desired *B. subtilis* strains were grown over day in 4 ml LB medium (supplemented with antibiotics where needed) at 30°C. 150 ml CSE medium were inoculated with 100 µl or 50 µl of the over day cultures and shaken over night at 30°C or 37°C, respectively. The cultures were harvested by centrifugation (10 min; 4,000 rpm, room temperature), the pellets were washed twice in 1x C-salts, resuspended and the OD_{600} was determined. For monitoring the growth in minimal medium, 10 ml C-minimal medium (supplemented with glucose or glycerol) were inoculated with the preculture to an OD_{600} of 0.1 and incubated shaking at 37°C. The growth rate of the culture was determined by measuring its OD once per hour.

Serial drop dilution plate assay

Overnight cultures of the strains to be tested were prepared in 4 ml LB-medium. The next day, the overnight cultures were transferred into a falcon tube and centrifuged for 10 min at 4,000 rpm. The pellets were washed twice and resuspended in 5 ml C-minimal medium. The OD_{600} was measured and an OD = 1 was adjusted with C-minimal medium. Serial tenfold dilutions (in C-medium) were prepared and 5 µl of each dilution were dropped in a row on selective plates. The assay was incubated for 1-2 days at 37°C.

Determination of wet weight of *M. pneumoniae* cultures

The supernatant of a 100 ml culture was decanted and the adhering cells were washed twice with 1xPBS buffer pH 7.4. Subsequently, the cells were scraped off with a cell scraper in 1.5 ml 1 x

phosphate buffered saline (PBS). The cells were transferred to a previously weighed reaction tube and centrifuged (13,000 rpm, 4°C). The supernatant was removed completely and the weight of the pellet was determined using a special accuracy weighing machine. The wet weight resulted from the weight of the reaction tube with the harvested cells minus its weight without cells (Großhennig, 2011).

PBS (10 x)		
	2 g	KCl
	2 g	KH_2PO_4
	14.24 g	Na_2HPO_4 x 2 H_2O
	80 g	NaCl
	ad 1 l	dH_2O
	adjust pH 7.4 or 6.5	

2.2.3 Transformation of bacteria

Transformation of *E. coli* cells

Preparation of competent E. coli *cells*
20 ml LB medium were inoculated with a single colony of the *E. coli* strain grown on a LB agar plate. The culture was incubated for 20 h at 28°C. 250 ml SOB medium in a 2 l baffled flask were inoculated with 6 ml of this preculture and incubated overnight at 18°C and 200-250 rpm until the cells reached an OD_{600} of 0.5 – 0.9. Then, the culture was placed on ice for 10 min and subsequently centrifuged at 5,000 rpm at 4°C for 10 min. The pellet was resuspended in 80 ml precooled TB buffer and incubated on ice for 10 min. The cells were centrifuged again at 4,000 rpm and 4°C for 10 min and the pellet was resuspended in 20 ml TB buffer. While gently rotating the tube, 1.4 ml DMSO were added to final concentration of 7%. The cells were shortly incubated on ice, divided in 200 µl aliquots and rapidly frozen in liquid nitrogen. The competent cells were stored at -80°C until further use (modified from Rempeters, 2011).

TB-buffer (500 ml, pH 6.7)		
	1.51 g	PIPES
	1.1 g	$CaCl_2$ x H_2O
	ad 472.5 ml	deionized H_2O
	autoclave, then addition of:	
	27.5 ml	$MnCl_2$ (1 M, sterile)

SOB medium (1 l)	20 g	Tryptone
	5 g	Yeast extract
	0.584 g	NaCl
	0.188 g	KCl
	ad 1 l	deionized H_2O

autoclave, then addition of:

	10 ml	$MgCl_2$ (1 M, sterile)
	10 ml	$MgSO_4$ (1 M, sterile)

Transformation of E. coli *cells*

10-100 ng of DNA were added to an aliquot of 200 µl competent *E. coli* cells. The sample was incubated on ice for 30 min, followed by a heat shock for 90 sec at 42°C and incubation for 5 min on ice again. After addition of 500 µl LB-medium, the cells were shaken for 1 h at 37°C and 200 rpm. For each sample, 100 µl as well as the centrifuged and resuspended "rest" were plated on selective media. The plates were incubated over night at 37°C (adapted from Großhennig, 2011).

Transformation of *B. subtilis* cells

Preparation of competent B. subtilis *cells*

10 ml MNGE medium containing casamino acids were inoculated with a *B. subtilis* overnight culture to an OD_{600} of 0.1. The culture was incubated at 37°C and 200 rpm. At an OD_{600} of 1.3, one volume pre-warmed MNGE medium without casamino acids was added to the culture. After an additional hour of incubation at 37°C and 200 rpm the cells were competent.

Transformation of competent B. subtilis *cells*

400 µl competent cells were pipetted onto 0.1 to 1 µg DNA in a microcentrifuge tube and incubated at 37°C and 200 rpm for 0.5 h. 100 µl expression solution was added to the cells and incubation was continued for 1 h. Then the cells were spread on LB agar plates containing the appropriate antibiotics for selection (Rempeters, 2011).

Expression mix (1 ml)	500 µl	Yeast extract (5%)
	250 µl	Casamino acids (10%)
	250 µl	dH_2O
	50 µl	Tryptophan (5 mg/ml)

Transformation of *M. pneumoniae* by electroporation

The cells of a four days grown 100 ml *M. pneumoniae* culture were washed twice with electroporation buffer (8 mM HEPES, 272 mM Sucrose; pH 7.4) and scraped off in 1.5 ml of this buffer. The cells were centrifuged for 5 min at 10,000 rpm and 4°C, and the pellet was resuspended in 150 µl of ice cold electroporation buffer. For an electroporation sample, 50 µl *M. pneumoniae* cells, 5-10 µg Plasmid-DNA and 1 µl yeast tRNA were mixed and filled up with electroporation buffer to 80 µl. The samples were transferred to electroporation cuvettes (0.2 cm) and incubated 15 min on ice. Electroporation was performed at 2.5 kV, 25 µF and 100 Ω. Subsequent to electroporation, the cells were incubated for 15 min on ice again, followed by 2 h of incubation in 10 ml MP-Medium at 37°C. Afterwards, the cells were spun down for 5 min at 4,000 rpm and RT. In order to separate the cells, the pellet was resuspended in 1 ml MP-medium using a syringe with needle (0.55 mm diameter) and dilution series were prepared. Of each dilution ($10^{-1} - 10^{-7}$), 200 µl were plated on MP-plates containing gentamycin and tetracycline. The plates were incubated 7-14 days at 37°C. Clones were picked with sterile tooth picks and inoculated in 1 ml MP-Medium (Großhennig, 2011).

Electroporation buffer (1l)	1.91 g	HEPES
	93.11 g	Sucrose
	ad 1 l	dH$_2$O
	adjust pH 7.4	

2.2.4 Bacterial adenylate cyclase two hybrid (BACTH)

The bacterial adenylate cyclase two hybrid system is a method for detection of protein-protein-interactions *in vivo*. It is based on the reconstruction of the *Bordetella pertussis* adenylate cyclase in *E. coli*. This enzyme consists of two domains (T25 and T18) and is only active when these domains are in close proximity. For investigation of protein-protein-interactions, the proteins to be tested are fused to the T25 or T18 domain of the *B. pertussis* adenylate cyclase, respectively. In case of interaction of the two proteins, the domains get close to each other and are able to form the active enzyme adenylate cyclase which synthesizes the central transcription regulator cAMP. This molecule then binds the catabolite activator protein CAP which is responsible for activation of catabolic operons like the *lac*-operon.

For detection of *in vivo-* interactions, the proteins to be tested were fused N-terminally and C-terminally to the domains of the adenylate cyclase using a set of plasmids. For construction of fusions, four distinct plasmids were used, respectively: two "low-copy" vectors for expression of T25-fusions (pKT25 and p25-N) and two "high-copy" vectors for expression of T18-fusions (pUT18 and pUT18C). Genes for transport- and lipoproteins were cloned into the low-copy or high-copy vectors using the methods described above and the *E. coli* strain XL-1 blue. For the interaction experiment, the *E. coli* strain BTH101, which lacks the adenylate cyclase, was co-transformed with one high-copy and one low-copy plasmid. The transformation was performed in microtiter plates. For this purpose, 30 µl BTH101 cells were mixed with 1 µl of each plasmid and incubated on ice for 30 min, followed by a heat shock for 90 sec at 42°C. As positive control, the plasmids pKT25-zip and pUT18C-zip that form a functional leucin zipper were used. Afterwards, 120 µl LB medium were added to the cells and the plate was incubated at 30°C for 2 h. Finally, 5 µl of the respective cell suspensions were dropped on LB plates supplemented with ampicillin, kanamycin, IPTG and X-Gal. The transformation plates were incubated for 2 days at 30°C.

Protein-protein-interactions were detected visually and monitored by scanning. In case of interaction blue colonies should be formed due to production of cAMP by the functional adenylate cyclase and final activation of β-galactosidase expression. The enzyme β-galactosidase is able to convert the colorless compound X-Gal to a blue dye leading to growth of blue colonies (adapted from Großhennig, 2011).

2.2.5 Preparation and analysis of DNA

Isolation of plasmid DNA by modified Alkali / SDS lysis

Plasmid isolation was performed by means of alkaline lysis followed by chromatographic purification. For that, 4 ml of an overnight culture (and accordingly 10 ml for preparation of "low-copy" plasmids) were used. The isolation was done using the NucleoSpin˚ Plasmid Kit (MACHEREY-NAGEL) according to manufacturer's manual (Großhennig, 2011).

Isolation of *M. pneumoniae* chromosomal DNA

The supernatant of 100 ml *M. pneumoniae* culture that had been grown for four days was poured away, the cells were washed twice with 1xPBS buffer (pH 6.5) and were scraped off in 1.5 ml of this

buffer. The suspension was centrifuged for 1 min at 13,000 rpm and 4°C. The pellet was resuspended in 540 µl Lysis buffer and 10 µl RNaseA (20 mg/ml) were added. Afterwards, the sample was incubated for at least 25 min at 37°C and chromosomal DNA was isolated via the DNeasy˚ Blood and Tissue Kit (50) (QIAGEN) according to manufacturer's manuals (Großhennig, 2011).

Lysis buffer	20 mM	Tris pH 8.0
	2 mM	EDTA pH 8.0
	50 mg	Lysozyme
	ad 2.5 ml	dH_2O

Sequencing of DNA

Sequencing was done at the Göttingen Genomics Laboratory (G_2L), Seqlab (Göttingen) or LGC Genomics (Berlin) using the chain termination sequencing technique by Sanger.

Restriction and ligation of DNA

Restriction with the desired endonucleases (FERMENTAS) was performed using buffers as recommended by the manufacturer. The amount of enzyme conformed to the amount of DNA and the sample volume. Restriction samples were incubated at 37°C overnight or for 1h in case of use of Fast Digest™ enzymes. Ligation of DNA fragments was carried out with T4-DNA-ligase (FERMENTAS) and the appropriate manufacturer's buffer. The reaction sample was set up with 10-100 ng of vector DNA and 2-5 fold excess of insert DNA, and incubated for at least 1h at room temperature (Großhennig, 2011).

Dephosphorylation of DNA

In order to dephosphorylate the 5'end of DNA fragments, 1 µl of FastAP™ Thermosensitive Alkaline Phosphatase (FERMENTAS) was added to a mixture containing a final concentration of 3-10 ng/µl restricted DNA. The sample was incubated for 30 min at 37°C and subsequently purified using the QIAquick PCR purification Kit (QIAGEN) (Großhennig, 2011).

Polymerase chain reaction (PCR)

Polymerase chain reactions were performed using chromosomal DNA or plasmid DNA as templates. The samples were mixed and the reactions were set up in a thermocycler using the respective programs.

Reaction set-up for *Taq* polymerase (50 µl)

1 µl	Primer (fwd) (20 pmol)
1 µl	Primer (rev) (20 pmol)
1 µl	Template DNA (approx. 100 ng)
5 µl	10x *Taq* polymerase buffer
1 µl	*Taq* polymerase (5 U/µl)
2 µl	dNTPs (12.5 µmol/ml)
39 µl	dH$_2$O

Reaction	Temperature	Duration	Number of cycles
Initial denaturation	95°C	5 min	1
Denaturation	95°C	1 min	
Annealing	52°C	1 min	30/50
Elongation	72°C	1-2 min / 1 kb	
Final elongation	72°C	10 min	1
Cool down	16°C	∞	1

In case of screens for *M. pneumoniae* transposon mutants, 50 cycles were run.

Reaction set-up for *Phusion*® DNA polymerase (50 µl)

2 µl	Primer (fwd) (20 pmol)
2 µl	Primer (rev) (20 pmol)
0.5 µl	Template DNA (approx. 100 ng)
10 µl	5 x *Phusion* HF buffer
0.5 µl	*Phusion*® DNA polymerase (2 U/µl)
2 µl	dNTPs (12.5 µmol/ml)
33 µl	dH$_2$O

Reaction	Temperature	Duration	Number of cycles
Initial denaturation	98°C	30 s	1
Denaturation	98°C	10 s	
Annealing	52°C	30 s	30
Elongation	72°C	30 s / 1 kb	
Final elongation	72°C	10 min	1
Cool down	16°C	∞	1

Reaction set-up for *ACCUZYME*™-Polymerase (50 μl)

2 μl   Primer (fwd) (20 pmol)

2 μl   Primer (rev) (20 pmol)

2 μl   Template DNA (approx. 100 ng)

5 μl   10x *ACCU* buffer

1 μl   *ACCUZYME*™ polymerase (2.5 U/μl)

2 μl   dNTPs (12.5 μmol/ml)

36 μl   dH$_2$O

Reaction	Temperature	Duration	Number of cycles
Initial denaturation	95°C	5 min	1
Denaturation	95°C	1 min	
Annealing	52°C	1 min	30
Elongation	72°C	1 min / 1 kb	
Final elongation	72°C	10 min	1
Cool down	16°C	∞	1

Isolation of *M. pneumoniae* transposon mutants

Isolation of transposon insertion mutants was performed by means of the so called haystack method (Halbedel *et al.*, 2006). This strategy is based on an ordered collection of pooled random mutants which can be screened for junctions between the transposon and the gene of interest due to transposon insertion. The transposon mutants are grouped in 64 pools containing 50 clones, respectively. Cells of each pool were used in a PCR to detect the occurrence of products corresponding to junctions between the transporter genes of interest and the mini transposons using the gene-specific oligonucleotides as

described in the appendix (**Tab. 7.1**) and the transposon-specific oligonucleotides SH29 and SH30. From pools that gave a positive signal, colony PCR with the 50 individual mutants was performed. The clones delivering positive PCR signals were isolated and grown in 1 ml liquid MP-medium. Additionally, a dilution series was prepared and plated on solid MP-medium supplemented with gentamycin. Depending on their growth, positive clones were grown to broth passage P3 or P4 before starting further experiments. Each passage was checked for wt contaminations by PCR using the gene-specific primers (adapted from Großhennig, 2011).

Long flanking homology PCR (LFH-PCR)

The *B. subtilis glpF* gene was deleted by the LFH-PCR technique (Wach, 1996). A chloramphenicol resistance cassette was amplified from the pGEM-cat plasmid using the primers cat-fwd (kan) and cat-rev (kan) without terminator to allow expression of downstream genes. Additionally, two fragments of about 1 kb were amplified. One comprised the region upstream of the *glpF* gene and 55 nt of the beginning of the gene (upstream fragment). The other comprised the region downstream of *glpF* including 67 nt of the end of the gene (downstream fragment). The upstream fragment was amplified using the primers SG43 and SG40, the downstream fragment was amplified using the primers SG41 and SG44. The extension of the fragments into the gene ensured that all expression signals of genes up- and downstream of the *glpF-glpK* operon stayed intact. To the 3' end of the upstream fragment and the 5' end of the downstream fragment a 25 nt sequence was added by the primers. This sequence was complementary to the 5' end and the 3' end of the resistance cassette, respectively, and allowed base pairing which is crucial for the joining PCR. In the joining PCR all three purified fragments (150 ng of the up- and downstream fragments and 300 ng of the resistance cassette) were added to one PCR and a single fragment comprising all three fragments was generated. Competent *B. subtilis* cells were transformed with 7,5 µl and 15 µl of the PCR product and selected for chloramphenicol resistance on SP plates.

The clones were subsequently checked for the integrity of the resistance cassette by check PCR using the cat-check primers. The DNA sequence of the flanking regions was verified by sequencing with primers SG43 and SG44 (modified from Rempeters, 2011).

Reaction setup for the LFH PCR:

0.5 µl PhusionTM polymerase (5 U/µl)

2 µl dNTPs (12.5 µmol/ml)

2.2 µl Upstream fragment (150 ng)

3.3 µl Downstream fragment (150 ng)

5.3 µl Resistance cassette (300 ng)

10 µl 5 x Phusion HF buffer

20.8 µl dH$_2$O

during the break of the PCR (see below), addition of:

3 µl Forward primer (30 pmol)

3 µl Reverse primer (30 pmol)

Reaction	Temperature	Duration	Number of cycles
Initial denaturation	98°C	1 min	1
Denaturation	98°C	10 s	
Annealing	53°C	30 s	10
Elongation	72°C	1 min 15 s	
Break	15°C	∞	1
Addition of primers			
Denaturation	98°C	10 s	
Annealing	53°C	30 s	21
Elongation	72 °C	1 min 15 s	
Final elongation	72°C	10 min	1
Final hold	15°C	∞	1

Gel electrophoresis

For analytical and preparative DNA separation, gel electrophoresis was performed with gels containing 1% agarose in 1 x TAE. The samples were mixed with 5 x DNA loading dye and loaded on the gel. A voltage of 120 V was applied until the bromophenol blue band of the loading dye reached the last third of the gel. In case of screening for *M. pneumoniae* mutants, a large gel chamber was used and a voltage of 200 V was applied. After the run, the gels were stained in ethidium bromide solution (10-30 min), briefly destained with H$_2$O and subsequently photographed under UV-light (λ = 254 nm). For estimation of the size of DNA fragments, a marker of *Eco*RI and *Hin*dIII digested λ-DNA was applied

to the gel. In order to dissect DNA from a preparative gel, the fragments were detected at λ = 365 nm and cut out with a scalpel. Purification of DNA from the gel slice was done using the QIAquick gel extraction kit (QIAGEN) according to manufacturer's manuals (Großhennig, 2011).

DNA-Loading Dye (5 x)	5 ml	100% Glycerol
for DNA gel electrophoresis	200 µl	50 x TAE
	10 mg	Bromophenol blue
	10 mg	Xylene cyanol
	4.5 ml	dH_2O
TAE buffer (50 x)	242 g	Tris
	57.1 ml	Acetic acid
	100 ml	0.5 M EDTA pH 8.0
	ad 1l	dH_2O

Southern Blot

M. pneumoniae chromosomal DNA was digested with appropriate enzymes for 1 h at 37°C. Digested DNA as well as a DIG-labeled DNA marker (DNA molecular weight marker III DIG-labeled, 0.12-21.2 kbp ROCHE) were loaded on a 1% agarose gel and run at 120 V. Ethidium bromide staining and detection after the gel run were omitted. The transfer of DNA to a positively charged nylon membrane was conducted via a vacuum blot apparatus (VacuGene™XI). The nylon membrane (ROCHE) was saturated with dH_2O and placed free from air bubbles on the moistened porous carrier plate. The blot was sealed with a plastic mask and the agarose gel was laid on the membrane. A vacuum of 60 mbar was applied to the chamber and the gel was sequentially covered with the following solutions:

1. Depurinization buffer	30 min
2. Denaturing buffer	30 min
3. Neutralization buffer	30 min
4. 20 x SSC	2-3 hours

Before addition of the new buffer, the rest of the previous solution was decanted. After addition of 20 x SSC, a vacuum of 80 mbar was applied for blotting. Following the blotting steps, the DNA was crosslinked to the membrane via UV-light (90 sec) (Großhennig, 2011).

Depurinization buffer	250 mM	HCl

Denaturing buffer	1.5 M	NaCl
	0.5 M	NaOH
	ad 1 l	dH$_2$O

Neutralization buffer	1 M	Tris-HCl pH 7.5
	1.5 M	NaCl
	ad 1 l	dH$_2$O

SSC (20 x)	3 M	NaCl
	0.3 M	Sodium citrate x 2 H$_2$O
	ad 1 l	dH$_2$O
	adjust pH 7.0	

Hybridization of membrane bound DNA with DIG-labeled RNA probes

The nylon membrane carrying the crosslinked DNA was transferred to a hybridization tube containing 25 ml prehybridization buffer and incubated rotating for 1 h at 68°C in a hybridization oven. Subsequently, the prehybridization solution was replaced by the probe (15 μl in 5 ml prehybridization solution) and hybridization occurred overnight at 68°C. The next day, the probe was removed and, in order to remove unspecifically bound RNA probes, the membrane was washed twice for 10 min in buffer PI at RT, followed by two washing steps in buffer PII at 68°C for 15 min. Afterwards, the membrane could be used for detection of DIG-labeled DNA-RNA-hybrids (Großhennig, 2011).

Prehybridization solution	5 x	SSC
(for Southern Blot)	1%	Blocking Solution
	0.1%	N-laurylsarcosine
	0.02%	SDS
	ad 30 ml	dH$_2$O

Buffer PI	2 x	SSC
	0.1%	SDS
	ad 1 l	dH$_2$O

Buffer PII	0.1 x	SSC
	0.1%	SDS
	ad 1 l	dH$_2$O

Detection of DNA-RNA-hybrids

The membrane was incubated for 5 min in 1 x Dig P1 followed by 30 min in 1 x Dig P1 + 1% Blocking solution. Afterwards, detection of hybridized probes was done for 30 min using Anti-Digoxigenin antibodies coupled to Alkaline Phosphatase that were diluted 1:10,000 in 1 x Dig P1 + 1% Blocking solution. Then, the membrane was washed three times 10 min in 1 x Dig P1 followed by 10 min washing in Buffer III. The membrane was placed between two clean plastic foils and moistened with 1 ml Buffer III containing 10 µl CDP* (ROCHE) chemoluminescence substrate for alkaline phosphatase. After a short incubation time, the signals were detected using the ChemoCam imager (INTAS) with exposure times varying from 1 to 30 min (Großhennig, 2011).

Dig P1 buffer (5 x)	0.5 M	Maleic acid
	0.75 M	NaCl
	ad 1 l	dH$_2$O
	adjust pH 7.5	

Blocking solution (10%)	5 g	Blocking reagent
	50 ml	1 x Dig P1

Buffer PIII	100 mM	Tris

Detection buffer for	100 mM	NaCl
RNA-DNA-hybrids	ad 1 l	dH$_2$O
	adjust pH 9.5	

2.2.6 Preparation and analysis of RNA

Isolation and precipitation of *M. pneumoniae* total RNA

Preparation of total RNA from *M. pneumoniae* was done using the RNeasy Midi-Kit 50 (QIAGEN). Except for PBS, all utilized buffers were included in the kit.

The supernatant of a 4 days grown 100 or 200 ml culture was discarded and the cells were washed twice with 1 x PBS. Subsequently, the cells were scraped off in 2 ml RLT buffer + 1% β-mercaptoethanol and transferred to a falcon tube. This step was repeated using 3 ml RLT buffer + 1% β-mercaptoethanol. The suspension was vortexed while 5 ml 100% ethanol were added slowly. The sample was stepwise transferred to a spin column, briefly centrifuged at 4,000 rpm and the flow-through was discarded. That followed washing steps with 4 ml buffer RW1 and two times 2.5 ml buffer RPE containing ethanol. Again, the flow-through was discarded. The column was placed in a new tube and the RNA was eluted using 400 μl RNase-free water.

For precipitation of isolated RNA, 40μl 3.3 M Sodium acetate and 1 ml 96% ethanol were added to 400 μl eluat. Precipitation took place overnight at -20°C (Großhennig, 2011).

Isolation and precipitation of *B. subtilis* total RNA

Cultivation of B. subtilis *cells*

4 mL of LB were inoculated with the respective *B. subtilis* strain and grown shaking over day at 30 °C or 37°C. 50 μl of the over day preculture were used to inoculate 15 mL CSE-glucose medium and grown overnight at 30°C or 37°C with agitation. The next morning, the OD_{600} of the overnight culture was determined and a new 100 ml CSE-glucose culture was inoculated to an OD_{600} of 0.1. The culture was incubated at 37°C until an OD_{600} of 1.0 was reached. For cell harvest, 25 ml of the cell suspension was added to 15 ml frozen Killing buffer in a 50 ml falcon tube and mixed until the buffer was melted. The mixture was centrifuged at 0°C and 4000 rpm for 10 min. The supernatant was discarded and the pellet was shock frozen in liquid nitrogen and stored at -80°C until further use.

Killing buffer	20 mM	Tris-HCl, pH 7.5
	5 mM	$MgCl_2$
	autoclave, then addition of:	
	20 mM	NaN_3

Preparation of RNA from B. subtilis *cells*

The RNA preparation was done using a Mikro-Dismembrator (Sartorius) and the RNeasy Plus kit (QIAGEN). To open the cells, the pellet obtained from the harvesting (see above) was resuspended in 200 μl RNase-free water. The sample was pipetted into the sample box of the Mikro-Dismembrator which had been precooled and filled with liquid nitrogen. The Mikro-Dismembrator was run for 3 min

49

at 1,800 rpm. The sample was resuspended in 2 ml RLT buffer containing 20 µl of β-mercaptoethanol and transferred to 2 ml Eppendorf reaction tubes. The samples were centrifuged for 5 min at 13,000 rpm and 4°C. The following steps were done with the QIAGEN RNeasy Plus kit according to the manufacturer's manuals. The RNA was eluted in 150 µl RNase-free water and stored at -70°C.

DNaseI treatment

Digestion of isolated RNA was performed using DNaseI and the appropriate included buffer (FERMENTAS). The following reaction was prepared in a PCR tube:

1.25 µg / 2.5 µg / 3.75 µg RNA

2.5 µl   10 x Buffer

5 µl   DNaseI

ad 25 µl   dH$_2$O

The mixture was incubated in a PCR cycler for 30 min at 37°C. Afterwards, 2.5 µl EDTA were added and the samples were incubated again in a PCR cycler for 10 min at 65°C.

For radical elimination of DNA from the RNA isolates, the DNaseI treated samples were purified again using the RNeasy Mini Kit 50 (QIAGEN) including the gDNA elimination column according to manufacturer's manual. Subsequently, the eluted RNA was once more precipitated and treated with DNaseI as mentioned above (Großhennig, 2011).

***In vitro* transcription for preparation of RNA probes**

In order to produce DIG-labeled transcripts, PCRs using genomic M129 DNA as template were set up to amplify about 500 bp long, intern fragments of the gene of interest. The reverse primers for these PCRs each contained a signal sequence for the T7-RNA polymerase (ROCHE) at their 5' end.

For *in vitro* transcription, the following components were mixed in a reaction tube:

13 µl   PCR product

2 µl   10x DIG RNA labeling mix (ROCHE)

2 µl   10 x Transcription buffer for T7-RNA polymerase (ROCHE)

2 µl   T7-RNA polymerase (ROCHE)

1 µl   RNase inhibitor (ROCHE)

The samples were incubated for 2 h at 37°C. Afterwards, the *in vitro* transcription was stopped by addition of 1 µl 0.5 M EDTA pH 8.0, and 2.5 µl 4 M LiCl and 75 µl of ice-cold 96% ethanol were added. Precipitation took place overnight at -20°C. The next day, the labeled probes were pelletized by 15 min centrifugation at 13,000 rpm and 4°C. The supernatant was discarded. The pellet was washed with ice-cold ethanol (70%). After repeated centrifugation, the supernatant was discarded and the probes were dried at RT to remove remaining ethanol. Finally, the RNA was dissolved in 100 µl RNase-free H_2O containing 1 µl RNase Inhibitor (ROCHE) (Großhennig, 2011).

Analysis of mRNA amounts using Slot Blots

In order to analyze mRNA amounts, slot blots were used to transfer total RNA of the wild type or mutants directly onto a nylon membrane without prior gel electrophoresis. For this purpose, total RNA was isolated from *M. pneumoniae* cells and a twofold dilution series (2 µg – 0.25 µg) in 10 x SSC was prepared. For control, equal amounts of chromosomal DNA and yeast tRNA (ROCHE) were used. The RNA extracts were blotted through small slots onto a positively charged nylon membrane by means of the PR 648 Slot Blot Manifold (AMERSHAM BIOSCIENCES) to which a vacuum of 100 mbar was applied for up to 1 h. The following hybridization of membrane bound RNA with DIG-labeled RNA probes as well as the detection of RNA-RNA hybrids were performed as described for Southern blots except for the recipe of the prehybridization buffer (Großhennig, 2011).

Prehybridization buffer	200 ml	Formamide
(for Slot Blots)	100 ml	20 x SSC
	4 ml	N-laurylsarcosine (10%)
	8 g	Blocking reagent
	28 g	SDS
	ad 400 ml	dH_2O

Reverse transcription quantitative real-time PCR (qRT-PCR)

In order to analyze the expression of specific genes, qRT-PCR was carried out by means of the iScript™ One-Step RT-PCR Kit with SYBR® Green (BIO-RAD). The reactions were performed in a 96-well-plate with each well containing the following set up:

Reaction set up for RT-PCR (20 μl):

10 μl	2x SYBR Green RT-PCR Reaction Mix
1.2 μl	Primer forward
1.2 μl	Primer reverse
x μl	RNA template (80 - 100 ng / μl)
0.4 μl	iScript Reverse Transcriptase
ad 20 μl	Nuclease-free H_2O

The samples were pipetted in a 96-well-plate and the following reaction was set up in an iCycler (Bio-Rad) according to the manufacturer:

Reaction protocol for RT-PCR:

cDNA synthesis	10 min at 50°C
iScript reverse Transcriptase inactivation	5 min at 95°C
PCR cycling and detection	10 sec at 95°C
(30 to 45 cycles)	10 sec at 60°C
Melt curve analysis (optional)	1 min at 95°C
	1 min at 55°C
	10 sec at 55°C
	(80 cycles, increasing each by 0.5°C each cycle)

2.2.7 Work with proteins

Overproduction of recombinant proteins in *E.coli* and cell disruption by French press

For overexpression of *Strep*-tagged proteins in *E. coli* BL21, 500 ml LB + ampicillin were inoculated to an OD_{600} of 0.1 using an overnight culture of the respective *E.coli* strain carrying the overexpression plasmid. The culture was shaken at 37°C until an OD_{600} of 0.6-0.8 was reached and the overexpression was induced using 1mM IPTG. After 2.5 h of induction, the culture was harvested by centrifugation at 5,000 rpm for 20 min and 4°C. The pellet was resuspended in 15 ml buffer W and centrifuged in a falcon tube for 15 min at 4°C and 8,500 rpm. The supernatant was discarded and the pellet was used for cell disruption or stored at -20°C until further use.

52

The disruption of *E. coli* cells after protein overexpression was performed using the SLM Aminco 2-FA-078-E1 French Press Cell (SLM Aminco) at 18000 psi and repeated 2 times. The disrupted suspension was centrifuged for 20 min at 4°C and 8,500 rpm to remove the major cell debris. Afterwards, the supernatant was centrifuged for an additional hour at 35,000 rpm and 4°C in an ultracentrifuge. The pellet was discarded and the supernatant containing the soluble proteins was used as crude extract for purification.

Purification of proteins via *Strep*-Tactin® sepharose column

The proteins that were supposed to be purified were tagged with a *Strep*-tag II, an eight amino acids short peptide (WSHPQFEK), and purified using a *Strep*-Tactin® sepharose column (IBA) with a matrix volume of 0.5 ml. This *Strep*-Tactin® matrix binds specifically and with high affinity to the Strep-tag II of the desired proteins thereby separating them from the mixed protein solution. The column was equilibrated with 5 ml buffer W and loaded with the crude extract. The flow through was collected and the column was washed 4 times with 1.25 ml buffer W. For elution of the bound protein, initially 0.25 ml followed by three times 0.5 ml of buffer E were added. The elution fractions (E1-E4) as well as the last washing fraction (W4), the crude extract (CE) and the flow through (FT) were analyzed on a 12% SDS-PAA-gel.

Buffer W	100 mM	Tris-HCl pH 8.0
	150 mM	NaCl
	1 mM	EDTA
Buffer E	100 mM	Tris-HCl pH 8.0
	150 mM	NaCl
	1 mM	EDTA
	2.5 mM	Desthiobiotin

Denaturing polyacrylamide gel electrophoresis (SDS-PAGE)

The denaturing gels were prepared according to Laemmli *et al.*, 1970. These gels are poured to a thickness of 1 mm and consist of a stacking gel to accumulate the proteins in the sample and a running gel to separate the proteins according to their size. The samples were mixed with SDS-Loading dye (2 x) and boiled at 95°C for 5-10 min. After applying the samples, the gels were run at 120 V. In case of the Hoefer-SE-400 device, the gels were run over night at 30 V.

Stacking gel	1.3 ml	Rotiphorese® Gel 30 (37.5:1)
	0.87 ml	Tris-HCl pH 6.8 (1.5 M)
	50 µl	SDS (20%)
	100 µl	APS (10%)
	20 µl	TEMED
	6.3 ml	dH$_2$O

Running gel (12%)	4 ml	Rotiphorese® Gel 30 (37.5:1)
	2.6 ml	Tris-HCl pH 8.8 (1.5 M)
	50 µl	SDS (20%)
	100 µl	APS (10%)
	10 µl	TEMED
	3.3 ml	dH$_2$O

5 x SDS loading dye	1.4 ml	Tris-HCl 1 M pH 7.0
	3 ml	Glycerol
	2 ml	SDS (20%)
	1.6 ml	β-Mercaptoethanol
	10 mg	Bromophenol blue
	2 ml	dH$_2$O

Running buffer (10 x)	1.92 M	Glycerin
	0.5 M	Tris
	10%	SDS

Coomassie staining of polyacrylamide gels

After the gel run, the PAA gel was incubated for 15 min in fixing solution, stained with Coomassie staining solution for 5-10 min and destained until an optimal contrast between protein bands and background was observable. All steps were performed at room temperature with gentle shaking.

Fixing solution	500 ml	Methanol
	100 ml	Acetic acid
	ad 1 l	dH$_2$O

Staining solution	2.5 g	Coomassie brilliant blue R250
	100 ml	Acetic acid
	500 ml	Methanol
	ad 1 l	dH$_2$O

Destaining solution	150 ml	Acetic acid
	100 ml	Methanol
	ad 1 l	dH$_2$O

Silver staining of polyacrylamide gels

The silver staining of protein bands in SDS-gels was performed according to the method of Nesterenko (1994). This was done by incubating the gels at room temperature and with gentle shaking in the following solutions:

Step	Reagent	Duration
Fixing	Fixing solution	1 -24 h
Washing	50% ethanol	3 x 20 min
Reduction	Thiosulfate solution	1 min
Washing	dH$_2$O	3 x 20 s
Staining	Impregnating solution	25 min
Washing	dH$_2$O	2 x 20 s
Developing	Developer	Until sufficiently stained
Washing	dH$_2$O	5 s
Stopping	Stop solution	5 min

Fixing solution	50 ml	Methanol
	12 ml	Acetic acid
	100 µl	Formaldehyde (37%)
	ad 100 ml	dH$_2$O

Thiosulfate solution	20 mg	Na$_2$S$_2$O$_3$ x 5 H$_2$O
	ad 100 ml	dH$_2$O

Impregnating solution	0.2 g	$AgNO_3$
	37 μl	Formaldehyde (37%)
	ad 100 ml	dH_2O

Developer	6 g	Na_2CO_3
	2 ml	Thiosulfate solution
	50 μl	Formaldehyde (37%)
	ad 100 ml	dH_2O

| Stop solution | 1.86 g | EDTA |
| | ad 100 ml | dH_2O |

Western Blot

The Western blot was employed to detect *Strep*-tagged proteins from an SDS gel using an anti-*Strep* antibody (PromoKine) after protein purification. Using a semi-dry blotting apparatus (Peqlab), the proteins were transferred from the gel onto a polyvinylidene difluoride (PVDF) membrane (Bio-Rad).

At first, three Whatman papers were soaked in transfer buffer and placed onto the transfer device. The membrane was briefly activated in 100% methanol, equilibrated in transfer buffer and placed on top of the Whatman papers. The acrylamide gel was equilibrated in transfer buffer and placed onto the PVDF membrane. Finally, three Whatman papers soaked in transfer buffer were placed on the polyacrylamide gel. Bubbles were removed, the transfer device was closed and a current of 0.8 mA/cm² was applied for 1 to 1.5 h. After the transfer of the proteins to the membrane, the membrane was incubated 1xTBS for 2 h. Subsequently, the membrane was incubated with the primary antibody (anti-*Strep*-antibody) overnight at 4°C. The anti-*Strep*-antibody was diluted 1:1,000 in TBS-tween.

Afterwards, the primary antibody was removed and three washing steps of 30 min in blocking solution followed. The membrane was incubated for 30 min with the secondary antibody, a polyclonal goat anti-rabbit immunoglobulin conjugated with alkaline phosphatase which was diluted 1:100,000 with blocking solution. The membrane was subsequently rinsed with deionized water and incubated in buffer III for 5 min. The membrane was placed between a transparent foil and the membrane was covered with a mixture of 500 μl buffer III and 5 μl CDP*. The luminescence was detected with a Chemolumineszenz Imager (modified from Rempeters, 2011).

Blocking solution	100 ml	10 x TBS
	25 g	Milk powder
	1 ml	Tween® 20
	ad 1 l	dH$_2$O
Buffer III (1 l)	0.1 M	Tris
	0.1 M	NaCl
	ad 1 l	dH$_2$O
	adjust	pH 9.5
10 x TBS (1 l)	60 g	Tris-HCl pH 7.6
	90 g	NaCl
	ad 1 l	dH$_2$O
Transfer buffer (5 l)	15.1 g	Tris
	72.1 g	Glycerol
	750 ml	Methanol
	ad 5 l	dH$_2$O

Preparation of *M. pneumoniae* protein extracts

The cells of a 100 ml culture were harvested after four days of growth in 1.5 ml PBS pH 7.4 in a 2 ml Eppendorf reaction tube. The cells were centrifuged (10 min, 11,000 x g, 4°C), washed three times and resuspended in 500 µl PBS. The cell suspension was transferred into a 2 ml screw-cap reaction tube containing 0.5 g glass beads (0.1 mm diameter). The cells and beads were vortexed 10 times for 30 s at 1 min intervals and subsequently centrifuged. The resulting supernatant contained the protein extract of the lysed *M. pneumoniae* cells.

2.2.8 Enzyme activity tests

The characteristics and activity levels of the purified proteins were assessed by measuring the production rate of H$_2$S, pyruvate or alanine. Hemolysis and hemoxidation assays with the proteins are described in 2.2.10.

Hydrogen sulfide assays

Methylene blue method

The quantification of H_2S by the methylene blue method was performed as described previously (Schmidt, 1987). In presence of $FeCl_3$ at a very low pH, N',N'-dimethyl-p-phenylenediamine can form a complex with H_2S which turns blue ("methylene blue") and has its absorption maximum at $\lambda = 670$ nm. A reaction setup of 1 ml was composed of 100 mM potassium phosphate buffer (pH 7.6), 2.5 mM dithioerythritol (DTE), 10 μM pyridoxal-5-phosphate (PLP), 1-2 μg of the purified enzyme(s) and substrate in various concentrations. The mixture was incubated for 2 hours at 37°C, or various time periods when needed, and the reaction was terminated by addition of 100 μl solution I (20 mM N',N'-dimethyl-p-phenylenediamine dihydrochloride in 7.2 M HCl) and 100 μl of solution II (0.03 M $FeCl_3$ in 1.2 M HCl). After 30 min incubation at room temperature, the formation of methylene blue was determined spectrophotometrically at $\lambda = 670$ nm.

Bismuth chloride method

The bismuth chloride method is based on the reaction of bismuth ($BiCl_3$) with sulfide (H_2S) to produce Bi_2S_3 which is visible and measurable as a black precipitate. For a 1 ml reaction setup, 1-10 μg purified protein were incubated with various cysteine concentrations in a visualization solution at 37°C. After 2 hours, or different time points when needed, the OD of the reaction mix was measured at $\lambda = 405$ nm and compared to a sodium sulfide standard curve.

Visualization solution (1 ml)		
	100 mM	Triethanolamine
	10 μM	Pyridoxal-5-phosphate (PLP)
	1%	Triton X-100
	10 mM	EDTA (pH 8.0)
	0.5 mM	$BiCl_3$
	0-70 mM	L-Cysteine

Pyruvate assay

The pyruvate assay is based on the derivatization of pyruvate with 3-methyl-2-benzothiazolinone hydrazone (MBTH) (Sigma-Aldrich) in an acidic environment. This results in the formation of a coloured complex that can be detected photometrically. The assay was carried out in a 250 μl potassium phosphate buffer setup containing 10 μM PLP, 2-5 μg purified enzyme and various cysteine concentrations. The mixtures were incubated for 10, 30, 60, 120 min or overnight at 37°C. To

terminate the reaction, 125 µl of 4.5% trichloroacetic acid (Sigma-Aldrich) were added. The samples were centrifuged for 5 min at 13,000 rpm. 300 µl of the supernatant were transferred into a new tube containing 900 µl of 0.017% 3-methyl-2-benzothiazolinone hydrazone in 0.67 M sodium acetate (pH 5.2). After 30 min incubation at 50°C, the OD at λ = 335 nm was measured.

Sample preparation for alanine and pyruvate detection using GC-MS

To identify products other than hydrogen sulfide that derive from the enzymatic reaction of MPN487, gas chromatography coupled to mass spectrometry (GC-MS) was performed by Dr.Till Ischebeck in the Department for Plant Biochemistry in Göttingen.

A 1 ml reaction setup contained 400 µl sodium carbonate buffer (pH 9.2), 10 µM PLP, 2.5 mM DTE, 5 µg of the purified enzyme and 1, 5 or 10 mM L-cysteine. Control samples without enzyme or without substrate, respectively, were prepared and treated the same way. The mixtures were incubated over night at 37°C and added to 2 ml of extraction solution (methanol/chloroform/water 32.25:12.5:6.25 [v/v/v]) in a Kimble glass. Extraction and derivatization of samples was done as described previously (Bellaire *et al.*, 2014). The extracts were vortexed and incubated shaking for 2 h at 4°C. After a centrifugation step for 5 min at 2,000 x g and 4˚C, the supernatant was transferred into a new Kimble glass. 200 µl of the extract were dried under nitrogen, redissolved in 30 µl freshly prepared methoxylamine (Mox) solution (30 mg/ml in pyridine) and incubated overnight at RT. After the addition of 60 µl pure N-methyl-trimethylsilyltrifluoroacetamid (MSTFA) for derivatization (silylation) and volatization of the ingredients, the samples were incubated for at least 1 h but not more than 8 h and could subsequently be used for GC-MS analysis. In that procedure, the samples were analyzed on an Agilent 5973 Network mass selective detector connected to a Agilent 6890 gas chromatograph equipped with a capillary HP5-MS column (30 m x 0.25 mm; 0.25 µm coating thickness; J&W Scientific, Agilent). Helium was used as carrier gas (1 ml/min). The inlet temperature was set to 230°C and the temperature gradient applied was 50°C for 2 min, 50 – 330°C at 5 K/min 330°C for 2 min. Electron energy of 70 eV, an ion source temperature of 230°C, and a transfer line temperature of 330°C was used. Spectra were recorded in the range of 71-600.

For quantification, the ions with the following mass-to-charge ratio were used: pyruvate (1 TMS (trimethylsilyl-), 1 MEOX (methoximino-)), 174 Da/e; alanine (2 TMS), 116 Da/e; alanine (3 TMS), 188 Da/e.

2.2.9 Methods for characterization of *M. pneumoniae* strains

Growth assays

For generation of a growth curve, 100 ml cultures were inoculated with 2.5 mg of *M. pneumoniae* cells and incubated at 37°C. The wet weight of these cultures was determined after two, four and six days of growth as described in 2.2.2.

Determination of *in vivo* H_2O_2 production

M. pneumoniae cells were harvested in 1.5 ml 1 x H_2O_2 assay buffer as described earlier. The cells were spun down for 10 min at 10,000 x g and 4°C. The supernatant was discarded. The cells were washed again in 1 ml buffer, transferred into a falcon tube and centrifuged again for 15 min at 4,000 rpm and 4°C. The pellet was resuspended in 3.5 – 4 ml buffer and 1 ml of this solution was used for determination of optical density at λ = 550 nm. For measurement of H_2O_2 production, the amount of cells corresponding to 1.0 OD_{550} unit in a final volume of 1 ml was used. The 1 ml set-up was incubated in a reaction tube for 1 h at 37°C. Afterwards, 1 µl 100 mM glycerol, 1 µl 100 mM glucose, 1 µl 100 mM glycerol-3-phosphate (G3P) or 2 µl 50 mM GPC were added to the samples. This point was set as t = 0. The amount of produced hydrogen peroxide was measured prior to addition of carbon sources, as well as at t = 5 min, 15 min, 30 min, 60 min and 120 min. For this purpose, peroxide test strips (MERCK) were briefly dipped into the tubes. These strips contain a peroxidase which transfers oxygen from the produced H_2O_2 to an organic redox indicator, which is then converted to a blue-colored product. After 15 sec, the resulting blue color of the strip was compared to the enclosed color chart (adapted from Großhennig, 2011).

H_2O_2 assay buffer	67.6 mM	HEPES (pH 7.3)
	140 mM	NaCl
	7 mM	$MgCl_2$
	ad 1 l	dH_2O

Determination of cytotoxicity towards HeLa cells

Preparation of HeLa cells

Infection assays were performed in 24-well-plates. For this purpose, previously harvested HeLa cells were counted in a Neubauer chamber as mentioned above. For calculation of the desired cell number per well (2.5×10^4), the following formula was used:

$$x \text{ ml} = 2.5 \times 10^4 / \text{number of HeLa cells per ml}$$

The respective amount of cell suspension was pipetted in each well to be infected and was filled up with DMEM to a final volume of 700 µl. The titer plates were incubated for 24 hours at 37°C and 5% CO_2.

Cell harvest and infection

After 4 days growth, *M. pneumoniae* cultures were harvested in 1.5 ml 1 x H_2O_2 assay buffer as described above. Then, the cells were centrifuged for 5 min at 4°C and 10,000 x g. The supernatant was discarded and the pellet was resuspended in 1 ml buffer using a syringe with a 0.4 x 20 mm hollow needle. Depending on the size of the pellet, the suspension was diluted in 5 – 8 ml buffer. Subsequently, 1 ml was used for measurement of optical density at $\lambda = 550$ nm. The amount corresponding to 0.1 OD_{550} units was transferred to a new reaction tube and centrifuged again for 5 min at 10,000 x g and 4°C. The supernatant was removed and the pellet was resuspended in 125 µl fresh MP-medium with a syringe and a 0.4 x 20 mm hollow needle. The *M. pneumoniae* cells were added to the incubated HeLa cells and incubated for 2 h at 37°C and 5% CO_2. Afterwards, the supernatant was removed from the wells and replaced by 700 µl fresh DMEM. The assay was monitored for 6 days by staining and photographing the cells (adapted from Hames, 2008).

Quantification of cytotoxixity

To quantify the cytotoxixity of *M. pneumoniae* or an enzyme towards HeLa cells, the amount of surviving HeLa cells in the assay was determined 2, 4 or 6 days past infection by crystal violet stain. For this purpose, the infection assay was set up as described above and the DMEM was removed from the wells after the desired time of incubation. The HeLa cells were fixed with 500 µl 10% buffered formalin for 10 min at room temperature. Afterwards, the fixing solution was removed and the cells were stained for 30 min with 150 µl 0.1% aqueous crystal violet solution which only binds to intact cell tissues. After staining, the crystal violet was discarded and the cells were washed with water until all unbound crystal violet was removed. For visual documentation, the stained cells were photographed (Olympus EVOLT E-420). For quantification, the stained cells were destained again using 500 µl 0.5%

SDS solution and the OD_{595} was determined. The OD_{595} of an uninfected HeLa cell control was set to 100% surviving cells. The cytotoxicity of an *M. pneumoniae* strain was calculated as follows:

$$\% \text{ cytotoxicity} = 100 - (OD_{595} \text{ sample} / OD_{595} \text{ control})$$

| Buffered formalin | 10 ml | 37% Formaldehyde |
| | 90 ml | 1 x PBS pH7.4 |

| Crystal violet solution | 0.1 g | Crystal violet |
| | 100 ml | dH_2O |

Determination of *in vivo* H_2S production

M. pneumoniae *cell harvest*

M. pneumoniae cells were harvested in 1.5 ml 1 x PBS (pH 7.4) as described above. After centrifugation for 10 min at 11,000 x g and 4°C, the pellet was resuspended in 1 ml PBS using a syringe and a needle (0.4 mm diameter). Depending on the size of the pellet, the solution was transferred into a falcon tube and diluted with 3-5 ml cold PBS. The optical density of the cell suspension was determined at $\lambda = 550$ nm. For investigation of H_2S production, *M. pneumoniae* cells corresponding to an OD_{550} of 1 were used in a 1 ml set-up.

Setup with lead acetate test strips

For the lead acetate sample, the *M. pneumoniae* cells were incubated in 1 ml 1x PBS pH 7.4 or in MP-medium supplemented with different cysteine concentrations in 2 ml Eppendorf reaction tubes. Lead acetate test strips (Aldrich) were fixed under the lid of the tube (without contact to the liquid) to catch the produced hydrogen sulfide. The lead covering the strips reacts with the sulfide to form black PbS resulting in a dark staining of the test paper. After an overnight incubation at 37°C, the coloration of the test strips was examined and photographed.

Setup with $BiCl_3$ visualization solution

The harvested *M. pneumoniae* cells were resuspended in 1 ml visualization solution (see 2.2.8) and incubated at 37°C overnight. When H_2S is produced by the cells, Bi_2S_3 is formed which appears as a dark discoloration and precipitate that can be detected visually and spectrophotometrically at $\lambda = 405$ nm. A sample that was incubated in visualization solution without $BiCl_3$ was used as control. The amount of H_2S was determined by comparing the OD_{405} to a sodium sulfide standard curve.

2.2.10 Work with blood

Preparation of red blood cells from whole sheep blood

To isolate erythrocytes, 5 ml of defibrinated sheep blood were transferred into a 15 ml falcon tube and centrifuged for 10 min at 900 x g and 4°C. The supernatant was discarded and the red blood cells were washed three times with 1x PBS pH 7.4 by inverting the tube. After the last centrifugation step, the amount of erythrocytes was estimated on the scale on the falcon tube. The according amount of 1x PBS was added to the RBCs to get a final solution of 20% RBCs in PBS. The erythrocytes were gently resuspended and stored at 4°C for up to three days.

Blood agar plates

To analyze hemolytic activity of *M. pneumoniae*, serial tenfold dilutions of each strain of interest were prepared in MP-medium. 200 µl of the 10^{-4} dilutions were distributed on MP-glucose plates and incubated for 7-14 days at 37°C until colonies were visible. 0.75% agar in 1x PBS pH 7.4 was autoclaved and cooled down to 42°C. Defibrinated sheep blood was added to a final concentration of 5% and mixed carefully. The *M. pneumoniae* colonies were overlayed with 5 ml blood agar and the plates were incubated for 1-2 days at 37°C. Pictures were taken using the Lumar V.12 stereo fluorescence microscope (Zeiss).

Hemolysis- and hemoxidation assays

Assays with proteins

To test the ability of proteins to lyse erythrocytes or to oxidize hemoglobin, a 10 ml mixture of 2% washed sheep RBCs and 2 µg/ml enzyme in PBS (pH 7.4) was set up. In case of MPN487 being the enzyme of interest, 10 µM PLP and 1 or 10 mM freshly prepared cysteine were added to the set up. For a mixture using GlpD as protein, 1 mM glycerol-3-phosphate was applied as substrate. The samples were incubated in a falcon tube at 37°C and gentle rotation at 110 rpm. 1 ml samples were withdrawn after different time points and transferred into 1.5 ml Eppendorf reaction tubes. The tubes were centrifuged for 10 min at 1,400 x g and 4°C. The supernatant was removed carefully, transferred into a new reaction tube and stored for later analysis. The pellet was resuspended in 1 ml dH$_2$O to lyse the erythrocytes and release the hemoglobin. The supernatant and the lysed pellet were photographed and their spectra from $\lambda = 370$ to 700 nm were measured using the platereader SynergyMX (Biotek).

Assays with M. pneumoniae *cells*

In order to analyze the hemolytic or hemoxidative activities of different *M. pneumoniae* strains, 100 ml cultures were harvested in 1 x PBS as described above. After determination of the optical density at λ=550 nm, the appropriate amount of *Mycoplasma* suspension referring to an OD of 1 was incubated with 5% defibrinated sheep blood or 2% washed sheep RBCs in PBS (pH 7.4) and various supplements (1 mM glycerol, 1 mM glycerol-3-phosphate and 1 or 10 mM L-cysteine) in a final volume of 1 ml. The samples were incubated at 37°C and 100-110 rpm for several hours. One reaction tube for each time point and condition of interest was prepared. After the desired incubation time, the tubes were centrifuged at 4°C and 1,400 x g and the supernatant was transferred carefully into a new tube. The pellet was resuspended and lysed in 1 ml dH$_2$O. Both supernatant and pellet were photographed and the spectra were recorded photometrically from λ = 370 to 700 nm.

Hemagglutination assay

The cells of a *M. pneumoniae* culture were harvested after 5 days growth as described earlier and their OD at λ = 550 nm was determined. The amount of cells needed for an OD$_{550}$ of 5 was transferred into an Eppendorf tube and centrifuged for 5 min at 4°C and 11,000 x g. The supernatant was removed and the pellet was resuspended in 150 µl PBS.

The hemagglutination assay was performed in a 96 well microtiter plate with round bottom. For each strain, serial twofold dilutions in PBS (50 µl cells + 50 µl PBS) were prepared starting from an undiluted 100 µl cell suspension in the first well of each row. Subsequently, 50 µl of 2% defibrinated sheep blood in PBS was added to each well. The plate was incubated at 37°C for 1-2 hours or overnight and pictures were taken.

Preparation of a blood smear for microscopy

5-10 µl blood solution (with or without *Mycoplasma*) were dropped onto a glass slide and distributed using a second slide to form a thin film. The blood smear was heat fixed with a Bunsen burner, cooled down and used for staining or microscopy. Blood microscopy was done using the Axioskop 40 FL fluorescence microscope (Zeiss).

3. RESULTS

3.1 Transport systems in *Mycoplasma pneumoniae*

3.1.1 Attempts to express *M. pneumoniae* transporters in *B. subtilis*

In order to analyze or confirm the function of essential transporters whose substrates are not certainly known, heterologous expression of these systems in *Bacillus subtilis* was attempted. For this, *B. subtilis* transporter mutants were to be prepared, transformed with the *Mycoplasma* copy of the suspected homologous transporter gene and checked for complementation success. To test the functionality of this approach, the glycerol facilitator, GlpF, from *Mycoplasma pneumoniae* was expressed in a *B. subtilis* strain lacking its own glycerol facilitator. GlpF seemed to be the ideal test protein for several reasons: (1) *M. pneumoniae* and *B. subtilis* possess GlpF homologs; (2) as a facilitator, GlpF is a single protein with a simple transport function; (3) its substrate is known; (4) the absence and presence of a functional carbon source transporter can be easily tested when growing *B. subtilis* on minimal medium supplied with the respective carbon source, i.e. glycerol; (5) GlpF is the only glycerol transporter in *B. subtilis*.
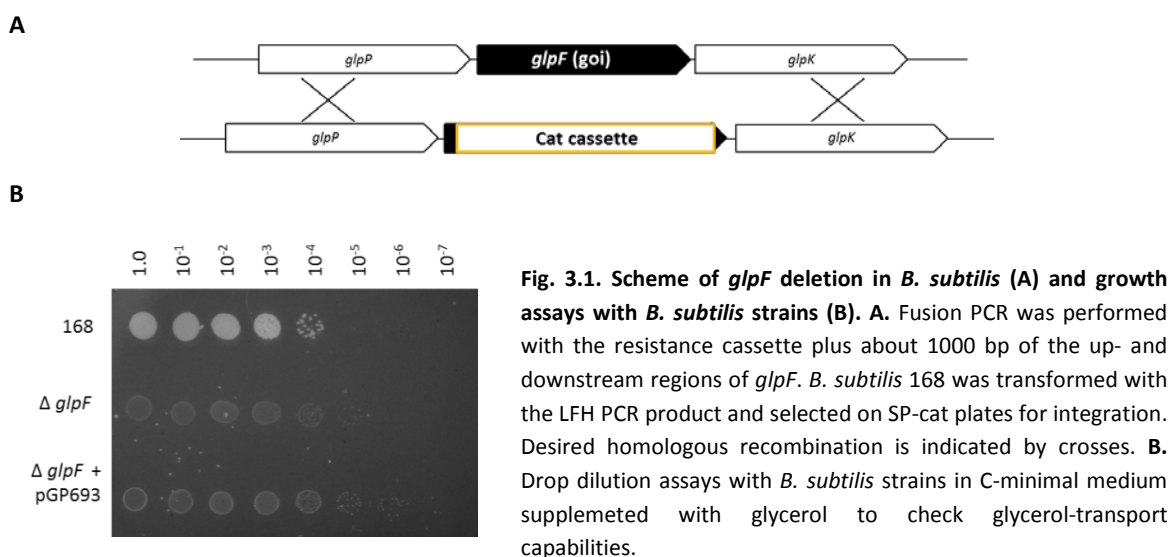

Fig. 3.1. Scheme of *glpF* deletion in *B. subtilis* (A) and growth assays with *B. subtilis* strains (B). A. Fusion PCR was performed with the resistance cassette plus about 1000 bp of the up- and downstream regions of *glpF*. *B. subtilis* 168 was transformed with the LFH PCR product and selected on SP-cat plates for integration. Desired homologous recombination is indicated by crosses. **B.** Drop dilution assays with *B. subtilis* strains in C-minimal medium supplemeted with glycerol to check glycerol-transport capabilities.

A $\Delta glpF$ mutant of *B. subtilis* was generated by long flanking homology PCR (LFH) and homologous recombination (**Fig. 3.1 A**). The knockout was confirmed by the growth defect of the $\Delta glpF$ strain on C-minimal medium containing glycerol (**Fig. 3.1 B**). The *glpF* gene from *M. pneumoniae* was amplified from pGP663 containing the gene without internal TGA codons (Großhennig, 2011). The gene was cloned into pBQ200 (resulting in pGP693) which would allow for constitutive *glpF*-expression from the plasmid. Subsequent growth assays with *B. subtilis* strains 168, $\Delta glpF$ and $\Delta glpF$ containing pGP693 revealed that the growth defect of the mutant could not be restored by GlpF$_{Mpn}$ (**Fig. 3.1 B**). The same was true for a $\Delta glpF$ strain carrying $glpF_{mpn}$ integrated into the genome (data not shown). To rule out whether the ineffective complementation was due to $glpF_{mpn}$ not being properly expressed or due to a negative effect of the gene replacement on expression of the downstream gene *glpK*, quantitative real-time PCR with *B. subtilis* RNA was performed (data not shown). The results showed that expression of *glpK*, which is absolutely needed for glycerol metabolism, was not affected by replacement of the native *glpF* by the chloramphenicol resistance cassette. However, no $glpF_{mpn}$ transcripts could be detected in the $\Delta glpF$ strain containing pGP693 indicating that with the applied system the expression of $glpF_{mpn}$ is not possible in *B. subtilis* (data not shown).
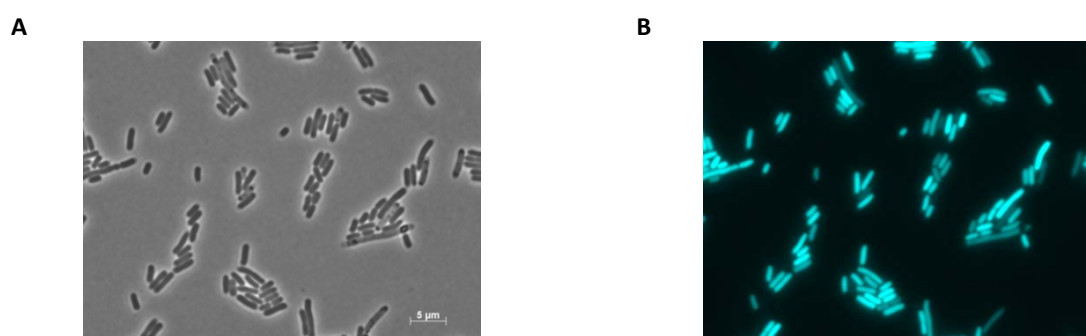

Fig. 3.2. Fluorescence microscopy images of *E. coli* cells expressing C-terminally tagged GlpF$_{Mpn}$. **A.** Bright field. The scale is 5µm. **B.** GlpF-CFP fusion in the same cells detected with CFP filter. Expression of GlpF-YFP was examined accordingly and gave the same result. The pictures were taken with the Axioskop 40 FL fluorescence microscope (Zeiss).

Using fluorescence microscopy, it was tested if and where $glpF_{mpn}$ is expressed in *E. coli*. Therefore, the gene including the constitutively promoter P$_{degQ}$ was cloned into the fluorescence vectors pBP19 and pBP20, respectively. The resulting plasmids were named pGP697 and pGP698 and encode GlpF$_{Mpn}$ being C-terminally fused to YFP and CFP, respectively. The *E.coli* DH5α strains that harbored the correct plasmids were subsequently examined by fluorescence microscopy (**Fig. 3.2**). Both the YFP- and the CFP-fusion constructs were expressed from pGP697 and pGP698 in *E. coli*. However, it seems

that GlpF$_{Mpn}$ is not located at the cell membrane but rather inside the cytosol. This might be due to a misfolding of the protein, a steric hindrance by the fluorescence tag or simply the lack of a signal peptide which could prevent proper transport of the protein to and its correct insertion into the membrane. Moreover, as *M. pneumoniae* and *E. coli* are only distantly related, it is highly probable that their membrane composition differs. All these options, in general, make heterologous expression of membrane proteins especially challenging. Taken together, heterologous expression of *M. pneumoniae* transporters in *B. subtilis* or *E. coli* is not a practicable tool for studies of transport systems.

3.1.2   Characterization of *M. pneumoniae* transporter mutants

Of the 70 putative transport proteins listed in **Tab. 3.1**, 31 are expected to be non-essential (Lluch-Senar *et al.*, in press). To assess the function of these non-essential proteins and their relevance for growth and virulence, mutants for as many transport systems as possible were planned to be identified. In case of ABC transporters, isolation of the indispensable ATP binding protein of the complex was chosen to be sufficient.

Isolation of transporter mutants

In *M. pneumoniae*, mutants cannot be constructed as in other bacteria, e.g. by LFH, since they do not possess a system for homologous recombination. Therefore, mutants need to be created and isolated by means of "haystack mutagenesis". In this approach, an ordered pool of random mutants is produced by transposon mutagenesis (Halbedel and Stülke, 2007). This ordered library containing about 3,000 clones can then be screened step by step for transposon insertions in the gene of interest by PCR combinations, each using a gene specific and a transposon specific oligonucleotide (**3.3**). In **3.3 A**, a representative scheme for the isolation of *mpn096*::Tn is shown and will be explained subsequently. For the mutant screen, the gene specific primers SG65 and SG66 were designed and used in combination with the transposon binding oligonucleotides SH29 and SH30. The products of the PCR combinations that identify the positive isolated clone are depicted in **Fig. 3.3 B**. Sequencing of this clone revealed that the transposon was inserted after 148 bp in *mpn096*. This results in a truncated protein of 49 amino acids with one additional amino acid and the stop codon carried by the transposon. No PCR product appeared in the lane with only gene specific primers, assuring that the culture was not contaminated with another mutant. To confirm that the transposon inserted in

Tab. 3.1. Overview of proteins that are involved in transmembrane transport processes in *M. pneumoniae*.

MPN #	Gene name [1,2]	Mutant	MPN #	Gene name [1,2]	Mutant
018	*pmd1*	f	274		e
019	*msbA*	nt	308	*apc*	+
043	*glpF*	-	318	*apc*	f
048		-	319	*gap1*	f
049		-	333		-
055	*potA*	e	334	*bcrA*	nt
056	*potB*	e	335		-
057	*potI*	e	415	*phnD*	f
076		+ [3]	416	*phnC*	f
077		+ [3]	417	*phnE*	f
078	*fruA*	f	421	*glpU*	+ [3]
080	*ybbP*	e	431	*cbiQ*	e
081	*glnQ*	e	432	*artP*	e
095		+	433	*cbiO*	e
096		+	435		e
112		+ [4]	448	*folT*	e
113		+ [4]	460	*ktrB*	e
134	*ugpC*	e	461	*ktrA*	e
135	*ugpA*	e	494	*sgaA*	f
136	*ugpE*	e	495	*sgaB*	nt
193	*cbiO1*	f	496	*sgaT*	+
194	*cbiO2*	e	508		-
195	*cbiQ*	f	509		-
207	*ptsG*	e	510		f
209	*mgtA*	f	511		nt
215	*oppB*	e	512		-
216	*oppC*	f	571	*lcnDR3*	+
217	*oppD*	e	609	*pstB*	+
218	*oppF*	e	610	*pstA*	-
234		-	611	*pstS*	-
236		e	651	*mtlA*	+
258	*mglA*	e	653	*mtlF*	-
259		+	683	*devA*	nt
260	*rbsC*	f	684		f
268		f	685	*cysA*	f

[1] Himmelreich *et al.*, 1996; [2] KEGG; [3] Großhennig *et al.*, 2013; [4] Großhennig, 2011; e essential; f fitness (Lluch-Senar *et al.*, in press); - no mutant isolated; + mutant isolated and experimentally tested; nt mutant isolated but not tested

mpn096 and nowhere else in the genome, Southern blot analysis of the mutant in comparison to the wild type M129 was performed. For that, chromosomal DNA of both strains was prepared and digested with *Nco*I and *Xho*I (**Fig. 3.3 A**). The digested DNA was blotted and afterwards hybridized with two different probes (**Fig. 3.3 C**).
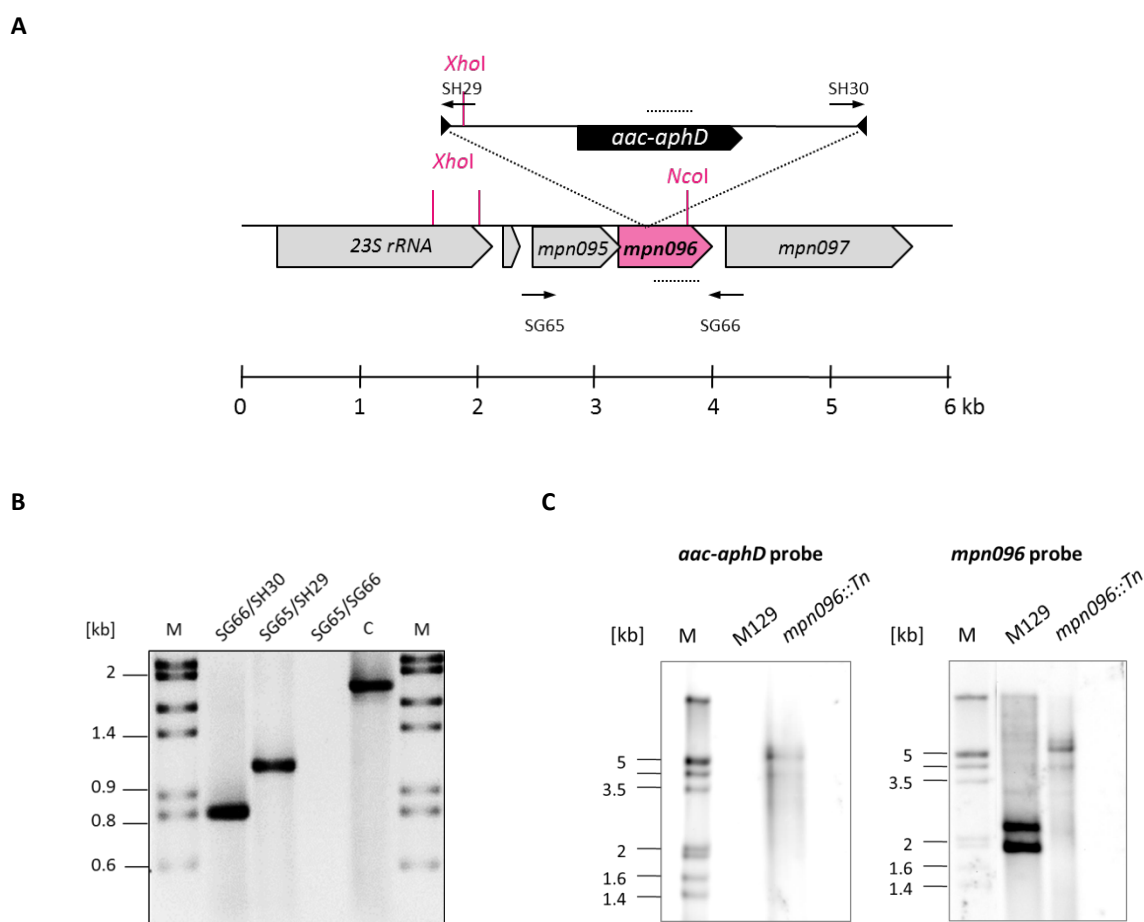

Fig. 3.3. Schematic illustration of transposon insertion in the isolated *mpn096*::Tn mutant of *M. pneumoniae*. A. The transposon was inserted after 148 bp in *mpn096* and is depicted to scale. Oligonucleotides SG65 and SG66 were designed for the mutant screen. Restriction sites for Southern blots are marked in pink. Probe binding sites are indicated by dotted lines. *aac-aphD* is the gene conferring gentamycin resistance in the mutant. **B.** PCR products with the respective primers from an isolated clone. No product was obtained with only gene specific primers. M = marker, C = positive control with M129 chromosomal DNA and SG65/SG66. **C.** Southern blot wich chromosomal DNA from M129 and *mpn096*::Tn. Hybridization was done with a probe specific for the *aac-aphD* gene on the transposons (left) and for the gene *mpn096* (right).

The *aac-aphD* probe binds to the gentamycin resistance cassette that is carried by the transposon and inserted into *mpn096* in the mutant strain but not in M129. Therefore, hybridization of this probe is supposed to occur only with the mutant chromosomal DNA. As shown, only in the lane containing the mutant DNA a band appeared at the expected size of about 5 kbp. The *mpn096* probe binds to the

respective gene as indicated by the dotted line in **A**. Due to transposon insertion and the appearance of a new *Xho*I restriction site, the digestion pattern changes in the mutant DNA in comparison to the wild type chromosomal DNA. This is visible in the band shift. The double bands may be the result of incomplete digestion at the transposon or the two *Xho*I restriction sites upstream of *mpn096*. The bands in the lanes containing mutant DNA hybridized with the *aac-aphD* and the *mpn096* probe match, which rules out the possibility of the transposon being additionally inserted elsewhere in the genome. The resulting strain was designated GPM31.

According to the procedure described above, all mutants were isolated and verified and used for following characterization.

Growth experiments for characterizing selected *M. pneumoniae* transporter mutants

Since growth and viability are a crucial determinant for *M. pneumoniae* dispersion and pathogenesis, the importance of several transport systems in survival and growth rate was tested. For that, the respective mutant strains were grown in liquid MP-medium supplemented with glucose and the increase of cell density was monitored over six days. The chosen import systems were: MPN095, MPN096 and MPN308 as putative amino acid transporters; MPN259 as part of a putative ribose/galactose uptake system; MPN496 as the EIIC protein of a putative ascorbate PTS; MPN609 as part of a putative phosphate import system and MPN651 as EIIBC component of a mannitol PTS. The resulting growth curves of M129 and mutant strains are depicted in **Fig. 3.4**. Except for the amino acid permease mutants *mpn095*::Tn and *mpn096*::Tn, none of the mutants exhibited a phenotype that differs from the wild type. During the harvest of *mpn095*::Tn and *mpn096*::Tn, the strains turned out to have an adhesion defect. Usually, *M. pneumoniae* cells grow attached to the host cell or, *in vitro*, attached to surface of the cell culture flask. The two amino acid transporter mutants, however, only partially grew adhesively while most of the cells were dispersed in the medium. This effect was even stronger in *mpn096*::Tn than in *mpn095*::Tn indicating that their impact on this process might be of different intensity.
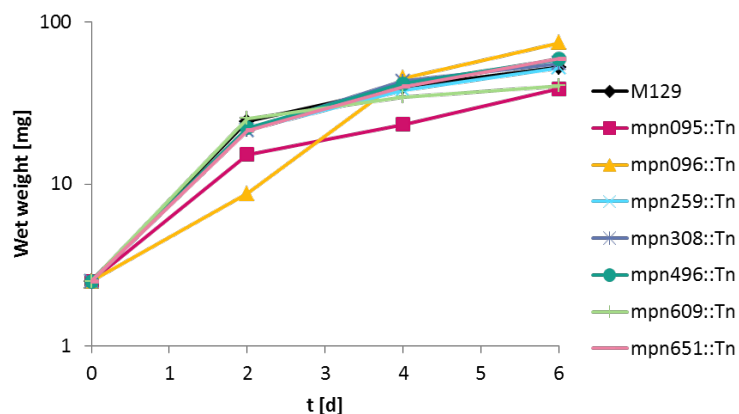
Fig. 3.4 Growth assay with *M. pneumoniae* wild type and mutant strains. *Mycoplasma* cultures were inoculated with 2.5 mg cells from the pre-culture and grown in MP-glucose medium for 2, 4 and 6 days, respectively. Total cells were harvested and their wet weight was determined

Investigation of the putative hemolysin transporter MPN571 and the putative hemolysin MPN159

Among the transport systems encoded in the *M. pneumoniae* genome, a putative hemolysin ABC transporter, MPN571, is predicted (Himmelreich *et al.*, 1996). Since a hemolysin transporter logically needs a corresponding hemolysin to transport, the genome was searched for genes encoding hemolysin-like proteins. In fact, the search retrieved the gene *hlyC* which encodes a hypothetical protein, MPN159 (KEGG). Both, MPN159 and MPN571, were tested for their role in viability, cytotoxicity and hemolysis to confirm or disprove their function as hemolysin (transporter). This was done again by isolating mutants from the transposon mutant library and determining their phenotype.

Isolation of mutants

As described above, *mpn159*::Tn and *mpn571*::Tn mutants were identified by screening the mutant library pools with respective oligonucleotides. Both screens resulted in the isolation of a mutant.

The genomic context of *mpn159*::Tn and its transposon insertion in *mpn159* are shown in **Fig. 3.5**. The transposon was inserted in antisense direction after 435 base pairs leading to a perfect disruption of the gene. In **Fig. 3.6**, a scheme for the genomic insertion of the transposon into *mpn571* is shown. Although the transposon inserted rather near the 3' region of *mpn571*, which is usually not sufficient for a reliable knockout strain, it hit the nucleotide binding domain of the protein. Therefore, the protein was regarded as unable to fulfil its function as an ABC transporter rendering the according mutant as acceptable. For both mutant strains, Southern blots were performed and confirmed the correctness of the transposon insertions. The *mpn159*::Tn strain was designated GPM34, the *mpn571*::Tn strain is GPM32.
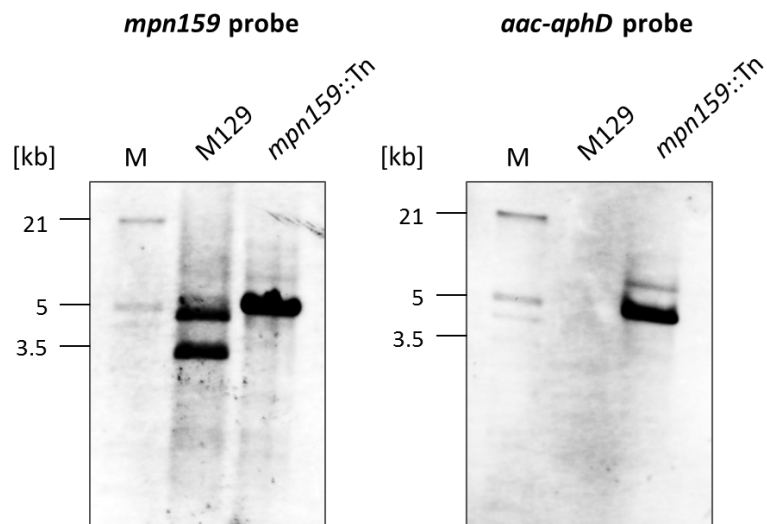
A
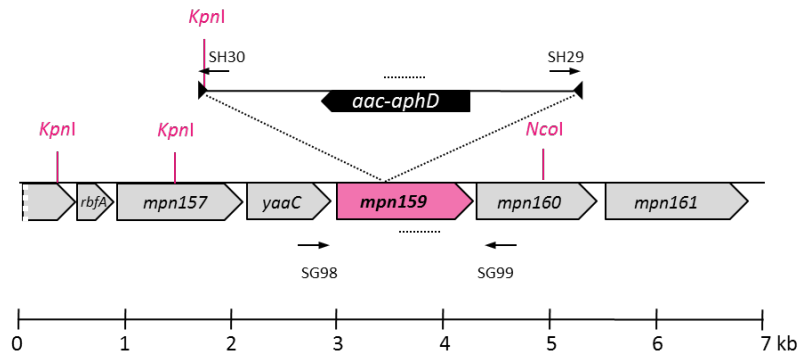
B

Fig. 3.5. Scheme of transposon insertion in *mpn159* and verification of the *mpn159*::Tn mutant using Southern blots. A. Genome organization around *mpn159*. The transposon inserted after 435 bp in *mpn159*. Dotted lines indicate the binding sites of probes for the Southern blot. Oligonucleotide binding sites are marked by arrows, restriction sites are highlighted pink. **B.** Southern blots to confirm integration of the transposon only into *mpn159*. Left: hybridization with the gene specific probe. A band shift is seen between the M129 chromosomal DNA and the mutant DNA after transposon insertion. The double bands are probably caused by an incomplete digestion with *Kpn*I (see restrictions sites in **A.**). Hybridzation with the transposon-specific *aac-aphD* probe expectedly does only occur in the mutant chromosomal DNA. For the *mpn159*::Tn chromosomal DNA, hybridization with each probe results in the same band size.

72
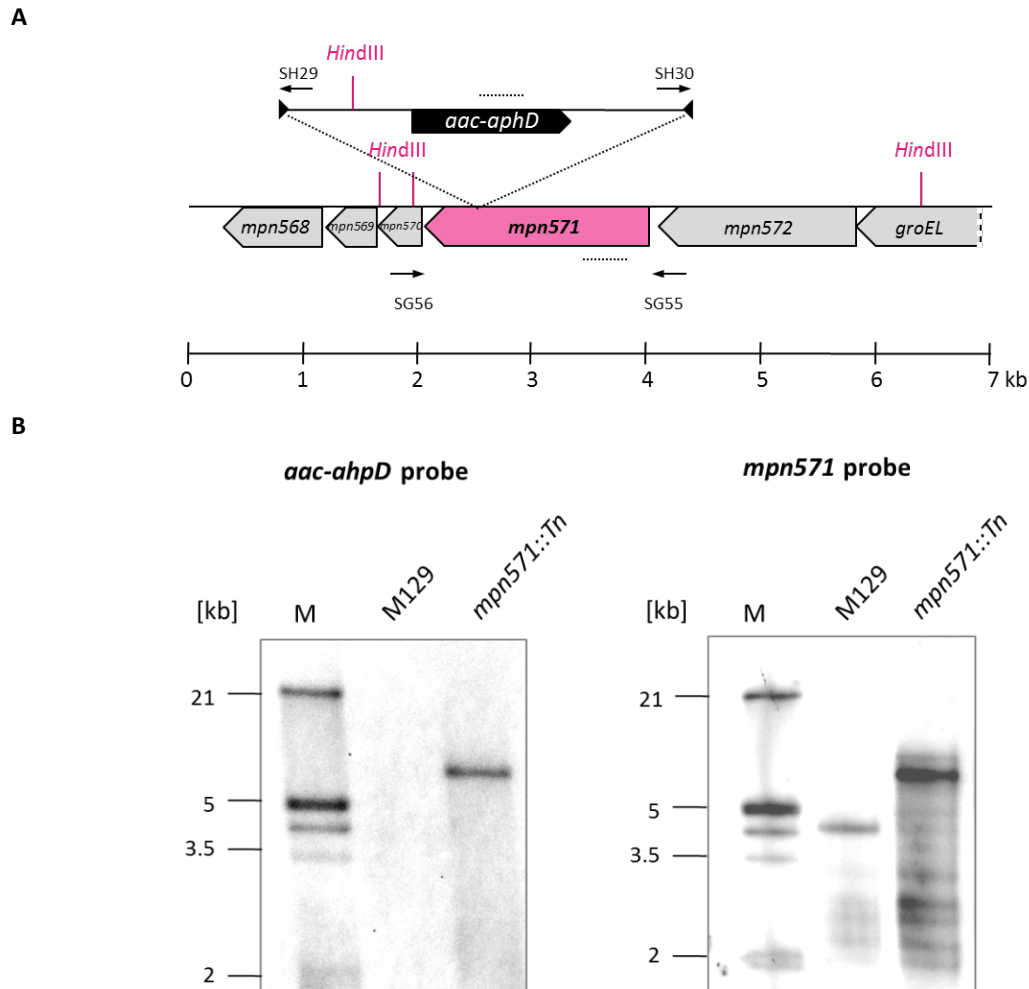
Fig. 3.6. Scheme and proof of transposon insertion into *mpn571*. A. Genomic organization including the inserted transposon in *mpn571*::Tn. The transposon is depicted to scale. Oligonucleotides used for mutant screen are indicated by arrows, binding sited of the respective probes are indicated by dotted lines. *Hind*III restriction sited for Southern blots are marked in pink. **B.** Southern blot analysis to prove the insertion of the transposon in *mpn571*. On the left side, hybridization with the *aac-ahpD* probe to the transposon resulted in one band in the *mpn571*::Tn chromosomal DNA lane. After hybridization with the gene-specific probe, a band shift is seen (right).

Implication of mpn159*::Tn and* mpn571*::Tn in growth, hydrogen peroxide production and pathogenicity*

The impact of MPN159 and MPN571 in *M. pnumoniae* growth and pathogenicity was assessed as described earlier. The results are depicted in **Fig. 3.7**. For both knockout strains, no difference in growth behavior as compared to the wild type strain M129 could be observed. This indicates that these proteins are, at least *in vitro*, dispensable for survival and replication of the cells.

Since hydrogen peroxide has long been regarded as the hemolysin of *M. pneumoniae*, possible roles of the proteins in H_2O_2 production or release were tested by a hydrogen peroxide assay (Somerson, 1965). As a reference, M129 and the *glpD*::Tn mutant were examined as well. Since GlpD is the hydrogen peroxide producing enzyme in *M. pneumoniae*, it has been shown that the respective mutant is incapable of H_2O_2 production with glycerol and glycerophosphocholine as substrates (Hames *et al.*, 2009; Schmidl *et al.*, 2011). As can be seen in **Fig. 3.7 B**, no hydrogen peroxide is produced without addition of a carbon source in all strains. Addition of glucose leads to a very slight H_2O_2 production in all strains which cannot be explained so far. Maximal amounts of H_2O_2 are produced by M129 with glycerol as substrate, which is also true for *mpn571*::Tn. However, not only *glpD*::Tn but also *mpn159*::Tn was not able to produce hydrogen peroxide with glycerol. Using GPC, all strains except for *glpD*::Tn were able to produce intermediate amounts of H_2O_2. The impairment of the *mpn159*::Tn mutant to produce H_2O_2 with glycerol might hint at MPN159 being involved to some extent in the pathogenicity of the bacterium.
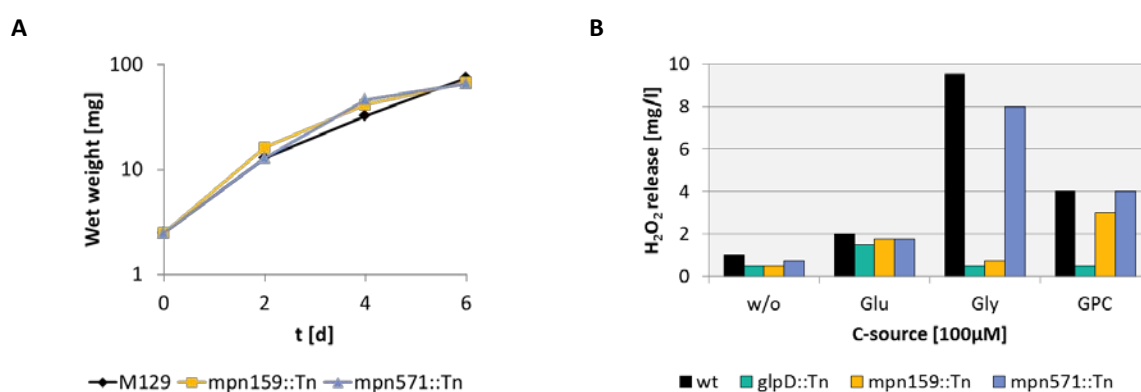
Fig. 3.7. Growth and hydrogen peroxide production of the *M. pneumoniae* wt and *mpn159*::Tn and *mpn571*::Tn mutants. A. Growth curves were performed by inoculating 2.5 mg cells in MP-glucose medium and harvesting after 2, 4 and 6 days of growth. No difference between M129 and the mutant strains is observed. **B.** Hydrogen peroxide assays were done by incubating *M. pneumoniae* cells with 100 μM of several carbon sources and measuring the released H_2O_2 amount using peroxide test strips. The *glpD*::Tn mutant, which cannot produce hydrogen peroxide, served as control.

To pursue the question, if and how MPN159 and MPN571 are involved in cytotoxicity, HeLa cell infection assays were performed (**Fig. 3.8**). The HeLa cell control grew plain in the well. Incubation with M129 and *mpn571*::Tn led to a complete destruction of the HeLa cell layer except for a clot in the middle. The calculated cytotoxicity of both strains accounted for more than 80 and 70%, respectively. This percentage might actually be higher, since the value was probably slightly adulterated by the clot in the middle of the well. As in the experiments before, the behavior of the *mpn571*::Tn mutant did not differ from the wild type. The *glpD*::Tn mutant, which was proven to have a strongly reduced cytotoxicity due to a lack of hydrogen peroxide production, behaved as expected (Hames *et al.*, 2009). This was also true for the *mpn159*::Tn mutant. For both strains, a high amount of HeLa cells survived during the assay and the cytotoxicity was reduced to about 25%. This probably matches the result of the H_2O_2 test, since hydrogen peroxide is the major toxin of *M. pneumoniae*.

The actual hemolytic effect of the putative hemolysin MPN159 and the putative hemolysin ABC transporter MPN571 were detected by hemolysis assays using the respective mutant strains. The results of these assays are summarized in the following sections.

A
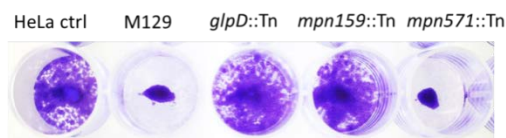
B
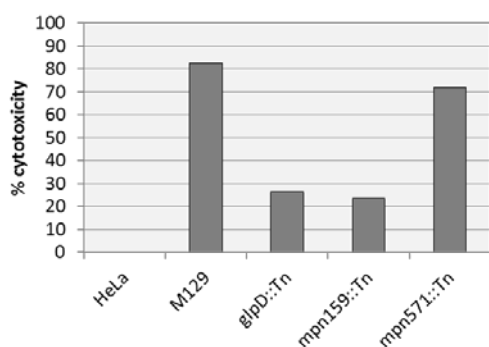
Fig. 3.8. Cytotoxicity assay using HeLa cells. A. Picture of HeLa cells 2 dpi with *M. pneumoniae* M129 and mutant strains. The infected cells were fixed with 4% buffered formalin and stained with crystal violet as described. **B.** Quantification of cytotoxicity calculated in %. The crystal violet bound by intact HeLa cells is solved with 0.1% SDS and measured photometrically at λ = 595 nm. The OD_{595} of the HeLa cell control (HeLa ctrl) was set as 100% surviving cells referring to 0% cytotoxicity. The % cytotoxicity of the *M. pneumoniae* strains was calculated using the OD_{595} set in relation to the control.

3.2. Hemolytic and hemoxidative activities in *M. pneumoniae*

3.2.1 Hemolytic activity of *M. pneumoniae* strains on plates

Analysis of the potential role of MPN159 and MPN571 in hemolysis

MPN571 is annotated as putative hemolysin ABC transporter, while MPN159 is supposed to be a putative hemolysin HlyC. In order to confirm their potential involvement in hemolysis, either as transporter or as hemolysin itself, hemolysis assays with the respective mutant strains on blood agar plates were performed. Assuming the annotation is correct, a lack of the hemolysin MPN159 or the hemolysin transporter MPN571 would result in a non-hemolytic phenotype in their corresponding mutant strains. The results of the blood agar test after two days of incubation are shown in **Fig. 3.9**. All *M. pneumoniae* strains exhibit clear zones of β-hemolysis around their colonies. Due to the black background under the photographed plates, the clear zones appear dark. Neither the *mpn159*::Tn nor the *mpn571*::Tn mutant seems to be impaired in their hemolytic function. Since hydrogen peroxide has been said to be the hemolysin of *M. pneumoniae*, it seemed possible that the halos are mainly caused by H_2O_2 and that its effect exceeds that of the putative additional hemolysin. Therefore, blood agar tests with high amounts of catalase were performed. As can be seen, for none of the strains, addition of catalase was able to abolish the hemolytic effect. This suggests that there is a hemolysin in addition to H_2O_2. However, neither MPN159 nor MPN571 are involved.

Comparative analysis of hemolysis caused by other *M. pneumoniae* strains

In addition to the *mpn159*::Tn and *mpn571*::Tn mutants, the hemolytic effect of the *prkC*::Tn, *glpD*::Tn and *mpn372*::Tn strains in comparison to the lab wild type (M129) was examined. All these proteins are involved in virulence which suggested them to play a potential role in hemolysis as well (Schmidl *et al.*, 2010; Hames *et al.*, 2009; Kannan *et al.*, 2006). However, none of the strains showed a lack of hemolysis (**Fig. 3.10**). Even the *glpD* mutant, which does not produce substantial amounts of hydrogen peroxide, forms halos around their colonies. This, and the fact that the addition of high amounts of catalase (1000 U per plate) did reduce but not abolish the hemolytic effect of the *M. pneumoniae* strains, indicate the presence of a different source of hemolysis.
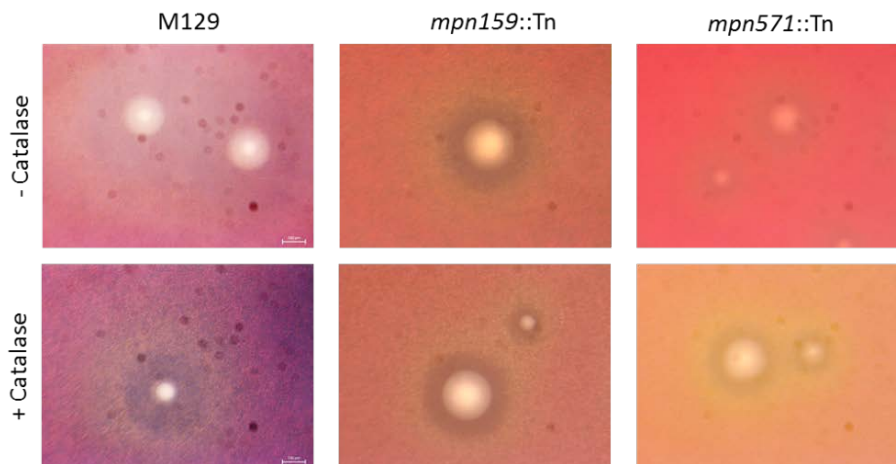
Fig. 3.9. Hemolytic activity of _M. pneumoniae_ M129, _mpn159_::Tn and _mpn571_::Tn strains on blood agar plates. _M. pneumoniae_ was grown on MP-glucose plates for 7-10 days until colonies were visible. The cultures were overlaid with 5 ml of blood agar and incubated for two more days at 37°C. The blood agar consisted of 2% defibrinated sheep blood and 0.75% agar in PBS with or without 1000 U catalase per plate. Pictures were taken using the Lumar V.12 stereo fluorescence microscope (Zeiss). Scale bar = 100 µm.

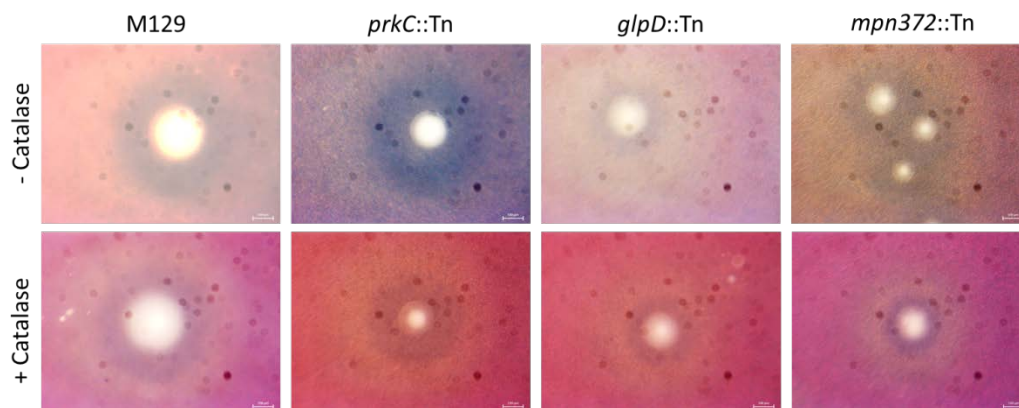**Fig. 3.10. Hemolytic activity of M129, _prkC_::Tn, _glpD_::Tn and _mpn372_::Tn strains on blood agar plates.** _M. pneumoniae_ was grown on MP-glucose plates for 7-10 days and subsequently overlaid with blood agar as described above. Scale bar = 100 µm.

3.2.2 Hemolysis and hemoxidation in liquid blood culture

Assessment of hemoxidative activity in reaction tubes

To get more insight into the hemolytic activities, blood lysis was also examined in liquid culture. For this purpose, 5% defibrinated sheep blood in PBS was incubated with *M. pneumoniae* strains of an $OD_{550} = 1$ in a glass reaction tube at 37°C and gentle shaking overnight. To estimate the effect of H_2O_2 on hemolysis, the assay was done with and without catalase. After incubation, the sedimented pellets were photographed, resuspended and photographed again. The results are shown in **Fig. 3.11**.
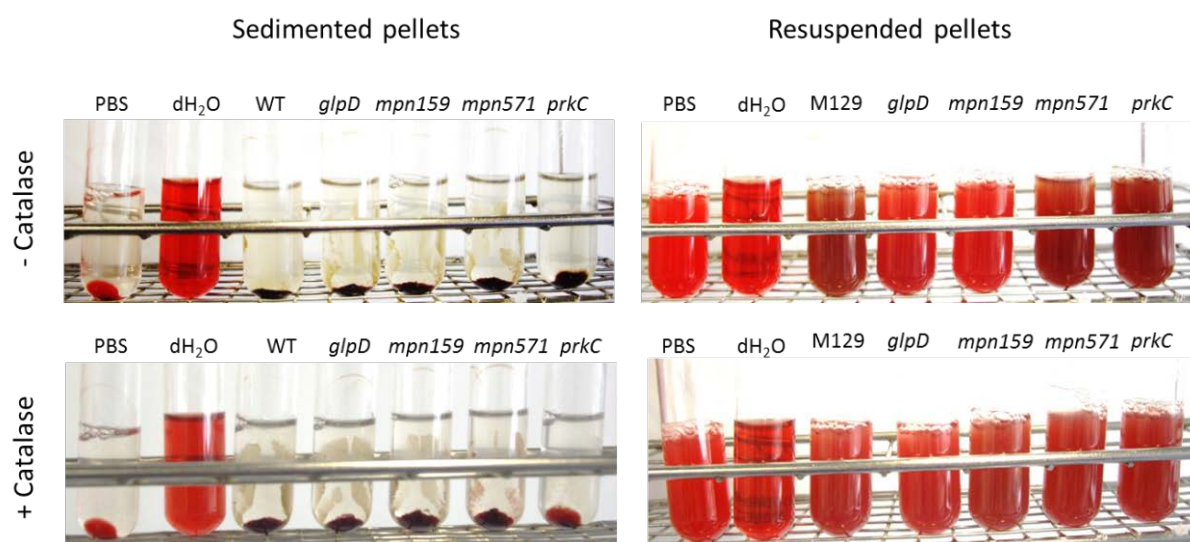
Fig. 3.11. Hemolysis assay with liquid blood culture. *M. pneumoniae* cells of an $OD_{550} = 1$ were incubated with 5% sheep blood in PBS with or without 500 U catalase. The sedimented pellets after overnight incubation (left) were photographed and subsequently resuspended. Pictures were taken of the resuspended pellets (right). Control samples are 5% blood in PBS (left most tube) as hemolysis negative control and 5% blood in dH_2O as hemolysis positive control.

The sedimented pellet of the negative control consisting of 5% sheep blood in PBS had a bright red color and a smooth consistence. The pellet contains the intact red blood cells including the hemoglobin whereas the supernatant is clear. In contrast, the positive hemolysis control, which consisted of 5% sheep blood in dH_2O, did not show a pellet, since all the erythrocytes were lysed in water, releasing their hemoglobin into the supernatant. As for the negative control, the hemoglobin of the positive control had a bright red color. On the contrary, the sedimented pellets of all cultures infected with *M. pneumoniae* strains had a viscous and clotted texture and a brownish color indicating that α-hemolysis (hemoxidation) had occurred. Interestingly, this was also the case in the samples containing catalase. The supernatant in all samples was clear which means that all hemoglobin is kept

inside the erythrocytes of the pellet and no "real" (β-) hemolysis occurred. After resuspension of the pellets, the hemoxidizing effect of the *M. pneumoniae* cells got even more visible in the brownish discoloration of the blood samples. All strains were able to oxidize hemoglobin, with *glpD*::Tn and *mpn159*::Tn having a slightly reduced hemoxidative effect, which might correlate with their impaired H_2O_2 production. Addition of catalase seemed to result in slight reduction of hemoxidation but the brown discoloration as compared to the control samples was still present.

Spectrophotometric measurements of hemoglobin

Hemoxidation can be examined in detail by measuring the absorption spectra of hemoglobin in the respective samples. Therefore, 1 ml of the blood solution was centrifuged, to pellet the red blood cells, and the supernatant was removed. The pellet was lysed in 1 ml dH_2O to dissolve the hemoglobin and 100 μl of that solution were used in a microtiter plate to photometrically measure the hemoglobin spectrum. **Fig. 3.12** displays the spectra of hemoglobin after incubation with M129 and different amounts of catalase (0, 500, 5000 units). The classic hemoglobin spectrum (black) has one huge peak at about 410 nm and two smaller ones at about 530 and 570 nm. After incubation with M129, the peak at 410 nm slightly shifted to the left, the peaks at 530 and 570 nm decreased and a new peak appeared at about 630 nm **(Fig. 3.12)**. This pattern of peaks is typical for oxidized hemoglobin. As can be seen, even the addition of 5000 U of catalase did not seem to alter the peaks at 530, 570 and 630 nm in comparison to the "M129" sample (yellow) indicating that hemoxidation is not only caused by hydrogen peroxide.

Taken together, *M. pneumoniae* is able to perform hemolysis on blood agar plates, which is mainly independent from hydrogen peroxide production, whereas no complete hemolysis occurs after overnight incubation in liquid culture. Instead, clumping of red blood cells and strong hemoxidation can be seen in liquid culture, which cannot be abolished by addition of catalase. These results suggest that *M. pneumoniae* possesses a hemolysin different from hydrogen peroxide and which acts on blood agar plates but not in liquid culture.
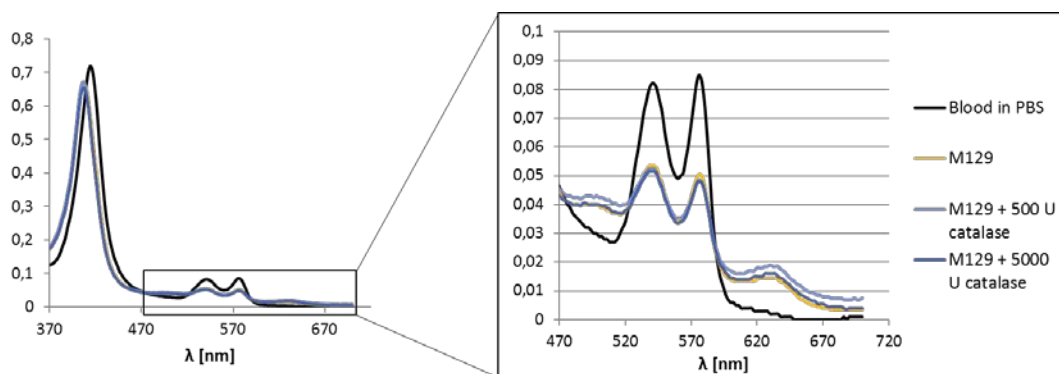
Fig. 3.12. Spectra of hemoglobin incubated with *M. pneumoniae* M129 without and with different amounts of catalase. Complete spectrum of hemoglobin recorded from 370 to 700 nm (left) and detailed section of the spectra from 470 to 700 nm (right box). The black curve is the lysed control of 5% sheep blood in PBS. The spectrum was recorded in the SynergyMX platereader from BioTek.

3.2.3 Test for efficiency and effect of catalase

In order to confirm the functionality of the applied catalase and to exclude a hemoglobin altering effect by the catalase itself, H_2O_2 assays using test strips and hemoglobin spectra with addition of various units of catalase were performed. In **Fig. 3.13 A**, the y-axis is cut off at 25 mg/l H_2O_2 since the test strips could not detect a higher concentration. Nevertheless, the effect of catalase is perfectly seen with lower concentrations of H_2O_2. The presence of 10-40 U catalase is sufficient to erase 10 mg/l H_2O_2 (**Fig. 3.13 A**). Also, the initially added 100 mg/l hydrogen peroxide are consistently degraded by 10-40 U catalase. After 120 min incubation, the catalase setups were retreated with the respective hydrogen peroxide amounts to mimic the steady production of H_2O_2 by *M. pneumoniae* in a hemolysis assay. Since the initial amount of additional 10 mg/l is reduced after 180 min incubation, the catalase can be assumed active. Incubation of the respective hydrogen peroxide levels with 1000-4000 U catalase completely abolished their detection in the assay indicating that the catalase successfully converted all externally applied H_2O_2 even after repeated addition (data not shown). A hemolysis assay using 5% sheep blood in PBS with and without addition of 500 U or 5000 U catalase was performed to exclude a hemoxidative effect of catalase itself. In both cases, the presence of catalase does not alter the hemoglobin spectrum which indicates that the hemoxidative effect described above is only committed to the *M. pneumoniae* cells.

A

B
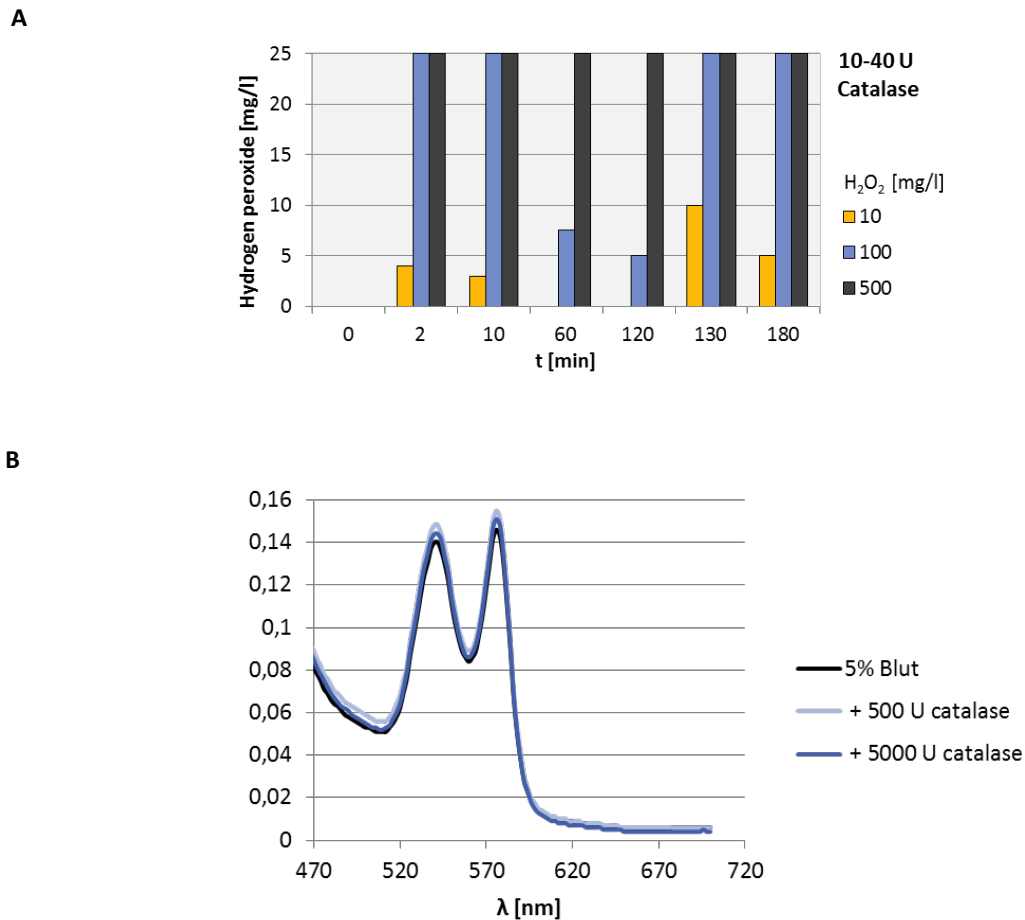
Fig. 3.13. Hydrogen peroxide assay and hemolysis assay with addition of catalase. A. 10, 100 and 500 mg/l hydrogen peroxide were used and incubated with $10 - 40$ U catalase. After 120 min incubation at 37°C, the same amount of hydrogen peroxide was added again to see if the catalase retained active. **B.** Spectrum of hemoglobin incubated with high 500 U or 5000 U of catalase, respectively. No change in spectrum as compared to the control can be observed.

A   **B**
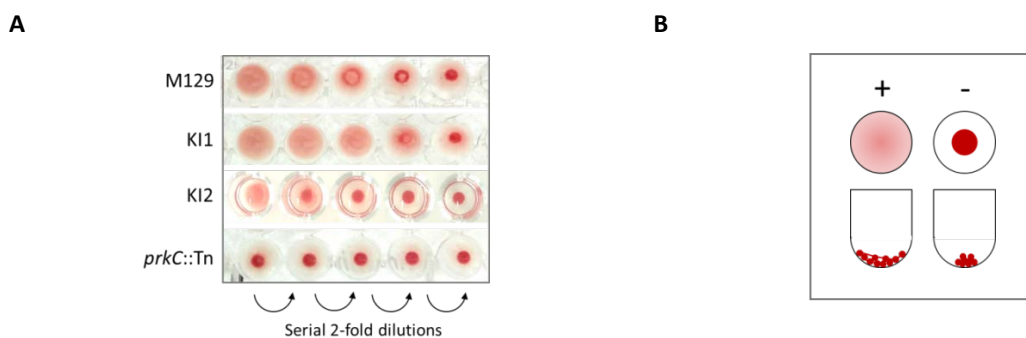
Fig. 3.14. Hemagglutinating effect of *M. pneumoniae* strains. A. Hemagglutination assay in a 96-well microtiter plate. Starting with 100 µl of a mycoplasma culture with an $OD_{550} = 5$ in the left most well, serial twofold dilutions in PBS were prepared. 2% sheep blood in PBS was added and the plate was incubated at 37°C without shaking. **B.** Scheme of agglutinated (+) and non-agglutinated (-) red blood cells. During hemagglutination, red blood cells form a connected, net-like structure covering the bottom of the well. Without hemagglutination, single red blood cells sink to the bottom which can be observed as a small red dot.

3.2.4 Hemagglutination

To address the question why the blood pellet is tough and clotted after incubation with Mycoplasma cells in contrast to the control pellet, the hemagglutinating effect of the cells was tested. Hemagglutination is a process in which the red blood cells are clumped and connected to a net-like structure **(Fig. 3.14 B)**. It is usually caused by viruses and antibodies, but also by some bacteria (Neter *et al.*, 1954). For that, serial twofold dilutions of *M. pneumoniae* suspensions were prepared in a round-bottom 96-well plate and incubated with 2% sheep blood in PBS at 37°C. When hemagglutination occurs, the red blood cells cover the whole bottom of the well due to their net-like connection. When no hemolysis occurs, the red blood cells sink to the bottom to form a little red dot. As can be seen in **Fig. 3.14 A**, the wild type M129 and the clinical isolate KI1 have a hemagglutinating effect. In contrast, the clinical isolate KI2 and the *prkC* mutant strain are strongly impaired in hemagglutination. Since both strains exhibit an adhesion deficient phenotype, it seems conclusive that these *M. pneumoniae* cells cannot bind to and thereby connect the red blood cells.

3.2.5 Microscopic analyses of blood

Red blood cells typically exhibit a "donut" shaped cell form, a biconcave disk with a flattened center. However, they can assume different shapes upon exposure to certain kinds of stress or membrane altering effects. In order to see which effect *M. pneumoniae* cells have on erythrocytes, microscopic analyses of blood cultures with or without *M. pneumoniae* cells were performed. Blood smears were prepared, fixed by heat and examined under the microscope. **Fig. 3.15** shows two independent experimental setups. The upper panel and the lower panel, respectively, represent one experiment. In **A** and **C**, pure blood cells in PBC can be seen. They show their typical regular round shape which is called discocyte. In contrast, a high proportion of red blood cells that were incubated with *M. pneumoniae* M129 (**B** and **D**), possess an irregular, rather "prickly" shape which can be caused by lipid depletion in the RBC membrane or by osmotic imbalance and might have severe effects on the integrity of erythrocytes (see section 4.3.3).
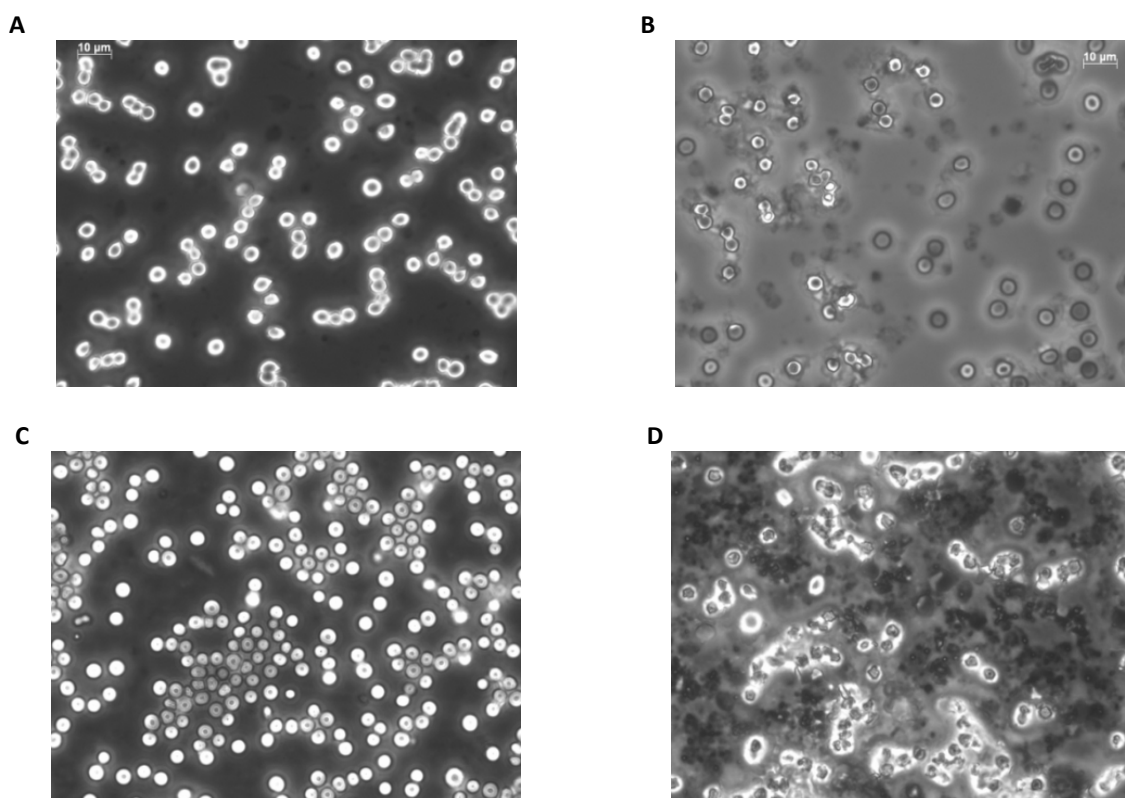
Fig. 3.15. Phase contrast microscopic images of blood cells after overnight incubation with or w/o *M. pneumoniae* cells from two independent experiments. **A** and **C**. Blood cells w/o *M. pneumoniae*. **B** and **D**. Blood samples after incubation with *M. pneumoniae* strains. All pictures were taken at the same magnification with the Axioskop 40 FL fluorescence microscope (Zeiss). Scale bar is 10 µM.

3.2.6 Cysteine-dependent hemolysis and hemoxidation

In many bacteria, like *Streptococcus pneumoniae*, hemolysins are oxygen-labile. Since *M. pneumoniae* strains were found to cause hemolysis only on blood agar plates in the absence of oxygen and not in liquid culture where oxygen is present, the existence of an oxygen-labile hemolysin in *M. pneumoniae* was considered. To test this option, hemolysis assays in liquid blood culture were performed with addition of cysteine as reducing agent to protect the potential hemolysin from oxygen.

Figures 3.16 – 3.20 present the outcome after RBC incubation with the *M. pneumoniae* strains for 1h and 18 h, respectively. **A** and **B** show independent experiments. **Fig. 3.21** shows the control samples which were incubated with the same additives except for the *M. pneumoniae* cells to rule out an effect being caused by glycerol, G3P or cysteine alone. As can be seen in the control, only addition of 10 mM cysteine led to a very slight hemoxidation after 18 h of incubation. For all the strains, incubation for 1 h did not lead to hemolysis in any of the samples, since the supernatant (S) was clear and the pellet (P)

contained the hemoglobin. However, all strains, except for *glpD*::Tn, caused hemoxidation with glycerol already after 1 h. This can be recognized by the brown color in the respective pellet wells (**A**) and the change of peaks at 530, 570 and 630 nm in the spectrum of hemoglobin (**B**) as the result of a high production of hydrogen peroxide which strongly oxidizes hemoglobin. Expectedly, this was not possible in the mutant lacking the hydrogen peroxide producing enzyme GlpD. Remarkably, the clinical isolate 2 (KI2) was also able to oxidize hemoglobin with 1 mM and 10 mM cysteine after a short incubation time. After 18 h, all strains exhibited a slight hemoxidative effect which was even observed without addition of glycerol or cysteine. This indicates that, indeed, red blood cells per se do contain substrates leading to hemoxidation by *M. pneumoniae*. As expected from the results after 1 h incubation, this hemoxidative activity was enhanced in the presence of glycerol leading to strongly oxidized hemoglobin and partial hemolysis after 18 h of incubation time. Again, this was not true for the *glpD*::Tn mutant. Interestingly, addition of 1 mM and 10 mM cysteine also led to a strong oxidation of hemoglobin by all strains after 18 h. In addition, the presence of 10 mM cysteine caused nearly complete hemolysis in all strains. This can be recognized by the red-brown supernatant and the bright pellet fractions in the respective wells and by the high hemoglobin peaks in the supernatant spectra which are proportionately reduced in the pellet spectra. Surprisingly, the hemolytic effect of cysteine in most cases exceeded that of glycerol which suggests that H_2O_2 is not the major hemolysin in *M. pneumoniae* but another compound which is cysteine-dependent. Since addition of cysteine initially caused hemoxidation followed by hemolysis, it can be excluded that cysteine acts a reducing agent which protects a potential oxygen-labile hemolysin. Instead, it implies that cysteine itself is a substrate for the production of a hemoxidative and hemolytic factor which, so far, has not been known in *M. pneumoniae*.

Another surprising aspect is the strong hemoxidation and hemolysis that is caused by M129 cells in presence of glycerol-3-phosphate (G3P). In fact, G3P is the substrate for the enzyme GlpD and will therefore lead to production of H_2O_2 and hemoxidation. However, based on results from hydrogen peroxide assays, it has been assumed that *M. pneumoniae* cannot take up G3P (Schmidl *et al.*, 2011). These present data strongly suggest that G3P can be utilized by *M. pneumoniae* M129 cells leading to strong hemoxidation and hemolysis.
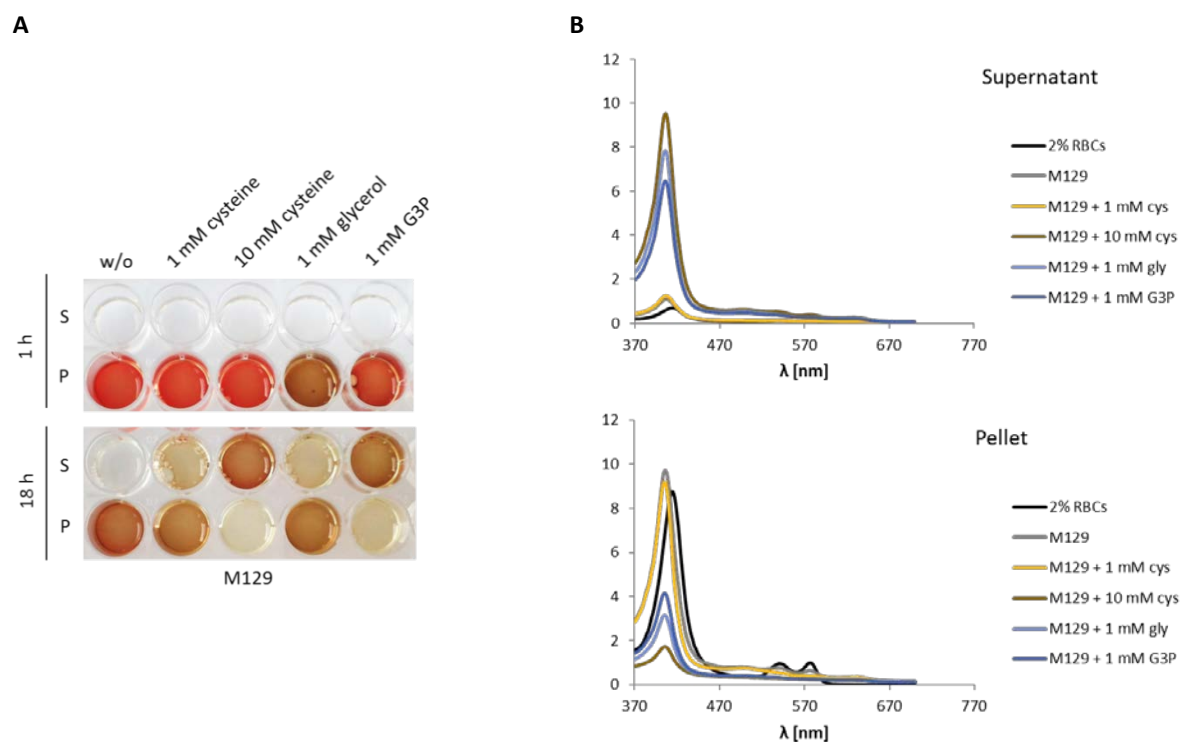
Fig. 3.16. Heme assays with M129 and 2% RBCs in PBS. A. Pictures of supernatant (S) and pellet (P) fractions of the blood samples in a 24-well-plate. **B.** Spectra of hemoglobin in the supernatant and the pellet, respectively, after 18 h of incubation. Cys: cysteine; gly: glycerol; G3P: glycerol-3-phosphate
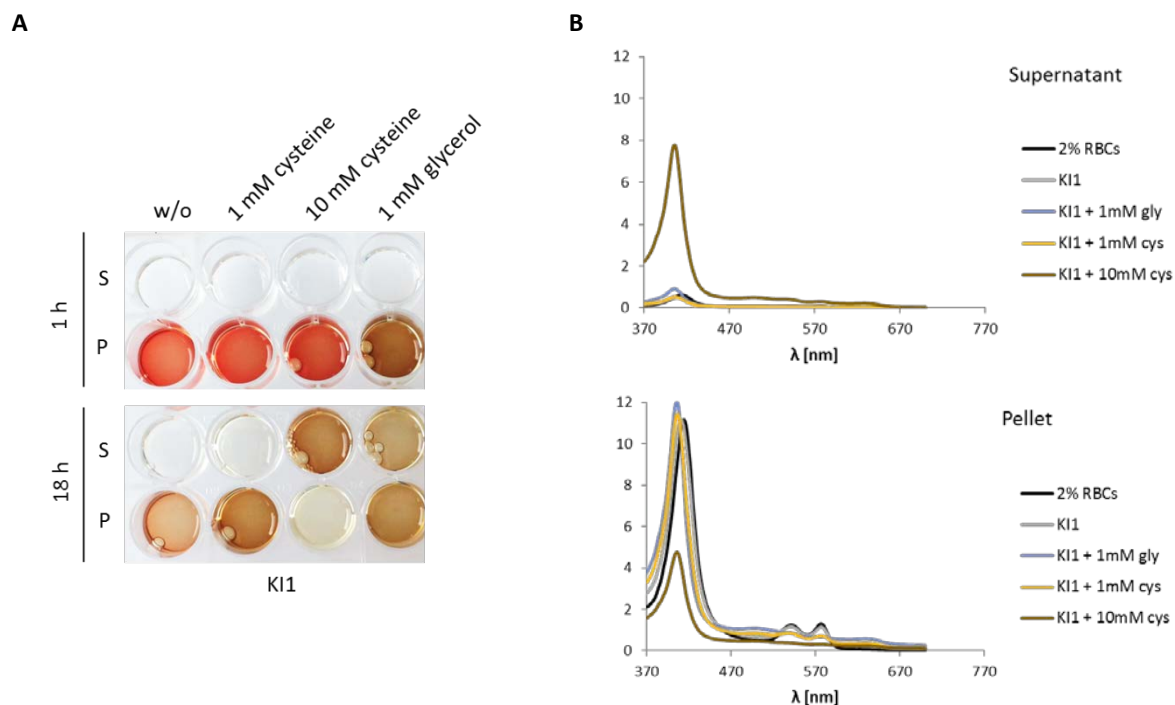
Fig. 3.17. Heme assays with clinical isolate KI1. A. Supernatant (S) and pellet (P) fractions of the blood samples photographed in a 24-well-plate. **B.** Spectra of hemoglobin of supernatant and pellet after 18 h incubation.
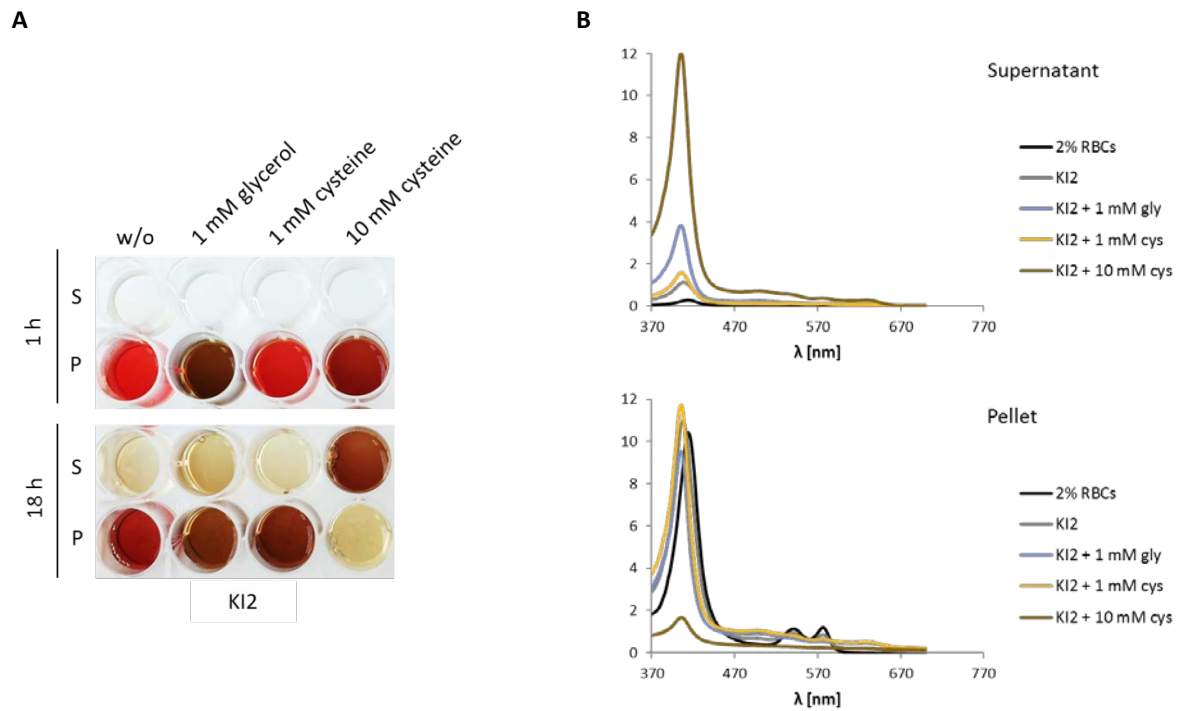
Fig. 3.18. Heme assays with clinical isolate KI2. A. Supernatant (S) and pellet (P) fractions of the blood samples in a 24-well-plate. **B.** Spectra of hemoglobin of supernatant and pellet after 18 h incubation.
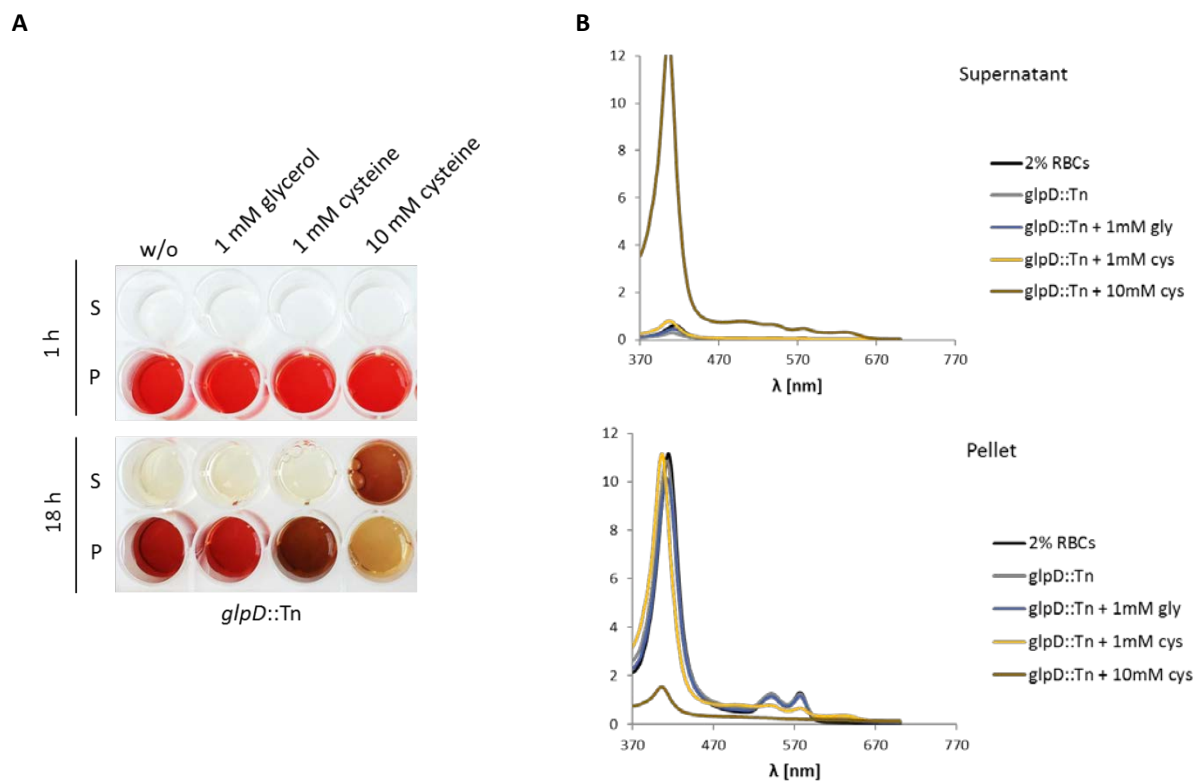
Fig. 3.19. Heme assays with *glpD*::Tn. A. Supernatant (S) and pellet (P) fractions of the blood samples photographed in a 24-well-plate. **B.** Spectra of hemoglobin of supernatant and pellet after 18 h incubation.
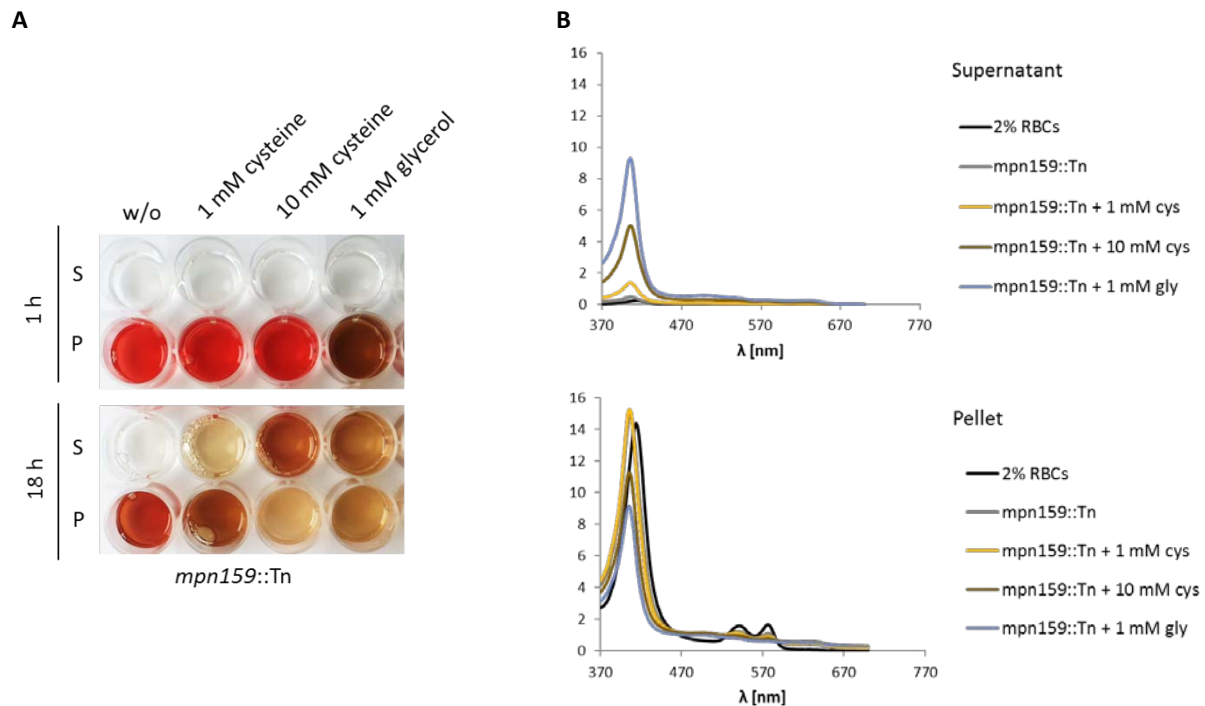
Fig. 3.20. Heme assays with *mpn159*::Tn. A. Photos of supernatant (S) and pellet (P) fractions of the blood samples in a 24-well-plate. **B.** Hemoglobin spectra of supernatant and pellet after 18 h incubation. **A.** and **B.** show independent experiments
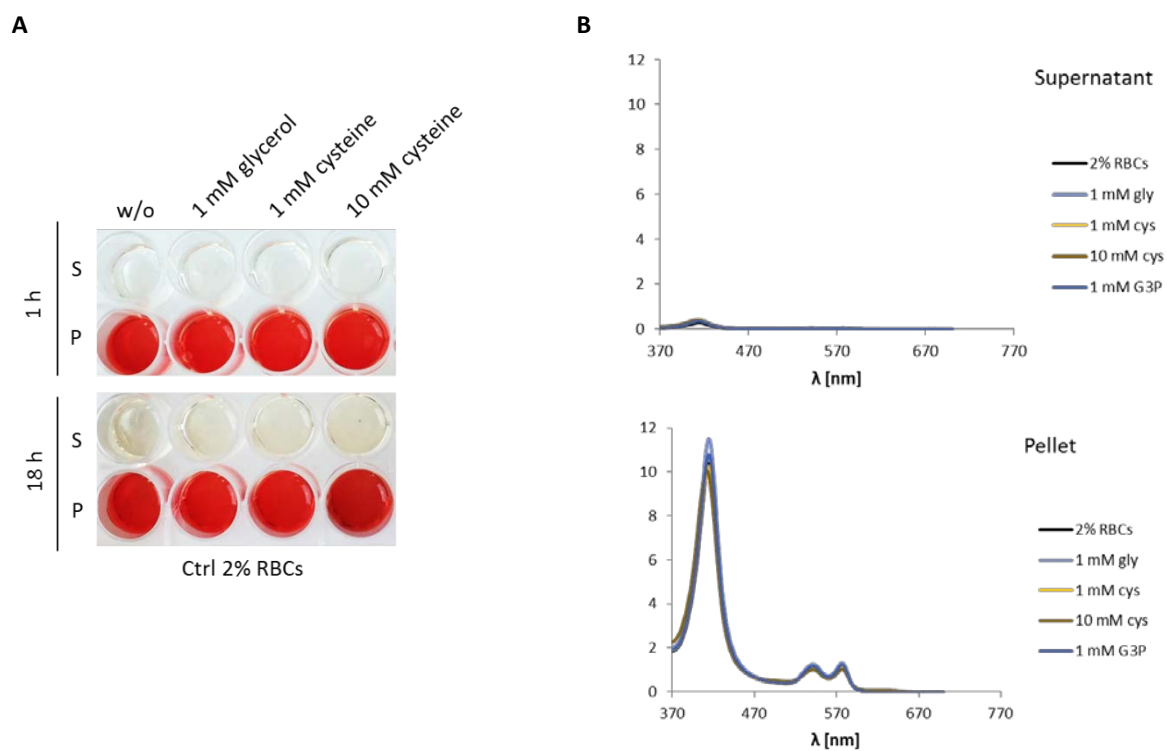
Fig. 3.21. Control heme assays with*out M. pneumoniae* cells. A. Supernatant (S) and pellet (P) fractions of the blood samples in a 24-well-plate. **B.** Hemoglobin spectra of supernatant and pellet after 18 h incubation.

87

3.2.7 H₂S production in *M. pneumoniae*

Cysteine-mediated hemoxidation and hemolysis is a feature of a variety of oral pathogenic bacteria, like *Treponema denticola*. These pathogens produce hydrogen sulfide from cysteine by enzymes called L-cysteine desulfhydrases. In order to clarify if the cysteine-dependent hemoxidation and hemolysis in the *M. pneumoniae* strains can be caused by hydrogen sulfide production of the bacterium, several H₂S tests were performed. At first, simple lead acetate strips were used. *M. pneumoniae* M129 cultures were incubated with cysteine over night at 37°C in Eppendorf tubes containing a lead acetate strip wedged under the lid. The gaseous hydrogen sulfide reacts with the lead on the strips to give a black discoloration. In fact, an increasing dark color change can be seen on the strips that were incubated with M129 and 3, 6 and 12 mM cysteine, respectively **(Fig. 3.22 A)**.
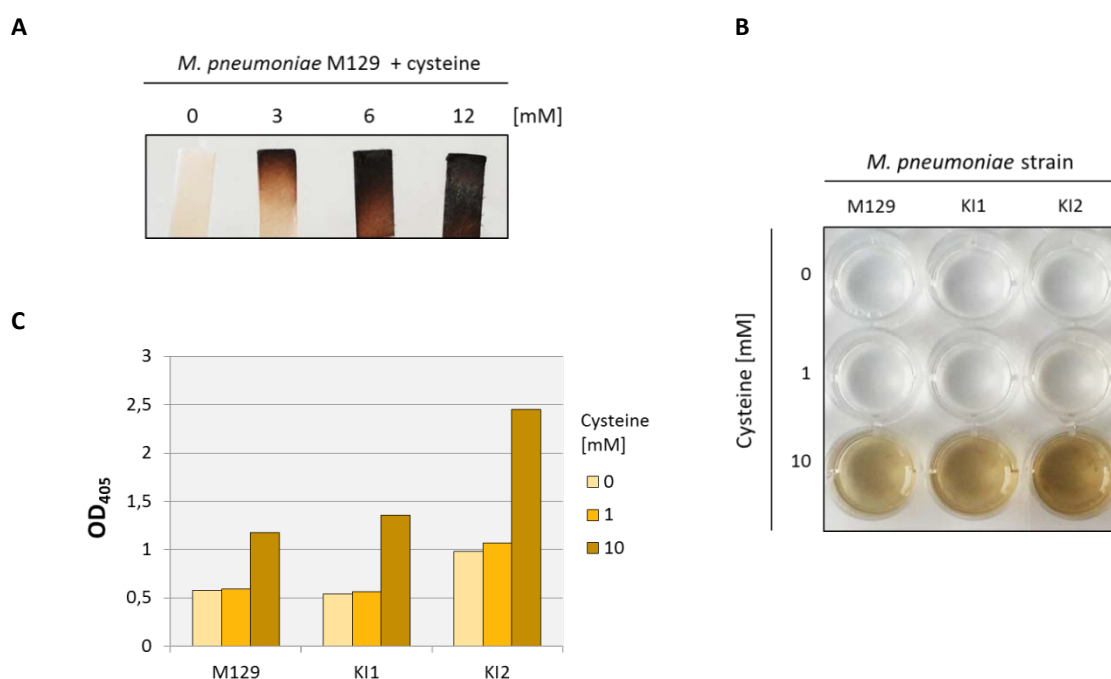
Fig.3.22. Hydrogen sulfide assays with *M. pneumoniae* strains. A. Incubation of M129 in PBS with different concentrations of cysteine and lead acetate strips overnight. The black discoloration results from PbS formation after reaction of lead with hydrogen sulfide. **B.** and **C.** Bismuth sulfide assays with M129 and clinical isolates 1 and 2 and different L-cysteine concentrations. Bismuth reacts with hydrogen sulfide to Bi₂S₃ which forms a dark precipitate. **B.** shows photos of an overnight incubation of *M. pneumoniae* strains in BiCl₃ solution. **C.** presents photometric measurements of solutions in B. Bi₂S₃ can be measured at 405 nm.

To compare the hydrogen sulfide production in the clinical isolates KI1 and KI2 with the lab wild type M129, the bismuth chloride assay was chosen. In this assay, freshly harvested *M. pneumoniae* cells are

resuspended in an assay mixture containing bismuth chloride ($BiCl_3$). Bismuth can react with sulfide similar to the lead on the strips mentioned above. The release of hydrogen sulfide by the *M. pneumoniae* cells would lead directly to a reaction with the $BiCl_3$ in the solution resulting in the formation of black Bi_2S_3. This precipitate can be measured photometrically. In **Fig. 3.22 B and C**, the hydrogen sulfide assay and its photometric measurement are shown. As can be seen, the results for 0 mM and 1 mM cysteine were nearly identical in all strains. Apparently, 1 mM cysteine was not sufficient for the cells to produce detectable amounts of hydrogen sulfide. However, in the presence of 10 mM cysteine, the brown precipitate was easily visible in all strains. The H_2S production rates of the laboratory wild type strain M129 and the clinical isolate KI1 appeared to be similar. In contrast, the clinical isolate KI2 seemed to form slightly increased amounts of hydrogen sulfide.

3.3. Characterization of MPN487

In many oral pathogens, hydrogen sulfide is produced by enzymes called L-cysteine desulfhydrases. These pyridoxal-5'-phosphate dependent desulfhydrases convert L-cysteine to NH_4^+, pyruvate and H_2S. In *M. pneumoniae*, no such enzyme is present. However, it possesses the putative L-cysteine desulfurase, MPN487, which is supposed to use L-cysteine for Fe-S-cluster biogenesis. In this section, the characterization of MPN487 and its unexpected role as H_2S producing enzyme is described.

3.3.1 Expression of *mpn487* in *E. coli* and purification of *Strep*-tagged proteins

The gene *mpn487* and the adjoining gene *mpn488*, which is supposed to be a scaffold protein following MPN487 in Fe-S-cluster formation, were expressed in *E. coli* BL21 and subsequently purified. For that, both genes were cloned into the overexpression vector pGP172. This vector places the gene of interest under control of a T7 promoter. Upon addition of IPTG to the BL21 culture carrying the plasmid, the expression of the T7 polymerase in the BL21 strain is induced, and the gene can be transcribed with a high rate. Moreover, overexpression form pGP172 fuses an N-terminal *Strep*-tag to the protein which allows its purification via a *Strep*-Tactin-sepharose-column.

Cloning of *mpn487* into pGP172 and MMR

The gene *mpn487* was amplified from chromosomal DNA of M129 in a PCR using the oligonucleotides SG142 and SG143 (see Appendix **Tab. 7.1**). The product was cut with *Sac*I and *Bam*HI and cloned into the *Bam*HI and *Sac*I digested vector pGP172 resulting in pGP2245. Since *mpn487* contained one TGA codon for tryptophan, a multiple mutation reaction (MMR) of *mpn487* had to be performed using pGP2245 and the primers SG142, SG143 and SG144 to mutate the A on position 345 to a G. This way, the TGA codon is converted to a TGG codon which codes for tryptophan in both *M. pneumoniae* and *E. coli*, ensuring a correct expression of the gene in BL21. The MMR product was digested as described above and cloned again into pGP172. The resulting vector was designated pGP2246 and used for overexpression and purification later.
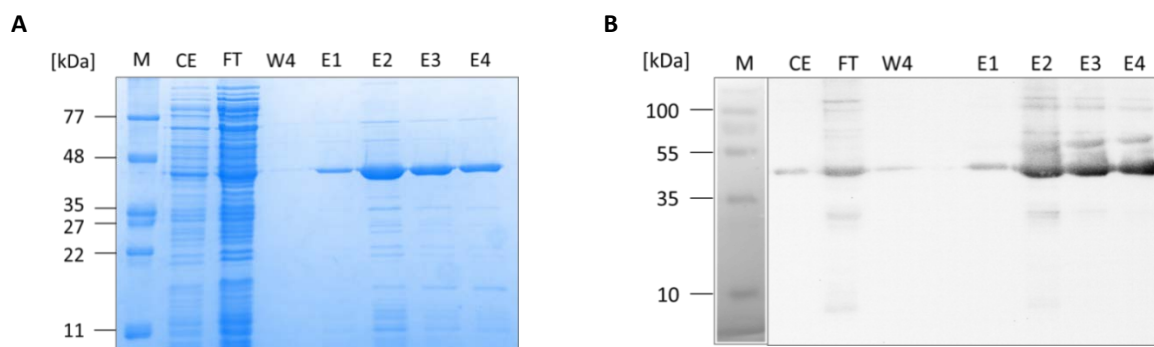
Fig. 3.23. *Strep*-tag purification and Western blot of *Strep*-MPN487. A. Coomassie stained 12% SDS gel of the purification fractions. Only the 46-kDa protein MPN487 is eluted from the column in fractions E2-E4. **B.** Western blot with an α-*Strep* antibody. A 12% SDS gel was run after purification of the protein and the blot was performed using an antibody against the *Strep*-tag fused to the protein MPN487. M: marker, CE: crude extract, FT: flow through, W4: washing fraction 4, E1-4: elution fractions 1-4.

Purification and Western blot

After overexpression and harvest of the BL21 cells, the respective proteins were purified using their *Strep*-tag. Afterwards, a Western blot was performed to confirm the existence of the *Strep*-tagged protein in the elution fractions. For *Strep*-MPN487, the purification procedure was successful. A high amount of protein with only a little background could be eluted from the *Strep*-Tactin sepharose column (**Fig. 3.23**). The Western blot proved the presence of a *Strep*-tag in the elution fractions at the size of MPN487.

3.3.2 Enzymatic assays

To find out, if MPN487 is the responsible enzyme for hydrogen sulfide production in *M. pneumoniae*, several enzyme assays were performed. Moreover, the identity of the protein as L-cysteine desulfurase or L-cysteine desulfhydrase was attempted to be clarified by determining the additional products of the enzyme reaction.

Assay of H_2S formation

Hydrogen sulfide production can be measured by two different methods. One is the methylene blue method, the second is the $BiCl_3$ assay. Since none of these methods had been applied before in this laboratory, both were tested. To quantify the amount of hydrogen sulfide, standard curves had to be prepared for each method using sodium sulfide (Na_2S). Finally, to determine the enzymatic characteristics of MPN487, kinetic studies were performed.

Preliminary tests for H_2S production using methylene blue and $BiCl_3$ assays

Prior to elaborate enzyme assays, it should be given a trial, if in fact hydrogen sulfide can be detected and if the desired methods for detection, which had not been established in this laboratory so far, are working. For this, 5 and 12 µg of the purified MPN487 were used in methylene blue and $BiCl_3$ assays as described in 2.2.9 with 24 mM cysteine as substrate. As depicted in **Fig. 3.24**, hydrogen sulfide could be detected in the samples containing purified enzyme. In the controls, which contain only 24 mM L-cysteine without enzyme, no H_2S formation was detected. This proves that MPN487 is a hydrogen sulfide producing enzyme in *M. pneumoniae* and that its function is obviously not inhibited by the N-terminal *Strep*-tag. In the methylene blue assays, the typical spectrum for methylene blue appeared and could be applied for quantification using the peak at OD_{670}. In the $BiCl_3$ test, the Bi_2S_3 amount that results from reaction of bismuth with the produced sulfide is measured. This assay gave results that are very similar to those of the methylene blue assay, indicating that both methods work and could be used in parallel to determine enzyme characteristics. Since the methylene blue method is the primary method that is used for hydrogen sulfide quantification in enzyme assays in literature, this assay was initially chosen for the following tests.

A

B

C
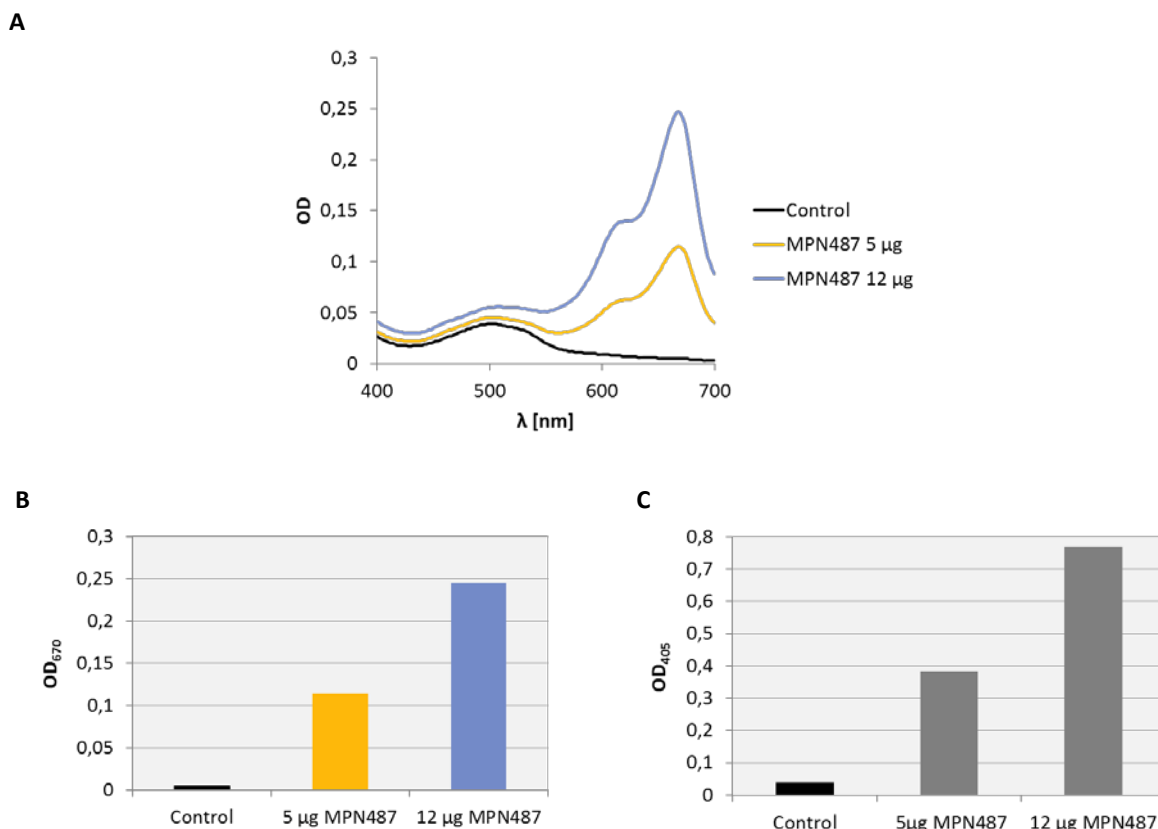
Fig. 3.24. First tests for H₂S production of the purified enzyme directly after *Strep*-tag purification. A. Typical spectrum of methylene blue for H$_2$S detection. The peak at 670 nm represents the wavelength at which the methylene blue complex referring to the amount of H$_2$S can be measured. **B.** Optical density of the methylene blue complex at OD$_{670}$ for the respective samples from the purification steps. **C.** Bismuth chloride assay to prove hydrogen sulfide production of the purified enzyme. The amount of Bi$_2$S$_3$ is measured at OD$_{405}$. A negative control without addition of proteins, and two different amounts of MPN487 were used in each test.

In the next step, the enzymes as well as the assays had to be tested for their functionality with different amounts of cysteine as substrate. For this, 2 µg of purified MPN487 were used in the methylene blue and the BiCl$_3$ setups and the OD was determined after to 2 h of incubation at λ = 670 or 405 nm, respectively. The results are shown in **Fig. 3.25.** In the BiCl$_3$ assay, the OD$_{405}$ increased with increasing cysteine concentrations, which shows that more hydrogen sulfide could be produced by the enzyme and detected in the assay. In contrast, the methylene blue assay only seemed to work for very low cysteine concentrations. Higher amounts of cysteine probably inhibit the complex formation of color development of methylene blue. Since enzyme kinetics needs to make use of different substrate concentrations, the BiCl$_3$ assay was the method of choice for further characterization of the enzyme.
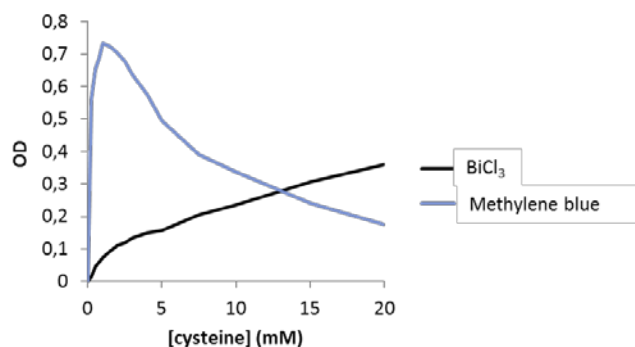
Fig. 3.25. Comparison of BiCl₃ and methylene blue assays for hydrogen sulfide production with different concentrations of cysteine in the experimental setup. In both reactions, 2 µg MPN487 were used. The OD was measured at λ = 405 nm for Bi_2S_3 and at λ = 670 nm for the methylene blue assay.

Preparation of a Na₂S standard curve

In order to relate the optical density measured in the BiCl₃ assays to the respective sulfide concentration, sulfide calibration curves were prepared (**Fig. 3.26**). For that, sodium sulfide was used as substitute for hydrogen sulfide, since this substance is not gaseous and more convenient to handle. Different concentrations of Na₂S were applied in a BiCl₃ assay setup without cysteine or enzyme and the resulting OD was measured at λ = 405 nm. The deriving slope of y = 0.0011x is later used for calculation of hydrogen sulfide amounts produced by MPN487 in the respective assays. As can be seen, the assay works fine in a range of 0 – 250 mM sulfide. Only with sulfide concentrations above 250 mM it starts to get slightly insensitive and imprecise
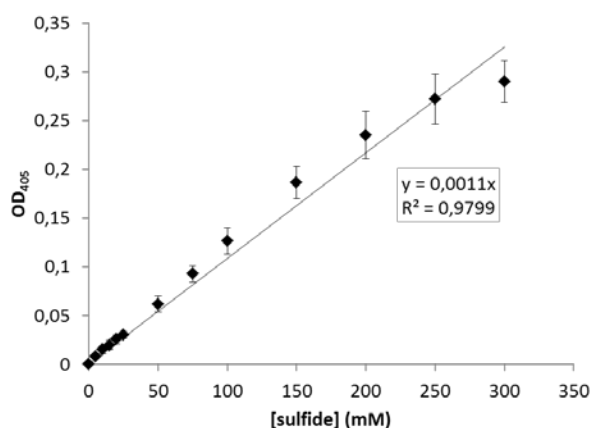
Fig. 3.26. Sulfide calibration curve using different concentrations of Na₂S. The slope of the curve delivers a linear relation between the sulfide concentration and the measured OD at λ = 405 nm. This can be used for quantification of hydrogen sulfide amounts in the following enzyme assays.

Kinetic properties of MPN487 in a bismuth chloride assay

Using the BiCl₃ assay and the corresponding standard curve, the kinetics of H₂S formation from interaction of MPN487 with different cysteine concentrations were determined (**Fig. 3.27**). 0.5 µg purified enzyme were incubated in 100 µl BiCl₃ assay setups containing different cysteine concentrations. The assay was started by adding the enzyme and the change of absorption at OD₄₀₅ was

measured over 30 min at 37°C in a plate reader. Using the rate of H_2S production, a K_m value of 11.21 and a $V_{max} = 6.9$ µmol H_2S / min / mg enzyme were calculated.

A

B
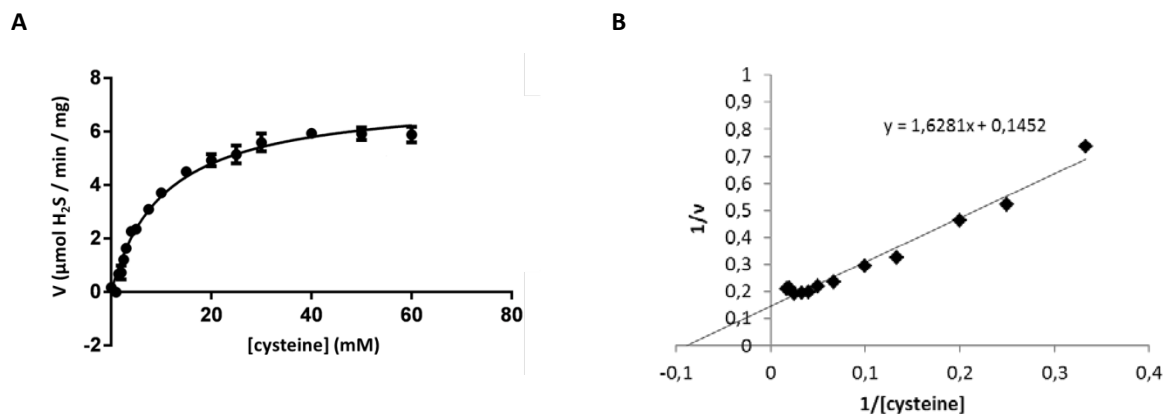
Fig. 3.27. MPN487 kinetics of hydrogen sulfide production. A. Michaelis-Menten substrate saturation curves in which the velocity of H_2S formation is plotted against the applied cysteine concentrations. **B.** Lineweaver-Burke graph as double-reciprocal plot of H_2S formation in A.

Assay for detection of pyruvate formation

In contrast to L-cysteine desulfurases which form alanine from cysteine, L-cysteine desulfhydrases are capable of producing not only H_2S but also pyruvate. To get more insight into the catalytic function of MPN487 and its possible additional products, a pyruvate assay was established.

Preparation of a sodium pyruvate standard curve

As for hydrogen sulfide, a calibration curve for the pyruvate assay had to be prepared in order to relate the measured OD to an actual pyruvate concentration. For that, sodium pyruvate was used in the pyruvate assay setup instead of enzyme and substrate. The OD_{335} was plotted against the pyruvate concentration and the slope was determined for later calculation (**Fig. 3.28**).

Pyruvate assay

The pyruvate assay was performed in 250 µl setups containing 2-5 µg MPN487, 10 µM PLP as cofactor and various cysteine concentrations in potassium phosphate buffer. The mixtures were incubated for several hours or overnight at 37°C. Afterwards, the reaction was stopped and a solution for color development was added which enabled measurement of the product at OD_{335}. After 30, 60 and 120 min of incubation time, no pyruvate could be detected (not shown) which suggested the inability of the

enzyme to form this product. However, after incubation overnight, pyruvate could in fact be detected indicating a very slow reaction rate for pyruvate formation under the given conditions (**Fig. 3.29**).
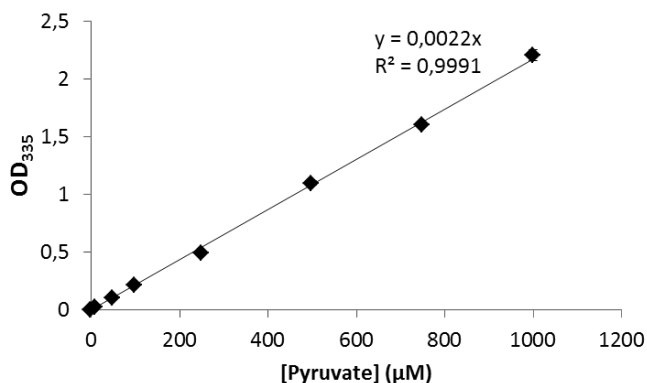
Fig.3.28. Pyruvate standard curve for determination of pyruvate concentrations produced from MPN487. Sodium pyruvate was used in the setup and measurements were performed in triplicates.

	w/o enzyme	0 mM cys	0,5 mM cys	1 mM cys	5 mM cys	10 mM cys	20 mM cys
■ µM Pyruvate	9,9	10,2	196,1	349,8	461,1	296,8	268,6
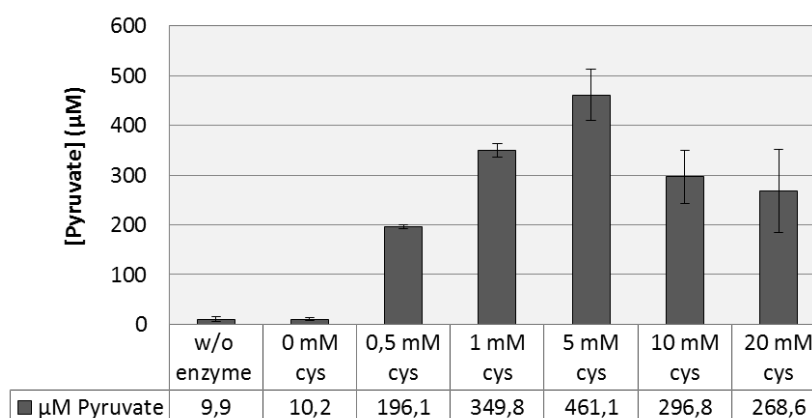
Fig. 3.29. Pyruvate formation from different amounts of cysteine. An assay contained 5 µg purified MPN487, 10 µM PLP and various substrate concentrations. The setup was incubated overnight (16 hours) at 37°C.

3.3.3 GC-MS

To get a general impression which products are formed from L-cysteine by MPN487, GC-MS analyses of the reaction mix were performed. In this procedure, the components of the reaction sample are separated via gas chromatography, where they elute after a specific retention time. The eluted components can subsequently be ionized, measured and identified according to their mass/charge ratio using the mass spectrometer. For GC-MS measurements, 5 µg of purified enzyme were incubated in a 1 ml sodium carbonate buffer set up including the cofactor and various cysteine concentrations for several hours or overnight. As control, samples without enzyme or without substrate, respectively,

were prepared as well. The reactions were stopped, mixed with 2 ml extraction solution (methanol / chloroform / water 32.25:12.5:6.25 [v/v/v]) in a Kimble glass and vortexted. The samples were subsequently analyzed by Dr. Till Ischebeck at the department of Plant Biochemistry of the Georg-August-Universität Göttingen.
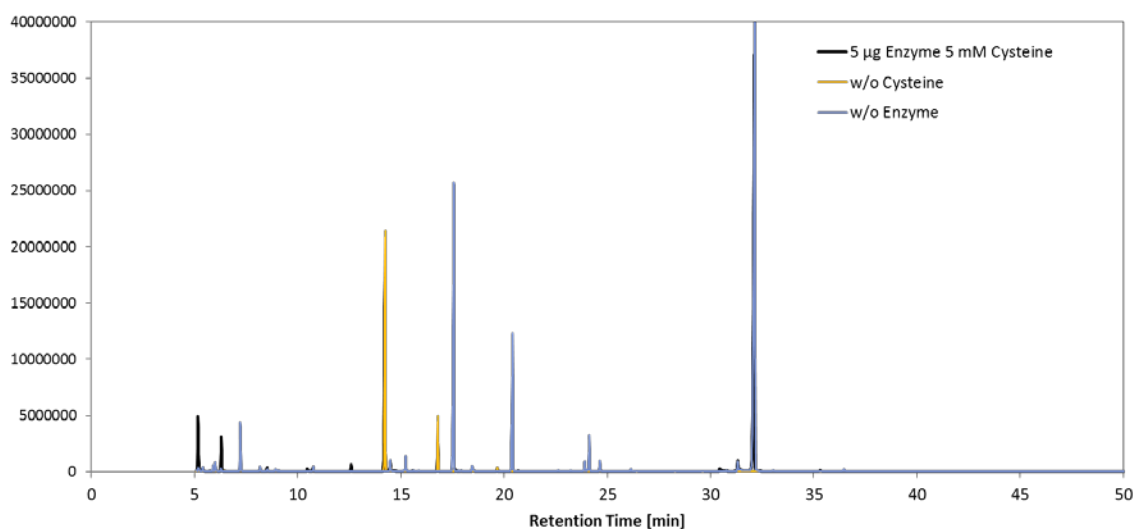
Fig 3.30. **Total ion count of GC-MS samples**. The enzyme assays were incubated over night at 37°C. A control without enzyme plus a control without cysteine were incubated and treated the same way (blue and yellow graph). The figure shows one representative chromatogram. Measurements were performed in triplicates.

The overlay chromatograms for the samples are shown in **Fig. 3.30**. In these chromatograms, the abundance of all ions (total ion count, TIC) that were eluted at a certain time point and measured by mass spectrometry, is depicted. The huge peak that appears after 32 min retention time in the "+enzyme +cysteine" and the "w/o enzyme" samples, refers to cystine which is probably spontaneously formed by oxidation of cysteine. The other peaks appearing only in the "w/o enzyme" control (blue) refer to cysteine derivatives (cysteine sulfonic acid). At a retention time 0f about 14 min, a peak turns up in the enzyme samples, which could not be identified by the software and is probably caused by a component of the elution buffer from protein purification. Three additional peaks emerge only in the sample containing enzyme and substrate (black line) after about 5, 6 and 12 min. These correspond to the retention times of pyruvate (5 min) and alanine (6 and 12 min). External standards were run for both alanine and pyruvate to be able to determine the amount and ratio of the products that are formed in the reaction. Using the standards, the content of the pyruvate and alanine masses in the total ion count was calculated. **Fig. 3.31** shows the specific chromatograms of the respective pyruvate and

alanine masses. Since alanine can appear as 2TMS (alanine derivatized with two trimethylsilyl groups) and 3TMS alanine (alanine derivatized with three trimethylsilyl groups) which elute at different time points, both masses have to be considered for calculation. In total, the averaged GC-MS result of one run revealed a production of about 0.24 µmol pyruvate and about 0.1 µmol alanine. This proves that MPN487 catalyzes the formation of both alanine and pyruvate from cysteine, with pyruvate being produced at an about 2.4 times higher rate than alanine. Since only a small proportion of the enzymatic assay setup is used for chromatography, it has to be noted that the calculated amounts are no absolute values reflecting the catalysis rate of the enzyme. Instead, these measurements are simply supposed to prove the existence and the ratio of the formed products.

A

B

C
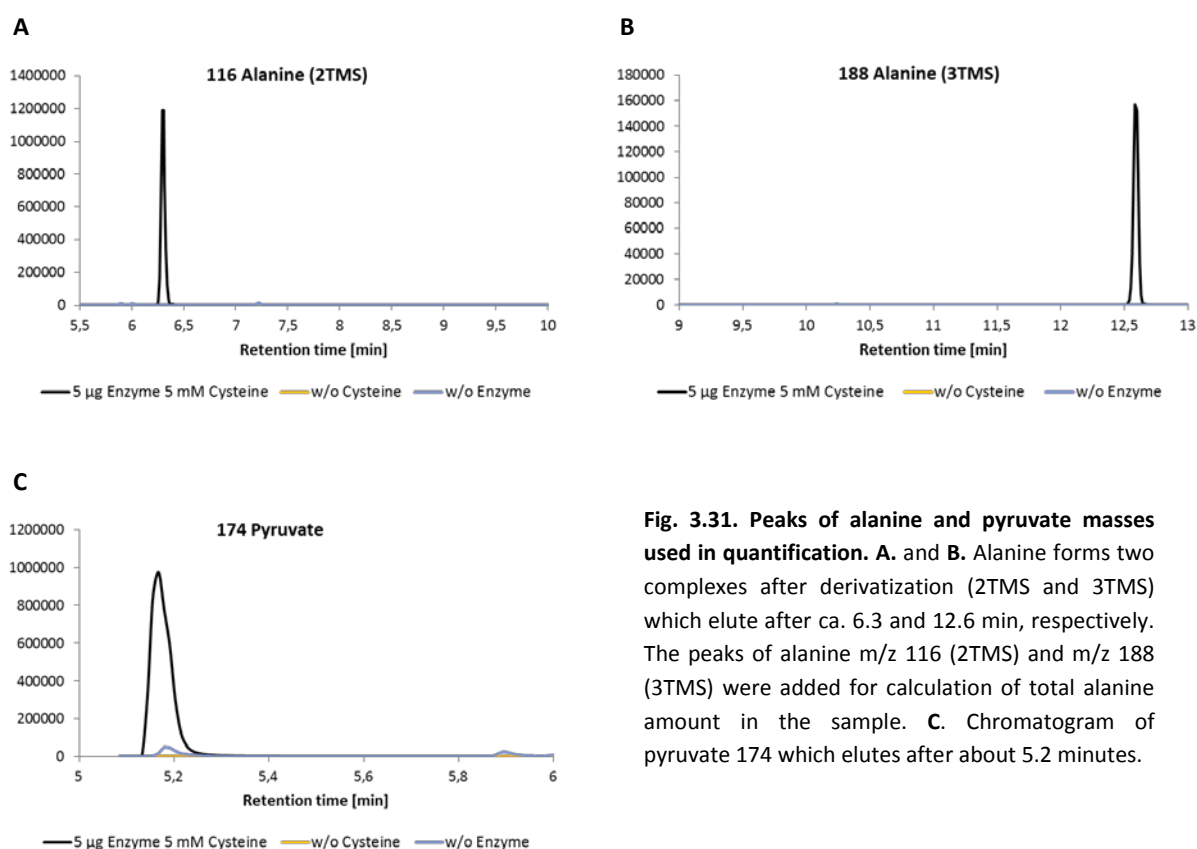
Fig. 3.31. Peaks of alanine and pyruvate masses used in quantification. A. and **B.** Alanine forms two complexes after derivatization (2TMS and 3TMS) which elute after ca. 6.3 and 12.6 min, respectively. The peaks of alanine m/z 116 (2TMS) and m/z 188 (3TMS) were added for calculation of total alanine amount in the sample. **C**. Chromatogram of pyruvate 174 which elutes after about 5.2 minutes.

3.3.4 Analysis of expression levels using Slot Blots

To get insight into the roles of MPN487 in the bacterial cell, its expression level under different conditions were examined. This was done by Slot Blot analyses using an *mpn487*-specific probe. In Slot blots, the intensity of the slot signals correlates with the amount of RNA which can be bound

specifically by the applied probe. For this purpose, total RNA from *M. pneumoniae* M129 cells that had been grown for four days in MP-medium with glucose or glycerol was isolated. Prior to harvest, the cells were treated with 10 mM cysteine, 2% blood, 0.02% H_2O_2 or 0.5 mg/ml of the iron-chelator 2,2-dipyridyl for 1 h or 4 d. In order to see, if the adjacent gene *mpn488* is expressed similar to *mpn487*, which would hint at them being involved in the same pathway, the blots were also performed with an *mpn488*-specific probe.

A

B

C
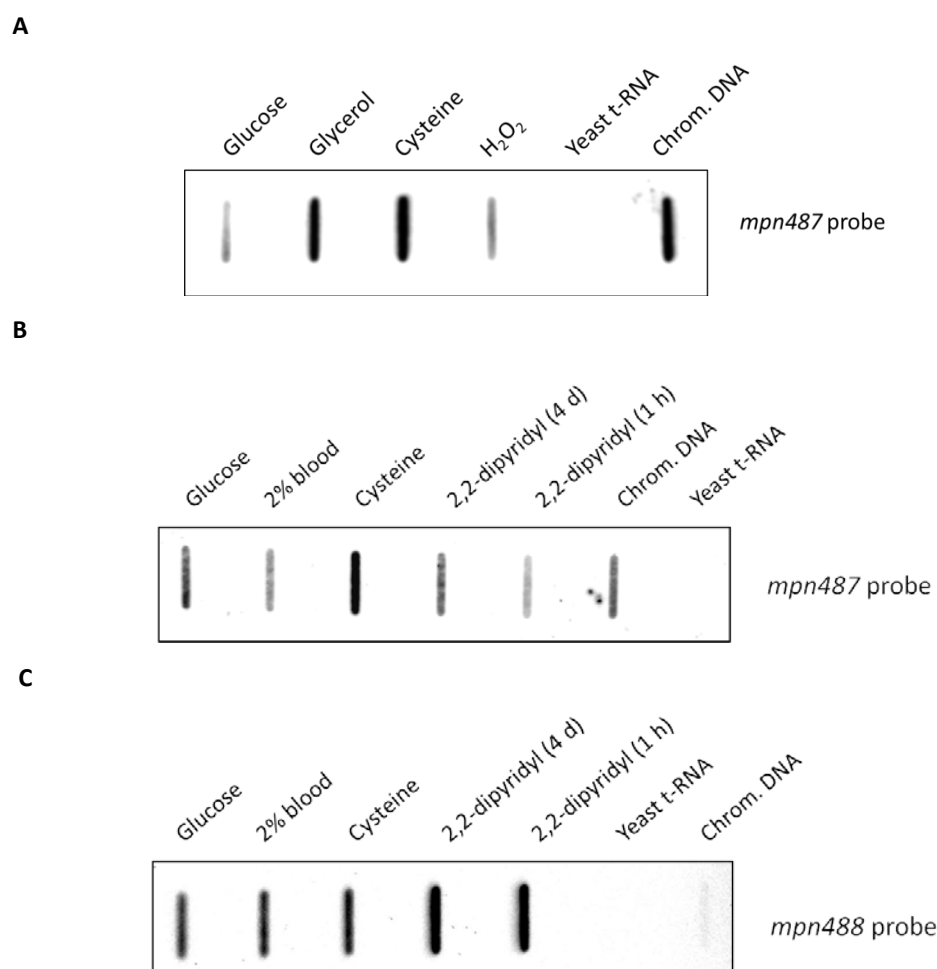
Fig. 3.32. Slot blot analyses to check the expression of *mpn487* and *mpn488* under the described conditions. *M. pneumoniae* M129 RNA was isolated after 4 days growth in MP medium. Prior to harvest, the cells were treated with cysteine, blood, H_2O_2 or 2,2-dipyridyl for 1 h unless mentioned otherwise.

As shown in **Fig. 3.32 A**, the expression of *mpn487* strongly increased after treatment with cysteine. Also, the presence of glycerol seemed to enhance *mpn487* transcription, whereas H_2O_2 did not seem to have an effect. In **Figures 3.32 A** and **B**, the expression of *mpn487* and *mpn487* under the respective conditions is compared. At a first glance, it appears that the expression patterns of both genes are not

identical. Whereas *mpn487* was significantly upregulated only in presence of cysteine, expression of *mpn488* was strongly enhanced after incubation with the iron-chelator 2,2-dipyridyl for 1 hour or 4 days and only slightly enhanced upon incubation with cysteine. This suggests that MPN487 is needed when elevated cysteine amounts are available, whereas MPN488 seems to become important under iron-depletion. These results indicate that both of the proteins might have different roles or priorities in the organisms.

3.3.5 Investigation of protein-protein-interactions using MPN487 in a bacterial-two-hybrid (BACTH) study

To assess the question whether MPN487 and MPN488 are working together in the same metabolic pathway, protein-protein-interaction studies were performed.

For the bacterial-two-hybrid screen, genes coding for the proteins MPN487 and MPN488 were cloned into BACTH specific vectors (pUT18/C and pKNT25) and fused each to one domain of the adenylate cyclase of *Bordetella pertussis*. This enzyme consists of two domains (T18 and T25) and separation of these domains results in a non-functional enzyme. Interaction of two proteins that are fused to either one of the two domains, respectively, results in a spatial proximity of the formerly separated adenylate cyclase domains and therefore in a functional enzyme. The presence of a functional adenylate cyclase results in the expression of reporter genes in the *E. coli* strain and possible protein-protein-interactions can be recognized in blue colonies.

The vectors that were constructed for the BACTH containing either *mpn487* or *mpn488*, are listed in in the appendix. The BACTH showed self-interaction of MPN488 but not MPN487 (**Fig. 3.33**). Moreover, no interactions between MPN487 and MPN488 could be detected. This might indicate that, indeed, MPN487 and MPN488 are not interacting. However, the BACTH is an artificial system in which the proteins reside in a different organism, where they might not be properly folded or modified. Therefore, the appearance of only white colonies does not necessarily mean that these proteins are not able to interact in *M. pneumoniae*. In this BACTH, an interaction of MPN487 and MPN488 could not be proven but is still not excluded.
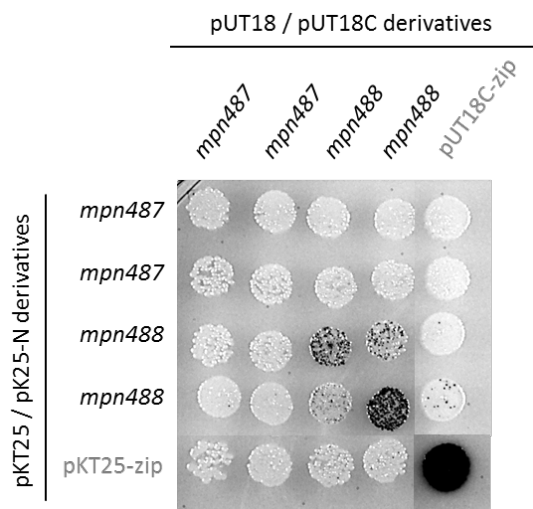
Fig. 3.33. Bacterial-two-hybrid screen for detection of potential interactions between MPN487 and MPN488. 5 µl *E. coli* BTH101 cells transformed with a pUT18- and a pKT25 derivative were dropped on an LB plate containing X-Gal and incubated at 30°C for two days. Discoloration of colonies indicates interaction of the proteins encoded by the respective plasmids. Down right is the positive control.

3.3.6 Hemoxidative and hemolytic effect of MPN487

The L-cysteine desulfhydrases in oral pathogens like *Treponema denticola*, which produce H_2S and pyruvic acid, were also demonstrated to possess hemoxidative and hemolytic activity (Chu *et al.,* 1997). Since MPN487 could be shown to also possess desulfhydrase activity, it was subsequently investigated, if it also possesses hemoxidative and hemolytic activity. To compare the effect of the enzyme with the effect of the H_2O_2 producing enzyme GlpD, both were purified and tested in parallel. Moreover, the homologous L-cysteine desulfurase from *B. subtilis*, SufS, was tested for comparison.

Cloning and purification of GlpD$_{Mpn}$ and SufS$_{Bsu}$

All enzymes were purified using a *Strep*-tag fused to the protein and a *Strep*-Tactin sepharose matrix. For that, the genes were cloned into the overexpression vector pGP172, overexpressed in *E. coli* BL21 and purified as described in section 3.3.1. The vector containing GlpD$_{Mpn}$ (pGP2031) was already existing (Schmeisky, 2013). For cloning of SufS, the gene was amplified from *B. subtilis* 168 chromosomal DNA using gene specific oligonucleotides SG196 and SG197. The PCR product was digested *Bam*HI / *Sac*I and cloned into the *Bam*HI / *Sac*I digested pGP172. **Fig. 3.34** shows the respective fractions of the GlpD and SufS purifications on a 12% SDS gel.
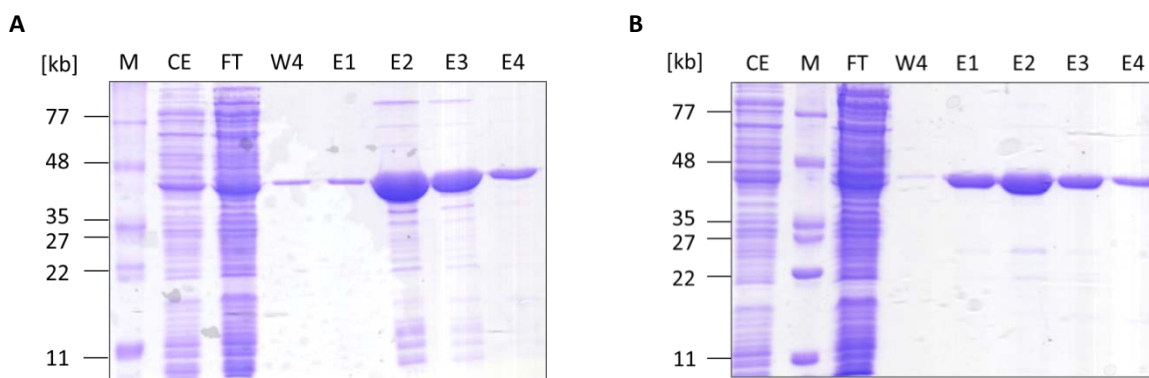
Fig. 3.34. Purification of Strep-GlpD_{Mpn} (A) and Strep-SufS_{Bsu} (B). Proteins were overexpressed in *E. coli* BL21 and then purified via their Strep-tag and a Strep-Tactin sepharose column. Proteins from the elution fraction E2 or E3 were used in further experiments.

Hemolysis assays using MPN487, GlpD_{Mpn} and SufS_{Bsu}

To test their hemolytic activity, 2 µg/ml of the purified proteins were incubated with (or w/o) their substrates and 2% RBCs in PBS pH 7.4 for several hours. The mixtures were shaken slowly at 100 rpm and 37°C. After the desired incubation time, 1 ml was withdrawn from each sample, centrifuged and the supernatant was collected. The pellet was resuspended in 1 ml dH_2O. Both fractions were photographed in a 24-well plate and their spectrum was recorded photometrically.

Comparison of the hemolytic activities of MPN487 and GlpD

After three hours of red blood cell incubation with either MPN487 or GlpD, the supernatants of all samples were clear and the hemoglobin was kept inside the pellets (**Fig. 3.35**). This implies that no hemolysis occurred. However, the hemoglobin was slightly oxidized in the MPN487 sample and strongly oxidized in the GlpD sample. In fact, the hemoglobin in the GlpD sample was already completely oxidized after 30 min (data not shown). This suggests that GlpD is a highly active enzyme whereas for MPN487 the rate of catalysis is comparatively low. Similarly, after 20 h of incubation, no hemolysis was detectable. Still, the hemoglobin in the MPN487 sample showed stronger oxidation. In contrast, after 44 hours, strong hemolysis was visible in the sample containing both MPN487 and 1 mM cysteine. The strongly oxidized hemoglobin was not only present in the pellet but also in the supernatant indicating that a high proportion of erythrocytes had undergone lysis to release their hemoglobin. Hemolysis did not appear in the control samples containing only 2% RBCs in PBS with or without 1 mM cysteine. Incubation with GlpD and 1 mM G3P led to a strong hemoxidation and a slight hemolysis which was, however, not comparable to that caused by MPN487 and cysteine. These

results are confirmed by the measurements of the respective hemoglobin spectra of the samples (**Fig. 3.36**).

After incubation for 44 hours, all control samples showed only a very little hemoglobin peak in the supernatant indicating that only a little amount of hemoglobin was present in the supernatant and most of it kept in the pellet (**Fig. 3.36**). For the sample containing 1 mM G3P + GlpD, a larger peak was detectable referring to a higher hemolysis rate. The largest peaks in the supernatant fractions were observed for the samples containing cysteine and MPN487. This result was the same for the sample containing 1 mM cysteine as for the one containing 10 mM cysteine. From that, it seems that 1 mM cysteine is sufficient for MPN487 to exhibit its hemolytic function. On the other hand, the hemoglobin peaks in the resuspended pellet fractions were very large in each of the control samples. This means that the pellet contained all the hemoglobin and hemolysis did not take place. In contrast, the peak of the sample containing 1 mM G3P + GlpD was reduced which fits to the respective higher peak in the supernatant fraction. The peaks of the samples containing MPN487 + 1 mM or 10 mM cysteine were even more reduced indicating an enhanced hemolysis rate. In fact, the respective peaks for those samples were equally intense in both the supernatant and the pellet fractions. Consequently, hemoglobin was present in equal parts in the supernatant and the pellet, respectively, meaning that about half the erythrocytes had been lysed by the concerted action of MPN487 and cysteine. Moreover, the hemoglobin in the samples containing GlpD and MPN487 with their corresponding substrates, had an altered spectrum in the region of $\lambda= 500\text{-}650$ nm. This refers to oxidized hemoglobin which is also visible by its brown discoloration in **Fig. 3.35**.
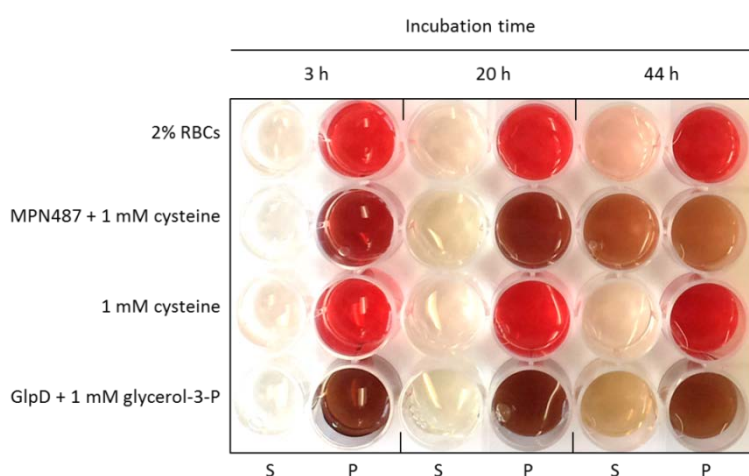
Fig. 3.35. Hemolysis assay with 2% RBCs in PBS incubated with MPN487 and cysteine for indicated time periods. As controls, only 2% RBCs in PBS and a sample with cysteine but without enzyme were chosen. For comparison, a setup containing RBCs, GlpD and 1 mM glycerol-3-phosphate (glycerol-3-P) was prepared as well. Brown discoloration indicates hemoxidation. S: supernatant. P: pellet.

Comparing MPN487 with SufS from B. subtilis

MPN487 is a putative L-cysteine desulfurase, which unexpectedly turned out to be involved in virulence and hemolysis. To rule out if its hemolytic attributes are unique for the *M. pneumoniae* enzyme or also present *in vitro* in L-cysteine desulfurases of non-pathogenic bacteria, its homolog from *B. subtilis*, SufS, should be tested for similar effects on sheep blood. For that, 2 µg / ml enzyme were incubated with cysteine, PLP and 2% RBCs in PBS as described above. **Figures 3.37** and **3.38** show the pellet and supernatant fractions in a 24-well-plate and in forms of their spectra, respectively.
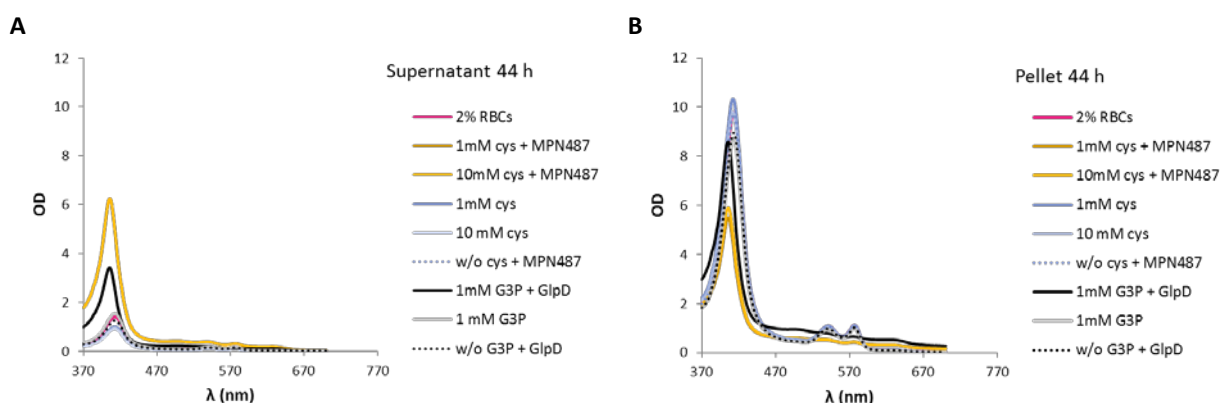
Fig. 3.36. Spectra of hemoglobin after 44 h of incubation with MPN487 and GlpD. The spectra of the supernatants are shown in **A**, those of the pellets are shown in **B.** The samples were incubated with gentle shaking at 37°C. After centrifuging, the supernatant was removed and the pellet was resuspended in 1 ml dH$_2$O. For measurement of the spectra, 100 µl of the supernatant and a 1:5 dilution of the resuspended pellet in 100 µl were pipetted in a 96 well plate. Recording of the spectra was done using the platereader SynergyMX (Biotek). cys: cysteine. G3P: glycerol-3-phosphate.

As for the experiment before, no hemolysis was detectable after 3 h (not shown) or 20 h of RBC incubation with either of the enzymes. This can be recognized from the clear supernatant in all the samples meaning that all the hemoglobin is inside the entire RBCs in the pellets. However, with 10 mM cysteine, already a slight hemoxidation could be seen in both pellet fractions that were incubated with MPN487 and SufS$_{Bsu}$ (**Fig. 3.37**). After 40 h, the hemoxidation is in an advanced state in all setups. It is noteworthy that 10 mM L-cysteine solution already seemed to have a slight hemoxidative and hemolytic effect on RBCs. Nevertheless, this hemolytic effect was stronger in the samples incubated with 10 mM cysteine and SufS and with 10 mM cysteine and MPN487, respectively. In fact, the hemolytic activity of MPN487 outnumbered that of SufS, since the hemoglobin appeared to be present nearly exclusively in the supernatant fraction. In contrast, less than 50% of the red blood cells seemed to be lysed in the SufS sample (**Fig. 3.37**). The results shown in **Fig. 3.37** are supported by those in **Fig.**

3.38. Here, the hemoglobin spectra of an independent experimental setup are depicted. In all cases, a concentration of 1 mM L-cysteine was not enough to cause hemolysis. The presence of 10 mM cysteine led to strong hemoxidation in all samples which is implied by the change of the absorption spectra at of λ= 500-650 nm. A high proportion of hemoglobin was detectable in the supernatant fraction of the sample incubated with 10 mM cysteine and MPN487 (**Fig. 3.38 A**, yellow curve). Consequently, the respective amount of hemoglobin is lower in the pellet fraction. In this experiment, the grey curve of the sample containing SufS + 10 mM L-cysteine even seemed to match the negative control with only 10 mM L-cysteine present. This result indicates that the observed hemolysis is already caused by L-cysteine alone and cannot be referred to the activity of SufS. Although the results are, unfortunately, not 100% reproducible due to fluctuations in the quality of L-cysteine and sheep RBCs, a trend can be observed.

Definitely, SufS from *B. subtilis* can also cause hemoxidation probably due to release of low amounts of H_2S. However, the enzyme has significantly less hemolytic activity than MPN487. This means that MPN487 either simply releases much higher amounts of hydrogen sulfide than SufS or it has additional hemolytic properties, which are not known so far. Either way, MPN487 is a unique enzyme in *M. pneumoniae* which is similar to L-cysteine desulfurases but definitely has hemolytic functions - probably due to its high hydrogen sulfide production rate.
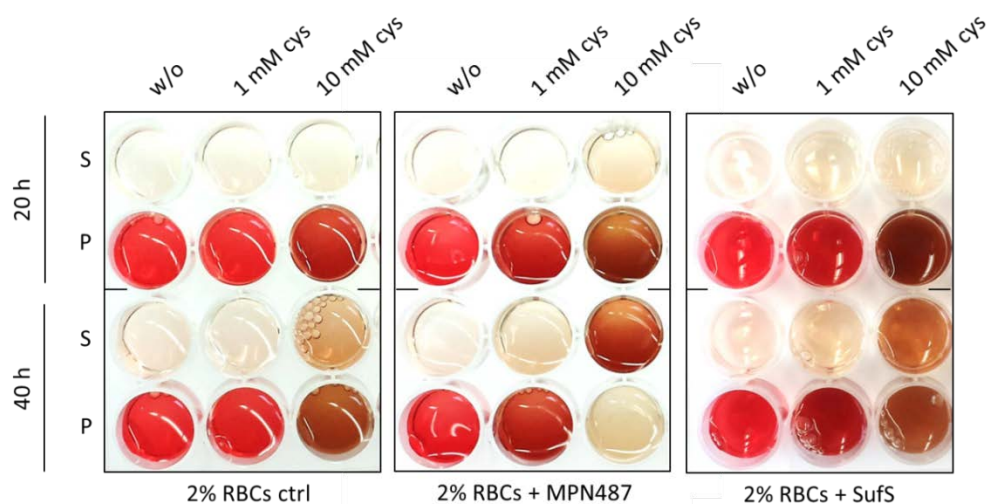
Fig. 3.37. Hemolysis assay to compare possible hemolytic effects of SufS_{Bsu} and MPN487. 2% RBCs were incubated with 2 µg/ml of the respective enzyme and 1 mM or 10 mM of the substrate. 1 ml samples were withdrawn after 3, 20 and 40 h incubation time. After 3 h no change was detectable. S: supernatant; P: pellet; cys: cysteine.
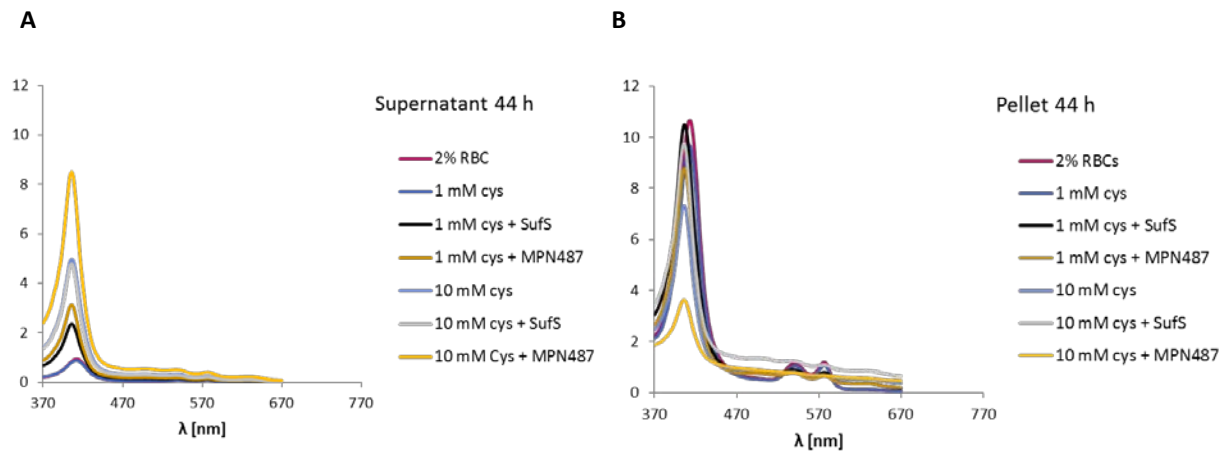
Fig. 3.38.. Hemoglobin spectra of 2% RBC cultures incubated with or without L-cysteine and MPN487 or SufS$_{Bsu}$ for 44 h at 37°C. **A.** Spectra of supernatant fractions. **B.** Spectra of pellet fractions that were previously lysed in 1 ml of distilled water. Samples were prepared as described in Fig. 3.3.14, and measured in a 96 well plate in the platereader SynergyMX (Biotek).

105

4. DISCUSSION

4.1 The role of transport systems in *M. pneumoniae* pathogenicity

Identification of *M. pneumoniae* transporters

Transport systems are of various natures and therefore fulfill various functions in the bacterial cell. They are responsible for the import of sugars for energy generation, amino acids for protein biosynthesis, metal ions as cofactors or electrolytes to maintain the osmotic balance. Their export function is essential for protection from toxic compounds that accumulate inside the cell, for communication - or for secreting virulence factors that aim at promoting bacterial survival.

For *M. pneumoniae*, transport systems are of particular importance. The genome-reduced pathogen is strongly dependent on external nutrient supply due to the lack of most biosynthetic pathways. This is reflected in the fact that the bacterium has about 10% of its genome coding for proteins which are involved in transport, even though it lives in an environment with steady conditions and a predictable, comprehensive nutrient supply (Himmelreich *et al.*, 1996; Ren and Paulsen, 2007). In contrast, *B. subtilis*, which is a soil bacterium that has also been shown to live and sporulate in the gastrointestinal tract of animals, needs to be prepared for environmental changes and distinct nutrient availability (Serra *et al.*, 2014). Still, it dedicates only 7% of its genome for transport systems (Ren and Paulsen, 2007). This is surely possible, because *Bacillus* possesses a lot more anabolic and catabolic pathways for self-supply than *Mycoplasma*. Considering the fact that about another 10% of the *M. pneumonie* genome encode lipoproteins, which in many cases function as high-affinity substrate-binding proteins for ABC transporters, the total number of proteins involved in transmembrane transport processes in the human pathogenic *M. pneumoniae* is probably even higher (Hallamaa *et al.*, 2006). By ensuring the pathogen's survival, sequestering iron from the host tissue or exporting toxins, transporters play a crucial role in general virulence processes. Therefore, their relevant functions in *M. pneumoniae* were to be tested in this work.

In order to identify the roles of certain transport systems for growth, survival and infection, the genome was searched for genes encoding transmembrane transporters and accessory proteins, e.g. ATP binding domains in ABC-transporters. This was done using genome annotations (Himmelreich

et al., 1996; Dandekar *et al.*, 2000), databases (KEGG, Uniprot, String, TCDB, SubtiWiki) and BLAST searches (NCBI, Molligen). Altogether 70 proteins could be found (**Tab. 3.1**), 39 of which are essential (Lluch-Senar, in press). Eleven transport proteins are annotated as putative exporters (membrane exporters, multidrug resistance transporters or hemolysin exporters), whereas expectedly, the major part is annotated as putative importers (for detailed annotation and essentiality see Appendix **Tab. 7.7**).

Among the import systems, 16 transporters are annotated to be responsible for the uptake of carbon sources, e.g. glycerol, glycerophosphocholine, glycerol-3-phosphate, glucose, fructose/mannose, mannitol, and ribose. The GPC uptake system has been previously described to be involved in growth and virulence, because it transports a precursor for membrane synthesis and for formation of H_2O_2 and a glycolytic feeder (Großhennig *et al.*, 2013). Likewise, the glycerol facilitator GlpF might be involved in pathogenicity, although this hypothesis could not be confirmed due to the lack of a corresponding mutant. In *Mycoplasma mycoides*, the glycerol facilitator is prevalently present to enable uptake of glycerol. In addition, some *M. mycoides* subsp. *mycoide*s SC strains possess an efficient ABC transporter for glycerol uptake which makes them highly virulent as compared to the others (Vilei and Frey, 2001). In *M. pneumoniae*, the supposedly non-essential GlpF is the only glycerol transporter that is known so far. This is quite interesting given the fact that the production of H_2O_2 from glycerol is thought to be its major virulence determinant. Instead, the genome encodes an essential ABC transporter, MPN134-136, which is similar to the sn-glycerol-3-phosphate ABC transporter UgpB-AEC in *E. coli* (Wuttge *et al.*, 2012). As G3P is the immediate substrate of GlpD and necessary for membrane phospholipid biosynthesis, it would be reasonable for the cell to exhibit a corresponding transport system. Using a H_2O_2 assay, it was shown earlier that several *M. pneumoniae* strains are not capable of producing H_2O_2 when only G3P is available (Schmidl *et al.*, 2011). From this approach, it would be concluded that G3P cannot be taken up by these bacteria. In this present work, it was revealed that *M. pneumoniae* cells are able to oxidize hemoglobin in the presence of G3P, most probably due to H_2O_2 release. This indicates that, unexpectedly, the cells are capable of G3P transport in a hemolysis assay approach and therefore need to possess a respective transport system which has not been known so far. For sure, the putative Ugp-system encoded by *mpn134-136* represents one potential G3P transporter candidate. However, due to the essentiality of the genes, this question remains unsolved by now.

From a first glance at the transporter genes, it appeared that *M. pneumoniae* encodes two putative cobalt ABC transporters (CbiO), MPN193-195 and MPN431-433. Upon further investigation and

BLAST searches, these transporters actually turned out to be members of the energy-coupling factor (ECF) transporter family. These systems belong to the ubiquitous class of ATP-binding cassette (ABC) transporters, although the organization of the components differs from classical ABC systems (**Fig. 4.1**). Typical ABC transporters form heteromultimeric complexes containing two identical transmembrane proteins for substrate translocation, two identical cytoplasmic nucleotide-binding domains (NBDs) that hydrolyze ATP and drive the transport reaction, and, most often, extracellular high-affinity substrate-binding proteins (BP). Members of this group transport a variety of substrates including rare elements, peptides or sugars (Davidson *et al.*, 2008). In contrast, ECF transporters consist of a general, non-specific ECF module and a substrate-specific S component. The ECF modules are composed of three proteins: a transmembrane component (T) for translocation of the captured substrate and two similar cytosolic ATP-binding proteins (A and A') which, in contrast to the ABC transporters, are encoded each by their own corresponding genes (Henderson *et al.*, 1977; Henderson *et al.*, 1979). Interestingly, one ECF module can transport a large variety of different substrates which are all bound specifically by their respective binding proteins. These small integral-membrane S components can then deliver their substrate to the transmembrane protein of the ECF module for translocation. ECF transporters typically transport micronutrients like transition metal ions (Ni^{2+} or Co^{2+}), as well as water-soluble vitamins, such as riboflavin, thiamin, folate or biotin and their precursors (Rodionov *et al.*, 2009). ECF transporters are especially abundant in pathogenic bacteria of the Firmicutes e.g. *L. monocytogenes* or *M. pneumoniae* which are unable of synthesizing vitamins like thiamin (Schauer *et al.*, 2009). Consistent with this, *M. pneumoniae* carries transporter genes coding for even two general CbiO ECF modules all of which are essential. Indeed, *M. pneumoniae* lacks biosynthetic genes for all vitamins, which means that these necessarily have to be taken up, e.g. by ECF transporters. Although there are two ECF modules encoded, no typical S component is annotated. Since ECF transporters rely on their S components for specific binding of the substrates, the *Mycoplasma* genome was searched for genes similar to S protein coding genes in other organisms. Overall 21 different S component families have been identified in different organisms so far. What is conserved in all of them is their very high substrate specificity (Rodionov *et al.* 2009). However, they share extreme low sequence similarities (10-20%), which makes their identification in *M. pneumoniae* considerably complicated. Nevertheless, at least one potential S component could be spotted by BLAST: MPN448, a protein which is similar to the folate binding S component from *Lactobacillus* FolT. MPN448 is annotated as hypothetical protein, but according to KEGG, it has an ECF-ribofla_trS

/ DUF3816 domain, which is typical for S compounds. Analysis at TCDB revealed 7 transmembrane segments (TMS), which supports its function in transport.

For most of the non-essential transport systems, mutants were isolated either in this work or previously (Großhennig, 2011; Großhennig *et al.*, 2013). Of the eight mutants tested here, only the two amino-acid transporters MPN095 and MPN096 seemed to play a minor role in virulence, insofar as their disruption seems to lead to an adhesion defect of the cell, which cannot be explained by now. Interestingly, decreased adhesion after transposon insertion into an amino acid transporter gene has also been described for group B streptococci (Tamura *et al.*, 2002). Transcriptome-, proteome- and interaction studies with the mutants or the tagged proteins *in vivo* would possibly give insight into the underlying mechanisms.

Fig. 4.1 Transport systems. **A.** Composition of ECF transporters. S: S component for substrate binding, T: Transmembrane domain, A: ATP hydrolyzing domain. **B.** Illustration of classic ABC transporters for import. SBP: extracellular substrate binding protein, TMD: transmembrane domain, NBD: nucleotide binding domain for ATP hydrolysis. **C.** Structure of a MgtE dimer for magnesium transport. The CBS domains are shown in rose. (A and B: Erkens *et al.*, 2012: C: Moomaw and Maguire, 2008)

MPN159, MPN571 and the hemolysin system

Among the export proteins, *M. pneumoniae* possesses a putative hemolysin transporter, MPN571. This transporter is structurally similar to bacteriocin transporters and carries a C39-peptidase domain which is also present in the *E.coli* hemolysin ABC transporter HlyB (KEGG). The search for genes encoding a potential hemolysin to be transported by MPN571 resulted in the discovery of *mpn159*, which is annotated as *hlyC* (Himmelreich *et al.,* 1996). In *E. coli* as in other pathogenic bacteria, HlyC and HlyB are part of a prevalent hemolysin synthesis and –secretion machinery encoded by the *hlyCABD* operon (Felmlee *et al.,* 1985). The 110 kDa pore-forming hemolysin (HlyA) is herein encoded by the gene *hlyA*. HlyA is synthesized as a non-toxic precursor and needs to be activated in the cytoplasm by internal acylation. This task is fulfilled by the acyltransferase HlyC(Albrecht *et al.,* 1996; Goebel and Hedgpeth, 1982; Hardie *et al.,* 1991). Finally, the translocation of the toxic form of HlyA is mediated by the two membrane-localized proteins HlyB and HlyD (Gentschev *et al.,* 1992; Schulein *et al.,* 1992). According to its annotation as HlyC, MPN159 would play the part of the activating acyltransferase in this system. Nevertheless, mutants for both putative Hly proteins were tested for growth, cytotoxicity and hemolysis defects. It turned out that the *mpn571* mutant was not impaired in any of these processes indicating that its function is not the transport of a pore-forming hemolysin A. Because of the presence of a Peptidase C39 domain, the protein might instead be involved in the proteolytic cleavage (and simultaneous activation) of peptides containing double-glycine (GG) leader motifs. In gram-positive bacteria, these play a key role in peptide secretion systems involved in quorum sensing and bacteriocin production (Havarstein *et al.,* 1995).

The *mpn159* mutant strain was impaired in H_2O_2 production with glycerol and HeLa cell lysis similar to a *glpD* mutant. Accordingly, less hemoxidation was seen in a hemolysis assay. These results suggest that MPN159 is somehow involved in virulence of *M. pneumoniae* but rather via regulation of H_2O_2 production than as an independent pore-forming hemolysin. A closer look at the structure of the protein reveals 4 transmembrane domains in the N-terminal region, which is also designated as DUF21 domain. Directly behind these transmembrane sequences, the protein carries two CBS (cystathionine-beta synthase) domains. CBS domains are often found in enzymes to bind adenosyl groups (AMP and ATP, or s-adenosylmethionine) and regulate the activity of the catalytic domains (Kemp, 2004). Additionally, in combination with transmembrane domains, CBS domains may be part of dimeric magnesium or cobalt channels like the Mg^{2+} channel MgtE (**Fig. 4.1**). The CBS domains in the magnesium channel are thought to act as sensors for the availability of magnesium inside the cell

which regulates organization and gating of the ion-translocating pore (Moomaw and Maguire, 2008). It seems that MPN159 is actually not a hemolysin but another transport protein in *M. pneumoniae* and ensures the availability of Mg^{2+} and the osmotic balance of the cell. Its function in H_2O_2 production can only be hypothesized. Magnesium is needed as a cofactor in several enzymes. Even though this is not true for GlpD, the prior enzyme in glycerol metabolism, GlpK, needs Mg^{2+} as cofactor. MPN159 might be involved in virulence via sensing and regulation of cofactor supply. Interestingly, the implication of magnesium transport in virulence has been reported for several pathogens, especially for the PhoP/PhoQ dependent systems in *Salmonella enterica*. Moreover, the magnesium channel CorA was shown to be required for *Salmonella* virulence in mice as well as for invasion of epithelial cells, although it is presently not clear how exactly CorA contributes to *Salmonella* pathogenicity (Papp-Wallace *et al.*, 2008; Smith *et al.*, 1998). Also, the Mg^{2+} transporter MgtE was reported to be involved in virulence-associated phenotypes in some bacteria. In *Aeromonas hydrophila*, MgtE is required for adherence to surfaces and biofilm formation, whereas it is needed for expression of a type III secretion system in *Pseudomonas aeruginosa* (Merino *et al.*, 2001; Anderson *et al.*, 2010).

4.2   Hemolytic activities in *M. pneumoniae* and *Mycoplasma*-blood interactions

4.2.1   Human blood, a habitat with benefits

About 6-8% of the human body mass are made up of blood. It serves as important transport and communication system which is essential for the maintenance of normal bodily functions. By means of the blood stream, oxygen, nutrients and hormones are transported to the organs and tissues and metabolites are removed. Blood mediates an equal distribution of water between the vasculature, the intra cellular and extracellular space and transports heat through the human body. Finally, it possesses several very important mechanisms for (self-) protection against pathogenic bacteria, viruses, fungi, or pathologically altered cells, as well as against excessive blood loss e.g. after injury (Walzog and Fandrey, 2010).

Blood consists of sundry cells, electrolytes, water-soluble nutrients, metabolites, vitamins, gases and proteins in an aqueous solution called the blood plasma. The most prevalent metabolites are glucose (3.6-6.1 mM), lactate (0.4-1.8 mM), urea (3.5-9 mM), amino acids (2.3-4 mM) and lipids (5.5-6 g/l).

Cellular components of blood comprise erythrocytes (red blood cells, RBCs), leukocytes (white blood cells) and thrombocytes (blood platelets). Thrombocytes are cellular fragments that serve to contract and close an injured vessel in a process called hemostasis. Leukocytes are divided in granulocytes, monocytes and lymphocytes all of which are involved in immune response and protection. While granulocytes and monocytes are the cellular components of the innate immune system, lymphocytes belong to the acquired, specific immune response which is developed after birth and serve, amongst others, for the production of pathogen-specific antibodies. In general, leukocytes are responsible for maintaining infections as short-termed as possible to prevent the body from permanent damage. Therefore, important constituents of the innate immune system are macrophages and neutrophil granulocytes which phagocytize intruding organisms. Prior opsonization of pathogens by antibodies or complement factors leads to a 5,000 fold enhancement of phagocytosis efficiency. However, microbial pathogens have evolved several mechanisms to evade phagocytosis, like antigenic variation, which would hamper their recognition. Some of them, like *Salmonella*, are even able to grow inside macrophages (Caroll *et al.*, 1979). Among the cellular components of the human blood, erythrocytes (RBCs) are the most prevalent (5×10^{12} / l). Normally, they are small biconcave discs with a diameter of 7.5 μm and an average thickness of 1.5 μm. This shape provides an optimal surface-volume-ratio for gas transport and –exchange. Their flexible membrane skeleton enables them to change their shape when needed, e.g. for passing narrow capillaries. These cells do not contain a nucleus, any kind of DNA or mitochondria and gain energy exclusively via glycolysis. The main function of RBCs is the transport of O_2 and CO_2. Erythrocytes consist for the most part of hemoglobin, a heterotetrameric protein containing heme groups with a central divalent iron ion, which is able to bind O_2 with a high affinity **(Fig. 1.2)**. While O_2 is poorly water-soluble (3.2 ml in 1 l blood plasma), hemoglobin can bind up to 220 ml O_2. The life span of a mature red blood cell in the blood circulation accounts for about 120 days before it is eliminated in the liver or spleen (Koolman and Röhm, 2003; Walzog and Fandrey, 2010).

The high availability of metabolites and especially the high frequency of hemoglobin molecules turn blood into an attractive source of nutrients and iron for pathogenic bacteria. In fact, it has been shown that *Staphylococcus aureus* enters erythrocytes and specifically binds human hemoglobin in order to get access to the growth limiting factor iron (Skaar *et al.*, 2004). Intentional invasion of erythrocytes and other blood components for nutrition, survival, evasion of the host immune system or even replication and distribution has been described for several pathogens: Multiple *Bartonella* and *Brucella* species were shown to be able to persist in their host's blood for several weeks. Most *Bartonella* species

113

even perform non-hemolytic parasitism and maintain within the erythrocytes without having a significant effect on their physiology (Vitry *et al.*, 2014; Schulein *et al.*, 2001). The causative agent of tularemia, *Francisella tularensis*, can infect and replicate in leukocytes and erythrocytes and exhibits an extracellular phase in the blood of the host (Barker and Klose, 2007; Horzempa *et al.*, 2011; Forestal *et al.*, 2007). Furthermore, a recent study on *Streptococcus pneumoniae* infection revealed that these pathogenic bacteria are able to invade human erythrocytes suggesting a novel infection strategy and a way to evade the host immune system. Interestingly, in this study it was also shown that the survival rate of *S. pneumoniae* in cultures containing erythrocytes was increased by 3-fold as compared to those without erythrocytes (Yamaguchi *et al.*, 2013). Obviously, the erythrocyte and blood niches can confer a growth advantage by providing nutrients, protection from both, the immune system and antibiotic substances, and a means of transportation to distinct infection sites, thereby promoting the survival and dissemination of their invading pathogenic bacteria.

Beside the above mentioned bacterial pathogens like *Bartonella* spp., some *Mycoplasma* species including *M. suis*, and *M. gallisepticum* can establish intraerythrocytic infections (Schulein *et al.*, 2001; Kocan *et al.*, 2007; Groebel *et al.*, 2009; Vogl *et al.*, 2008). The avian pathogen *M. gallisepticum* was proven to invade chicken erythrocytes not only after *in vitro* infection but also *in vivo* which indicates a previously unknown infection strategy for pathogenic mycoplasmas (Vogl *et al.*, 2008). *Mycoplasma suis*, a porcine pathogen belongs to the group of so called hemotropic mycoplasmas (hemoplasmas). These are uncultivable mycoplasmas that parasitize mammalian erythrocytes to cause mostly chronic blood infections with hemolytic anemia and several accessory symptoms (Messick, 2004). Severe acute anemia due to *M. suis* infection can cause death in young piglets or pregnant sows. Chronic infections established by hemotropic mycoplasmas like *M. suis* or *M. ovis*, a bovine pathogen, might lead to abortion, reproductive inefficiency, decreased milk production or weight loss, which makes the issue of major economic importance (Hoelzle, 2007; Smith *et al.*, 1990). Typically, hemoplasmas commit surface parasitism on red blood cells which provides them with amino acids, fatty acids, cholesterol or vitamins and other essential compounds which cannot be synthesized by the bacteria due to their reduced genome. However, *M. suis* was shown to even enter erythrocytes. Blood smears of infected pigs with an acute clinical attack on day seven past infection, show a high number of *M. suis* cells which are predominantly successfully attached to the RBC surface. On day 11, the number of *M. suis* cells on the erythrocyte surface is strongly reduced due to RBC entrance. Remarkably, at this stage, red blood cells have turned from discocytes to echinocytes which might be caused by draught or phospholipid depletion. Due to the intraerythrocytic lifestyle and the concomitant protection of the

bacteria from external antimicrobial substances, the usual treatment of *Mycoplasma* infections with tetracycline is strongly hampered (Groebel *et al.*, 2009).

4.2.2 *M. pneumoniae*-blood interactions

So far, not much is known about a potential lifecycle of *M. pneumoniae* in human blood. However, there are several indications for an interaction with red blood cells and the contact with the blood stream: (i) *M. pneumoniae* has been isolated and cultivated from several extrapulmonary infection sites like the synovial fluid or the cerebrospinal fluid. Extrapulmonary manifestations might affect nearly each organ, among them the skin, the hematologic, the cardiovascular and the nervous system. They occur in up to 25% of all *M. pneumoniae* infected patients. Encephalitis is one of the most severe manifestations and supposed to be caused by the direct presence of *M. pneumoniae* in the brain causing inflammation. Therefore, *M. pneumoniae* has to enter the blood stream at its primary infection site, i.e. the lung tissue, disseminate through the blood (probably attached to cellular blood components) and finally cross the blood-brain barrier (Narita, 2009; Narita, 2010). The possible interaction of *M. pneumoniae* with RBCs is reflected in early studies which used erythrocytes as a model to analyze their adhesion behavior and showed that the attachment to RBCs is mediated by sialic acid residues (Baseman *et al.*, 1982). Using electron microscopy it was proven that the mycoplasmas even produce depressions in the surface of human erythrocytes thereby deforming them – a feature which it shares with hemotropic mycoplasmas (Deas *et al.*, 1979; Messick, 2009). In this work, it could be shown that *M. pneumoniae* can cause hemagglutination which is most probably mediated by surface proteins which are needed to attach the bacterium to host cells. The functionality of these adhesins relies on the protein kinase PrkC (Schmidl *et al.*, 2010). Here, it could be shown that also the process of hemagglutination is strongly reduced in a *prkC* mutant indicating that PrkC activity is needed for the binding and clumping of erythrocytes **(Fig. 3.14)**. Hemagglutination is typically seen in pathogenic avian mycoplasmas like *M. gallisepticum* and *M. synoviae*, where it is procured by a large family of variable lipoprotein hemagglutinins (*vlhA*). These lipoproteins are important surface proteins for cytadherence, host-cell-interaction and antigenic variation. Different *M. gallisepticum* strains possess about 30-70 genes encoding VlhA variants. *M. pneumoniae* does not possess homologs of the VlhA family. However, this organism also has an astonishingly high proportion of lipoprotein genes which partially are differentially expressed according to external conditions (Hallamaa *et al.*,

2006; Hallamaa *et al.*, 2008). It is tempting to speculate that also in *M. pneumoniae* lipoproteins play a role in hemagglutination and phase variation which would facilitate a (transient) lifestyle in human blood. In fact, the expression of *M. pneumoniae* lipoproteins *in vitro* seems to be dynamically altered in response to the presence of sheep blood in the surrounding medium as suggested by preliminary RNA seq. experiments (data not shown).

4.2.3   Hemolytic and hemoxidative activities in *M. pneumoniae*

Hemolytic activity has been described for a multitude of pathogenic bacteria. In *Mycoplasma* species, including *M. pneumoniae*, hemolysis and host cell damage has mainly been attributed to the production of H_2O_2 (Cole *et al.*, 1968; Hames *et al.*, 2009). In 1965, Somerson *et al.* tentatively identified hydrogen peroxide as the hemolysin in *M. pneumoniae*. Three years later, Cole *et al.* published a study about hemolysis related to hydrogen peroxide production in different *Mycoplasma* spp. In this study, they showed that *M. pneumoniae,* as well as most other tested *Mycoplasma* species, cause strong β-hemolysis on sheep blood agar plates. Interestingly, this β-hemolysis appeared to be completely reversed upon addition of catalase in all tested cases except for *M. neurolyticum, M. mycoides* and *M. bovigenitalium*, in which catalase could only reduce the β-hemolysis. From that, it could be concluded that H_2O_2 is the only hemolytic compound in *M. pneumoniae* (Cole *et al.,* 1968). In this present work, the ability of *M. pneumoniae* to perform β-hemolysis on plates overlaid with sheep blood agar could be confirmed. However, in contrast to the previous findings, this effect was not completely remedied by addition of even high amounts of catalase. In fact, even the *glpD* mutant, which is deficient in H_2O_2 production, was able to perform β-hemolysis in both the absence and presence of catalase. In principle, several explanations for that observation could be considered: (i) *M. pneumoniae* produces very high amounts of H_2O_2 independent from GlpD; (ii) the catalase is not efficient enough; (iii) *M. pneumoniae* possesses a hemolysin or β-hemolytic compound other than H_2O_2. Indeed, *M. pneumoniae* is able to produce H_2O_2 with glucose or PTS sugars as substrate as could be shown in H_2O_2 assays (Schmeisky, 2013; data not shown). However, these amounts are extremely low in comparison to the G3P- dependent release catalyzed by GlpD. Moreover, it can be excluded that the catalase is not adequately efficient. The average amount of H_2O_2 produced by M129 with 100 μM glycerol as substrate accounts for 10 mg/l (Schmidl *et al.*, 2011). This is easily removed by only 10-40 units of catalase **(Fig.3.13)**. 1000-4000 U catalase, a concentration which is used in the hemolysis

assays, are even able to rapidly erase 500 mg/l hydrogen peroxide. Also, it could be shown that the catalase per se is not causing hemoxidation. In fact, erythrocytes naturally contain catalases and are able to eliminate elevated levels of H_2O_2 to some extent (Eaton *et al.*, 1972). These points suggest that the obvious β-hemolysis halos around the *M. pneumoniae* colonies originate from a source other than H_2O_2. This assumption is supported by the fact, that in *Streptococcus pneumoniae*, H_2O_2 production leads to a strong α-hemolysis on blood agar plates (Duane *et al.*, 1993). Actually, this feature is typically used to distinguish this bacterium from its β-hemolytic relative *S. pyogenes* which produces the pore-forming streptolysin O but no H_2O_2 **(Fig. 1.2 B)**. In further support of the assumption that H_2O_2 is not responsible for *M. pneumoniae* β-hemolysis, it could be hypothesized that in a rather anaerobic environment, as it is established after overlaying the *M. pneumoniae* colonies with blood agar, there is less O_2 available for GlpD as electron acceptor. As a consequence, less H_2O_2 could be produced.

For a better understanding of the hemolytic activity of *M. pneumoniae*, accessory hemolysis assays in liquid culture were performed and the spectra of hemoglobin were measured to discover potential modifications. Surprisingly, these assays revealed that *M. pneumoniae* does not display beta-hemolysis in liquid culture. Instead, strong α-hemolysis (hemoxidation) was observed in all samples, which is probably caused by H_2O_2. The hemoxidative effect was also present in the *glpD* mutant and could partially, but not entirely, be removed by addition of catalase. This finding would also exclude H_2O_2 as the hemolysin and therefore matches the results obtained from the blood agar plates which suggest the existence of another hemolytic or hemoxidative compound. Though the hemoxidative effect of *M. pneumoniae* in liquid blood culture perfectly fits the production of the hemoxidative compound H_2O_2, the significant discrepancy between α-hemolysis in liquid culture and β-hemolysis on blood agar plates appeared rather puzzling. A similar conflict concerning hemolysis in liquid culture and on blood agar plates was observed in a study about hemolytic activities in *Mycoplasma penetrans*. This bacterium turned out to behave beta-hemolytic on blood agar plates and alpha-hemolytic in liquid culture. The beta-hemolysis of *M. penetrans* on plates was mainly attributed to the action of a membrane-associated phospholipase C. Beside pore-forming toxins, phospholipases A and C represent a large group of typical hemolysins, which destroy erythrocytes by cleaving and degrading special phospholipids in the cell membrane (Titball, 1993). In their investigations, Kannan and Baseman suggested that the presence of alpha or beta-hemolysis might be due to the presence or absence of oxygen in the respective culture. Since the overlay of *M. penetrans* or *M. pneumoniae* colonies with blood agar produces partial anaerobic environments, potential oxygen-labile hemolysins might be protected and

active only on plates. To prevent or reverse the possible oxidative damage in liquid culture, cysteine was added as reducing agent. In *M. penetrans*, the addition of cysteine indeed lead to a strongly increased hemolytic activity indicating the presence of a typical oxygen-labile hemolysin, similar to streptolysin O or listeriolysin O, which relies on a reduced cysteine residue for lytic activity (Kannan and Baseman, 2000). To clarify, if maybe a similar mechanism is working in *M. pneumoniae*, the hemolysis assays in liquid culture were repeated with addition of various cysteine concentrations and gave an unexpected result. Not only did cysteine cause β-hemolysis after an overnight incubation of *M. pneumoniae* with sheep RBCs, it also strongly promoted a rapid, preceding hemoxidation. The combination of cysteine-dependent hemolysis and hemoxidation is not typical for oxygen-labile hemolysins and points at the existence of yet another type of hemolytic and hemoxidative compound. Indeed, a cysteine-dependent hemoxidation and hemolysis has been described for several oral pathogenic bacteria like *Treponema denticola*, *Prevotella intermedia* or *Streptococcus anguinosus* (Chu *et al.*, 1997; Yano *et al.*, 2009; Yoshida *et al.*, 2002). In these organisms, L-cysteine is converted to ammonia, pyruvate and H_2S in a PLP-dependent β carbon-sulfur (βC-S) lyase reaction that leads to a modification of hemoglobin and to hemolysis. On the basis of these reports, the ability of *M. pneumoniae* to produce hydrogen sulfide from L-cysteine was examined. Astonishingly, *M. pneumoniae* cells really release H_2S when cysteine is present – a previously unknown behavior for this organism. Since H_2S can modify hemoglobin to form sulfhemoglobin or methemoglobin, the alteration of the hemoglobin spectrum in the hemassay containing *M. pneumoniae* and cysteine can be attributed to H_2S release. However, it has to be considered that there is always an interplay of a variety of toxic compounds and pathogenicity factors which might lead to hemoxidation and hemolysis *in vivo*. A combined action of H_2O_2, H_2S and superoxide anions produced by *M. pneumoniae* might cause eventually irreversible oxidative damage and hemoglobin modification in erythrocytes. The noxious effect of *M. pneumoniae* on erythrocytes in liquid culture is also underlined by the microscopic images in **Fig. 3.15.** It is clearly visible that the shape of RBCs seems to turn from discocytes to echinocytes, similar to those incubated with *M. suis*.

4.3 The importance of HapE and H$_2$S formation for viability, virulence and hemolytic activity of *M. pneumoniae*

4.3.1 Which enzyme generates H$_2$S in *M. pneumoniae*?

After the finding, that *M. pneumoniae* is able to release H$_2$S, the responsible enzyme for H$_2$S production was to be found. BLAST searches for an L-cysteine desulfhydrase or a βC-S lyase in *M. pneumoniae* did not yield a hit. Aside from that, the protein that appeared most obvious to fulfill a similar function was the putative L-cysteine desulfurase MPN487, which is also PLP-dependent. To rule out or confirm its potential involvement in H$_2$S production, the protein was subsequently investigated.

Overexpression and purification of a *Strep*-tagged version of MPN487 was feasible without difficulties. Initial hydrogen sulfide assays confirmed that MPN487 is a hydrogen sulfide producing enzyme *in vitro*. In order to determine whether MPN487 produces H$_2$S in a Michaelis-Menten-like manner, enzyme kinetics were performed using different cysteine concentrations. The analysis yielded a typical Michaelis-Menten substrate saturation curve for H$_2$S production indicating that this finding is not an artifact but relates to a true catalytic function (**Fig. 3.27**). Still, it has to be noted that the calculated K_{m} value is very high, which indicates that the enzyme has a rather low affinity for its substrate.

Further investigations using GC-MS revealed that, surprisingly, MPN487 also releases pyruvate and alanine *in vitro,* with pyruvate being produced at a twofold higher rate than alanine. According to this unexpected combination of products, MPN487 was for now renamed in HapE (**H**$_2$S, **a**lanine and **p**yruvate producing **E**nzyme).

A

```
CSD_MYCPN     1  --------MTK------------------------------------------------    3
Q56257_TREDN  1  MIYDFTTKISRKNLGSLKWDLMYSQNPEVGNEVVPLSVADMEFKNPPELIEGLKKYLDET   60
                         :::

CSD_MYCPN     4  ----TKFNPYQFRKQFKWFKNNPQWVNFDNAATSIALDTVSQACKEYYELFSVNPHNKTP   59
Q56257_TREDN 61  VLGYTGPTEEYKKTVKKWMKDRHQWDIET-------------------------------   89
                     *   .   :.  **:*:.* **

CSD_MYCPN    60  DLNNQIIAIIAETRQLVADWFNVTALEIIFTSSATESINLFAHGLKPWIKPGDEIVLKGD  119
Q56257_TREDN 90  ------------------DWIINT----------AGVVPAVFNAVREFTKPGDGVIIITP  121
                                   **:  *        :  :  . ..:: : **** :::

CSD_MYCPN   120  EHSANVLPWVALAKQT------------------------------------------KA  137
Q56257_TREDN 122 V----YYPFFMAIKNQERKIIECELLEKDGYYTIDFEKLEKLSKDKNNKALLFCSPHNPV  177
                       *:.    *:                                              .

CSD_MYCPN   138  RLVWVEKQANQSLEDTFKSLINPKTKVVAITATSNLFGNSIDFAQIADYLKQVNPKAFVA  197
Q56257_TREDN 178 GRVWKKDELQK--------------IKDIVLKSDLMLWSDEIHFDLIMPGYE---HTVFQS  221
                  **  :.: :*                * :.:.*.* *      :       ..* :*

CSD_MYCPN   198  VDAVQTVQHKQIDIAKTQIDFLAFSTHKFYGPTGLGVAYIKKSLQPQLQ-PLKLGGDIFT  256
Q56257_TREDN 222 ID---------EQLADKTITFTA--PKTFNIAGMGMSNIIIKN-PDIRERFTKSRDI-T   268
                  :*          ::*.* * *TREDN  * :  : *:*:*::  *   *:::  :.  .** *

CSD_MYCPN   257  QIDPDNTIHFKSTPLK------------------------FEAGTPNIMA---------  282
Q56257_TREDN 269 SGMPFTTLGYKACECYKECGKWLDGCIKVIDKNQRIVKDFFEVNHPEIKAPLIEGTYLQ  328
                  .  * .*: :*:  :        **.   *:* *

CSD_MYCPN   283  ---------------IYALNKLLRFFKQKFNFAQMMAYGHQLKQQAYELLNSNPQIVLAN  327
Q56257_TREDN 329 WIDFRALKMDHKAMEEFMIHKAQIFFDEGYIFG-------------------------  361
                  : :.:*  :**.:: *.

CSD_MYCPN   328  HDQDVPIFSFKHRQLATIDLATFLNINKIMVRQGSICVGRYRNKDYFVRVSLMHYNTV--  385
Q56257_TREDN 362 ------------------------------DGGIGFE--------RINLAAPSSVIQ   380
                                                :*.*. .     *:.*    .:*

CSD_MYCPN   386  KELQYLAKLLATDTKTIIKNVIK   408
Q56257_TREDN 381 ESLERLNKALKD----LKNRHLK   399
                  :.*:* *** *        : :. :*
```

B

```
CSD_MYCPN     1  --MTKTKFNPYQFRKQFKWF---KNNPQWVNFDNAATSIALDTVSQACKEYYELFSVNPH   55
SUFS_BACSU    1  -------MNITDIREQFPILHQQVNGHDLVYLDSAATSQKPRAVIETLDKYYNQYNSNVH   53
CSD_SYNY3     1  MVALQIPSLAATVRQDFPILNQEINGHPLVYLDNAATSQKPRAVLEKLMHYYENDNANVH   60
                   .* :: .        *  :   *. : *  :**.**** :**  : * .   **:  .* ***

CSD_MYCPN    56  NKTPDLNNQIIAIIAETRQLVADWFNVT-ALEIIFTSSATESINLFAHGL-KPWIKPGDE  113
SUFS_BACSU   54  RGVHTLGTRATDGYEGAREKVRKFINAKSMAEIIFTKGTTTSLNMVALSYARANLKPGDE  113
CSD_SYNY3    61  RGAHQLSVRATDAYEAVRNKVAKFINARSPREIVYTRNATEAINLVAYSWGMNNLKAGDE  120
                  .  .  *  :      .   * *  : . .:*: * **::*  :*  ::*:.* .   :* ***

CSD_MYCPN   114  IVLKGDEHSANVLPWVALAKQTKARLVWVEKQANQSLE-DTFKSLINPKTKVVAITATSN  172
SUFS_BACSU  114  VVITYMEHHANIIPWQQAVKATGATLKYIPLQEDGTISLEDVRETVTSNTKIVAVSHVSN  173
CSD_SYNY3   121  IITTVMEHHSNLVPWQMVAAKTGAVLKFVQLDEQESFDLEHFKTLLSEKTKLVTVVHISN  180
                  ::  .   **.*::**    .   * * * :   : : :::.  .:  .  :**:*:*  **

CSD_MYCPN   173  LFGNSIDFAQIADYLKQVNPKAFVAVDAVQTVQHKQIDIAKTQIDFLAFSTHKFYGPTGL  232
SUFS_BACSU  174  VIGTVNPIKEMAKIAHD--NGAVIVVDGAQSTPHMKIDVQDLDCDFFALSSHKMCGPTGV  231
CSD_SYNY3   181  TIGCVNPAEEIAQLAHQ--AGAKVLVDACQSAPHYPLDVQLIDCDWLVASGHKMCAPTGI  238
                  :* .     ::*.  ::       *   **.  *: * .:*   .   *:: .  * *:. ***:

CSD_MYCPN   233  GVAYIKKSLQPQLQPLKLGGDIFTQIDPDNTIHFKSTPLKFEAGTPNIMAIYALNKLLRF  292
SUFS_BACSU  232  GVLYGKKALLENMEPAEFGGEMIDFVGLYE-STWKELPWKFEAGTPIIAGAIGLGAAIDF  290
CSD_SYNY3   239  GFLYGKEEILEAMPPFFGGGEMIAEVFFDH-FTTGELPHKFEAGTPAIAEAIALGAAVDY  297
                  *. .*:    : :*    : **::    . *   .   * ******* :  .* : *  :

CSD_MYCPN   293  FKQKFNFAQMMAYGHQLKQQAYELLNSNPQIVLAN----HDQDVPIFSFKHRQLATIDLA  348
SUFS_BACSU  291  LE-EIGLDEISRHEHKLAAYALERFRQLDGVTVYGPEE----RAGLVTFNLDDVHPHDVA  345
CSD_SYNY3   298  LT-DLGMENIHNYEVELTHYLWQGLGQIPQLRLYGPNPKHGDRAALASFNVAGLHASDVA  356
                  :    .: : :: :   *     : .:    : :    :        . : :*: : *:*

CSD_MYCPN   349  TFLNINKIMVRQGSICVGRY---RNKDYFVRVSLMHYNTVKELQYLAKLLATDTKTIIKN  405
SUFS_BACSU  346  TVLDAEGIAVRAGHHCAQPLMKWELDVTATARASFYLYNTEEEIDKLVEALQKTKEYFTNV  405
CSD_SYNY3   357  TMVDQDGIAIRSGHHCTQPLHRLFDASGSARASLYFNTKEEIDLFLQSLQATIRFFSDD  416
                  *.::  : * :* *  . *     .   :       *   *** :*:: :  * * : *

CSD_MYCPN   406  VIK-   408
SUFS_BACSU  406  F---   406
CSD_SYNY3   417  DFTV   420
```

Fig. 4.2. Alignments of the putative L-cysteine desulfurase MPN487 (CSD_MYCPN) with similar proteins. **A**. Alignment with the cystalysin Hly from *T. denticola* (Q56257_TREDN). **B**. Alignment with SufS from *B. subtilis* (SUFS_BACSU) and Slr0077, a putative NifS from *Synechocystis* with desulfurase and lyase activity (CS_SYNY3). Identical residues (dark grey) are indicated by asterisks, similar residues (lighter grey) are marked by dots. Yellow: catalytic cysteine for persulfide binding. Red: PLP binding site. Blue: residues which, beside the PLP binding Lys, are invariant in aminotransferases.

4.3.2 Is HapE working as an L-cysteine desulfhydrase or an L-cysteine desulfurase?

The production of pyruvate and H_2S from L-cysteine is a typical feature of L-cysteine desulfhydrases which catalyze a PLP-dependent β carbon-sulfur (βC-S) lyase reaction. However, an alignment between the desulfhydrase Hly from *T. denticola* and HapE (MPN487) shows only 10.3% similarity. Beside a conserved cysteine in the active center, the lysine for PLP binding and three additional residues that are invariant in aminotransferases, both proteins do not share substantial similarities (**Fig. 4.2 A**). This is remarkably different in the alignment of MPN487 with the L-cysteine desulfurase SufS from *B. subtilis* which share 29% identity. Indeed, according to genome annotations, MPN487 is a putative L-cysteine desulfurase Csd (UniProt) or NifS (KEGG) (Himmelreich *et al.*, 1996). These enzymes are normally involved in acquiring sulfur as a first step of iron-sulfur-cluster biogenesis (**Fig. 4.3 C**). In this reaction, free cysteine binds the PLP cofactor of the desulfurase, forming a PLP-cysteine adduct. The SH-group of this cysteine is then attacked by a cysteine in the active center of the enzyme to generate a very stable persulfide bond (R-S-SH) while releasing alanine as a side product. The activated sulfur is transmitted to a scaffolding protein, which additionally acquires iron from external sources, and builds either a rhombic [2Fe-2S] or a cubic [4Fe-4S] iron-sulfur-cluster. By means of special trafficking enzymes, the cluster is subsequently transferred to proteins which are in need for iron-sulfur-clusters to finally form functional holoenzymes (Fe-S proteins) (Ayala-Castro *et al.*, 2008; Py and Barras, 2010).

Proteins involved in Fe-S cluster formation usually belong to one of the NIF (nitrogen fixation), ISC (iron-sulfur cluster) or SUF (sulfur mobilization) systems. In *B. subtilis*, the Suf system comprises SufCDSUB and SufA with SufS being the sulfur-binding L-cysteine desulfurase, while SufU is an important adjacent scaffolding protein (Tokumto *et al.*, 2004; Selbach *et al.*, 2013). The SufBCD complexes from *B. subtilis* and *E. coli* share high sequence similarities and form a pseudo ABC transporter which functions in sulfur mobilization and FeS-cluster assembly. Finally, SufA is supposed to be another cluster scaffold or a shuttle protein which can be transferred to apoprotein targets (Vinella *et al.*, 2009, Ayala-Castro *et al.*, 2008). The genes involved in the process of Fe-S cluster generation are typically organized in one operon (**Fig. 4.3 A**).
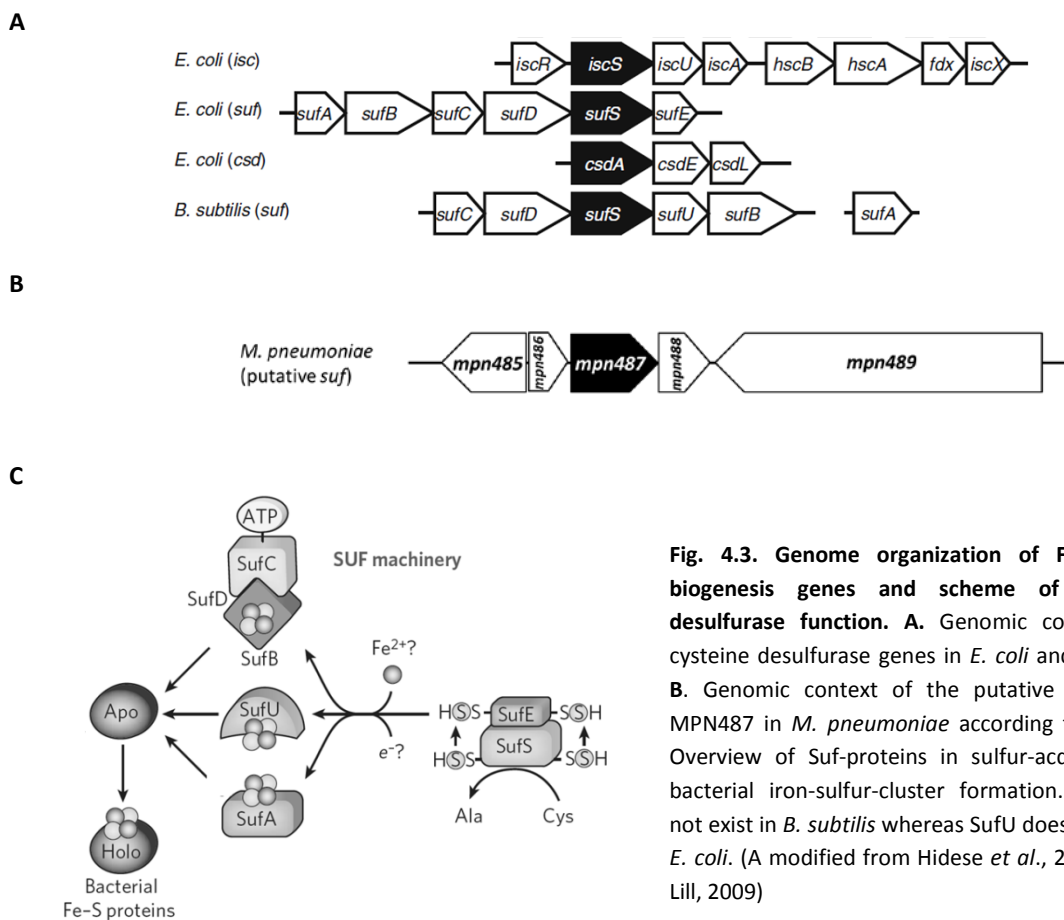
A

B

C

Fig. 4.3. Genome organization of Fe-S cluster biogenesis genes and scheme of L-cysteine desulfurase function. A. Genomic context of L-cysteine desulfurase genes in *E. coli* and *B. subtilis*. **B**. Genomic context of the putative desulfurase MPN487 in *M. pneumoniae* according to KEGG. **C**. Overview of Suf-proteins in sulfur-acquisition for bacterial iron-sulfur-cluster formation. SufE does not exist in *B. subtilis* whereas SufU does not exist in *E. coli*. (A modified from Hidese *et al.*, 2011, C from Lill, 2009)

The activity of SufS in *B. subtilis* strongly depends on the presence of and interaction with the scaffolding-protein SufU (Selbach *et al.*, 2010). Their mechanism of sulfur transfer starts with a non-covalent binding of SufU to SufS, which is loaded with the persulfide. Subsequently, the persulfide is transferred from the desulfurase to the cysteine 41 of its scaffold SufU. After this intermolecular sulfur transfer, SufU dissociates from the complex and performs an intramolecular sulfur transfer to other cysteine residues (Albrecht *et al.*, 2011). SufS alone exhibits a very modest activity. In contrast, when SufU was present, the rate of sulfide and alanine production is increased more than 100-fold. It was concluded that SufU plays an active role in the catalytic mechanism of SufS (Selbach *et al.*, 2010).

In comparison to reports about SufS$_{Bsu}$, both the v$_{max}$ (6.9 µmol S^{2-}/min/mg) and the K_m value (11.21 mM as compared to 86 µM in *B. subtilis*) for the rate of H$_2$S formation by HapE are substantially higher. The K_m value of catalysis determines the affinity of the enzyme towards its substrate: the higher the value, the lower the affinity. It seems that HapE has a relatively low affinity for L-cysteine, since H$_2$S is only formed with comparatively high substrate concentrations. Still, the maximum velocity is more than six-fold higher than for SufS$_{Bsu}$, suggesting that HapE activity does not necessarily rely on

the presence of a putative SufU. Nevertheless, *M. pneumoniae* encodes MPN487/HapE (putative SufS) and MPN488 (putative SufU) in a putative Suf operon (**Fig. 4.3 B**). Most of their adjacent genes code for hypothetical proteins and are oriented antisense, which supports the assumption that they are not part of a larger operon comprising additional *suf* genes. To test a potential interaction of HapE with the putative SufU, MPN488, B2H studies were performed in this work. Interestingly, in these tests, clear self-interactions of MPN488 could be seen (**Fig.3.33**), which is common for some scaffolding proteins like IscU (Ayala-Castro *et al.*, 2008; Chandramouli *et al.*, 2007). On the contrary, no interaction between MPN487 and MPN488 was detectable in the B2H, suggesting that MPN487 and MPN488 are not involved in the same pathway *in vivo*. One reason for this B2H result might of course be a lack of interaction between the two proteins. However, since the B2H makes use of heterologous expression in *E. coli*, the *Mycoplasma* proteins could exhibit differential functions or even be misfolded and inactive at all. Thus, this negative result might give a hint at a lack of interaction, but it nevertheless cannot be excluded. The interaction and sulfur transfer from SufS to SufU in *B. subtilis* was shown to rely on the presence of three cysteine residues (Cys41, Cys66, Cys128) and one aspartate residue (Asp43) coordinating an essential zinc atom. Cysteine 41 is located in the center of 6 amino acids long flexible loop, which probably has in important influence on the efficiency of persulfide transfer (Albrecht *et al.*, 2011; Selbach *et al.*, 2014). The alignment of SufU$_{Bsu}$ and MPN488 shows that these residues are also conserved in the *M. pneumoniae* protein (**Fig.4.4**). However, it might be possible that for some reason the flexibility of the loop carrying cysteine 41 is altered. Likewise, SufS proteins contain an important loop and their activity and the delivery of the sulfur to the acceptor molecule is strongly dependent on its flexibility. Therefore, it should be taken into consideration that there might have been conformational changes in the evolution of these proteins which would not allow for proper interaction of MPN488 with MPN487.

The Suf operon, e.g. from *E. coli,* was shown to be up-regulated upon iron-limitation and under conditions of oxidative stress (Hantke, 2002; Zheng *et al.*, 2001). Assuming MPN487 and MPN488 were part of a classical Suf operon and involved in the same pathway, their genes would be expected to be up-regulated under similar conditions. The expression of the *mpn487* and *mpn488* genes was thus examined in Slot Blot analyses in response to iron-deprivation, oxidative stress and the availability of cysteine (**Fig. 3.32**). Interestingly, incubation with the iron chelator 2,2-dipyridyl led to an induction of *mp488* expression, whereas the impact of L-cysteine was rather low as compared with the *mpn487* transcription rate. In contrast, neither H_2O_2 stress nor iron-limitation, but L-cysteine did result in an up-regulation of *mpn487* expression. This result is especially striking considering the fact that the

genes are located directly behind each other. It seems that MPN488 behaves similarly as typical Suf proteins, whereas MPN487 does not.
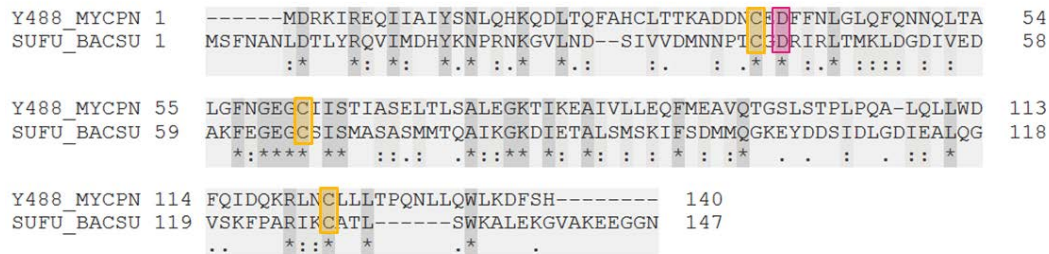
```
Y488_MYCPN   1  ------MDRKIREQIIAIYSNLQHKQDLTQFAHCLTTKADDNCHDFFNLGLQFQNNQLTA   54
SUFU_BACSU   1  MSFNANLDTLYRQVIMDHYKNPRNKGVLND--SIVVDMNNPICSDRIRLTMKLDGDIVED   58
                 :*   *:  *:  *.* :.*   *.:     :.     :  .  * : .*  :::: : :

Y488_MYCPN  55  LGFNGEGCIISTIASELTLSALEGKTIKEAIVLLEQFMEAVQTGSLSTPLPQA-LQLLWD  113
SUFU_BACSU  59  AKFEGEGCSISMASASMMTQAIKGKDIETALSMSKIFSDMMQGKEYDDSIDLGDIEALQG  118
                 *:**** **  ::..:  .*::** *:  *: : : *  : :*   . .   :   . :: *

Y488_MYCPN 114  FQIDQKRLNCLLLTPQNLLQWLKDFSH--------  140
SUFU_BACSU 119  VSKFPARIKCATL------SWKALEKGVAKEEGGN  147
                 ..        *::*  *         .*    .
```

Fig. 4.4. Alignment of the putative SufU from *M. pneumoniae* MPN488 (Y488_MYCPN) with SufU from *B. subtilis* (SUFU_BACSU). The zinc binding aspartate 43 is marked red. The cysteine residues that are important for persulfide transfer are yellow. Both proteins share 18.7% identity.

Fe-S proteins are found ubiquitously in nearly each organism and it is supposed that Fe-S clusters belong to the earliest catalytic biomolecules. In *E. coli*, nearly 80 Fe-S proteins have been described (Blattner *et al.*, 1997; Py and Barras, 2010). A high proportion of those are involved in respiration (e.g. nitrate reductase and NADH dehydrogenase complexes), biosynthetic pathways, especially vitamin biosynthesis, the TCA cycle or regulation of gene expression including post-transcriptional and post-translational modification. In a review by Py and Barras (2010) about bacterial strategies to build Fe-S proteins, all Fe-S enzymes from *E. coli* are listed. Astonishingly, BLAST analyses of each single protein did not give a single hit in *M. pneumoniae* or *M. genitalium*. Unlike in other *Mycoplasma* spp., the same is true for BLAST searches of all *B. subtilis* Fe-S proteins listed in SubtiWiki. These results strongly indicate that *M. pneumoniae* (and probably also *M. genitalium*) does not possess Fe-S proteins. Of course this conclusion is a daring thesis given the fact that Fe-S clusters are ubiquitously found. However, it might still be possible as a result of extreme, reductive evolution. The high K_m value of HapE, which refers to a low substrate affinity, might support this theory. In case Fe-S cluster proteins were existing and essential in *M. pneumoniae*, their biogenesis should be guaranteed already at very low cysteine concentrations as seen for other essential L-cysteine desulfurases. Instead, it seems that HapE activity is only needed when higher cysteine levels are available. In fact, high intracellular cysteine concentrations can become toxic for the cell due to promotion of oxidative DNA damage by the Fenton-reaction (Park and Imlay, 2003). The conversion of excessive cysteine might hence also represent a mechanism of protection.

The screen for an *mpn487* mutant in our transposon mutant library was not successful (data not shown). Since the probability to find a mutant for a non-essential gene in the mutant library is 99.999%, this outcome indicates that the gene is essential for *M. pneumoniae* (Halbedel and Stülke, 2007). The possible lack of iron-sulfur-clusters in *M. pneumoniae* of course raises the question, why HapE is indispensable. As a matter of fact, cysteine desulfurases can be involved in important processes aside from Fe-S cluster synthesis and iron homeostasis. These include amongst others thiamin biosynthesis, molybdopterin biosynthesis, biotin biosynthesis and t-RNA modification (**Fig. 4.5. A**) (Mihara and Esaki, 2002; Hidese *et al.*, 2011). The generation of the important sulfur-containing nucleosides 4-thiouridine (s^4U) and 5-methylaminomethyl-2-thiouridine (mnm^5s^2U) at positions 8 and 34, respectively, in bacterial tRNAs mostly relies on the action of L-cysteine desulfurases for initial acquisition of sulfur (**Fig 4.5. B**) (Bjök, 1996). For biosynthesis of s^4U, IscS/SufS removes the sulfur from free cysteine as described above to form a persulfide which is transferred via ThiI to the tRNA forming s^4U8 (Kambampati and Lauhon, 2000).
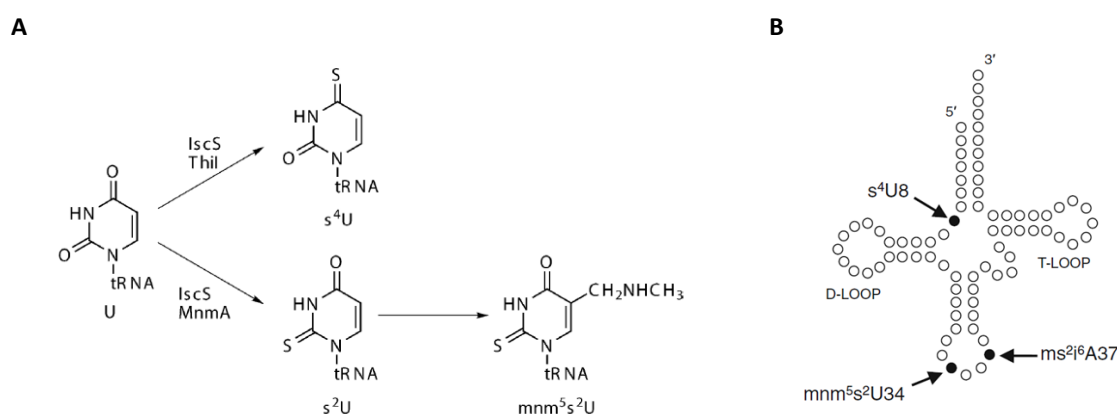
Fig. 4.5. Representative tRNA modifications in bacteria. A. Proposed pathways for the formation of s^4U and mnm^5s^2U depending on the sulfur mobilization by IscS/SufS. **B.** Thiomodification sites in bacterial tRNA from *E. coli*. Filled circles indicate 4-thiouridine 8, 5-methylaminomethyl-2-thiouridine 34 and 6-N-dimethyallyl-2-methylthioadenosine 37.

The formation of mnm^5s^2U requires IscS/SufS, MnmA and a 2-thiolation step (Sullivan *et al.*, 1985). While 4-thiouridine (s^4U) can serve as near UV-photosensors, the modification of uridines into 2-thiouridine at wobble position 34 in tRNA[Lys], tRNA[Glu] and tRNA[Gln] is crucial for precise decoding of the genetic code. Interestingly, recent publications about *Salmonella enterica* revealed that, in these bacteria, the initial step of sulfur mobilization for thiamine thiazole is conditionally mediated by a cysteine desulfhydrase, CdsH (Palmer *et al.*, 2014). In *M. pneumoniae*, genes coding for both a putative ThiI (MPN550) and a putative MnmA (MPN422) are present. This implies that HapE might also be

involved in the mobilization of sulfur for crucial tRNA modifications, which would give one possible explanation for its essentiality in the organism.

Another aspect, which should be taken into account when discussing the biochemical function of HapE, is the finding that several PLP containing enzymes can catalyze an abortive transamination as a side reaction (Mihara *et al.*, 2000). In this process, the amino group of the cysteine is transferred to the cofactor PLP resulting in its conversion to pyridoxamine phosphate (PMP) and the subsequent inactivation of the enzyme. In case of L-cysteine desulfurases, the substrate is thereby converted to pyruvate as a side product. Thus, one might argue that HapE does not produce pyruvate on purpose but as a side product of abortive transamination and that H_2S is only released *in vitro* because the bound persulfide cannot be transferred to the following enzyme in its natural pathway. Then again, this might be refuted by the fact that *M. pneumoniae* indeed releases H_2S *in vivo* meaning that there has to be a hydrogen sulfide-generating enzyme present in the organism. Moreover, by means of the GC-MS studies, pyruvate has been shown to be produced even in a higher rate than alanine. This would actually suggest that abortive transamination is preferentially catalyzed. In the studies of Mihara *et al.*, it was shown that the conversion of PLP to PMP can be derived from a change in their photometric spectrum, and that the abortive process is reversible upon addition of higher concentrations of PLP or external pyruvate. For HapE, the analysis of the photometric spectrum did not yield useful results. The spectra of HapE and the PLP control looked quite similar, however neither of them showed the typical spectrum of PLP. In order to test the reversibility of a potential abortive transamination in HapE, hemolysis assays with HapE plus pyruvate or the 10-fold concentration of PLP were performed (data not shown). In both cases, no difference to the controls was detectable indicating that either reversion did not work or no abortive transamination occurred. On the other hand, the formation of both pyruvate and alanine from cysteine has been reported for the protein Slr0077 from the cyanobacterium *Synechocystis*. This enzyme, which shares 49% similarity with $SufS_{Bsu}$ and 28% similarity with HapE, has cysteine desulfurase and cysteine lyase activity. Depending on the redox conditions either the formation of pyruvate or alanine is favored although both reactions are catalyzed at a very low rate (Kessler, 2004). This example supports the idea of HapE being involved in both functions.

Though *T. denticola* Hly and HapE share only 10.3% sequence similarity, there are certain aspects which argue for an L-cysteine desulfhydrase function of HapE and accompanying advantages for the bacterium. The production of pyruvate and H_2S from L-cysteine in a PLP-dependent β carbon-sulfur (βC-S) lyase reaction is a typical feature of L-cysteine desulfhydrases. Although these enzymes are

126

usually involved in amino acid metabolism, i.e. the biosynthesis of methionine via homocysteine, there are increasing reports about additional functions (Soda, 1987). In *E. coli*, there are several cysteine desulfhydrases. Its major cysteine desulfurase is the tryptophanase TnaA which primarily catabolizes tryptophane but also can also degrade cysteine *in vivo*. The degradation of cysteine proceeds with a K_m of 11 mM which is strongly reminiscent of HapE (Snell, 1975). TnaA expression is induced by cysteine and thought to contribute to energy generation by production of pyruvate. Similarly, *mpn487* transcription was shown to be up-regulated in the presence of cysteine (**Fig. 3.32**). In *M. pneumoniae*, the only ways of ATP generation are glycolysis and the final step of acetate production from pyruvate by the acetate kinase AckA. An effective conversion of cysteine to pyruvate could therefore represent a convenient source of energy for the minimal organism. The newly described cysteine desulfhydrase CdsH from *Salmonella enterica* was shown to play an important role in the regulation of potentially toxic intracellular cysteine levels, since a *cdsH* mutant strain exhibited more sensitivity towards exogenous cysteine. Also, the gas H_2S has been proven to protect a variety of bacteria from antibiotics (Shatalin *et al.*, 2011). Likewise, the high activity of HapE at high cysteine concentrations and the production of hydrogen sulfide could represent efficient mechanisms of self-protection.

A potential multifunction of HapE is not anything unusual. The genome reduction in bacteria like *M. pneumoniae* often goes along with the evolution of multitasking bacterial moonlighting enzymes. These proteins have activities in addition to their primary functions which are in many cases related to virulence. A widespread moonlighting function is the host cell adhesion and plasminogen-binding by glycolytic enzymes including aldolase, enolase, glyceraldehyde 3-phosphate dehydrogenase (GAPDH), phospholycerate mutase (PGM) and others. The adhesive properties of GAPDH is mainly found in streptococci and staphylococci, but was also shown for *M. genitalium* and *M. pneumoniae* binding to mucin (Alvarez *et al.*, 2003; Dumke *et al.*, 2011; Hernderson and Martin, 2011). Also, the pyruvate dehydrogenase subunit B and enolase have been identified as plasminogen-binding proteins in *M. pneumoniae* (Thomas *et al.*, 2013). Therefore, an additional enzymatic function for MPN487 (HapE) or a change of its role in *M. pneumoniae* is definitely to be considered.

4.3.3 Are HapE and hydrogen sulfide formation involved in virulence?

As a toxic gas, H_2S acts as a virulence factor in a variety of oral pathogens. Its toxicity is based on a multitude of destructive effects on proteins and cells. Once released from the bacterium, H_2S can react

with diverse metalloproteins, inhibit oxidative phosphorylation and break disulfide bonds of proteins in surrounding cells (Beauchamp *et al.*, 1984). These cells may not only include host cells but also bacterial competitors to establish a niche. There have been several studies on the impact of H_2S on host tissues in the habitat of oral bacteria like *T. denticola, Porphyromonas gingivalis* or *S. intermedius*. In these, H_2S was described to increase the permeability of oral mucosal tissue, increase the collagen solubility or decrease the protein synthesis in human gingival fibroblasts (Johnson *et al.*, 1992; Ng and Tonzetich, 1984). Similarly, hydrogen sulfide produced by *M. pneumoniae* might have analogous effects on lung mucosal tissue and epithelial cells or promote selective advantages and defense against other lung pathogens.

The L-cysteine desulfhydrase of *T. denticola* has been studied intensely concerning biochemical properties and its role in virulence. Beside a growth promoting effect due to pyruvate production and the beneficial alteration of the periodontal ecology by H_2S release, the enzyme was significantly involved in modification of hemoglobin and hemolysis (Hespell and Canle-Parola, 1971; Chu *et al.*, 1997; Chu *et al.*, 1999; Kurzban *et al.*, 1999). Initial incubation of erythrocytes with *T. denticola* led to a cysteine-dependent alteration of hemoglobin, referring to the formation of methemoglobin, and to a change of erythrocyte morphology from discocytes to spiky echinocytes (Chu *et al.*, 1994). In further studies, the accumulation of modified forms of hemoglobin, especially methemoglobin and sulfhemoglobin, was clearly assigned to cysteine-dependent production of hydrogen sulfide by the *T. denticola* cystalysin and even caused hemolysis (Chu *et al.*, 1999; Kurzban *et al.*, 1999).

The investigation of *M. pneumoniae* behavior in blood culture followed by subsequent analysis of HapE in this work, gave similar results. As described in 3.2 and 4.2, incubation of red blood cells with *M. pneumoniae* led to echinocytosis and modification of hemoglobin, which is strongly enhanced in the presence of L-cysteine. The same is true for incubation of RBCs with HapE and cysteine. As for the cystalysin, HapE causes hemoxidation as formation of sulfhemoglobin or methemoglobin due to the production of H_2S. This modification of hemoglobin is finally accompanied by real hemolysis indicating that H_2S formation by HapE is causing hemolysis thereby representing a virulence factor similar to cystalysin in *T. denticola*. To compare the hemoxidative and hemolytic effect of HapE to the one caused by H_2O_2 from GlpD, hemolysis assays with both proteins and their substrates were performed in parallel. Hemoxidation by formation of H_2O_2 from GlpD proceeded very fast and efficiently. In contrast, hemoxidation due to H_2S release went comparatively slowly, which is in good agreement with the different activities of both enzymes. However, while hemoxidation caused by GlpD stayed on a constant level, hemoxidation by HapE induced strong beta-hemolysis indicating that,

concerning hemolysis *in vitro*, HapE has a surprisingly higher impact than GlpD. This might originate from their distinct mechanisms of hemoglobin modification. While H_2O_2 leads to formation of methemoglobin, reaction with H_2S generates higher amounts of sulfhemoglobin than methemoglobin. As a matter of fact, treatment of RBCs with either H_2S or H_2O_2 could be shown to result in modification of hemoglobin and formation of echinocytes (Moxness *et al.*, 1996). However, only sulfhemoglobin was shown to substantially contribute to phospholipid extraction from the RBC membrane, which finally results in hemolysis.

From these findings, the following possible virulence mechanism for *M. pneumoniae* in blood can be proposed: Upon initial intracellular production of H_2S, the toxic compound diffuses out of the cell to reach and enter erythrocytes. Once inside the RBC, H_2S leads to formation of sulfhemoglobin resulting in lipid depletion, echinocytosis and ultimate hemolysis. The attachment of *M. pneumoniae* to RBCs facilitates this process. Following hemolysis, important nutrients and fresh supplies of cysteine become available to the mycoplasmas, promoting further formation of H_2S and more hemolysis.

Attempts to investigate the role of HapE or *M. pneumoniae* plus cysteine in a HeLa cell infection assay failed (data not shown), which is why RBCs have been the only potential host cells tested so far. Assuming that lipid depletion by sulfhemoglobin formation is the reason for RBC lysis by HapE, this might not work for other cells, e.g. the lung epithelium. However, since H_2S was shown to be toxic for oral mucosa and fibroblasts, a similar effect in the lung tissue cannot be excluded (Johnson *et al.*, 1992; Ng and Tonzetich, 1984). Likewise, the release of H_2O_2 does not cause hemolysis but significant lysis of HeLa cells. Probably, the effect of H_2S on different cell types can also be quite diverse.

L-cysteine is present in the blood plasma of a healthy person in a concentration of about 0.25 mM and it is thought to contribute to the plasma's redox homeostasis (El-Khairy *et al.*, 2001). In erythrocytes, cysteine is present in higher concentrations (about 1 mM) and cysteine influx and efflux are tightly regulated. It is assumed that erythrocytes can import and store cysteine from blood plasma, since high cysteine concentrations can be toxic there (Yildiz et al., 2006). If higher cysteine levels are needed for the redox status of the plasma, erythrocytes might export cysteine again. Erythrocytes are not capable of protein synthesis, which is why they do not need this amino acid for incorporation into proteins. However, they strongly rely on the presence of cysteine for the synthesis of glutathione (GSH), a tripeptide consisting of glutamate, cysteine and glycine. GSH is an important antioxidant which protects living cells from free radicals and lipid peroxidation and is therefore abundant throughout the human body, especially in regions where free radicals can cause the most damage (Gille and Sigler, 1995; Clemens and Walker, 1987). Surprisingly, for *T. denticola*, it was reported that glutathione

promotes cell growth and H$_2$S synthesis (Chu *et al.*, 2002). Although the cystalysin cannot directly use glutathione as substrate, it is assumed to be the final element in a stepwise degradation of glutathione yielding glutamate, glycine, pyruvate, ammonia and hydrogen sulfide. It would therefore be interesting to learn whether *M. pneumoniae* can also metabolize glutathione, since it is not only present in blood but also abundant in lung tissue as primary habitat. Lung infections and injury like the chronic obstructive pulmonary disease (COPD) have been treated with N-acetylcysteine (NAC), for quite a while now. This medication is a cysteine-derivative which by providing sulfhydryl groups, can induce cysteine metabolism and act both as a precursor of reduced glutathione and as a direct ROS scavenger in the lung tissue (Huang and Ling, 2001; Sadowska *et al.*, 2007). This is an interesting aspect considering the finding that cysteine and glutathione can promote the virulence of certain bacteria, perhaps including *M. pneumoniae.* Nevertheless, the question whether the formation of hydrogen sulfide is in a sufficient rate to be important for the establishment or support of virulence *in vivo* remains difficult to assess. In contrast to glycerol, cysteine concentrations in the environment need to be relatively high to induce cell lysis by *M. pneumoniae* suggesting that H$_2$S production plays a minor role in overall virulence. On the other hand, the diversity of virulence factors might represent some sort of bacterial adaptation according to their efficiency in different environments.

A realistic evaluation of the involvement of HapE in virulence *in vivo* is even more exacerbated considering reported discrepancies between potential virulence factors *in vitro* and *in vivo.* In *M. pneumoniae*, the CARDS toxin (MPN372) is one example. Whereas an *mpn372* mutant does not exhibit reduced cytotoxicity *in vitro*, the protein was clearly shown to have an impact *in vivo* in a mouse model and in infected patients (Kannan and Baseman, 2006). In contrast, the production of H$_2$O$_2$ from glycerol is a virulence factor in a lot of mycoplasmas and is evidentially cytotoxic for cocultured eukaryotic cells. A recent publication about *M. gallisepticum,* however, revealed that a *glpO* mutant, which is deficient of hydrogen peroxide production, is still completely virulent in the respiratory tracts of chicken indicating that *in vivo* pathogenicity is mediated by a so far unknown additional factor in this *Mycoplasma* species (Szczepanek *et al.*, 2014). An indispensable method to unequivocally assess the function of HapE in pathogenicity would therefore include an *in vivo* infection study with a *hapE* mutant strain, which is unfortunately not available. Interestingly, HeLa cell assays with a *M. agalactiae* transposon library found the SufS/SufU locus to be crucial for proliferation of this ruminant pathogen in the presence of HeLa cells (Baranowski *et al.*, 2010). In later studies, the importance of the locus for *in vivo* infectivity was tested using knockout mutants in the natural host. Indeed, none of the tested mutants was able to survive and colonize the host. From these results

Baranowski and colleagues concluded that this gene locus plays a so far not elucidated key role in the infection process of *M. agalactiae* – and most probably in other *Mycoplasma* species as well (Baranowski *et al.*, 2014).

4.4   Conclusions and future perspectives

To get more insight into the interplay between *M. pneumoniae* and blood, further blood infection assays could be performed with M129, the clinical isolates and mutant strains and analyzed microscopically for deformations of erythrocytes and echinocytosis. For comparison, erythrocytes could be incubated with hydrogen peroxide or hydrogen sulfide. Since no *hapE* mutant can be isolated, it might be interesting to construct and analyze a *Mycoplasma* strain containing additional copies of *hapE*. This strain would be investigated for higher H_2S production and hemolysis for an clearer assignment of these functions to HapE. Moreover, with a *M. pneumoniae* strain containing a highly expressed, *Strep*-tagged version of HapE, a SPINE could be performed. This would shed light on the *in vivo* interaction partners and functions of HapE – possibly by interacting with ThiI or MnmA for tRNA modification. For a better understanding of the biochemical function and catalysis of HapE, time course experiments to monitor the formation of alanine and pyruvate are performed and compared to the activity of SufS from *B. subtilis*. Also, different substrate concentrations might be tested to see if the availability of cysteine has an influence on the reaction type of HapE favouring alanine of pyruvate production. Another important task poses the purification of MPN488 to investigate its influence on HapE or possibly $SufS_{Bsu}$ activity in H_2S, alanine and pyruvate formation. Finally, alternative substrates like homocysteine, glutathione or selenocysteine could be applied in enzyme assays for a comprehensive view of HapE activities

.

5. SUMMARY

The human pathogen *Mycoplasma pneumoniae* is a remarkable minimal organism which primarily colonizes the human lung tissue. To reach distant infection sites, it probably also enters the blood stream. The *Mycoplasma* genome has constantly undergone reductive changes due to strong adaptation to the convenient conditions and high nutrient availability in its habitat. In turn, this adaptation renders the bacterium dependent on the exploitation of the host tissue. This dependence is reflected by a high number of genes coding for transport proteins with most of them being essential. In the initial part of this work, the importance of several *M. pneumoniae* transporters for survival and virulence was addressed. However, except for two putative amino acid transporters and one potential Mg^{2+} transporter, none of the isolated transporter mutants showed a significant effect indicating that the influence of the analyzed transporters in growth and cytotoxicity is negligible. Following the analysis of a putative hemolysin transporter, general hemolytic activities in *M. pneumoniae* were investigated in the second part of this work. It appeared that the organism causes β-hemolysis on blood agar plates but α-hemolysis (hemoxidation) in liquid culture. Surprisingly, the long assumed hemolysin H_2O_2 caused only hemoxidation and no real hemolysis. Addition of L-cysteine to liquid blood culture unexpectedly resulted in strong hemoxidation followed by complete hemolysis. In several oral pathogens, such as *Treponema denticola*, similar effects are caused by production of H_2S by so called L-cysteine desulfhydrases. H_2S is a toxic gas which leads to modification of hemoglobin and subsequent hemolysis. For *M. pneumoniae*, none of these processes in response to cysteine have been described before. In this work, the bacteria were proven to be capable of producing H_2S. The search for a potential H_2S producing enzyme in *Mycoplasma* retrieved MPN487, an essential putative L-cysteine desulfurase which is actually supposed to be involved in FeS-cluster formation. In enzyme assays, it turned out that MPN487 indeed produces H_2S in a Michaelis-Menten-like behavior and additionally forms alanine and pyruvate. Thus, MPN487 was renamed in HapE (H_2S, alanine and pyruvate producing enzyme). Since alanine formation is a feature of L-cysteine desulfurases, whereas pyruvate- and H_2S production are performed by L-cysteine desulfhydrases, HapE might be a novel enzyme which combines both functions or has changed its activity in a process of reductive evolution. In hemolysis assays, HapE showed strong hemoxidation and hemolysis of erythrocytes when incubated with cysteine. This *in vitro* hemolysis rate even exceeded that of the major virulence factor H_2O_2, produced by the enzyme GlpD. Even though the *in vivo* effect in the human host can only be hypothesized by now, the formation of H_2S and pyruvate by HapE might represent an important new way to ensure virulence and energy generation of this minimal pathogen.

6. REFERENCES

Albrecht AG, F Peuckert, H Landmann, M Miethke, A Seubert, and MA Marahiel. 2011. Mechanistic characterization of sulfur transfer from cysteine desulfurase SufS to the iron-sulfur scaffold SufU in *Bacillus subtilis*. FEBS Lett. **585**:465-470.

Alvarez RA, MW Blaylock, and JB Baseman. 2003. Surface localized glyceraldehyde-3-phosphate dehydrogenase of *Mycoplasma genitalium* binds mucin. Mol Microbiol**. 48**:1417-1425.

Ayala-Castro C, A Saini, and FW Outten. 2008. Fe-S cluster assembly pathways in bacteria. Microbiol Mol Biol Rev. 7**2**:110-125.

Baranowski E, S Guiral, E Sagné, A Skapski, and C Citti. 2010. Critical role of dispensable genes in *Mycoplasma agalactiae* interaction with mammalian cells. Infect Immun. **78**:1542-1551.

Baranowski E, D Bergonier, E Sagné, MC Hygonenq, P Ronsin *et al*. 2014. Experimental infections with *Mycoplasma agalactiae* identify key factors involved in host-colonization. PLoS One. **9**:e93970.

Barile MF. 1979. *Mycoplasma*-tissue cell interactions, p. 425–474. In J. G. Tully and R. F. Whitcomb (ed.), The *Mycoplasmas* II. Human and animal mycoplasmas, vol. 2. Academic Press, New York, N.Y.

Barker JR and KE Klose. 2007. Molecular and genetic basis of pathogenesis in *Francisella tularensis*. Ann N Y Acad Sci. **1105**:138–59.

Baseman JB. 1993. The cytadhesins of *Mycoplasma pneumoniae* and *M. genitalium*. Subcell Biochem. **20**:243-59.

Baseman JB, M Banai, and I Kahane. 1982. Sialic acid residues mediate *Mycoplasma pneumoniae* attachment to human and sheep erythrocytes. Infect Immun. **38**:389-391.

Beauchamp Jr. RO, JS Bus, JA Popp, CJ Boreiko, and DA Andjelkovich. 1984. A critical review of the literature on hydrogen sulfide toxicity. Crit Rev Toxicol. **13**:25–97.

Bellaire A, T Ischebeck, Y Staedler, I Weinhaeuser, A Mair, *et al*. 2014. Metabolism and development - integration of micro computed tomography data and metabolite profiling reveals metabolic reprogramming from floral initiation to silique development. New Phytol. **202**:322-335.

Ben-Menachem G, U Zähringer, and S Rottem. 2001. The phosphocholine motif in membranes of *Mycoplasma fermentans* strains. FEMS Microbiol Lett. **199**:137-141.

Bhakdi S, N Mackman, JM Nicaud, and IB Holland. 1986. *Escherichia coli* hemolysin may damage target cell membranes by generating transmembrane pores. Infect Immun. **52**:63–69.

Bhakdi S and Tranum-Jensen. 1991. Alpha-toxin of *Staphylococcus aureus*. Microbiol Rev. **55**:733-751.

Bhugra B, LL Voelker, N Zou, H Yu, and K Dybvig. 1995. Mechanism of antigenic variation in *Mycoplasma pulmonis*: interwoven, site-specific DNA inversions. Mol Microbiol. **18**:703–714.

Bjök GR. 1996. Stable RNA modification. In: Neidhardt FC. (ed) *Escherichia coli* and *Salmonella*: cellular and molecular biology. ASM Press, Washington, DC, pp 861–886.

Blanchard A and C Bébéar. 2011. The evolution of *Mycoplasma genitalium*. Ann N Y Acad Sci. **1230**:E61-64.

Blattner FR, G Plunkett 3rd, CA Bloch, NT Perna *et al*. 1997. The complete genome sequence of *Escherichia coli* K-12. Science. **277**:1453-1462.

Boschiroli ML, S Ouahrani-Bettache, V Foulongne, S Michaux-Charachon, G Bourg, *et al*. 2002. Type IV secretion and *Brucella* virulence. Vet Microbiol. **90**:341–348.

Bradford MM. 1976. A rapid sensitive method for the quantification of microgram quantities of protein utilizing the principle of protein dye binding. Anal Biochem. **72**:248-254.

Braun V and T Focareta. 1991. Pore-forming bacterial protein hemolysins (cytolysins). Crit Rev Microbiol. **18**:115-158.

Burns DL. 2003. Type IV transporters of pathogenic bacteria. Curr Opin Microbiol. **6**:1–6.

Calderwood SB and JJ Mekalanos. 1987. Iron regulation of Shiga-like toxin expression in *Escherichia coli* is mediated by the fur locus. J Bacteriol. **169**:4759.

Carroll MEW, PS Jackett, VR Aber, and DB Lowrie. 1979. Phagolysosome formation, cyclic adenosine 3':5'-monophosphate and the fate of *Salmonella typhimurium* within mouse peritoneal macrophages. J Gen Microbiol. **110**:421-429.

Carstensen EL, J Maniloff, and CW Einolf. 1971. Electrical properties and ultrastructure of *Mycoplasma* membranes. Biophys J. **11**:572-581.

Cavalieri SJ, Bohach GA, Snyder IS. 1984, *Escherichia coli* alpha-hemolysin: characteristics and probable role in pathogenicity. Microbiol Rev. **48**:326-343.

Censini, S, C Lange, Z Xiang, JE Crabtree, P Ghiara, *et al*. 1997. Cag, a pathogenicity island of *Helicobacter pylori*, encodes type I-specific and disease-associated virulence factors. Proc Natl Acad Sci USA. **93**:14648–14653.

Chandramouli K, MC Unciuleac, S Naik, DR Dean, BH Huynh, and MK Johnson. 2007. Formation and properties of [4Fe-4S] clusters on the IscU scaffold protein. Biochemistry. **46**:6804–6811.

Chanock RM, L Hayflick, and MF Barile. 1962. Growth on artificial medium of an agent associated with atypical pneumonia and its identification as a PPLO. Proc Natl Acad Sci U S A. **48**:41-9.

Chambaud I, H Wróblewski, and A Blanchard. 1999. Interactions between *Mycoplasma* lipoproteins and the host immune system. Trends Microbiol. **7**:493-499.

Chatfield MJ and GN La Mar. 1992. 1H nuclear magnetic resonance study of the prosthetic group in sulfhemoglobin. Arch Biochem Biophys. **295**:289-296.

Chu L and SC Holt. 1994. Purification and characterization of a 45 kDa hemolysin from *Treponema denticola* ATCC 35404. Microb Pathog. **16**:197–212.

Chu L, A Burgum, D Kolodrubetz, and SC Holt. 1995. The 46-kilodalton-hemolysin gene from *Treponema denticola* encodes a novel hemolysin homologous to aminotransferases. Infect Immun. **63**:4448-4455.

Chu L, J Ebersole, GP Kurzban, and SC Holt. 1997. Cystalysin, a 46-kilodalton cysteine desulfhydrase from *Treponema denticola*, with hemolytic and hemoxidative activities. Infect Immun. **65**:3231–3238.

Chu L, JL Ebersole, and SC Holt. 1999. Hemoxidation and binding of the 46-kDa cystalysin of *Treponema denticola* leads to a cysteine-dependent hemolysis of human erythrocytes. Oral Microbiol Immunol. **14**:293-303.

Chu L, Z Dong, X Xu, DL Cochran, and JL Ebersole. 2002. Role of glutathione metabolism of *Treponema denticola* in bacterial growth and virulence expression. Infect Immun. **70**:1113-1120.

Ciccarelli FD, T Doerks, C von Mering, CJ Creevey, B Snel, and P Bork. 2006. Toward automatic reconstruction of a highly resolved tree of life. Science. **311**:1283-1287.

Citti C, GF Browning, and R Rosengarten. 2005. Phenotypic diversity and cell invasion in host subversion by pathogenic *mycoplasmas*. In Blanchard A and G Browning (ed.). *Mycoplasmas*: molecular biology, pathogenicity and strategies for control. Horizon Bioscience, Norfolk, United Kingdom. pp. 439–483.

Citti C, LX Nouvel, and E Baranowski. 2010. Phase and antigenic variation in mycoplasmas. Future Microbiol. **5**:1073-1085.

Clemens MR and HD Waller. 1987. Lipid peroxidation in erythrocytes. Chem Phys Lipids. **45**:251-268.

Cohen G and NL Somerson. 1967. *Mycoplasma pneumoniae*: hydrogen peroxide secretion and its possible role in virulence. Ann N Y Acad Sci. **143**:85-87.

Cole BC, JR Ward, and CH Martin. 1968. Hemolysin and Peroxide Activity of *Mycoplasma* Species. J Bacteriol. **95**:2022-2330.

Coulter SN, WR Schwan, EY Ng MH Langhorne *et al*. 1998. *Staphylococcus aureus* genetic loci impacting growth and survival in multiple infection environments. Mol Microbiol. **30**:393–404.

Dallo SF and JB Baseman. 2000. Intracellular DNA replication and long-term survival of pathogenic mycoplasmas. Microb Pathog. **29**:301–309.

Dallo SF, TR Kannan, MW Blaylock, and JB Baseman. 2002. Elongation factor Tu and E1 β subunit of pyruvate dehydrogenase complex act as fibronectin binding proteins in *Mycoplasma pneumoniae*. Mol Microbiol. **46**:1041-1051.

Dandekar T, M Huynen, JT Regula, *et al*. 2000. Re-annotating the *Mycoplasma pneumoniae* genome sequence: adding value, function and reading frames. Nucl Acids Res. **28**:3278-3288.

Davidson AL, E Dassa, C Orelle, and J Chen. 2008. Structure, function, and evolution of bacterial ATP-binding cassette systems. Microbiol Mol Biol Rev. **72**:317-364.

Deas JE, FA Janney, LT Lee and C Howe. 1979. Immune electron microscopy of cross-reactions between *Mycoplasma pneumoniae* and human erythrocytes. Infect Immun. **24**:211.

Deutscher J, C Francke, and PW Postma. 2006. How Phosphotransferase System-related protein phosphorylation regulates carbohydrate metabolism in bacteria. Microbiol Mol Biol Rev. **70**:939.

Diethmaier C, N Pietack, K Gunka, C Wrede, M Lehnik-Habrink *et al*. 2011. A novel factor controlling bistability in *Bacillus subtilis*: the YmdB protein affects flagellin expression and biofilm formation. J Bacteriol. **193**:5997-6007

Duane PG, JB Rubins, HR Weisel, and EN Janoff. 1993. Identification of hydrogen peroxide as a *Streptococcus pneumoniae* toxin for rat alveolar epithelial cells. Infect Immun. **61**:4392–4397.

Dumke R, M Hausner, and E Jacobs. 2011. Role of *Mycoplasma pneumoniae* glyceraldehyde-3-phosphate dehydrogenase (GAPDH) in mediating interactions with the human extracellular matrix. Microbiol. **157**:2328-2338.

Eaton JW, M Boraas, and NL Etkin. 1972. Catalase activity and red cell metabolism. Adv Exp Med Biol. **28**:121-131.

El-Khairy L, PM Ueland, H Refsum, IM Graham, and SE Vollset. 2001. Plasma total cysteine as a risk factor for vascular disease: The European Concerted Action Project. Circulation. **103**:2544-2549.

Erkens GB, M Majsnerowska, J ter Beek, and DJ Slotboom. 2012. Energy coupling factor-type ABC transporters for vitamin uptake in prokaryotes. Biochemistry. **51**:4390-4396.

Fagerlund A, T Lindbäck, and PE Granum. 2010. *Bacillus cereus* cytotoxins Hbl, Nhe and CytK are secreted via the Sec translocation pathway. BMC Microbiol. **10**:304.

Felmlee T, S Pellett, and RA Welch. 1985. Nucleotide sequence of an *Escherichia coli* chromosomal hemolysin. J Bacteriol. **163**:94–105.

Finlay BB and S Falkow. 1997. Common themes in microbial pathogenicity revisited. Microbiol Mol Biol Rev. **61**:136-169.

Forestal CA, M Malik, SV Catlett, *et al*. 2007. *Francisella tularensis* has a significant extracellular phase in infected mice. J Infect Dis. **196**:134–137.

Fraser, CM, JD Gocayne, O White *et al*. 1995. The minimal gene complement of *Mycoplasma genitalium*. Science. **270**:397-403.

Fukamachi H, Y Nakano, M Yoshimura, and T Koga. 2002. Cloning and characterization of the L-cysteine desulfhydrase gene of *Fusobacterium nucleatum*. FEMS Microbiol Lett. **215**:75-80.

García E, D Llull, and R López. 1999. Functional organization of the gene cluster involved in the synthesis of the pneumococcal capsule. Int Microbiol. **2**:169-176.

Gentschev I and W Goebel. 1992. Topological and functional studies on HlyB of *Escherichia coli*. Mol Gen Genet. **232**:40–48.

Geofflroy C, J Raveneau, J-L Beretti, A Lechrolsey, J-A Vaquez-Boland *et al*. 1991. Purification and characterization of an extracellular 29-kilodalton phospholipase C from *Listeria monocytogenes*. Infect Immun. **59**:2382-2388.

Gille G and K Sigler. 1995. Oxidative stress and living cells. Folia Microbiol (Praha). **40**:131-152.

Goebel W and J Hedgpeth. 1982. Cloning and functional characterization of the plasmid-encoded hemolysin determinant of *Escherichia coli*. J Bacteriol. **151**:1290–1298.

Groebel K, K Hoelzle, MM Wittenbrink, U Ziegler, and LE Hoelzle. 2009. *Mycoplasma suis* invades porcine erythrocytes. Infect Immun. **77**:576–584.

Großhennig S. 2011. Implication of transport systems in *M. pneumoniae* pathogenicity. Master thesis.

Großhennig S, Schmidl SR, Schmeisky G, Busse J, and J Stülke. 2013. Implication of glycerol and phospholipid transporters in *Mycoplasma pneumoniae* growth and virulence. Infect Immun. **81**:896-904.

Güell M, V van Noort, E Yus, WH Chen *et al*. 2009. Transcriptome complexity in a genome-reduced bacterium. Science. **328**:1268-1271.

Hackett M, L Guo, J Shabanowitz, DF Hunt, and EL Hewlett. 1994. Internal lysine palmitoylation in adenylate cyclase toxin from *Bordetella pertussis*. Science **266**:433–435.

Halbedel S, C Hames, and J Stülke. 2004. *In vivo* activity of enzymatic and regulatory components of the phosphoenolpyruvate:sugar phosphotransferase system in *Mycoplasma pneumoniae*. J Bacteriol. **186**:7936-7943.

Halbedel S, J Busse, SR Schmidl, and J Stülke. 2006. Regulatory protein phosphorylation in *Mycoplasma pneumoniae*. A PP2C-type phosphatase serves to dephosphorylate HPr(Ser-P). J Biol Chem **281**:26253-26259.

Halbedel S, C Hames, and J Stülke. 2007. Regulation of carbon metabolism in the mollicutes and its relation to virulence. J Mol Microbiol Biotechn. **12**:147-154.

Halbedel S and J Stülke. 2007. Tools for genetic analysis of *Mycoplasma*. Int J Med Microbiol. **297**:37-44.

Hallamaa KM, GF Browning, and SL Tang. 2006. Lipoprotein multigene families in *Mycoplasma pneumoniae*. J Bacteriol. **188**:5393-5399.

Hallamaa KM, SL Tang, N Ficorilli, and GF Browning. 2008. Differential expression of lipoprotein genes in *Mycoplasma pneumoniae* after contact with human lung epithelial cells, and under oxidative and acidic stress. BMC Microbiol. **8**:124.

Hamada S and HD Slade. 1980. Biology, Immunology, and cariogenicity of *Streptococcus mutans*. Microbiol Rev **44**:331–384.

Hames, C. 2008. Glycerolmetabolismus und Pathogenität von *Mycoplasma pneumoniae*. PhD thesis.

Hames C, S Halbedel, **and J Stülke**. 2009. Glycerol metabolism is important for cytotoxicity of *Mycoplasma pneumoniae*. J Bacteriol. **191**:747-753.

Hantke K. 2002. Members of the Fur protein family regulate iron and zinc transport in *E. coli* and characteristics of the Fur-regulated FhuF protein. J Mol Microbiol Biotechnol. **4**:217–222.

Hardie KR, J-P Issartel, E Koronakis, C Hughes, and V Koronakis. 1991. *In vitro* activation of *Escherichia coli* prohaemolysin to the mature membrane-targeted toxin requires HlyC and a low molecular-weight cytosolic polypeptide. Mol Microbiol. **5**:1669–1679.

Havarstein LS, DB Diep, and IF Nes. 1995. A family of bacteriocin ABC transporters carry out proteolytic processing of their substrates concomitant with export. Mol Microbiol **16**:229–240.

Henderson GB, EM Zevely, and FM Huennekens. 1977. Purification and properties of a membrane-associated, folate-binding protein from *Lactobacillus casei*. J Biol Chem. **252**:3760–3765.

Henderson GB, EM Zevely, and FM Huennekens. 1979. Coupling of energy to folate transport in *Lactobacillus casei*. J Bacteriol. **139**:552–559.

Henderson B and A Martin. 2011. Bacterial virulence in the moonlight: multitasking bacterial moonlighting proteins are virulence determinants in infectious disease. Infect Immun. **79**:3476-3491.

Hespell RB and E Canle-Parola. 1971. Amino acid and glucose fermentation by *Treponema denticola*. Arch Mikrobiol. **78**:234–251.

Hidese R, H Mihara, and N Esaki. 2011. Bacterial cysteine desulfurases: versatile key players in biosynthetic pathways of sulfur-containing biofactors. Appl Microbiol Biotechnol. **91**:47-61.

Himmelreich, R, H Hilbert, H Plagens, E Pirkl, B-C Li, and R Herrmann. 1996. Complete sequence analysis of the genome of the bacterium *Mycoplasma pneumoniae*. Nucl Acids Res. **24**:4420-4449.

Hoelzle LE, K Hoelzle, M Helbling, H Aupperle, *et al.*. 2007. MSG1, a surface-localised protein of *Mycoplasma suis* is involved in the adhesion to erythrocytes. Microbes Infect. **9**:466-474.

Hoelzle LE. 2007. Significance of haemotrophic mycoplasmas in veterinary medicine with particular regard to the *Mycoplasma suis* infection in swine. Berl Muench Tieraerztl Wochenschr. **120**:34–41.

Horn DL, DC Morrison, SM Opal, R Silverstein, K Visvanathan, and JB Zabriskie. 2000. What are the microbial components implicated in the pathogenesis of sepsis? Report on a symposium. Clin Infect Dis. **31**:851-858.

Horzempa J, DM O'Dee, D Beer Stolz, JM Franks, D Clay, and GJ Nau1. 2011. Invasion of Erythrocytes by *Francisella tularensis*. J Infect Dis. **204**:51-59.
.
Huang XL and YL Ling. 2001. The antioxidant therapy of N-acetylcysteine to pulmonary injury. Int J Respir. **21**:64–69

Hutchings MI, T Palmer, DJ Harrington, and IC Sutcliffe. 2009. Lipoprotein biogenesis in Gram-positive bacteria: knowing when to hold 'em, knowing when to fold 'em. Trends Microbiol. **17**:13–21.

Inamine JM, TP Denny, S Loechel, U Schaper, CH Huang, KF Bott, and PC Hu. 1988. Nucleotide sequence of the P1 attachment-protein gene of *Mycoplasma pneumoniae*. Gene. **64**:217-229.

Ito S, H Nagamune, H Tamura, and Y Yoshida. 2008. Identification and molecular analysis of betaC-S lyase producing hydrogen sulfide in *Streptococcus intermedius*. J Med Microbiol. **57**:1411-1419.

Jacobs E. 1997. *Mycoplasma* infections of the human respiratory tract. Wien Klin Wochenschr. **109**:574-577.

Johnson PW, K Yaegaki, and J Tonzetich. 1992. Effect of volatile thiol compounds on protein metabolism by human gingival fibroblasts. J Periodont Res. **27**:553–561.

Kambampati R and CT Lauhon. 2000. Evidence for the transfer of sulfane sulfur from IscS to ThiI during the in vitro biosynthesis of 4-thiouridine in *Escherichia coli* tRNA. J Biol Chem. **275**:10727–10730.

Kannan TR and JB Baseman. 2000. Hemolytic and hemoxidative activities in *Mycoplasma penetrans*. Infect Immun. **68**:6419-6422.

Kannan TR and JB Baseman. 2006. ADP-ribosylating and vacuolating cytotoxin of *Mycoplasma pneumoniae* represents unique virulence determinant among bacterial pathogens. Proc Natl Acad Sci U S A. **103**:6724-6729.

Karimova G, N Dautin, and D Ladant. 2005. Interaction network among *Escherichia coli* membrane proteins involved in cell division as revealed by bacterial two-hybrid analysis. J Bacteriol. **187**:2233-2243.

Karimova G, J Pidoux, A Ullmann, and D Ladant. 1998. A bacterial two-hybrid system based on a reconstituted signal transduction pathway. Proc Natl Acad Sci USA. **95**:5752-5756.

Kemp BE. 2004. Bateman domains and adenosine derivatives form a binding contract. J Clin Invest. **113**:182–184.

Kenri T, R Taniguchi, Y Sasaki, N Okazaki, M Narita, *et al*. 1999. Identification of a new variable sequence in the P1 cytadhesin gene of Mycoplasma pneumoniae: evidence for the generation of antigenic variation by DNA recombination between repetitive sequences. Infect Immun. **67**:4557-4562.

Kessler D. 2004. Slr0077 of *Synechocystis* has cysteine desulfurase as well as cystine lyase activity. Biochem Biophys Res Commun. **320**:571-577.

Klose KE. 2001. Regulation of virulence in *Vibrio cholerae*. Int J Med Microbiol. **291**:81–88.

Kocan KM, J de la Fuente, and EF Blouin. 2007. Targeting the tick/pathogen interface for developing new anaplasmosis vaccine strategies. Vet Res Commun. **31**:91–96.

Koolman J and K-H Röhm. 2003. Taschenatlas der Biochemie. Georg Thieme Verlag, Stuttgart.

Krause DC. 1996. *Mycoplasma pneumoniae* cytadherence: unravelling the tie that binds. Mol Microbiol. **20**:247-253.

Krause DC and MF Balish. 2001. Structure, function, and assembly of the terminal organelle of *Mycoplasma pneumoniae*. FEMS Microbiol Lett. **198**:1-7.

Krause DC and D Taylor-Robinson. 1992. *Mycoplasmas* which infect humans. In: *Mycoplasmas*: Molecular Biology and Pathogenesis. J. *Maniloff,* R. N. McElhaney, L. R. Finch, and J. B. Baseman (eds.). American Society for Microbiology. Washington DC. pp. 417-444.

Kühner S, V van Noort, MJ Betts *et al*. 2009. Proteome organization in a genome-reduced bacterium. Science. **326**:1235-1240.

Kunst F, N Ogasawara, I Moszer, AM Albertini *et al*. 1997. The complete genome sequence of the gram-positive bacterium *Bacillus subtilis*. Nature. **390**:249-256.

Kurzban GP, L Chu, JL Ebersole, and SC Holt. 1999. Sulfhemoglobin formation in human erythrocytes by cystalysin, an L-cysteine desulfhydrase from *Treponema denticola*. Oral Microbiol Immunol. **14**:153-164.

Laemmli UK. 1970. Cleavage of structural proteins during the assembly of the head of Bacteriophage T4. Nature. **227**:680-685.

Lill R. 2009. Function and biogenesis of iron-sulphur proteins. Nature. **460**(7257):831-8.

Lluch-Senar M, J Delgado, C Weihua, J Wodke, A Vivancos *et al.* Excess of essential non-coding RNAs and novel short genes in a reduced bacterium: a new concept of minimal genome. Mol Syst Biol. In press.

Ludwig A, F Garcia, S Bauer, T Jarchau, R Benz *et al.* 1996. Analysis of the *in vivo* activation of hemolysin (HlyA) from *Escherichia coli*. J Bacteriol. **178**:5422-5430.

Lysnyansky I, K Sachse, R Rosenbusch, S Levisohn, and D Yogev. 1999. The *vsp* locus of *Mycoplasma bovis*: gene organization and structural features. J Bacteriol. **181**:5734-5741.

Mackay AD, JB Watt, and GR Jones. 1975. Myocarditis associated with *Mycoplasma pneumoniae* infection. Practitioner. **214**:390-392.

Maheswaran SK and RK Lindorfer. 1967. Staphylococcal beta-hemolysin. II. Phospholipase C activity of purified beta-hemolysin. J Bacteriol. **94**:1313-1319.

Markham PF, MD Glew, JE Sykes, TR Bowden, TD Pollocks *et al.* 1994. The organisation of the multigene family which encodes the major cell surface protein, pMGA, of *Mycoplasma gallisepticum*. FEBS Lett. **352**:347-352.

Martin-Verstraete I, M Débarbouillé, A Klier, and G Rapoport. 1994. Interactions of wild-type and truncated LevR of *Bacillus subtilis* with the upstream activating sequence of the levanase operon. J Mol Biol. **241**:178-192

Meiklejohn G, MD Beck and MD Eaton. 1944. Atypical pneumonia caused by psittacosis-like viruses. J Clin Invest. **23**:167-175.

Merino S, R Gavin, M Altarriba, L Izquierdo, ME Maguire, and TM Tomas. 2001. The MgtE Mg^{2+} transport protein is involved in *Aeromonas hydrophila* adherence. FEMS Microbiol Lett. **198**:189–195.

Merzbacher M, C Detsch, W. Hillen, and J Stülke. 2004. *Mycoplasma pneumoniae* HPr kinase/phosphorylase. Eur J Biochem. **271**:367-74.

Messick JB. 2004. Hemotrophic mycoplasmas (hemoplasmas): a review and new insights into pathogenic potential. Vet Clin Pathol. **33**:2-13.

Mihara H, T Kurihara, T Yoshimura, and N Esaki. 2000. Kinetic and mutational studies of three NifS homologs from *Escherichia coli*: mechanistic difference between L-cysteine desulfurase and L-selenocysteine lyase reactions. J Biochem. **127**:559-567.

Mihara H and N Esaki. 2002. Bacterial cysteine desulfurases: their function and mechanisms. Appl Microbiol Biotechnol. **60**:12-23.

Miles RJ. 1992. Catabolism in *mollicutes*. J Gen Microbiol. **138**:1773-1783.

Miyata M. 2008. Centipede and inchworm models to explain *Mycoplasma* gliding. Trends Microbiol. **16**:6-12.

Moomaw AS and Maguire ME. 2008. The unique nature of Mg^{2+} channels. Physiology (Bethesda). **23**:275-285.

Moxness MS, LS Brunauer, and WH Huestis. 1996. Hemoglobin oxidation products extract phospholipids from the membrane of human erythrocytes. Biochemistry. **35**:7181–7187.

Nakamura S, A Yamada, N Tsukagoshi, S Udaka, T Sasaki *et al*. 1988. Nucleotide sequence and expression in *Escherichia coli* of the gene coding for sphingomyelinase of *Bacillus cereus*. Eur J Biochem. **175**:213–220.

Nakao H and T. Takeda. 2000. *Escherichia coli* Shiga toxin. J Nat Toxins. **9**:299-313.

Narita M. 2009. Pathogenesis of neurologic manifestations of *Mycoplasma pneumoniae* infection. Pediatr Neurol. **41**:159-166.

Narita M. 2010. Pathogenesis of extrapulmonary manifestations of *Mycoplasma pneumoniae* infection with special reference to pneumonia. J Infect Chemother. **16**:162-169.

Nesterenko MV, M Tilley, and SJ Upton. 1994. A simple modification of Blum´s silver stain method allows for 30 minute detection of proteins in polyacrylamide gels. J Biochem Biophys Methods. **28**:239-242.

Neter E, EA Gorzynski, NJ Zalewski, R Rachman, and RM Gino. 1954. Studies on Bacterial Hemagglutination. Am J Public Health Nations Health. **44**:49–54.

Ng W and J Tonzetich. 1984. Effect of hydrogen sulfide and methyl mercaptan on the permeability of oral mucosa. J Dent Res. **63**:994–997.

Ochman H and NA Moran. 2001. Genes lost and genes found: evolution of bacterial pathogenesis and symbiosis. Science. **292**:1096–1099.

Papp-Wallace KM, M Nartea, DG Kehres, S Porwollik, M McClelland *et al*. 2008. The CorA Mg^{2+} channel is required for the virulence of *Salmonella enterica* serovar *typhimurium*. J Bacteriol. **190**:6517–6523.

Palmer LD, MH Leung, and DM Downs. 2014. The Cysteine Desulfhydrase CdsH Is Conditionally Required for Sulfur Mobilization to the Thiamine Thiazole in *Salmonella enterica*. J Bacteriol. **96**:3964-3970.

Park S and JA Imlay. 2003. High levels of intracellular cysteine promote oxidative DNA damage by driving the fenton reaction. J Bacteriol. **185**:1942-1950.

Persson S, MB Edlund, R Claesson, and J Carlsson. 1990. The formation of hydrogen sulfide and methyl mercaptan by oral bacteria. Oral Microbiol Immunol. **5**:195-201.

Py B and F Barras. 2010. Building Fe-S proteins: bacterial strategies. Nat Rev Microbiol. **8**:436-46.

Ramírez AS, A Rosas, JA Hernández-Beriain, JC Orengo, P Saavedra *et al*. 2005. Relationship between rheumatoid arthritis and *Mycoplasma pneumoniae*: a case-control study. Rheumatology **25**:912-914.

Razin S, S Kutner, H Efrati, and S Rottem. 1980. Phospholipid and cholesterol uptake by *Mycoplasma* cells and membranes. Biochim Biophys Acta. **598**:628-640.

Razin S, D Yogev, and Y Naot. 1998. Molecular biology and pathogenicity of *Mycoplasmas*. Microbiol Mol Biol Rev. **62**:1094-1156.

Reddy VS, MA Shlykov, R Castillo, EI Sun, and MH Saier Jr. 2012. The major facilitator superfamily (MFS) revisited. FEBS J. **279**:2022-2035.

Reizer J, AH Romano, and J Deutscher. 1993. The role of phosphorylation of HPr, a phosphocarrier protein of the phosphotransferase system, in the regulation of carbon metabolism in gram-positive bacteria. J Cell Biochem. **51**:19-24.

Rempeters L. 2011. Functional analysis of the glycolytic enzyme enolase and the DEAD-box RNA helicase CshA in the RNA metabolism of *Bacillus subtilis*. Master thesis.

Ren Q and IT Paulsen. 2007. Large-Scale Comparative Genomic Analyses of Cytoplasmic Membrane Transport Systems in Prokaryotes. J Mol Microbiol Biotechnol. **12**:165–179.

Rodionov DA, P Hebbeln, A Eudes, J ter Beek, IA Rodionova *et al.* 2009. A novel class of modular transporters for vitamins in prokaryotes. J Bacteriol. **191**:42–51.

Rosengarten R and KS Wise. 1991. The Vlp system of *Mycoplasma hyorhinis*: combinatorial expression of distinct size variant lipoproteins generating high-frequency surface antigenic variation. J Bacteriol. **173**:4782-4793.

Rottem S, L Adar, Z Gross, Z Neeman, and PJ Davis. 1986. Incorporation and Modification of Exogenous Phosphatidylcholines by *Mycoplasmas.* J Bacteriol. **167**:299-304.

Rottem S. 2003. Interaction of *Mycoplasmas* with host cells. Physiol Rev. **83**:417-432.

Sadowska AM, B Manuel-Y-Keenoy, and WA De Backer. 2007. Antioxidant and anti-inflammatory efficacy of NAC in the treatment of COPD: discordant in vitro and in vivo dose-effects: a review. Pulm Pharmacol Ther. **20**:9-22.

Saier M.H. 2000. A functional-phylogenetic classification system for transmembrane solute transporters. Microbiol Mol Biol Rev. **64:**354–411.

Sambrook J, EF Fritsch, and T Maniatis. 1989. Molecular cloning: a laboratory manual, 2nd ed. Cold Spring Harbor Laboratory, Cold Spring Harbor, N.Y.

Sanger F, S Nicklen, and AR Coulson. 1977. DNA sequencing with chain-terminating inhibitors. Proc Natl Acad Sci USA **74**:5463-5467.

Sasaki Y, J Ishikawa, A Yamashita, K Oshima, *et al.* 2002. The complete genomic sequence of *Mycoplasma penetrans*, an intracellular bacterial pathogen in humans. Nucl Acids Res. **30**:5293-5300.

SchaperU, JS Chapman, and PC Hu. 1987. Preliminary indication of unusual codon usage in the DNA coding sequence of the attachment protein of *Mycoplasma pneumoniae*. Isr J Med Sci. **23**:361-367.

Schauer K, J Stolz, S Scherer and TM Fuchs. 2009. Both thiamine uptake and biosynthesis of thiamine precursors are required for intracellular replication of *Listeria monocytogenes*. J Bacteriol. **191**:2218–2227.

Schiavo G, F Benfenati, B Poulain, O Rossetto, P Polverino de Laureto *et al.* 1992. Tetanus and botulinum-B neurotoxins block neurotransmitter release by proteolytic cleavage of synaptobrevin. Nature. **359**:832–835.

Schmeisky AG. 2013. Unteruchung zur kohlenstoffabhängigen Wasserstoffperoxidproduktion und Virulenz in *Mycoplasma pneumoniae* und *Mycoplasma genitalium*. PhD thesis.

Schmidl SR, C Hames, and J Stülke. 2007. Expression of *Mycoplasma* proteins carrying an affinity tag in *M. pneumoniae* allows rapid purification and circumvents problems related to the aberrant genetic code. Appl Environ Microbiol.**73**:7799-7801.

Schmidl SR, K Gronau, C Hames, J Busse *et al*. 2010. The stability of cytadherence proteins in *Mycoplasma pneumoniae* requires activity of the protein kinase PrkC. Infect Immun. **78**:184-192.

Schmidl SR, A Otto, M Lluch-Senar, J Pinol, J Busse *et al*. 2011. A trigger enzyme in *Mycoplasma pneumoniae*: Impact of the glycerophosphodiesterase GlpQ on virulence and gene expression. PLoS Pathog. **7**:e1002263.

Schmidt A. 1987. d-Cysteine desulfhydrase from spinach. Methods Enzymol. **143**:449–451.

Schmitt MP and RK Holmes. 1991. Iron-dependent regulation of diphtheria toxin and siderophore expression by the cloned *Corynebacterium diphtheriae* repressor gene *dtxR* in *C. diphtheriae* C7 strains. Infect Immun. **59**:1899-1904.

Schulein R, I Gentschev, H-J Mollenkopf, and W Goebel. 1992. A topological model for the haemolysin translocator protein HlyD. Mol Gen Genet. **234:**155–163.

Schulein R, Seubert A, Gille C, Lanz C, Hansmann Y, *et al*. 2001. Invasion and persistent intracellular colonization of erythrocytes. A unique parasitic strategy of the emerging pathogen *Bartonella*. J Exp Med. **193**:1077–1086.

Selbach B, E Earles, and PC Dos Santos. 2010. Kinetic analysis of the bisubstrate cysteine desulfurase SufS from *Bacillus subtilis*. Biochemistry. **49**:8794-8802.

Selbach BP, AH Chung, AD Scott, SJ George, SP Cramer, and PC Dos Santos. 2014. Fe-S cluster biogenesis in Gram-positive bacteria: SufU is a zinc-dependent sulfur transfer protein. Biochemistry. **53**:152-160.

Serra CR, AM Earl, TM Barbosa, R Kolter, and AO Henriques. 2014. Sporulation during Growth in a Gut Isolate of *Bacillus subtilis*. J Bacteriol. **196**:4184-4196.

Shatalin K, E Shatalina, A Mironov, and E Nudler. 2011. H_2S: a universal defense against antibiotics in bacteria. Science. **334**:986-990.

Shimizu T, Y Kida and K Kuwano. 2007. Triacylated lipoproteins derived from *Mycoplasma pneumoniae* activate nuclear factor-kappaB through toll-like receptors 1 and 2. Immunology. **121**:473-483.

Skaar EP, M Humayun, T Bae, KL DeBord, and O Schneewind. 2004. Iron-source preference of *Staphylococcus aureus* infections. Science. **305**:1626–1628.

Smith ML and SA Price. 1938. *Staphylococcus* gamma haemolysin. J Path and Bact. **47**:379-393.

Smith JA, MA Thrall, JL Smith, *et al*. 1990. *Eperythrozoon wenyonii* infection in dairy cattle. J Am Vet Med Assoc. **196**:1244-1250.

Smith RL, MT Kaczmarek, LM Kucharski, and ME Maguire. 1998. Magnesium transport in *Salmonella typhimurium*: regulation of *mgtA* and *mgtCB* during invasion of epithelial and macrophage cells. Microbiology. **144**:1835–1843.

Snell EE. 1975. Tryptophanase: structure, catalytic activities, and mechanism of action. Adv Enzymol Relat Areas Mol Biol. **42**:287–333.

Soda K. 1987. Microbial sulfur amino acids: an overview. Methods Enzymol. **143**:449–451.

Somarajan SR, TR Kannan, and JB Baseman. 2010. *Mycoplasma pneumoniae* Mpn133 is a cytotoxic nuclease with a glutamic acid-, lysine- and serine-rich region essential for binding and internalization but not enzymatic activity. Cell Microbiol. **12**:1821-1831.

Somerson NL, BE Walls, and RM Chanock. 1965. Hemolysin of *Mycoplasma pneumoniae*: tentative identification as a peroxide. Science. **150**:226-228.

Somerson NL, WD James, BE Walls, and RM Chanock. 1967. Growth of *Mycoplasma pneumoniae* on a glass surface. Ann N Y Acad Sci. **143**:384-389.

Spellerberg B, DR Cundell, J Sandros, BJ Pearce, I Idanpaan-Heikkila *et al*. 1996. Pyruvate oxidase, as a determinant of virulence in *Streptococcus pneumoniae*. Mol Microbiol. **19**:803–813.

Stein PE, A Boodhoo, GD Armstrong, LD Heerze, SA Cockle *et al*. 1994. Structure of a pertussis toxin-sugar complex as a model for receptor binding. Nat Struct Biol. **1**:591–596.

Steinhauer K, T Jepp, W Hillen, and J Stülke. 2002. A novel mode of control of *Mycoplasma pneumoniae* HPr kinase/phosphatase activity reflects its parasitic lifestyle. Microbiol. **148**:3277-3284.

Stülke J, H Eilers, and SR Schmidl. 2009. *Mycoplasma* and *Spiroplasma*. Encyclopedia of Microbiolgy. Oxford: Elsevier. pp.208-219.

Su CJ and JB Baseman. 1990. Genome size of *Mycoplasma genitalium*. J Bacteriol. **172:**4705-4707.

Sullivan MA, JF Cannon, FH Webb, and RM Böck. 1985. Antisuppressor mutation in *Escherichia coli* defective in biosynthesis of 5-methylaminomethyl-2-thiouridine. J Bacteriol. **161:**368–376.

Sutcliffe IC and RR Russell. 1995. Lipoproteins of gram-positive bacteria. J Bacteriol. **177:**1123–1128.

Szczepanek SM, M Boccaccio, K Pflaum, X Liao, and SJ Geary. 2014. Hydrogen Peroxide Production from Glycerol Metabolism Is Dispensable for Virulence of *Mycoplasma gallisepticum* in the Tracheas of Chickens. Infect Immun. **82:**4915-4920.

Talkington DF, KB Waites, SB Schwartz, and RE Besser. 2001. Emerging from obscurity: understanding pulmonary and extrapulmonary syndromes, pathogenesis, and epidemiology of human *Mycoplasma pneumoniae* infections. In WM Scheld, WA Craig, and JM Hughes (ed.). Emerging Infections 5. American Society for Microbiology, Washington, D.C. pp. 57–84.

Tamura GS, A Nittayajarn, and DL Schoentag. 2002. A glutamine transport gene, *glnQ*, is required for fibronectin adherence and virulence of group B streptococci. Infect Immun. **70:**2877–2885.

Taylor MJ, GN Burrow, B Strauch, and DM Horstmann. 1967. Meningoencephalitis associated with pneumonitis due to *Mycoplasma pneumoniae*. Jama. **199:**813-816.

Thomas C, E Jacobs, and R Dumke. 2013. Characterization of pyruvate dehydrogenase subunit B and enolase as plasminogen-binding proteins in *Mycoplasma pneumoniae*. Microbiology. **159:**352–365.

Tidhar, A, Y Flashner, S Cohen, Y Levi, A Zauberman *et al*. 2009. The NlpD lipoprotein is a novel *Yersinia pestis* virulence factor essential for the development of plague. PLoS One. **4:**e7023.

Titball RW. 1993. Bacterial phospholipases C. Microbiol Rev. **57:**347-366.

Tokumoto U, S Kitamura, K Fukuyama, and Y Takahashi. 2004. Interchangeability and distinct properties of bacterial Fe–S cluster assembly systems: functional replacement of the isc and suf operons in *Escherichia coli* with the nifSU-like operon from *Helicobacter pylori*. J Biochem. **136:**199–209.

Toumey C. 2011. Compare and contrast as microscopes get up close and personal. Nature Nanotechnology. **6:**191–193

Tonzetich J and PA Carpenter. 1971. Production of volatile sulphur compounds from cysteine, cystine and methionine by human dental plague. Arch Oral Biol. **16**:599-607.

Tryon VV and JB Baseman. 1992. Pathogenic determinants and mechanisms. In Maniloff J (ed.). *Mycoplasmas*: molecular biology and pathogenesis. American Society for Microbiology, Washington, D.C. pp. 457–471.

van Heyningen WE. 1941. The biochemistry of the gas gangrene toxins: Partial purification of the toxins of *Cl. welchii*, type A. Separation of alpha and theta toxins. Biochem J. **35**:1257-1269.

van Noort V, J Seebacher, S Bader, S Mohammed, I Vonkova *et al.* 2012. Cross-talk between phosphorylation and lysine acetylation in a genome-reduced bacterium. Mol Syst Biol. **8**:571.

Veldhuizen R, K Nag, S Orgeig, and F Possmayer. 1998. The role of lipids in pulmonary surfactant. Biochim Biophys Acta. **1408**:90-108.

Vilei EM and J Frey. 2001. Genetic and biochemical characterization of glycerol uptake in *Mycoplasma mycoides* subsp. *mycoides* SC: Its impact on H_2O_2 production and virulence. Clin Diagn Lab Immunol. **8**:85-92.

Vinella D, C Brochier-Armanet, L Loiseau, E Talla, and F Barras. 2009. Iron–sulfur (Fe/S) protein biogenesis: phylogenomic and genetic studies of A-type carriers. PLoS Genet. **5**:e1000497.

Vitry MA, Hanot Mambres, M Deghelt, K Hack, A Machelart, *et al.* 2014. *Brucella melitensis* invades murine erythrocytes during infection. Infect Immun. **82**:3927-3938.

Vogel J P, HL Andrews, SK Wong, and RR Isberg. 1998. Conjugative transfer by the virulence system of *Legionella pneumophila*. Science. **279**:873–876.

Vogl G, A Plaickner, S Szathmary, L Stipkovits, R Rosengarten, and MP Szostak. 2008. *Mycoplasma gallisepticum* Invades Chicken Erythrocytes during Infection. Infect Immun. **76**:71–77.

Wach A. 1996. PCR-synthesis of marker cassettes with long flanking homology regions for gene disruptions in *S. cerevisiae*. Yeast. **12**:259-265.

Waites KB and DF Talkington. 2004. *Mycoplasma pneumoniae* and its role as a human pathogen. Clin Microbiol Rev. **17**:697-728.

Walker T. 1998. Microbiology. Philadelphia: WB Saunders Company.

Walzog B and J Fandrey. 2010. Blut: ein flüssiges Organsystem. In: Klinke R, H-C Pape, A Kurtz, and S Silbernagel (ed.). Georg Thieme Verlag, Stuttgart. pp. 224-247.

Weed RI, CF Reed, and G Berg. 1963. Is hemoglobin an essential structural component of human erythrocyte membranes? J Clin Invest. **42**:581–588.

Williams LR and FE Austin. 1992. Hemolytic activity of *Borrelia burgdorferi*. Infect Immun. **60**:3224-3230.

Wilson ML, E Menjivar, V Kalapatapu, AP Hand, J Garber, and MA Ruiz. 2007. *Mycoplasma pneumoniae* associated with hemolytic anemia, cold agglutinins, and recurrent arterial thrombosis. South Med J. **100**:215-217.

Woodcock DM, PJ Crowther, J Doherty, S Jefferson, E DeCruz, *et al*. 1989. Quantitative evaluation of *Escherichia coli* host strains for tolerance to cytosine methylation in plasmid and phage recombinants. Nucleic Acids Res. **17**:3469-3478.

Wooldridge K. 2009. Bacterial Secreted Proteins: Secretory Mechanisms and Role in Pathogenesis. Caister Academic Press.

Wuttge S, M Bommer, F Jäger, BM Martins, S Jacob *et al*. 2012. Determinants of substrate specificity and biochemical properties of the sn-glycerol-3-phosphate ATP binding cassette transporter (UgpB-AEC2) of *Escherichia coli.* Mol Microbiol. **86**:908-920.

Yamaguchi M, Y Terao, Y Mori-Yamaguchi, H Domon, Y Sakaue, *et al*. 2013. *Streptococcus pneumoniae* Invades Erythrocytes and Utilizes Them to Evade Human Innate Immunity. PLoS One. **8**:e77282.

Yano T, H Fukamachi, M Yamamoto, and T Igarashi. 2009. Characterization of L-cysteine desulfhydrase from *Prevotella intermedia*. Oral Microbiol Immunol. **24**:485-492.

Yildiz D, C Uslu, Y Cakir, and H Oztas. 2006. L-cysteine influx and efflux: a possible role for red blood cells in regulation of redox status of the plasma. Free Radic Res. **40**:507-512.

Yoshida Y, Y Nakano, A Amano, M Yoshimura, H Fukamachi *et al*. 2002. lcd from Streptococcus anginosus encodes a C-S lyase with alpha,beta-elimination activity that degrades L-cysteine. Microbiology. **148**:3961-3970.

Zheng M, X Wang, LJ Templeton, DR Smulski, RA LaRossa, and G Storz. 2001. DNA microarray-mediated transcriptional profiling of the *Escherichia coli* response to hydrogen peroxide. J Bacteriol. **183**:4562–4570.

Zimmerman C-U and R Herrmann. 2005. Synthesis of a small, cysteine-rich, 29 amino acids long peptide in *Mycoplasma pneumoniae*. FEMS Microbiol Lett. **253:**315-321.

Zuo LL, YM Wu, and XX You. 2009. *Mycoplasma* lipoproteins and Toll-like receptors. J Zhejiang Univ Sci B. **10**:67-76.

7. APPENDIX

7.1 Material

7.1.1 Frequently used chemicals

Acrylamide	Roth, Karlsruhe
Agar	Roth, Karlsruhe
Agarose	Peqlab, Erlangen
Antibiotics	Sigma-Aldrich, München
	Serva, Heidelberg
	AppliChem, Darmstadt
Bismuth chloride	Sigma-Aldrich, München
Blocking reagent	Roche Diagnostic, Mannheim
Bromphenol blue	Serva, Heidelberg
CDP*	Roche Diagnostics, Mannheim
Coomassie Brilliant Blue R250	Serva, Heidelberg
Desthiobiotin	IBA, Göttingen
Dithioerythritol	Sigma-Aldrich, München
DMEM	Invitrogen, Karlsruhe
dNTPs	Roche Diagnostics, Mannheim
EDTA	Sigma-Aldrich, München
Ethidium bromide	Merck, Darmstadt
Fetal Bovine serum	Invitrogen, Karlsruhe
Glucose	Merck, Darmstadt
Glycerol	Merck, Darmstadt
Glycerol-3-Phosphate	Sigma-Aldrich, München
HEPES	Roth, Karlsruhe
Horse serum	Invitrogen, Karlsruhe
Hydrogen peroxide	Sigma-Aldrich, München
IPTG	Peqlab, Erlangen
L-α-Glycerophosphorylcholin	Sigma-Aldrich, München
L-Cysteine	Sigma-Aldrich, München
Natriumdodecylsulfat	Roth, Karlsruhe
N',N'-dimethyl-*p*-phenylenediamine dihydrochloride	Sigma-Aldrich, München (Fluka)
Phenol red	Roth, Karlsruhe
PPLO Broth	Becton, Dickinson and Company, France
Pyridoxal-5'-Phosphate	Sigma-Aldrich, München

Pyruvate	Sigma-Aldrich, München
Sheep blood, defibrinated	Oxoid, Heidelberg
Sodium hydroxide	Roth, Karlsruhe
Sodium sulfide	Sigma-Aldrich, München
Strep-Tactin sepharose	Iba, Göttingen
TEMED	Merck, Darmstadt
Triethanolamine	Sigma-Aldrich, München
Triton X-100	Roth, Karlsruhe
Tryptone	Oxoid, Heidelberg
X-Gal	Peqlab, Erlangen
Yeast extract	Oxoid, Heidelberg

Other chemicals were purchased from Merck, Serva, Fluka, Sigma or Roth.

7.1.2 Utilities

24-well microtiter plates	TPP, Switzerland
96-well flat bottom microtiter plates	Corning Inc., USA
96-well round bottom microtiter plates	Bio-Rad Laboratories GmbH, München
Cell scrapers (24 cm, 30 cm)	TPP, Switzerland
Centrifuge beaker	Beckmann, München
Cuvettes (microlitre, plastic)	Sarstedt, Nümbrecht
Eppendorf tubes	Greiner, Nürtingen
Falcon Tubes	Sarstedt, Nümbrecht
Gene Amp Reaction Tubes (PCR)	Perkin Elmer, Weiterstadt
Glass pipets	Brand, Wertheim
Membrane filter NC45 (0.2 µm pore size)	Schleicher und Schüll, Dassel
Mikrolitre pipets (2 µl, 20 µl, 200 µl, 1000 µl, 5000 µl)	Eppendorf, Hamburg
Needles	ROSE GmbH, Trier
Nylon membrane, positively charged	Roche Diagnostics, Mannheim
Pasteur pipets	VWR International
Petri dishes	Greiner, Nürtingen
Pipet tips	Greiner, Nürtingen
	Eppendorf, Hamburg
	Sarstedt , Nümbrecht
Polyethylene tubes	Greiner, Nürtingen
Poly-Prep Chromatography Columns	Bio-Rad Laboratories GmbH, München
Polyvinylidendifluorid-Membran (PVDF)	Bio-Rad Laboratories GmbH, München
Single use syringes (1 ml)	Becton, Dickinson & Company, France
Syringes (50 ml)	ERSTA CODAN Medical, Rodby
Tissue flasks (25 cm^2, 75 cm^2, 150 cm^2, 300 cm^2)	TPP, Switzerland

7.1.3 Equipment

Autoklave	Zirbus, Bad Grund
Blotting device VacuGene™XI	Amersham, Freiburg
Capillary HP5-MS column (for gas chromatography)	J&W Scientific, Agilent Technologies, USA
Centrifuges	Heraeus Christ, Osterode
	Thermo Scientific, Bonn
ChemoCam Imager	Intas, Göttingen
Clean bench Heraeus® HERAsafe®	Thermo Scientific, Bonn
CO_2-Incubator	Labotect, Göttingen
Fluorescence microscope Axioskop 40 FL	Zeiss
French Press	Spectonic Unicam, England
	SLM Aminco, New York (USA)
	(Now serviced by Fa. G. Heinemann, Schwäbisch Gmünd)
Gas chromatograph Agilent 6890 series	Agilent Technologies, USA
Gel documentation device Geldoc	Bio-Rad Laboratories GmbH, München
Gel electrophoresis device	EasyCast™ Minigelsystem, Peqlab, Erlangen
Heating block	Waasetec, Göttingen
High accuracy weighing machine Sartorius	Sartorius, Göttingen
Horizontal shaker	GFL, Burgwedel
Hybridization oven	Biometra, Göttingen
Ice machine	Ziegra, Isernhagen
Incubator shaker Innova® 40	New Brunswick, Neu-Isenburg
Incubator shaker Innova® 2300	New Brunswick, Neu-Isenburg
Incubation waterbath 1083	GFL, Burgwedel
Luminescence Imager ChemoCam	Intas, Göttingen
Magnet stirrer	JAK Werk, Staufen
Mass spectrometerMS 5973 Network	Agilent Technologies, USA
Mikrodismembrator	Sartorius, Göttingen
pH-meter	Knick, Berlin
Nanodrop ND-1000	Thermo Scientific, Bonn
Platereader SynergyMX	Biotek, Bad Friedrichshall
RT-PCR detection system iQ5	Bio-Rad Laboratories GmbH, München
Scale Sartorius universal	Sartorius, Göttingen
Slot Blot device Hoefer™ PR648	Amersham Biosciences, Freiburg
Spectral photometer Ultraspec 2100pro	Amersham, Freiburg
Standard power pac	Bio-Rad Laboratories GmbH, München
Stereo fluorescence microscope Lumar V.12	Zeiss
Thermocycler labcycler	SensoQuest, Göttingen
Thermocycler Tpersonal	Biometra, Göttingen

Ultracentrifuge Sorvall Ultra Pro 80 — Thermo Scientific, Bonn
Vortex Genie 2 — Bender & Hobeing AG Zürich
Water desalination plant — Millipore, Schwalbach
Western Blot apparatus — Peqlab, Erlangen

7.1.4 Commercially available systems

DIG RNA Labelling Mix — Roche Diagnostics, Mannheim
DNA ladder mix 1 kb DNA ladder — NEB Biolabs, Frankfurt am Main
DNA molecular weight marker III DIG-labeled — Roche Diagnostics, Mannheim
DNeasy Blood and Tissue Kit (50) — Qiagen, Hilden
Gene Ruler DNA ladder mix — MBI Fermentas, St. Leon-Rot
iScript One-Step RT-PCR kit with SYBR green — Bio-Rad Laboratories, München
Lambda DNA — MBI Fermentas, St. Leon-Rot
NucleoSpin® Plasmid-Kit — Macherey-Nagel, Düren
QIAquick® PCR Purification Kit 250 — Qiagen, Hilden
RNeasy Midi-Kit (50) — Qiagen, Hilden
RNeasy Mini-Kit (50) — Qiagen, Hilden

7.1.5 Antibodies and enzymes

Accuzyme Polymerase — Bioline, Luckenwalde
Alkaline Phosphatase (Fast AP) — MBI Fermentas, St. Leon-Rot
Ampligase — Epicentre, USA
Anti-Digoxigenin-AP, Fab Fragmente — Roche Diagnostics, Mannheim
Anti-*Strep* antibody — PromoKine, Heidelberg
Catalase — Sigma-Aldrich, München
Lysozyme from chicken egg white — Merck, Darmstadt
Phusion™ HF DNA-polymerase — Finnzymes, Espoo Finland
Restriction endonucleases — MBI Fermentas, St. Leon-Rot
— Thermo Scientific, Bonn

RNase inhibitor — Roche Diagnostics, Mannheim
Secondary antibody (α IgG gekoppelt mit AP) — Promega, Madison (USA)
T4-DNA-Ligase — Roche Diagnostics, Mannheim
T7-RNA-polymerase — Roche Diagnostics, Mannheim
Taq-DNA-Polymerase — MBI Fermentas, St. Leon-Rot

7.2 Oligonucleotides

Tab. 7.1 Oligonucleotides used in this study

Primer	Sequence 5' → 3'	Description
AS106	GGGAGGATAAGCAAGCTTTAAAAAG	*glpF* mutant screen fwd.
AS107	CCGTTTGTAATGTCTGTGGTCAG	*glpF* mutant screen rev.
cat check fwd	CTAATGTCACTAACCTGCCC	Sequencing from *cm*^{R} -cassette of pGem-*cat* for LFH-PCR
cat check rev	GTCTGCTTTCTTCATTAGAATCAATCC	Sequencing from *cm*^{R} -cassette of pGem-*cat* for LFH-PCR
cat- fwd (kan)	CGGCAATAGTTACCCTTATTATCAAG	Amplification of *cm*^{R} -cassette from pGem-*cat* for LFH-PCR
cat- rev (kan) w/o terminator	CGATACAAATTCCTCGTAGGCGCTCGGTT ATAAAAGCCAGTCATTAGGCCTATC	Amplification of *cm*^{R} gene with *kan* – flag w/o terminator for LFH-PCR
cat- rev (kan)	CCAGCGTGGACCGGCGAGGCTAGTTACCC	Amplification of *cm*^{R} -cassette from pGem-*cat* for LFH-PCR
CD13	AAA*CATATG*GCTAGCTGGAGCCACCCGCA GTTC	Amplification of the *Strep*-tag coding sequence, *Nde*I
M13fw	CGCCAGGGTTTTCCCAGTCACGAC	Sequencing and cloning of pBQ200 derivatives
M13_puc_for	GTAAAACGACGGCCAGTG	Sequencing primer for pBS plasmids and all puc-derivatives (e.g. pBQ200)
M13_puc_rev	GGAAACAGCTATGACCATG	Sequencing primer for pBS plasmids and all puc-derivatives (e.g. pBQ200)
NP20	GCAGCAGCCAACTCAGCTTCCTTTCGGGC	Sequencing of pGP172 rev.
SG39	CTAAAGAGCCGGCTGATGCCGC	*B. subtilis glpF* upstream fwd. for LFH-PCR
SG40	**CCTATCACCTCAAATGGTTCGCTG**CACCA AAAATGATAAGCAGCATCGTACCG	*B. subtilis glpF* upstream fragment rev., with **kan** flag for LFH-PCR
SG41	C**CGAGCGCCTACGAGGAATTTGTATCG**GT TAGGACTCTATGTTTATACGAAATCACA	*B. subtilis glpF* downstream fragment fwd., with **kan** flag for LFH-PCR
SG42	CTCCCTTCTAACGCATAGTTCACTTTTCC	*B. subtilis glpF* downstream rev. for LFH-PCR
SG43	CCGTGATCTTGGAGCAAAGCTTTTAGGT	*B. subtilis glpF* check fwd. for LFH-PCR
SG44	GATTCGCTTAGCGATGAATCCTGGAAC	*B. subtilis glpF* check rev. for LFH-PCR
SG45	TTT*GGTACC*CTAAACGATAACAGCCACAAG CAC	*glpF*$_{Mpn}$ for pGP888 rev., *Kpn*I
SG46	AAA*GGATCC***CTCACTTATTTAAAGGAGGA AACAATC**ATGTTTAATTTAAGTGATTTTAG TGAATTACCAC	*glpF*$_{Mpn}$ for pBQ200 Klonierung fwd. mit **Shine Dalgarno** (gap) Sequence, *Bam*HI
SG47	TTT*GTCGAC*CTAAACGATAACAGCCACAAG CAC	*glpF*$_{Mpn}$ for pBQ200 rev., *Sal*I
SG48	AAA*GGATCC*CTCACTTATTTAAAGGAGGAA ACAATCATGACAGCATTTTGGGGAGAAGT CATCG	*glpF*$_{Bsu}$ for pBQ200 fwd. with **Shine Dalgarno** (gap) sequence, *Bam*HI

SG49	TTT*GTCGAC*TTAAATATATTTAGAATTTTTTAGAATTTGATAATGTTTTAGCAGAATGTGATTATA	*glpF~Bsu~* for pBQ200 rev., *Sal*I
SG50	TTT*AGATCT*AACGATAACAGCCACAAGCACACCTAAGA	*glpF~Mpn~* rev w/o stop codon for pBP19/20, *Bgl*II
SG51	CAAATGCAAATAGCTGTTTACACTAACC	*mpn259-260* mutant screen fwd.
SG52	GTGAGTAATCGGCTTCGTTAAAACC	*mpn259-260* mutant screen rev.
SG53	CTTAATGGCCGCAAACCAGTTTG	*mpn308* mutant screen fwd.
SG54	GATCGTATGCAGTAGCTTGTTGG	*mpn308* mutant screen rev.
SG55	TAGTGTTAAGGGAGCAGGTTCATC	*mpn571* mutant screen fwd.
SG56	GTTTGTTCAGACAATTTTGCCCATAAG	*mpn571* mutant screen rev.
SG57	GGTGATTTTGTTAGATGAAACACTCAAC	*mpn569-570* mutant screen fwd.
SG58	CATAGGTGAAACCAACAAGTTATTCG	*mpn569-570* mutant screen rev.
SG59	CTCTCTGGTGGGCAAAAACAAC	*mpn019* mutant screen fwd.
SG60	GCCTTATTGAGGTATTTTTTGGGC	*mpn019* mutant screen rev.
SG61	GGGTCAAAAATTGCTACAATAAATACCG	*mpn055* mutant screen fwd.
SG62	GTTTTCATTTTGGAGTCCACTAACAATAATC	*mpn055* mutant screen rev.
SG63	GATTTTGTTACCCGTTTTGCTAGCTG	*mpn080* mutant screen fwd.
SG64	GGTTTAAAGCAACTCAAAAAGGATTACAAG	*mpn080* mutant screen rev.
SG65	GTCCATTTTATAGCTGTTTTTACTTTGCG	*mpn095-096* mutant screen fwd.
SG66	GTAACTCCCCAAAAGAAATTAAGCGC	*mpn095-096* mutant screen rev.
SG67	CCGGTGATCCTTACGAAGTTTTTATG	*mpn195* mutant screen fwd.
SG68	CGTGAAAGGTTTGGTTAATGGCATG	*mpn195* mutant screen rev.
SG69	AAA*GTCGAC***CTCACTTATTTAAAGGAGGAAACAAT**ATGTTGTGGGCAATTGTCTTGCTTG	*mpn076* for pBQ200 Klonierung fwd., with **Shine Dalgarno** sequence, *Sal*I
SG70	TTT*CTGCAG*CTATTTCAACAAGTCCGCGTAACG	*mpn076* for pBQ200 Klonierung rev., *Pst*I
SG71	AAA*GGATCC***CTCACTTATTTAAAGGAGGAAACAAT**CCTGTGAGGTCTCGTCTTACTTGG	*mpn077* for pBQ200 fwd., with **Shine Dalgarno** sequence, *Bam*HI
SG72	TTT*GTCGAC*TTATTTTAAGAGATCCGCGTAACGGT	*mpn077* for pBQ200 rev., *Sal*I
SG73	AAA*GAATTC*ATGTTTAATTTAAGTGATTTTAGTGAATTACCAC	*glpF~Mpn~* fwd for pBP15, *Eco*RI
SG74	TTT*AGATCT*CTAAACGATAACAGCCACAAGCACACCTAA	*glpF~Mpn~* rev with stop codon for pBP15, *Bgl*II
SG75	AAA*CTGCAG*ATGGAAACGAAACTTAGTTTAAAGAAACGG	*mpn421* for MMR in pBluescript fwd., *Pst*I
SG76	TTT*AAGCTT*TTAAGCATTGTCTAAGGTTCTCCAGC	*mpn421* for MMR in pBluescript rev., *Hin*dIII
SG77	**P**CTTAATCTTTTG**G**ACACCACTGTGG**G**AAGTTAGCGA	*mpn421* MMR 1 A411G, A423G
SG78	**P**GAACTGGAAGTTGTG**G**CTCTTGTCCTTCT	*mpn421* MMR 2 A762G

	TTTTAA	
SG79	**P**GGTTAATACTT**G**GGAGTTAAAGCGCTTG GGTAAAA	*mpn421* MMR 3 A1371G
SG80	AAA*GGATCC***CTCACTTATTTAAAGGAGGA AACAATC**ATGTTTTGTACATTTTTTGAAAA ACATCACCGGAAGTG	*mtsX* fwd. for pBQ200 with **Shine Dalgarno** sequence, *Bam*HI
SG81	TTT*TCTAGA*TTCTTTTTCTCCTTCTTCAGAT ACTGAGATGGAT	*mtsX* rev. for pBQ200, *Xba*I
SG82	AAA*GGATCC*ATGTTGTGGGCAATTGTCTTG CTTG	*mpn076* fwd. for FLAG-tag fusion in pGP1331, *Bam*HI
SG83	TTT*GTCGAC*TTTCAACAAGTCCGCGTAACG GTT	*mpn076* rev. for FLAG-tag fusion in pGP1331, w/o stop, *Sal*I
SG84	TTT*CTGCAG*TTTCAACAAGTCCGCGTAACG GTT	*mpn076* rev. for FLAG-tag fusion in pGP1331, w/o stop, *Pst*I
SG85	AAA*TCTAGA*ATGTTGTGGGCAATTGTCTTG CTTG	*mpn076* for *mpn076*-FLAG fusion in pGP699 fwd., *Xba*I
SG86	ATA*GTCGAC*TTATCACTTGTCGTCATCGTC TTTGTAGTC	Amplification 3xFLAG rev, *Sal*I
SG87	TTT*GGATCC*AATATATTTAGAATTTTTTAG AATTTGATAATGTTTTAGCAGAATGTGATT ATAGA	*glpF_{Bsu}* for pBP19/20 w/o stop, *Bam*HI
SG88	AAA*GTCGAC*ATGTTTAATTTAAGTGATTTT AGTGAATTACCAC	*glpF_{mpn}*-CFP/YFP for *mstX* fusion fwd. (binds to *glpF*), *Sal*I
SG89	TTT*CTGCAG*TCATTACTTATAAAGTTCGTC CATGCCAAGTGTAATG	*glpF_{mpn}*-CFP for *mstX* fusion rev. (binds to CFP, mod. KG206), *Pst*I
SG90	TTT*CTGCAG*TCATTACTTGTACAGCTCGTC CATGCCGA	*glpF_{mpn}*-YFP for *mstX* fusion rev. (binds YFP, mod. KG208), *Pst*I
SG91	AAA*GTCGAC*ATGTTTAATTTAAGTGATTTT AGTGAATTACCACGTTGG	*glpF_{Mpn}*-CFP/YFP for *mstX* fusion fwd. (binds *glpF*), *Sal*I
SG92	GCTTTTAATCGATCCTTACTTCTCCGGCA	Intern *glpK_{Bsu}* for RT-PCR fwd.
SG93	TGCGCTTTTCCGCCTGACATTTTCCAAA	Intern *glpK_{Bsu}* for RT-PCR rev.
SG94	GGTACGATGCTGCTTATCATTTTTGGTGC<u>A</u>	Intern *glpF_{Bsu}* for RT-PCR fwd.
SG95	GCTGATGCCGCCAACCGCGTAT	Intern *glpF_{Bsu}* for RT-PCR rev.
SG96	GGCGGTTGATGTAATGCTGGAAA	*mpn609* mutant screen fwd.
SG97	GTGCTGAAAGTAATCAAAAAAGAGTCCTA	*mpn609* mutant screen rev
SG98	CCAATTACCCGGGTGTAGGGT	*mpn159* mutant screen fwd.
SG99	CAAAGGTAACTAACTCTTCGGTCGT	*mpn159* mutant screen rev.
SG100	CGTTTATGAAGTACAAGGTGAACCGA	*mpn334* mutant screen fwd.
SG101	GATGATTAACAGCACTAAAGCCAGTAAAA A	*mpn334* mutant screen rev.
SG102	GAGTGCTTTGGGTTTGCATATCTGT	*mpn496* mutant screen fwd.
SG103	CTTGATTAGCATGCTCGTACCCAT	*mpn496* mutant screen rev.
SG104	CACCAGGAAAAGTACAGCTGCT	*mpn095* probe fwd.
SG105	**CTAATACGACTCACTATAGGGAGA**GCACA CTGGTTCACTTAACACTAA	*mpn095* probe rev., T7 RNA polymerase **signal sequence**

SG106	GGTTTTGTAATGTGAACGGGAAAGTT	*mpn096* probe fwd.
SG107	**CTAATACGACTCACTATAGGGAGA**GTTAAACACTGCTATTCCTAAATCTACAAA	*mpn096* probe rev., T7 RNA polymerase **signal sequence**
SG108	GGCAAGAAGTTTGGTCTCGAAATT	*mpn571* probe fwd.
SG109	**CTAATACGACTCACTATAGGGAGA**CCAAATAGCCCCGATACTGCT	*mpn571* probe rev., T7 RNA polymerase **signal sequence**
SG110	CTTAGTAATTTTGGCTACCGTTGGTTT	*mpn494-495* mutant screen fwd.
SG111	CGCTGTTAGTAAGATAGTGCCCA	*mpn494-495* mutant screen rev.
SG112	GCCATTAACACCATCTTGGTCGAAA	*mpn496* mutant screen fwd.
SG113	CACTTTGGCGGTGTAGCCCA	*mpn496* mutant screen rev.
SG114	GTTGCCATCTTATTTACGGTTAAGGT	*mpn570* probe fwd.
SG115	**CTAATACGACTCACTATAGGGAGA**CAAACAGCGCTTTGGACGGTAA	*mpn570* probe rev., T7-RNA polymerase **signal sequence**
SG116	CCCGCCGTGATGTTTACTTCTTTA	*mpn159* probe fwd.
SG117	**CTAATACGACTCACTATAGGGAGA**CCCCGACTAATTCCTCAATGATGT	*mpn159* probe rev., T7-RNA polymerase **signal sequence**
SG118	TA*GAGCTC***G**ATGGAAAGTGCCCCCAGTGGT	*mpn159* fwd. for pGP172, *Sac*I
SG119	TATA*GGATCC*CTAGTCCACAACATCACTCTTTTTGC	*mpn159* rev. for pGP172, *Bam*HI
SG120	**P**CTACATCCTTTTTTG**G**CCAATTACCAAGTTAGCCA	*mpn159* MMR 1 A450G
SG121	**P**CAAATCATGATTAAGTG**G**AACCGGGTGGTGTA	*mpn159* MMR 2 A639G
SG122	TA*GAGCTC***G**ATGATTGTTTCACCATG**G**AAGATGAAG	*mpn569* for pGP172 fwd., *Sac*I, A18G
SG123	TATA*GGATCC*TTATCGATTCCATAGTTTTAAAACGGTTTCAT	*mpn569* for pGP172 rev., *Bam*HI
SG124	AAA*GAGCTC***G**ATGCCAAATCCTGTTAGATTTGTTTACC	*mpn372* for pGP172 fwd., *Sac*I
SG125	TATA*GGTACC*CTAAAAGCGATCAAAACCATCTTTGAC	*mpn372* for pGP172 rev., *Kpn*I
SG126	**P**CCGTAGTGCTTG**G**CTAGTAGATGCTGTT	*mpn372* MMR 1 A444G
SG127	**P**CCAATGATCAACCATG**G**TTGCCAACACCA	*mpn372* MMR 2 A585G
SG128	**P**GTGCCCTGATTG**G**AGTCCACCTTCTA	*mpn372* MMR 3 A699G
SG129	**P**CGTGAACCAAAAGTG**G**AAAATGACACCGCA	*mpn372* MMR 4 A1092G
SG130	**P**GAAAATGGCTTGTTCTG**G**AATACCAAGAGTGG	*mpn372* MMR 5 A1176G
SG131	**P**GCTAGGCTGGTATTG**G**AGGGGTTATTACT	*mpn372* MMR 6 A1350G
SG132	**P**CCACAATTAAGTGGTTG**G**TCTTATCAGATGAAAACA	*mpn372* MMR 7 A1386G
SG133	**P**GTTACAGCTGGGATTG**G**GTAGAATGGCTA	*mpn372* MMR 8 A1524G

SG134	GTGTGATTGCTGTCATTATTGCCATT	*mpn651* mutant screen fwd.
SG135	GGTAATGAACTTGGTATTGTTTTTGCTTTT	*mpn651* mutant screen rev.
SG136	CCCAGGTCTTTTTAACCAACGTGT	*mpn683* mutant screen fwd.
SG137	CGGTGGCCATGCGAGCTAA	*mpn683* mutant screen rev.
SG138	AAA*TCTAGA*GATGATTGTTTCACCATGGAAGATGAAG	*mpn569* fwd. for BACTH vectors, *Xba*I
SG139	AAA*TCTAGA*GCTCGATTCCATAGTTTTAAACGGTTTCAT	*mpn569* rev. for BACTH vectors w/o stop, *Xba*I
SG140	AAA*GGTACC*GCTCGATTCCATAGTTTTAAACGGTTTCAT	*mpn569* rev. for BACTH vectors w/o stop, *Kpn*I
SG141	TATA*GGATCC*CTAAAAGCGATCAAAACCATCTTTGAC	*mpn372* for pGP172 rev., *Bam*HI
SG142	AAA*GAGCTC*GATGACCAAAACTAAGTTTAATCCGTACCAA	*mpn487* fwd. for pGP172, *Sac*I
SG143	TATA*GGATCC*TTACTTAATTACGTTTTTAATAATTGTCTTGGTATCA	*mpn487* rev. for pGP172, *Bam*HI
SG144	**P**CTAACGTTTTGCCCTG**G**GTTGCACTAGCTA	*mpn487* MMR A384G
SG145	TA*GAATTC*ATGGAAAGTGCCCCCAGTGGT	*mpn159* fwd. for pBP15, *EcoR*I
SG146	AAA*TCTAGA*GATGGAAAGTGCCCCCAGTGGT	*mpn159* fwd. for BACTH, *Xba*I
SG147	AAA*GGTACC*GCGTCCACAACATCACTCTTTTTGCGAA	*mpn159* rev. for BACTH w/o stop, *Kpn*I
SG148	GTGGTTTTACCTTGGCTTTGTCCAT	*mpn487* mutant screen fwd.
SG149	CCCGTTAAAACCAAGTGCTGTTAGT	*mpn487* mutant screen rev.
SG150	AAA*GAGCTC*GATGAAATTTAAGTATTGTGCCATCTTTTTCAGT	*mpn288* fwd. for pGP172, *Sac*I
SG151	**P**CTGCTACAAAAGATCTTTG**G**GAAAAAATAGAAGCTTCT	*mpn288* MMR 1 A642G
SG152	**P**CAAAATCAAAGAATCTTG**G**GGCGAATACCAAGAA	*mpn288* MMR 2 A822G
SG153	**P**GAGCATCTTCGAAAATTG**G**CATGACTTACTTGATT	*mpn288* MMR 3 A891G
SG154	**P**CAATACAGAAAGTTG**G**GAAGTTAAAAATGGAAAAGATTCCT	*mpn288* MMR 4 A2001G
SG155	CCCAACTCATTATTCACCTCTGTTTTT	*mpn288* probe fwd.
SG156	**CTAATACGACTCACTATAGGGAGA**GTTTTGTCTGATGGAATTTGACTTTTGTAAA	*mpn288* probe rev., T7-RNA polymerase **signal sequence**
SG157	AAA*GAGCTC*GGGTGCACGCGGCAAATTTGAC	*mpn284* fwd. w/o signal peptide
SG158	AAA*GAGCTC*GATGAAATTTAAGTATGGTGCCATTGTTTTCA	*mpn200* fwd. for pGP172, *Sac*I
SG159	TATA*GGATCC*CTATTTATCAAAATCAGAGCCTAATGCAG	*mpn200* rev. for pGP172, *Bam*HI
SG160	**P**CAAAATTAAAGAATCTTG**G**GGGTGCTTACCAAGAAGTA	*mpn200* MMR 1 A801G

SG161	**P**GCCATTGTTTTTGAAAACTG**G**CACGATCTAATTGATT	*mpn200* MMR 2 A870G
SG162	**P**AAATAAAACCGAAAGTTG**G**GAAGTTAAAGGAAACGGA	*mpn200* MMR 3 A2055G
SG163	CCTAATGCTTTACTATCTTCGGTGTTT	*mpn200* probe fwd.
SG164	**CTAATACGACTCACTATAGGGAGA**CTTTGATTCCGCTTGAGTTTTAGGTTT	*mpn200* probe rev., T7-RNA polymerase **signal sequence**
SG165	CTTTAAATTACCTCAAACACCGTTTTCT	*mpn259* probe fwd.
SG166	**CTAATACGACTCACTATAGGGAGA**GGCACTAACCACTTCATTAACCTTA	*mpn259* probe rev., T7-RNA polymerase **signal sequence**
SG167	GTACAAACTTTATCCAATAGCTGCCAT	*mpn651* probe fwd.
SG168	**CTAATACGACTCACTATAGGGAGA**CGAAATTAACAACGAAGTTACAGCTGA	*mpn651* probe rev., T7-RNA polymerase **signal sequence**
SG169	GGTCAACAATGTGGACTGGCAA	*fruA* probe fwd.
SG170	**CTAATACGACTCACTATAGGGAGA**ATTGATTTAACGCGTTTTTACGGTCAC	*fruA* probe rev., T7-RNA polymerase **signal sequence**
SG171	CCCAAAATTAGCTTTATAGCAGCGAT	*mpn308* probe fwd.
SG172	**CTAATACGACTCACTATAGGGAGA**CGGCGCTTACCACCATGTTTT	*mpn308* probe rev., T7-RNA polymerase **signal sequence**
SG173	AAA*GAGCTC*GATGAAAGGGTTTTCTTGCTCCAGAC	*mpn133* fwd. for pGP172, *Sac*I
SG174	TATA*GGATCC*TTAACTACCCTTTTGGGCTAATTTGGC	*mpn133* rev. for pGP172, *Bam*HI
SG175	AAA*GAGCTC*GACCCGCGACTATACTACCAAGAA	*mpn133* fwd. w/o signal peptide
SG176	AAA*GAGCTC*GATGAAATTGAAATATGGAACCATTATTTTCAGTG	*mpn284* fwd. for pGP172, *Sac*I
SG177	TATA*GGATCC*AATTTCACTACCCAAAGTGGCGATG	*mpn288*/*mpn284* rev. for pGP172, *Bam*HI
SG178	CAGAATTTTCGTTTTCCTGCTCCCA	*mpn288* mutant screen fwd.
SG179	CAGGGAATTCGCCTGGATTGTTTTT	*mpn288* mutant screen rev.
SG180	CGTGATGCCGTTAAGAGTACCTTTA	*mpn200* mutant screen fwd.
SG181	GCTGTTCAAGTAACATATTCACCATCAAA	*mpn200* mutant screen rev.
SG182	CCCCCACAATAAAACCCCTGAT	*mpn487* probe fwd.
SG183	**CTAATACGACTCACTATAGGGAGA**GCTAGGAAGTCGATCTGGGTTT	*mpn487* probe rev., T7-RNA polymerase **signal sequence**
SG184	TA*GAATTC***CTCACTTATTTAAAGGAGGAAACAATC**ACCCGCGACTATACTACCAAGAA	*mpn133* fwd. for pBP19/20 w/o signal peptide, *Eco*RI, RBS *gap*$_{Bsu}$
SG185	TA*GAATTC***CTCACTTATTTAAAGGAGGAAACAATC**ATGAAAGGGTTTTCTTGCTCCAGAC	*mpn133* fwd. for pBP19/20, *Eco*RI, RBS *gap*$_{Bsu}$
SG186	TATA*GGATCC*ACTACCCTTTTGGGCTAATTTGGC	*mpn133* rev. for pBP19/20 w/o stop codon, *Bam*HI
SG187	AAA*GTCGAC***T**ATGACCAAAACTAAGTTTAATCCGTACCAA	*mpn487* for BACTH fwd., S*al*I

SG188	TTT*GGATCC***TC**CTTAATTACGTTTTTAATA ATTGTCTTGGTATCAGT	*mpn487* for BACTH rev. w/o stop, *Bam*HI
SG189	AAA*TCTAGA***G**ATGGATCGCAAAATAAGGG AGCAAATT	*mpn488* for BACTH fwd., *Xba*I
SG190	TTT*GGTACC***CG**GTGCGAAAAATCTTTAAGC CACTGTA	*mpn488* for BACTH rev. w/o stop, *Kpn*I
SG191	AAA*GAGCTC***G**ATGGATCGCAAAATAAGGG AGCAAATT	*mpn488* fwd. for pGP172, *Sac*I
SG192	TATA*GGATCC*TTAGTGCGAAAAATCTTTAA GCCACTGT	*mpn488* rev. for pGP172, *Bam*HI
SG193	AAA*GCGGCCGC*TTACTTAATTACGTTTTTA ATAATTGTCTTGGTATCA	*mpn487* for SPINE, *Not*I
SG194	ATGGATCGCAAAATAAGGGAGCAAA	*mpn488* probe fwd.
SG195	**CTAATACGACTCACTATAGGGAGA**GTGCG AAAAATCTTTAAGCCACTGTA	*mpn488* probe rev., T7-RNA polymerase **signal sequence**
SG196	AAA*GAGCTC***G**ATGAATATCACAGATATTC GTGAACAGTT	*sufS*_{*Bsu*} fwd. for pGP172, *Sac*I
SG197	TATA*GGATCC*TTAAAAGACATTTGTAAAAT ACTCCTTTGTCTT	*sufS*_{*Bsu*} rev.for pGP172, *Bam*HI
SH29	ATGAGTGAGCTAACTCACAG	Sequencing and screen for pMT85 transposants (binds to transposon)
SH30	CAATACGCAAACCGCCTC	Sequencing and screen for pMT85 transposants (binds to transposon)
SH58	A*GAATTC*GTTAATAATGATGATTGAAGC	*M. pneumoniae ackA*_{*mpn*}-*lacZ* fusion fwd. for cloning of *ackA*_{*mpn*} promoter in pGP353, *Eco*RI
SS21	AAA*CTGCAG*CATTTTTATCTAATAGGTAAC AA	*M. pneumoniae ackA*_{*mpn*} promoter fragment from rev. for pMT85, *Pst*I
SS232	TTT*GGTACC*CGAACGATAACAGCCACAAG CACAC	*glpF (mpn043)* BACTH-Analyse rev., *Kpn*I

Italic, underlined: restriction sites; **P**: 5'phosphorylation; **bold red**: mutation; **bold blue**: additional inserted base for frame shift; **bold**: special signal sequences. Oligonucleotides were synthesized and purchased from Sigma-Aldrich, Steinheim.

7.3 Bacterial strains

Tab. 7.2 Bacterial strains used in this work.

Strain	Genotype / description	Reference / source
E. coli		
DH5α	*recA1 endA1 gyrA96 thi hsdR17rK- mK+relA1 supE44 Φ80ΔlacZΔM15 Δ(lacZYA-argF)U169*	Sambrook *et al.*, 1989
XL-1 Blue	*recA1 endA1 gyrA96 thi-1 hsdR17 supE44 relA1 lac [Fʿ proAB lacI�q ZΔM15* Tn*10 (Tetʳ)]*	Stratagene, Woodock *et al.*, 1989
BL21	B(834)-derivate *Fˉ lon ompT hsdS(rBmB) gal dcm[DE3]*	Novagen, Sambrook *et al.*, 1989
BTH101	*Fˉ cyaA-99 araD139 galE15 galK16 rpsL1 (Strʳ) hsdR2 mcrA1 mcrB1*	EUROMEDEX, Karimova *et al.*, 2005
B. subtilis		
168	*trpC2*	Lab collection
GP99	*trpC2 ΔglpF::catᴿ*	This work.
M. pneumoniae		
M129	Wild type	Somerson *et al.*, 1963
GPM8	*mpn372*::Tn4001m	Hames, 2008
GPM30	*mpn095*::Tn4001m	This work.
GPM31	*mpn096*::Tn4001m	This work.
GPM32	*mpn571*::Tn4001m	This work.
GPM33	*mpn570*::Tn4001m	This work.
GPM34	*mpn159*::Tn4001m	This work.
GPM35	*mpn334*::Tn4001m	This work.
GPM36	*mpn308*::Tn4001m	This work.
GPM37	*mpn496*::Tn4001m	This work.
GPM38	*mpn259*::Tn4001m	This work.
GPM39	*mpn651*::Tn4001m	This work.
GPM40	*mpn683*::Tn4001m	This work.
GPM41	*mpn609*::Tn4001m	This work.
GPM42	M129 + *mpn487* in pMT85 (pGP2231)	This work.
GPM52	*glpD*::Tn4001m	Hames *et al.*, 2009
GPM100	Clinical isolate 1	Roger Dumke, Dresden
GPM101	Clinical isolate 2	Roger Dumke, Dresden

7.4 Plasmids

Tab. 7.3 Plasmids constructed in this work.

Plasmid	Construction	Used restriction sites
pGP693	pBQ200 + $glpF_{mpn}$ from pGP663 (SG46/47)	*Bam*HI/*Sal*I
pGP694	pGP888 + $glpF_{mpn}$ from pGP663 (SG45/SS232)	*Xba*I/*Kpn*I
pGP696	pBQ200 + $glpF_{bsu}$ (SG48/49)	*Bam*HI/*Sal*I
pGP697	pBP19 + $glpF_{mpn}$ from pGP693 (M13fw/SG50)	*Eco*RI/*Bgl*II
pGP698	pBP20 + $glpF_{mpn}$ from pGP693 (M13fw/SG50)	*Eco*RI/*Bgl*II
pGP2226	pBQ200 + *mpn077* (SG71/SG72)	*Bam*HI/*Sal*I
pGP2227	pGP172 + *mpn372* (SG124/SG141)	*Sac*I/*Bam*HI
pGP2228	pBQ200 + *mpn076* + *mpn077* (SG69/SG72)	*Bam*HI/*Pst*I
pGP2229	pBP15 + $glpF_{mpn}$ from pGP663 (SG73/74)	*Eco*RI/*Bam*HI
pGP2230	pMT85 + *mpn487* from pGP2246 (SS22/SG193) + P_{ackA} from pGP1012 (SH58/SS21)	*Eco*RI/*Not*I
pGP2231	pBSK+ *mpn421* for MMR (SG75/76)	*Pst*I / *Hin*dIII
pGP2232	pBP19 + $glpF_{bsu}$ (M13fw/SG87)	*Eco*RI/*Bam*HI
pGP2233	pGP172 + *mpn569* A18G (SG122/123)	*Sac*I/*Bam*HI
pGP2234	pGP172 + *mpn159* (SG118/119)	*Sac*I/*Bam*HI
pGP2235	pGP172 + *mpn159* from pGP2234 A450G, A639G (SG118/119; SG120/121)	*Sac*I/*Bam*HI
pGP2236	pUT18 + *mpn569* from pGP2233 (SG138/SG140)	*Xba*I/*Kpn*I
pGP2237	pUT18C + *mpn569* from pGP2233 (SG138/SG140)	*Xba*I/*Kpn*I
pGP2238	PKt25 + *mpn569* from pGP2233 (SG138/SG140)	*Xba*I/*Kpn*I
pGP2239	PKNt25 + *mpn569* from pGP2233 (SG138/SG140)	*Xba*I/*Kpn*I
pGP2240	pBSK$^+$ + *mpn487* from pGP2246 (SG142/143)	*Sac*I/*Bam*HI
pGP2241	pUT18 + *mpn487* from pGP2246 (SG187/SG188)	*Bam*HI/*Sal*I
pGP2242	pGP172 + *mpn372* from pGP2227 A444G, A585G (SG124/SG141; SG126/127)	*Sac*I/*Bam*HI
pGP2243	pGP172 + *mpn133* from pGP686 (SG173/SG174)	*Sac*I/*Bam*HI
pGP2244	pUT18C + *mpn487* from pGP2246 (SG187/SG188)	*Bam*HI/*Sal*I
pGP2245	pGP172 + *mpn487* (SG142/SG143)	*Sac*I/*Bam*HI
pGP2246	pGP172 + *mpn487* from pGP2245 A384G (SG142/SG143; SG144)	*Sac*I/*Bam*HI
pGP2247	pGP172 + *mpn200* (SG158/SG159)	*Sac*I/*Bam*HI
pGP2248	pGP172 + *mpn288* (SG150/SG177)	*Sac*I/*Bam*HI
pGP2249	pKT25 + *mpn487* from pGP2246 (SG187/SG188)	*Bam*HI/*Sal*I
pGP2250	pKNT25 *mpn487* from pGP2246 (SG187/SG188)	*Bam*HI/*Sal*I
pGP2251	pUT18 + *mpn488* (SG189/SG190)	*Xba*I/*Kpn*I
pGP2252	pUT18C + *mpn488* (SG189/SG190)	*Xba*I/*Kpn*I
pGP2253	pGP172 + *mpn372* from pGP2242 A699G, A1092G	*Sac*I/*Bam*HI

	(SG124/SG141; SG128/129)	
pGP2254	pGP172 + *mpn372* from pGP2253 A1176G, A1350G (SG124/SG141; SG130/SG131)	*Sac*I/*Bam*HI
pGP2255	pGP172 + *mpn372* from pGP2254 A1386G, A1524G (SG124/SG141; SG132/SG133)	*Sac*I/*Bam*HI
pGP2256	pKT25 + *mpn488* (SG189/SG190)	*Xba*I/*Kpn*I
pGP2257	pKNT25 + *mpn488* (SG189/SG190)	*Xba*I/*Kpn*I
pGP2258	pGP172 + *mpn488* (SG191/SG192)	*Sac*I/*Bam*HI
pGP2259	pGP172 + *sufS* from *B. subtilis* (SG196/SG197)	*Sac*I/*Bam*HI

Tab. 7.4 Additional plasmids used in this work.

Plasmid	Construction / application	Reference
p25-N	Fusion of *goi* to N-terminus of T25-domain (BACTH)	Karimova *et. al.*, 1998
pBlueskript II SK(+)	Intermediate cloning	Stratagene
pBP15	Fusion of protein to N-terminal YFP	K. Gunka
pBP19	Fusion of protein to C-terminal YFP	K. Gunka
pBP20	Fusion of protein to C-terminal CFP	K. Gunka
pBQ200	Constitutive overexpression of proteins in *B. subtilis*	Martin-Verstraete *et al.*, 1994
pGP172	Fusion of protein with N-terminal *Strep*-Tag $^\circ$ II, overexpression in *E. coli*	Merzbacher *et al.*, 2004
pGP663	pUT18 + *glpF*$_{mpn}$ (MMR product)	Großhennig, 2011
pGP686	pUT18 + *mpn133* (MMR product)	Großhennig, 2011
pGP888	Allows for double homologous recombination of *goi* into the *lacA*-locus in *B. subtilis*	Diethmaier *et al.*, 2011
pGP1012	pMT85 + 239 bp promoter *ackA*$_{Mpn}$(-224…+3) + 1010 bp *Strep-hprK*$_{Mpn}$	Schmidl *et al.*, 2007
pGP2031	*glpD*$_{mpn}$ (MMR product) in pGP172	Schmeisky, 2013
pKT25	Fusion of *goi* to C-terminus of T25-domain (BACTH)	Karimova *et al.*, 1998
pKT25-zip	pKT25::*Kpn*I-*Eco*RI Fragment with Leucin zipper from GCN4 (positive control)	Karimova *et al.*, 2005
pMT85	Mini transposon for integration of *goi* and *aac-aphD* resistence in *M. pneumoniae* genome	Zimmermann and Herrmann, 2005
pUT18	Fusion of *goi* to N-terminus of T18-domain (BACTH)	Karimova *et. al.*, 1998

| **pUT18C** | Fusion of *goi* to C-terminus of T18-domain (BACTH) | Karimova *et. al.*, 1998 |
| **pUT18C-zip** | pUT18C::*EcoRI-KpnI* Fragment with Leucin zipper of GCN4 (positive control) | Karimova *et al.*, 2005 |

7.5 Bioinformatic tools and software

Tab. 7.5 Used bioinformatic tools and web pages.

Tool / URL	Provider	Application
KEGG http://www.genome.jp/kegg/	Kanehisa Laboratories	Genome sequence analysis and information about genes
BLAST http://blast.ncbi.nlm.nih.gov/Blast.cgi	National Center for Biotechnology Information	BLAST searches
PubMed http://www.ncbi.nlm.nih.gov/	National Center for Biotechnology Information	Literature research
OligoCalc http://www.basic.northwestern.edu/biotools/oligocalc	Northwestern University Chicago	Primer design
http://arep.med.harvard.edu/labgc/adnan/projects/Utilities/revcomp.html	Harvard University	Formation of reverse-complement sequences
Molligen http://services.cbib.u-ordeaux2.fr/molligen/	Université de Bordeaux	BLAST searches and genomanalyses in *Mollicutes*
MyMpn Project http://mympn.crg.eu/	Serrano group, CRG, Barcelona	Information about genes and proteins, genome organization in *M. pneumoniae*
ClustalW http://www.ebi.ac.uk/clustalw/	European Bioinformatics Institute	Sequence alignments
String http://string-db.org/	String consortium CPR, EMBL, KU, SIB, TUD and UZH	Information about protein-protein interactions
Subtiwiki http://subtiwiki.uni-goettingen.de/wiki/index.php/Main_Page	Stülke group, Georg-August University Göttingen	Information about genes and proteins in *B. subtilis*
TCDB http://www.tcdb.org/	Saier Lab. Group, University of California, San Diego	Information about transporter classes, identification of transmembrane domains
NEBcutter http://tools.neb.com/NEBcutter2/	New England Biolabs	Restiction site analysis
UniProt http://www.uniprot.org/	Uniprot Consortium EMBL-EBI, SIB, PIR	Information about protein functions, sequences and domains

Tab. 7.6 Used software.

Program	Producer	Application
AxioVision	Zeiss	Microscopic analyses of single cells
ChemoCam Imager Software	Intas	Analysis of chemiluminescence signals
Clone Manager	Sci-Ed Scientific & Educational Software	Sequence analysis, plasmid mapping, alignments
iCycler software	Bio-Rad	qRT-PCR data analysis
SeqMan™ II 5.07	DNASTAR	Analysis of sequencing results
Microsoft Office 2007 Microsoft Office 2010	Microsoft® Inc.	Text- and Dataprocessing
Gen5™ Data analysis software	BioTek®	Plate reader measurements of optical densities
Snap Gene Viewer	Snap Gene, GSL Biotech LLC	Plasmid mapping
Zen	Zeiss	Microscopic pictures of colonies

7.6   List of putative transporters in *M. pneumoniae*

Tab. 7.7 Putative proteins involved in transmembrane transport processes in *M. pneumoniae*.

MPN #	Gene name[1,2]	Essentiality[3]	Predicted Function[1,2]
MPN018	*pmd1*	F	ATP-bind prot.; Multidrug resist. ABC transporter
MPN019	*msbA*	NE	ATP-bind prot.; Multidrug resist. ABC transporter
MPN043	*glpF*	NE	Glycerol facilitator
MPN048		NE	Membrane export family
MPN049		NE	Membrane export familiy
MPN055	*potA*	E	ATP-bind. protein for polyamine transport
MPN056	*potB*	E	Transport permease (*potB* homolog)
MPN057	*potI*	E	Transport permease
MPN058		E	Lipoprotein, transport system substrate-binding protein
MPN076		NE	Hypothetical protein, MFS transporter
MPN077		NE	Hypothetical protein, MFS transporter
MPN078	*fruA*	F	Permease EIIA/B/C component
MPN080	*ybbP*	F	ABC transporter membrane protein, FtsX-like permease
MPN081	*ybbA/ glnQ*	E	ABC transporter ATP-binding protein
MPN095		NE	Amino acid permease
MPN096		NE	Amino acid permease

MPN112		NE	Permease
MPN113		NE	Permease

MPN133		NE	Lipoprotein / multiple sugar transport system substrate-binding protein / nuclease / MalE
MPN134	*ugpC*	E	Transport system permease, ATP binding protein
MPN135	*ugpA*	E	Transport system (ABC transporter) permease
MPN136	*ugpE*	E	Transport system (ABC transporter) permease

MPN193	*cysA/cbiO1/ecfA1*	F	Energy-coupling factor transporter ATP-binding protein
MPN194	*hisP/cbiO2/ecfA2*	E	Energy-coupling factor transporter ATP-binding protein
MPN195	*cbiQ*	F	Transport protein

MPN207	*ptsG*	E	PTS system, glucose-specific EIIABC component

MPN209	*mgtA / pacL*	F	Probable cation-transporting P-type ATPase

MPN215	*oppB*	E	Peptide ABC transporter permease
MPN216	*amiD / oppC*	F	Peptide ABC transporter permease
MPN217	*oppD*	E	Peptide ABC transporter ATP-binding protein
MPN218	*oppF*	E	Oligopeptide transport system ATP-binding protein, hypothetical protein

MPN234		NE	Membrane export family

MPN258	*yjcW/mglA*	E	Simple sugar ABC transporter, ATP-binding protein
MPN259		NE	Simple sugar ABC transporter permease
MPN260	*rbsC*	F	Simple sugar ABC transporter permease

MPN268		F	PTS system component EIIB/EIIC domain-containing protein

MPN274		E	ABC transporter permease

MPN308	*apc*	NE	Amino acid permease (sequence similarity zu mpn095/096)

MPN318	*apc*	F	Permease
MPN319	*gap1*	F	permease

MPN333		NE	Hypothetical membrane protein
MPN334	*bcrA*	NE	ABC transporter ATP binding protein (Multidrug-like transport?)
MPN335		NE	Hypothetical membrane protein

MPN415	*P37/ phnD*	F	High-affinity transport system substrate-binding protein P37
MPN416	*P29/ phnC*	F	ABC transport system ATP-binding protein P29
MPN417	*P69/ phnE*	F	ABC transport system permease protein P69

MPN421		NE	permease

MPN431	*cbiQ*	E	Transporter permease (CbiQ family)
MPN432	*artP*	E	Energy-coupling factor transporter ATP-binding protein
MPN433	*cbiO*	E	Energy-coupling factor transporter ATP-binding protein

MPN435		E	Permease

MPN448	*folT*	E	Hypothetical protein, ECF transporter S component

MPN460	*ktrB*	E	KtrB, Trk-type K$^+$ transport systems, membrane components, cation transporter
MPN461	*ktrA*	E	KtrA uptake protein, trk system potassium uptake protein TrkA

MPN494	*yjfU/ulaC (sgaA)*	F	PTS system: ascorbate-specific EIIA component
MPN495	*ulaB / sgaB*	NE	PTS system: EIIB
MPN496	*yjfU/sgaT/ulaA*	NE	PTS system: ascorbate-specific EIIC component, similar to phosphotransferase protein for pentitol from *E.coli*, SGAT homolog

MPN508		NE	Membrane export protein
MPN509		NE	Membrane export protein
MPN510		F	Membrane export protein
MPN511		NE	Membrane export protein
MPN512		NE	Membrane export protein

MPN571	*lcnDR3*	NE	Hemolysin ABC transporter, ABC transporter ATP binding protein

MPN608	*phoU / pstU*	NE	Phosphate transport system, regulatory protein
MPN609	*pstB*	NE	Phosphate import system, ATP-binding protein
MPN610	*pstA*	NE	Phosphate ABC transport system, permease protein
MPN611	*pstS*	NE	Phosphate transport system, substrate-binding protein

MPN651	*mtlA*	NE	Similar to mannitol-specific PTS EIIBC, EIICB-Mtl
MPN652	*mtlD*	NE	Mannitol-1-phosphate 5-dehydrogenase: D-mannitol 1-phosphate + NAD+ = D-fructose 6-phosphate + NADH
MPN653	*mtlF*	NE	Mannitol-specific PTS system component EIIA

MPN683	*devA*	NE	ABC transporter, ATP-binding protein
MPN684		F	ABC transporter permease
MPN685	*cysA*	F	ABC transporter ATP-binding protein

E essential; F fitness; NE non-essential. [1] Himmelreich *et al.*, 1996; [2] KEGG; [3] LLuch-Senar *et al.*, in press.

Curriculum vitae

STEPHANIE GROßHENNIG

Rosenwinkel 22
37081 Göttingen
Tel.: 0176/21896140
E-Mail: stgrosshennig@web.de

PERSONAL INFORMATION

Name	Stephanie Großhennig
Date of birth	04.05.1984
Place of birth	Wernigerode
Nationality	German

EDUCATION

Since 03/2012	**Ph.D. thesis** "Novel virulence determinants in *Mycoplasma pneumoniae*" in the group of Prof. Dr. Jörg Stülke, Department of General Microbiology, Georg-August University Göttingen
11/2011	**Master thesis** "Transport systems in *Mycoplasma pneumoniae*" in the group of Prof. Dr. Jörg Stülke, Department of General Microbiology, Georg-August University Göttingen
2009-2011	**M.Sc. Studies of Microbiology and Biochemistry**, Georg-August University Göttingen
08/2009	**Bachelor thesis** "Control of the intracellular glycerol-3-phosphate level in *Mycoplasma pneumoniae* – Influence of two homologous phosphodiesterases on the pathogenicity factor H_2O_2" in the group of Prof. Dr. Jörg Stülke, Department of General Microbiology, Georg-August University Göttingen
2006-2009	**B. Sc. Studies of Biology**, Georg-August University Göttingen
2004-2006	**Studies of Landscape architecture**, University Kassel
06/2003	**Abitur**, Heinrich-Heine-Gymnasium Ilsenburg

INTERNSHIPS

09/2010-11/2010	**Lab rotation** about "Fascinating Facilitators: Analysis of Transporters in *Mycoplasma pneumoniae*" in the group of Prof. Dr. Jörg Stülke, Department of General Microbiology, Georg-August University Göttingen
12/2010-02/2011	**Lab rotation** on „Characterization of *Aspergillus fumigatus ΔlaeA*, *ΔvelB*, *ΔvelC*, and *ΔvosA* mutants" with Dr. Henriette Irmer, Department for Molecular Microbiology and Genetics, Georg-August Universität Göttingen
02/2011-04/2011	**Internship** on "Analysis of listerial GpsB interactions with penicillin-binding proteins (PBPs) and construction of vectors for *pbp* gene replacement in *Listeria monocytogenes*" in the group of Dr. Sven Halbedel, FG 11 Bakterielle darmpathogene Erreger und Legionellen, Robert-Koch-Institut Wernigerode

CONTRIBUTION TO CONFERENCES

Presentation

10/2014	Microbiology and Infection2014, Gemeinsame Tagung der VAAM und DGHM, Dresden

Poster

12/2013	GGNB Poster session, Göttingen
3/2013	Jahrestagung der Vereinigung für Allgemeine und Angewandte Mikrobiologie (VAAM), Bremen

PUBLICATION

Großhennig S, Schmidl SR, Schmeisky G, Busse J, Stülke J., 2013
Implication of glycerol and phospholipid transporters in *Mycoplasma pneumoniae* growth and virulence. *Infect. Immun.* March 2013 *vol. 81* no. 3 896-904